

MARTIN MARIETTA ENERGY SYSTEMS LIBRARIES



3 4456 0250850 6

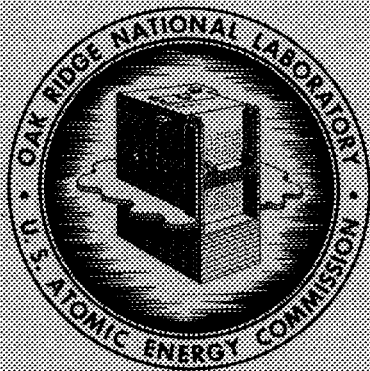
ORNL-3268
UC-34 - Physics
TID-4500 (17th ed.)

PHYSICS DIVISION
ANNUAL PROGRESS REPORT
FOR PERIOD ENDING JANUARY 31, 1962

CENTRAL RESEARCH LIBRARY
DOCUMENT COLLECTION
LIBRARY LOAN COPY

DO NOT TRANSFER TO ANOTHER PERSON

If you wish someone else to see this document, send in name with document and the library will arrange a loan.



OAK RIDGE NATIONAL LABORATORY
operated by
UNION CARBIDE CORPORATION
for the
U.S. ATOMIC ENERGY COMMISSION

Printed in USA. Price \$2.50 Available from the
Office of Technical Services
U. S. Department of Commerce
Washington 25, D. C.

LEGAL NOTICE

This report was prepared as an account of Government sponsored work. Neither the United States, nor the Commission, nor any person acting on behalf of the Commission:

- A. Makes any warranty or representation, express or implied, with respect to the accuracy, completeness, or usefulness of the information contained in this report, or that the use of any information, apparatus, method, or process disclosed in this report may not infringe privately owned rights; or
 - B. Assumes any liabilities with respect to the use of, or for damages resulting from the use of any information, apparatus, method, or process disclosed in this report.
- As used in the above, "person acting on behalf of the Commission" includes any employee or contractor of the Commission to the extent that such employee or contractor prepares, handles or distributes, or provides access to, any information pursuant to his employment or contract with the Commission.

ORNL-3268
UC-34 - Physics
TID-4500 (17th ed.)

Contract No. W-7405-eng-26

PHYSICS DIVISION
ANNUAL PROGRESS REPORT
for Period Ending January 31, 1962

J. L. Fowler, Director
E. O. Wollan, Associate Director

DATE ISSUED

MAY 23 1962

OAK RIDGE NATIONAL LABORATORY
Oak Ridge, Tennessee
operated by
UNION CARBIDE CORPORATION
for the
U. S. ATOMIC ENERGY COMMISSION

MARTIN MARIETTA ENERGY SYSTEMS LIBRARIES



3 4456 0250850 6

FOREWORD

This is the fourth Physics Division progress report made on an annual basis. As in previous years, the report contains the abstracts for papers which have been published or which have been prepared for publication. In such cases, reprints or preprints of the articles will be available. Preliminary results of work in progress are reported, as previously, in some detail. Since this work is of a preliminary nature, the authors should be contacted with regard to the inclusion of any of these results in other publications.

TABLE OF CONTENTS AND SUMMARY

NONSINGULAR FORMULATION OF THE BRUECKNER APPROXIMATION FOR AN INFINITE FERMI SYSTEM	
Richard L. Becker	1
Abstract of paper submitted to <i>Physical Review</i> .	
DIRECT NUCLEAR REACTIONS WITH POLARIZED TARGETS	
G. R. Satchler	1
Abstract of published paper: <i>Proceedings of the Rutherford Jubilee International Conference</i> , Manchester, England, 1961.	
FINITE-RANGE DISTORTED-WAVES CALCULATION OF DIRECT REACTIONS	
E. C. Halbert, R. M. Drisko, G. R. Satchler, and N. Austern	1
Abstract of published paper: <i>Proceedings of the Rutherford Jubilee International Conference</i> , Manchester, England, 1961.	
THE DISTORTED-WAVE THEORY OF DIRECT NUCLEAR REACTIONS. I: "ZERO-RANGE" FORMALISM WITHOUT SPIN-ORBIT COUPLING, AND THE CODE SALLY	
R. H. Bassel, R. M. Drisko, and G. R. Satchler	2
Abstract of published report: ORNL-3240 (Jan. 26, 1962).	
ROTATIONAL ENERGIES OF ASYMMETRIC ODD-A NUCLEI	
K. T. Hecht and G. R. Satchler	2
Abstract of paper to be published in <i>Nuclear Physics</i> .	
COLLECTIVE EFFECTS IN INELASTIC SCATTERING FROM NUCLEI	
W. T. Pinkston and G. R. Satchler	3
Abstract of published paper: <i>Nuclear Phys.</i> 27, 270 (1961).	
ENERGY DEPENDENCE OF THE $B^{10}(d, p)B^{11}$ ANGULAR DISTRIBUTION	
B. Zeidman, J. L. Yntema, and G. R. Satchler	3
Abstract of published paper: <i>Proceedings of the Rutherford Jubilee International Conference</i> , Manchester, England, 1961.	
RADIAL INTEGRALS WITH REALISTIC WAVE FUNCTIONS	
D. E. Arnurius, B. Buck, and G. R. Satchler	3
Abstract of paper to be published in <i>Proceedings of Conference on Electromagnetic Lifetimes and Properties of Nuclear States</i> , Gatlinburg, Tennessee, 1961.	
CALCULATION OF NUCLEAR PROPERTIES WITH THE SHELL MODEL	
J. N. Ginnochio, R. H. Bassel, and G. R. Satchler	4
Fractional-percentage coefficients are being computed for mixed neutron and proton configurations of the type j^n .	
ANALYSIS OF THE INELASTIC SCATTERING OF ALPHA PARTICLES	
R. H. Bassel, R. M. Drisko, and G. R. Satchler	4
The inelastic scattering of alpha particles has been analyzed by using a nonspherical generalization of the optical model and the distorted-waves method.	

GAMMA RAYS FROM INELASTIC SCATTERING OF HIGH-ENERGY NUCLEONS	
A. B. Clegg and G. R. Satchler	7
Abstract of published paper: <i>Nuclear Phys.</i> 27 , 431 (1961); also published in <i>Proceedings of the Rutherford Jubilee International Conference</i> , Manchester, England, 1961.	
THEORETICALLY STABLE AND CONFINED PLASMA	
T. K. Fowler	7
Abstract of research note to appear in <i>Physics of Fluids</i> , February 1962.	
PLASMA POTENTIAL AND ENERGY DISTRIBUTIONS IN HIGH-ENERGY INJECTION MACHINES	
T. K. Fowler and M. Rankin	7
Abstract of paper submitted to <i>Journal of Nuclear Energy: Part C</i> .	
PHENOMENOLOGICAL NUCLEAR POTENTIALS FOR CLOSED-SHELL NUCLEI	
J. L. Fowler	8
The interpretation of the interaction of neutrons with the closed-shell nucleus, O^{16} , is discussed in terms of phenomenological potentials, and the analysis is extended to the case of the interaction of neutrons with Pb^{208} .	
CHARGED-PARTICLE NUCLEAR CROSS-SECTION COMPILATION	
F. K. McGowan and M. R. Patterson	10
A literature search of charged-particle-induced reactions for the years 1959, 1960, and 1961 is 90% complete. Tabular data of results for the elements manganese through zinc are being collected.	
LEVEL STRUCTURE IN Ne^{22} AND Si^{30} FROM THE REACTIONS $O^{18}(\alpha, n)Ne^{21}$ AND $Mg^{26}(\alpha, n)Si^{29}$	
J. K. Bair and H. B. Willard	11
Abstract of paper to be submitted to <i>Physical Review</i> .	
ANGULAR CORRELATION STUDY OF THE $Be^9(\alpha, n)C^{12}(\gamma_{4.43})C^{12}$ REACTION	
J. Kjellman, T. Dazaj, and J. H. Neiler	11
Abstract of published paper: <i>Nuclear Phys.</i> 30 , 131 (1962).	
A STUDY OF THE REACTIONS $Be^9(He^3, n)C^{11}$, $Li^7(He^3, n)B^9$, AND $C^{13}(He^3, n)O^{15}$	
J. L. Duggan, P. D. Miller, and R. F. Gabbard	12
Abstract of paper to be submitted to <i>Nuclear Physics</i> .	
COULOMB EXCITATION OF THE FIRST 2^+ STATE OF EVEN-EVEN NUCLEI WITH $58 \leq A \leq 82$	
P. H. Stelson and F. K. McGowan	12
Abstract of paper to be published in <i>Nuclear Physics</i> .	
COULOMB EXCITATION OF SECOND 2^+ STATES IN Ge^{74}, Ge^{76}, Se^{76}, Se^{78}, AND Se^{80}	
F. K. McGowan and P. H. Stelson	13
Abstract of paper submitted to <i>Physical Review</i> .	
COULOMB EXCITATION OF LEVELS IN Se^{77}	
R. L. Robinson, F. K. McGowan, and P. H. Stelson	13
Abstract of paper to be published in <i>Physical Review</i> .	
COULOMB EXCITATION OF OSMIUM AND CHROMIUM NUCLEI	
F. K. McGowan, P. H. Stelson, and R. L. Robinson	14
Abstract of published paper: <i>Proceedings of Conference on Electromagnetic Lifetimes and Properties of Nuclear States</i> , Gatlinburg, Tennessee, Oct. 5--7, 1961.	

COULOMB EXCITATION OF Br⁷⁹	
R. L. Robinson, F. K. McGowan, and P. H. Stelson	14
Results on Coulomb excitation of seven levels in Br ⁷⁹ are reported.	
DECAY OF Rh¹⁰² → Ru¹⁰²	
F. K. McGowan and P. H. Stelson	18
Abstract of published paper: <i>Phys. Rev.</i> 123 , 2131 (1961).	
NUCLEAR LEVELS OF Ge⁷⁴	
E. Eichler, G. D. O'Kelley, R. L. Robinson, J. A. Marinsky, and N. R. Johnson	19
Abstract of paper submitted to <i>Nuclear Physics</i> .	
DECAY OF Cs¹³²	
R. L. Robinson, N. R. Johnson, and E. Eichler	19
The gamma-ray spectrum of Cs ¹³² has been studied with scintillation spectrometers. Energy-level diagrams of Xe ¹³² and Ba ¹³² have been proposed.	
TOTAL-NEUTRON CROSS SECTION OF Pb²⁰⁸	
J. L. Fowler and E. C. Campbell	23
Abstract of paper submitted to <i>Physical Review</i> .	
CHANNEL ANALYSIS OF FISSION: INTERPRETATION OF SOME EXPERIMENTAL DATA ACCORDING TO THE THEORY OF A. BOHR	
R. W. Lamphere	23
Formulas have been derived to facilitate the comparison of experimentally measured fission-fragment angular distributions with theory. They are of especial significance near threshold and have been applied to neutron-induced fission of U ²³⁴ , one of the few cases where adequate data exist to admit the possibility of identifying individual fission channels.	
CAPTURE CROSS SECTIONS FOR 30-kev NEUTRONS	
R. L. Macklin and T. Inada	40
A Moxon-Rae gamma-ray detector has been constructed and used with the ORNL 3-Mv Van de Graaff accelerator. The overall time resolution was about 15 nanoseconds (but should be capable of considerable improvement). By use of the Li ⁷ (p,n) reaction near threshold and a 19.7-cm flight path, neutron capture in several elements was compared. Cross-section results will be presented for Au, Ag, Cd, Sn, Mo, Pt, W, and Ta. Computer calculations of the relative efficiency of the detector confirm the anticipated proportionality to gamma-ray energy to ±25% over the energy range 0.5 to 8.0 Mev. This range covers most of the gamma rays resulting from neutron capture.	
DIRECT COMPARISON OF GAMMA-RAY SPECTRA OBTAINED FROM CAPTURE OF THERMAL AND (30 ± 10)-kev NEUTRONS	
F. W. K. Firk and J. H. Gibbons	42
Abstract of published paper: pp 213–19 in <i>Proceedings of the Symposium on Neutron Time-of-Flight Methods, Session II</i> , Saclay, France, July 24–27, 1961.	
GAMMA-RAY SPECTRA FROM 30-kev NEUTRON CAPTURE	
J. R. Bird, J. H. Gibbons, and W. M. Good	43
Prompt gamma rays from 30-kev neutron capture have been observed for a number of nuclides. In many cases the spectra result from capture in a single resonance of known spin and parity. In most cases the spectra are distinctly different from results obtained by using thermal neutrons.	

GENERAL SURVEY ON RADIATIVE CAPTURE MEASUREMENTS BY TIME-OF-FLIGHT	
J. H. Gibbons	47
Abstract of published paper: pp 151--66 in <i>Proceedings of the Symposium on Neutron Time-of-Flight Methods, Session II, Saclay, France, July 24--27, 1961.</i>	
PARAMETERS OF NEUTRON RESONANCES IN Pa²³¹	
J. R. Patterson and J. A. Harvey	47
Measurements have been made of the total neutron cross section of Pa ²³¹ from 0.04 to 200 ev. Resonance parameters up to 100 ev, the average level spacing, the s-wave neutron strength function, the neutron width distribution, and the level-spacing distribution were derived from the data.	
PARAMETERS OF NEUTRON RESONANCES IN W¹⁸⁴	
F. A. Khan and J. A. Harvey	52
Neutron transmission measurements have been made from 2.5 to 2000 ev upon a sample of normal tungsten and one enriched in W ¹⁸⁴ . Parameters for nine resonances up to 1271 ev have been derived from the data.	
MANGANESE BATH MEASUREMENTS OF η OF Pu²³⁹	
R. L. Macklin, G. deSaussure, J. D. Kington, and W. S. Lyon	54
Abstract of paper submitted to <i>Nuclear Science and Engineering.</i>	
FISSION FRAGMENT CORRELATION EXPERIMENTS	
F. J. Walter, J. H. Neiler, R. J. Silva, and H. W. Schmitt	54
A U ²³⁵ thermal-neutron-induced fission-fragment correlation experiment has been completed. Preliminary analysis of the data shows fine structure in the mass distribution. Results and experimental techniques are discussed.	
A PRECISION MEASUREMENT OF THE LONGITUDINAL POLARIZATION OF BETAS FOLLOWING P³² DECAY	
A. R. Brosi, A. I. Galonsky, B. H. Ketelle, and H. B. Willard	60
Abstract of paper submitted to <i>Nuclear Physics.</i>	
HALF-LIFE OF He⁶	
J. K. Bienlein and Frances Pleasonton	60
A preliminary value of $T_{1/2} = 0.78 \pm 0.01$ sec has been obtained for the beta decay of He ⁶ .	
AN ABSOLUTE DETERMINATION OF THE He⁶ BETA-DECAY ENERGY	
C. H. Johnson, Frances Pleasonton, and T. A. Carlson	61
Abstract of paper to be submitted to <i>Nuclear Physics.</i>	
RECOIL ENERGY AND CHARGE SPECTRA FOR THE Na²³ IONS FORMED FROM THE β^- DECAY OF Ne²³	
T. A. Carlson	62
Measurements have been made of both the charge and recoil spectra of the sodium ions resulting from the β^- decay of Ne ²³ . Less than 1/2% deviation was noted from the expected theoretical shape for recoil energy based on the assumption that the beta-neutrino interaction is pure axial vector; while the charge spectrum can be explained in terms of multiple shake-off arising from the sudden change in nuclear charge.	
ELECTRON SHAKE-OFF FOLLOWING THE β^- DECAY OF Ar⁴¹	
T. A. Carlson	65
Measurement of the charge spectrum of the potassium ions formed from the decay of Ar ⁴¹ completes a series of studies on the atomic consequence of beta decay. The data are explained by a sudden nonadiabatic change in the nuclear charge followed by one or more Auger processes when inner orbital electrons are removed.	

DECOMPOSITION OF $(CH_3Xe^{131})^+$ FOLLOWING THE NUCLEAR DECAY OF CH_3I^{131}	
T. A. Carlson and R. M. White	67
Abstract of paper to be published in <i>Journal of Chemical Physics</i> .	
MÖSSBAUER-PARITY EXPERIMENT	
F. E. Obenshain and H. H. Wegener	67
A Mössbauer-parity experiment has been designed to measure the sign of the ground-state magnetic moment of Ni^{61} . The relative sign of the ground and excited states is known from a previous experiment. The Mössbauer effect for Ni^{61} in the scattering position has been observed by using this apparatus.	
A MÖSSBAUER STUDY OF THE 77-keV GAMMA TRANSITION OF Au^{197} IN A SERIES OF FERROMAGNETIC ALLOYS. THE MAGNETIC MOMENT OF THE FIRST EXCITED STATE OF Au^{197}	
L. D. Roberts and J. O. Thomson	70
The s -state density on gold has been measured in the gold-nickel alloy system. This is related to the magnetic properties of these alloys and to previous theoretical considerations of this s -state density. The hyperfine structure splitting of gold dissolved in iron, cobalt, and nickel has been found to be proportional to the magnetic moment of the ferromagnetic metal. The measurements are interpreted to give a magnetic moment of the first excited state of Au^{197} .	
ISOMER SHIFT OF GOLD IN A NUMBER OF ALLOYS AND COMPOUNDS	
J. O. Thomson, H. Pomerance, C. F. Dam, and L. D. Roberts	74
The isomer shift of gold in a number of environments has been determined. These results may be related to the nuclear size change with the gamma-ray emission, to chemical bonding of the gold, and to electronegativity considerations.	
NEUTRON DIFFRACTION STUDY OF ANTIFERROMAGNETIC $FeCl_3$	
J. W. Cable, M. K. Wilkinson, E. O. Wollan, and W. C. Koehler	75
Abstract of paper to be submitted to <i>Physical Review</i> .	
THE MAGNETIC STRUCTURES OF THULIUM	
W. C. Koehler, J. W. Cable, E. O. Wollan, and M. K. Wilkinson	76
Abstract of paper submitted to <i>Physical Review</i> .	
INVESTIGATIONS OF PARAMAGNETIC NEUTRON SCATTERING FROM METALLIC CHROMIUM	
M. K. Wilkinson, E. O. Wollan, W. C. Koehler, and J. W. Cable	76
Neutron diffraction investigations performed on Cr^{52} indicate that localized atomic magnetic moments do not exist in metallic chromium above the Néel temperature.	
MAGNETIC ORDERING IN HoN	
H. R. Child, M. K. Wilkinson, J. W. Cable, E. O. Wollan, and W. C. Koehler	80
Neutron diffraction investigations on HoN in external magnetic fields have helped to clarify the unusual magnetic scattering from this compound below the Curie temperature. Specific values of the ordered atomic magnetic moments have been determined and a possible magnetic structure is suggested.	
MAGNETIC COUPLING IN Pd-DILUTE IRON GROUP ALLOYS	
E. O. Wollan	82
Abstract of published paper: <i>Phys. Rev.</i> 122 , 1710 (1961).	
NEUTRON DIFFRACTION INVESTIGATIONS OF FERROMAGNETIC PALLADIUM AND IRON GROUP ALLOYS	
J. W. Cable, E. O. Wollan, W. C. Koehler, and M. K. Wilkinson	82
Abstract of paper to be published in <i>Journal of Applied Physics (suppl)</i> .	

MAGNETIC MOMENT DISTRIBUTION IN PALLADIUM AND IRON GROUP ALLOYS	
E. O. Wollan, J. W. Cable, W. C. Koehler, and M. K. Wilkinson.....	82
Abstract of published paper: <i>Intern. Conf. Magnetism and Crystallography (Kyoto, Japan) 4</i> , 314 (1961).	
PHENOMENOLOGICAL DISCUSSION OF MAGNETIC ORDERING IN THE HEAVY RARE-EARTH METALS	
R. J. Elliott	83
Abstract of published paper: <i>Phys. Rev.</i> 124 , 346 (1961).	
NEUTRON DIFFRACTION BY HELICAL-SPIN STRUCTURES	
W. C. Koehler	83
Abstract of published paper: <i>Acta Cryst.</i> 14 , 535 (1961).	
RECENT PROGRESS IN MAGNETIC STRUCTURE DETERMINATIONS OF RARE-EARTH METALS	
W. C. Koehler, J. W. Cable, E. O. Wollan, and M. K. Wilkinson.....	83
Abstract of published paper: <i>Intern. Conf. Magnetism and Crystallography (Kyoto, Japan) 4</i> , 312 (1961).	
RECENT MAGNETIC NEUTRON SCATTERING INVESTIGATIONS AT OAK RIDGE NATIONAL LABORATORY	
M. K. Wilkinson, H. R. Child, W. C. Koehler, J. W. Cable, and E. O. Wollan	84
Abstract of published paper: <i>Intern. Conf. Magnetism and Crystallography (Kyoto, Japan) 4</i> , 311 (1961).	
NEUTRON DIFFRACTION	
M. K. Wilkinson, E. O. Wollan, and W. C. Koehler	84
Abstract of published chapter: <i>Ann. Rev. Nuclear Sci.</i> 11 , 303 (1961).	
OPTICAL PHYSICS	
G. W. Charles, P. M. Griffin, H. W. Morgan, O. B. Rudolph, P. A. Staats, K. L. Vander Sluis, T. A. Welton, and G. K. Werner	84
Preliminary work is described on the exploration of some promising two-component gas systems for optical amplification.	
INFRARED SPECTRA OF DILUTE SOLID SOLUTIONS	
H. W. Morgan and P. A. Staats	87
Abstract of published paper: <i>J. Appl. Phys. (suppl)</i> 33 , 364 (1962).	
SOLID-SOLUTION INFRARED SPECTRA. THE METABORATE ION, BO_2^-	
H. W. Morgan and P. A. Staats	88
Abstract of paper to be submitted to <i>Journal of Chemical Physics</i> .	
FRAGMENT AND CHARGE SPECTRA OF THE IONS FORMED FOLLOWING RADIOACTIVE DECAY OF $C_2H_5^{131}$ AND CH_3^{130}	
T. A. Carlson and R. M. White.....	88
The fragment and charge spectra following the nuclear decay of CH_3^{130} and $C_2H_5^{131}$ have been measured. From these data, the roles played by recoil energy and by the hydrocarbon in determining the stability of the parent xenon-hydrocarbon ion are evaluated.	
A 7090 PROGRAM FOR BUBBLE-CHAMBER TRACK RECONSTRUCTION	
H. O. Cohn, W. M. Bugg, and R. D. McCulloch	90
A 7090 computer program for bubble-chamber track reconstruction has been written. The input is punched tape from a Hermes film measuring device. The output includes azimuth angle, dip angle, end-point coordinates, and momenta evaluated at each end of a track.	

RESPONSE OF SILICON SURFACE-BARRIER DETECTORS TO FISSION FRAGMENTS	
H. W. Schmitt, J. H. Neiler, F. J. Walter, and R. J. Silva	94
The response of silicon surface-barrier detectors to fission fragments has been found not to be strictly proportional to fragment energy. The response is, in general, linear with a nonzero intercept. Systematics are discussed.	
BEHAVIOR OF SEMICONDUCTOR NUCLEAR-PARTICLE DETECTORS	
F. J. Walter, J. W. T. Dabbs, and L. D. Roberts	97
Abstract of paper to be published in <i>Proceedings of a Conference on Nuclear Electronics</i> , Belgrade, 1961.	
A SUPERCONDUCTING MAGNET STUDY	
L. D. Roberts and R. W. Boom	98
A partial report is made of the properties of a 33-kilogauss superconducting magnet.	
GENERAL SURVEY ON PULSED ELECTROSTATIC ACCELERATORS AS SOURCES OF PULSED NEUTRONS	
W. M. Good	98
Abstract of published paper: pp 309-19 in <i>Proceedings of the Symposium on Neutron Time-of-Flight Methods, Session III</i> , Saclay, France, July 24-27, 1961.	
NAPHTHALENE DERIVATIVE SCINTILLATORS AND GLASS LOADING POSSIBILITIES	
R. L. Macklin	98
Abstract of published report: AERE-R 3744 (June 1961).	
PULSE-SHAPE CALCULATIONS FOR A LARGE LIQUID SCINTILLATOR	
R. L. Macklin and J. H. Gibbons	99
A report is given of the application of Monte Carlo codes for calculating pulse-height distributions in liquid scintillators and the use of these results in pulsed Van de Graaff neutron capture studies.	
IMPROVED BEAM PULSER FOR 3-Mv VAN DE GRAAFF ACCELERATOR	
C. D. Moak, R. F. King, H. E. Banta, and J. W. Johnson	100
A report is given of the performance of a new pulser built for the duoplasmatron ion source, which has been installed in the terminal of the 3-Mv accelerator.	
COUNTDOWN CIRCUITS FOR PULSED VAN DE GRAAFF ACCELERATOR	
R. F. King and W. H. Du Preez	101
A synchronized countdown system has been built in which a set of electrostatic deflector plates is used to allow only one pulse out of eight to reach the target, while the remaining seven pulses are discarded.	
RELIABILITY IN HELIUM LIQUEFACTION	
J. W. T. Dabbs	101
Abstract of paper to be published in <i>Proceedings of a Conference of l'Institute International du Froid</i> , London, September 20-22, 1961.	
PUBLICATIONS	103
PAPERS PRESENTED AT SCIENTIFIC AND TECHNICAL MEETINGS	106
ANNOUNCEMENTS	110
ADVISORY COMMITTEE	112
ACTIVITIES RELATED TO EDUCATIONAL INSTITUTIONS	112
ORNL PHYSICS SEMINARS	119

NONSINGULAR FORMULATION OF THE BRUECKNER APPROXIMATION FOR AN INFINITE FERMION SYSTEM¹

Richard L. Becker

Singularities of the reaction matrix render Brueckner's integral for the average energy per particle a singular integral. By considering the infinite Fermi system to be a limit of finite systems, it is shown that the correct result in the approximation, neglecting any but single pair correlations, merely involves replacing Brueckner's ordinary integral over diagonal reaction matrix elements by a principal-value integral. In a finite system the level shift of a Bethe-Goldstone state differs from the diagonal reaction matrix element by a normalization factor which does not approach unity uniformly in the integration variable as the volume becomes infinite. In the neighborhood of

a singularity the expression for the two-particle energy shift takes the form

$$x |v_{bp}|^2 / (x^2 + V^{-1} |v_{bp}|^2).$$

Hence as $V \rightarrow \infty$ the sum over the energy x indeed approaches a principal-value integral. An alternative derivation, employing a modified reaction matrix for which there is no difference between level shift and matrix element, leads to the same result. The general derivations are preceded by a soluble example.

The connection of the Brueckner approximation with the phase-shift approximation for low-density systems is discussed. Some corrections to the higher-order terms in existing derivations of the "separation method" expansion of the Brueckner reaction matrix are given.

¹Abstract of paper submitted to *Physical Review*.

DIRECT NUCLEAR REACTIONS WITH POLARIZED TARGETS¹

G. R. Satchler

The advantages and the interpretation of nuclear reaction studies with polarized target nuclei are discussed, with particular reference to direct reactions.

¹Abstract of published paper: *Proceedings of the Rutherford Jubilee International Conference*, Manchester, England, 1961.

FINITE-RANGE DISTORTED-WAVES CALCULATION OF DIRECT REACTIONS¹

E. C. Halbert²

R. M. Drisko³

G. R. Satchler

N. Austern⁴

Current distorted-wave Born-approximation calculations of direct nuclear reactions employ a

zero-range interaction or an equivalent approximation. We have constructed an improved distorted-wave calculation which correctly treats finite-range interactions or finite-size projectiles.

¹Abstract of published paper: *Proceedings of the Rutherford Jubilee International Conference*, Manchester, England, 1961.

²Electronuclear Division.

³Consultant, University of Pittsburgh, Pittsburgh, Pa.

⁴University of Pittsburgh, Pittsburgh, Pa.

THE DISTORTED-WAVE THEORY OF DIRECT NUCLEAR REACTIONS. I: "ZERO-RANGE"
FORMALISM WITHOUT SPIN-ORBIT COUPLING, AND THE CODE SALLY¹

R. H. Bassel²R. M. Drisko³

G. R. Satchler

The distorted-wave theory of direct nuclear reactions is presented in a unified manner in which the effects of assuming various reaction mechanisms and nuclear models appear only in certain radial form factors. The zero-range approximation is used, and spin-orbit coupling is neglected in

the distorted waves. Formulas are given for transition amplitudes, cross sections, and polarizations. Then a description is given of the IBM 704 computer code SALLY, which is based on these formulas.

¹Abstract of published report: ORNL-3240 (Jan. 26, 1962).

²Electronuclear Division.

³Consultant, University of Pittsburgh, Pittsburgh, Pa.

ROTATIONAL ENERGIES OF ASYMMETRIC ODD-A NUCLEI¹

K. T. Hecht²

G. R. Stachler

The asymmetric rotator model of Davydov and Filippov has been extended to odd- A nuclei by coupling a single nucleon to an inert core of well-stabilized asymmetric equilibrium shape. Rotational energies are calculated for states with spin I through numerical diagonalization of $(I + \frac{1}{2}) \times (I + \frac{1}{2})$ rotational matrices which depend in a complicated way on the state of the odd nucleon. The state of the odd nucleon is described by single-particle wave functions such as those calculated by Newton, which are generalizations for the asymmetric case of the wave functions computed by Nilsson for axially symmetric nuclei. The rotational energy spectrum for a particular particle excitation is, in general, very rich in number of levels and may consist of a complicated sequence of spin values. In many cases, however, particularly for small asymmetries, the rotational spectra may consist of several well-separated or overlapping sequences of spin states

which resemble the rotational bands of axially symmetric nuclei, especially insofar as K (which gives the projection of I on the body-fixed z axis) may be approximately a good quantum number for each sequence.

In an initial survey of odd- A nuclei around A values of 190, no clear-cut evidence has been found for the existence of nuclei with a well-defined asymmetric equilibrium shape. Calculations for Ir^{191} and Re^{185} indicate only that it may be very difficult to distinguish between a symmetric and an asymmetric rotator model when the asymmetry is small. Calculations for Pt^{195} show that, although the observed level scheme can be reproduced by asymmetric rotator theory, the observed electromagnetic transition probabilities are not in agreement with the predictions of the simple asymmetric rotator model.

¹Abstract of paper to be published in *Nuclear Physics*.

²University of Michigan, Ann Arbor.

COLLECTIVE EFFECTS IN INELASTIC SCATTERING FROM NUCLEI¹W. T. Pinkston²

G. R. Satchler

Inelastic scattering is closely analogous to an electric multipole radiative transition and will show similar collective enhancement. This enhancement will vary with the scattering angle. In general, spin-flip transitions are little affected,

the enhancement being found in the spin-independent amplitudes; the consequences of this are discussed. The deformed nucleus model for C^{12} is used to illustrate these effects. Finally, the interaction form factors to be used for inelastic scattering are discussed.

¹Abstract of published paper: *Nuclear Phys.* 27, 270 (1961).

²Summer participant, Vanderbilt University, Nashville, Tenn.

ENERGY DEPENDENCE OF THE $B^{10}(d,p)B^{11}$ ANGULAR DISTRIBUTION¹B. Zeidman²J. L. Yntema²

G. R. Satchler

The angular distributions of the $B^{10}(d,p)B^{11}$ ground-state transition have been measured at incident energies of 12.5, 15.5, 18.5, and 21.5 Mev. The angular distributions at the higher energies cannot be fitted with Butler's theory

for (d,p) reactions. Excellent fits have been obtained with distorted-wave theory. There are indications that it is necessary to use an energy-dependent deuteron potential. Nonstripping processes appear to make very little contribution to this reaction.

¹Abstract of published paper: *Proceedings of the Rutherford Jubilee International Conference*, Manchester, England, 1961.

²Argonne National Laboratory, Argonne, Ill.

RADIAL INTEGRALS WITH REALISTIC WAVE FUNCTIONS¹D. E. Arnurius²B. Buck³

G. R. Satchler

A code has been written to compute the matrix elements of radial operators such as r^L and the collective surface-coupling interaction dU/dr , using radial wave functions for a nucleon moving

in a potential well of Saxon shape with spin-orbit and Coulomb forces included. Initial application has been to the $2s_{1/2}$ and $1d_{5/2}$ states in O^{17} and F^{17} and to the $E2$ transitions between them.

¹Abstract of paper to be published in *Proceedings of Conference on Electromagnetic Lifetimes and Properties of Nuclear States*, Gatlinburg, Tenn., Oct. 5-7, 1961.

²Mathematics Panel.

³Neutron Physics Division.

CALCULATION OF NUCLEAR PROPERTIES WITH THE SHELL MODEL

J. N. Ginnochio¹ R. H. Bassel² G. R. Satchler

A program of large-scale nuclear shell-model calculations is to be set up, by use of ORNL computer facilities, to diagonalize, for example, the large matrices involved. To evaluate the matrix elements to be used in such calculations, it is necessary to be able to construct properly antisymmetric wave functions for a number of nucleons. As a first step, a code is being written³

¹Consultant, University of Rochester, Rochester, N.Y.

²Electronuclear Division.

³The code is being prepared by N. M. Dismuke and J. E. Rayburn of the Mathematics Panel.

to compute the coefficients of fractional parentage for n equivalent nucleons, that is, mixed neutron and proton configurations of the type f^n . Initially, values of $j \leq \frac{9}{2}$ are being included, although it is hoped to extend these to $j \leq \frac{13}{2}$, at least for states of maximum isotopic spin. The calculation is based on a ladder process, devised by J. N. Ginnochio, which starts from the trivial case $n = 2$ and builds up to a half-filled shell with $n = 2j + 1$.

The advice of J. B. French and M. H. Macfarlane of the University of Rochester is gratefully acknowledged.

ANALYSIS OF THE INELASTIC SCATTERING OF ALPHA PARTICLES

R. H. Bassel¹ R. M. Drisko² G. R. Satchler

The inelastic scattering of alpha particles is interpreted as a direct interaction by use of the distorted-wave method.³ The collective, or surface-coupling, model for the interaction is used and is found to give results in good agreement with experiment. This model is a generalization of the optical model, including nonspherically-symmetric potential wells, and is particularly appropriate to the excitation of vibrational or rotational states. In the distorted-wave Born-approximation method, the shape of the inelastic angular distribution is entirely determined by the multipolarity of the transition and by the optical potential parameters needed to fix the observed elastic scattering. The magnitude of the observed inelastic cross section then determines the corresponding nuclear "deformation." Deformations obtained in this way agree reasonably well with those found by using other techniques such as Coulomb excitation. The

optical-model parameters which best reproduce the observed elastic scattering are determined by using an automatic search routine on the IBM 7090 computer and then used with the distorted-wave code⁴ to predict the inelastic scattering. The most intensive work so far has been on the reaction of 43-Mev alphas with nickel; a comparison of some of the results with the cross sections measured at Argonne National Laboratory⁵ is shown in Fig. 1. Two other examples are shown: a light nucleus Be⁹ at 48 Mev in Fig. 2, and Ar⁴⁰ at 18 Mev in Fig. 3. Both these results are somewhat preliminary; a good fit to the elastic data has not yet been found.

Some study has been made of the effects of including Coulomb excitation and its interference with the nuclear scattering. In addition, the

⁴R. H. Bassel, R. M. Drisko, and G. R. Satchler, *Phys. Div. Ann. Progr. Rept. Feb. 10, 1961*, ORNL-3085, p 10.

⁵H. W. Brock *et al.*, "Scattering of 43-Mev Alpha Particles by Ni⁵⁸ and Ni⁵⁰," to be published in *Physical Review*. We are indebted for the use of this data prior to publication.

¹Electronuclear Division.

²Consultant, University of Pittsburgh, Pittsburgh, Pa.

³E. Rost and N. Austern, *Phys. Rev.* **120**, 1375 (1960).

angular correlation of the inelastic alphas with de-excitation gamma rays has also been calculated. It is found that the correlation may differ markedly from the predictions of the adiabatic theory⁶ when alphas are detected away from the

⁶J. S. Blair and L. Wilets, *Phys. Rev.* 121, 1493 (1961).

⁷D. K. McDaniels and D. L. Hendrie, to be published.

peaks of the angular distribution, but that the predictions are in qualitative agreement with recent measurements.⁷

This work is being prepared for publication, when a more detailed interpretation will be given. The same model is also showing promise of giving a good description of neutron and proton inelastic scattering.

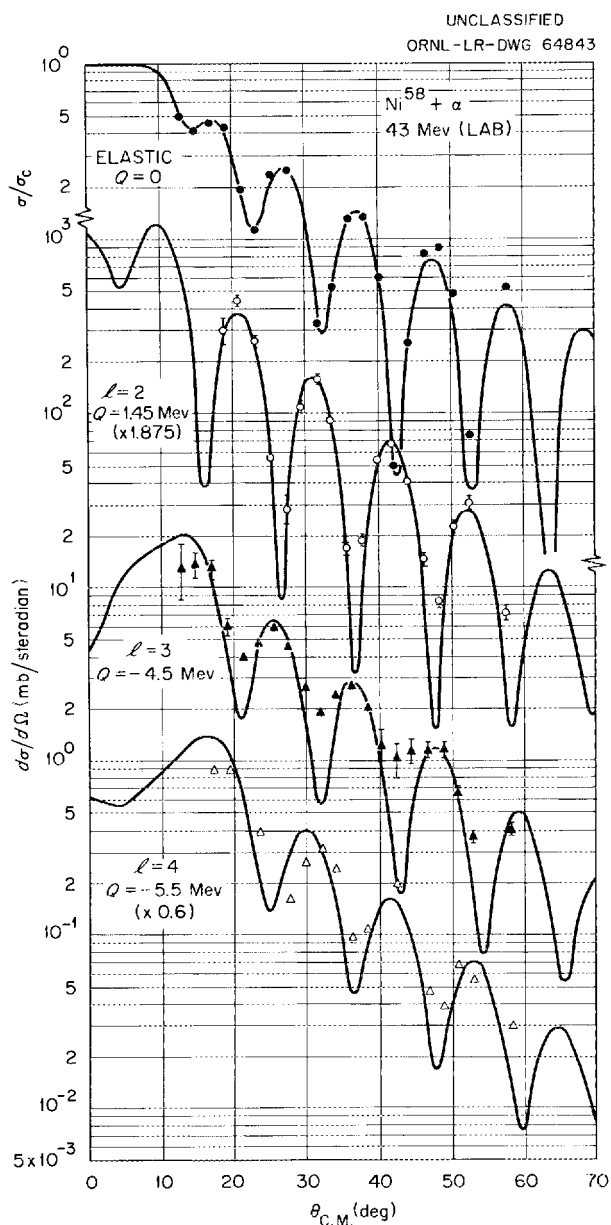


Fig. 1. Differential Cross Sections for 43-MeV Alpha Particles on Nickel. The theoretical curves are based upon analysis of preliminary elastic data which is extended only to 45° , and correspond to deformations of $\beta = 0.18$ ($l = 2$), 0.14 ($l = 3$), and 0.06 ($l = 4$).

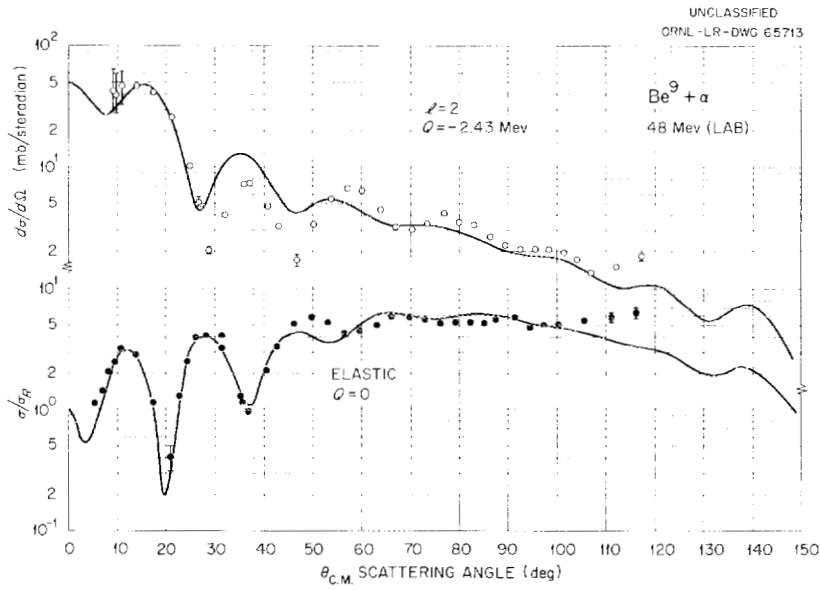


Fig. 2. Differential Cross Sections for 48-Mev Alpha Particles on Be^9 . The experimental data are from Summers-Gill, *Phys. Rev.* 109, 1591 (1958).

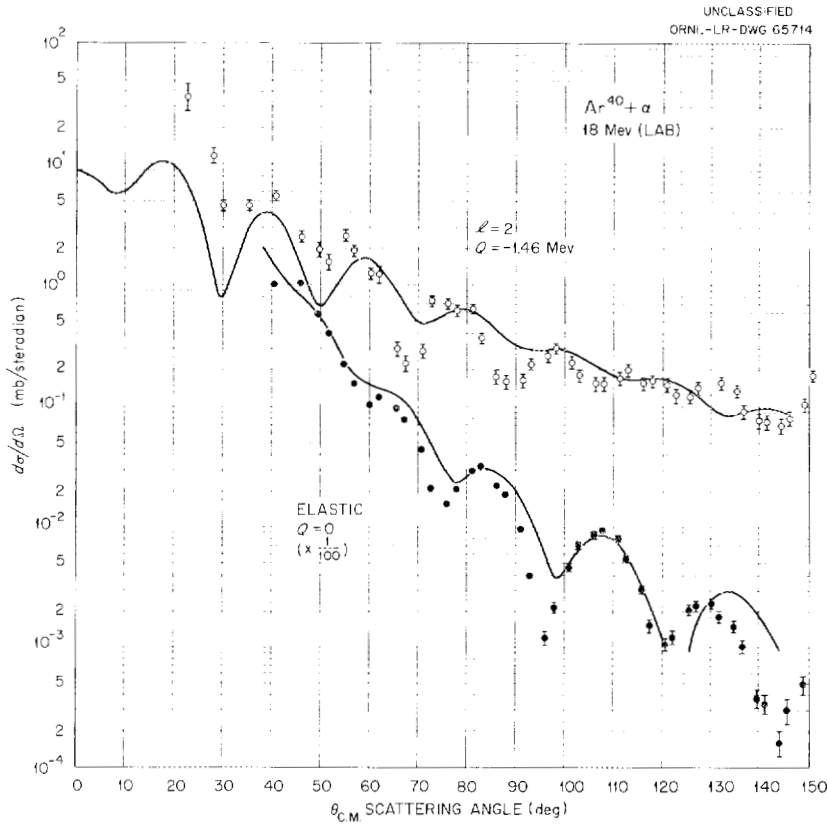


Fig. 3. Differential Cross Sections for 18-Mev Alpha Particles on Ar^{40} . The experimental data are from Seidlitz et al., *Phys. Rev.* 110, 682 (1958).

GAMMA RAYS FROM INELASTIC SCATTERING OF HIGH-ENERGY NUCLEONS¹

A. B. Clegg² G. R. Satchler

The angular distribution of de-excitation gamma rays following the inelastic scattering of high-energy nucleons by nuclei can give additional information on both nuclear structure and the

effective interaction. Formulas are derived by use of the impulse approximation; distortion effects due to elastic scattering of incident and outgoing nucleons are included. A simple case is first discussed in terms of individual scattering amplitudes; then the general formalism is introduced. The effect on the angular distribution of using polarized incident nucleons is also described and is shown to give further information about the scattering interaction.

¹Abstract of published paper: *Nuclear Phys.* 27, 431 (1961) and *Proceedings of the Rutherford Jubilee International Conference*, Manchester, England, 1961.

²Clarendon Laboratory, Oxford University, Oxford, England.

THEORETICALLY STABLE AND CONFINED PLASMA¹

T. K. Fowler

By means of a new technique capable of treating spatially inhomogeneous plasmas, it was shown previously² that certain distributions of plasma confined in a potential well are stable against a growth of space charge, as governed by the linearized Vlasov equation with only Coulomb interactions between particles. It has now been shown that these same distributions remain stable when magnetic as well as electrostatic forces

between particles are admitted. The plasmas proven stable include all those such that the equilibrium phase space distribution, f_0 , for each charge species can be written just as a function of the equilibrium energy for that species, H_0 ; and $\partial f_0 / \partial H_0 < 0$. An example is the Maxwell-Boltzmann distribution, $\exp(-H_0/T)$. The factor f_0 can depend on space through a spatially dependent potential term in H_0 . If this potential represents a net attraction for both ions and electrons, the stable systems include plasmas confined in this well. Stellar plasmas bound by their self-gravitational field are examples.

¹Abstract of Research Note to appear in *Physics of Fluids*, February 1962.

²T. K. Fowler, *Phys. Fluids* 4, 1393 (1961).

PLASMA POTENTIAL AND ENERGY DISTRIBUTIONS IN HIGH-ENERGY INJECTION MACHINES¹

T. K. Fowler M. Rankin²

Steady-state conditions have been calculated for the Oak Ridge DCX-2 and similar devices in which a plasma confined by magnetic mirrors is main-

tained continuously by the injection and trapping of energetic ions. The potential difference ϕ from plasma interior to exterior is determined in the course of the numerical solution of Fokker-Planck equations for ion and electron energy distributions. It is assumed that the only electron source is ionization of neutrals and that trapped ions are

¹Abstract of paper submitted to *Journal of Nuclear Energy: Part C, Plasma Physics-Accelerators-Thermonuclear Research*.

²Thermonuclear Division.

lost by charge exchange with neutrals and by Coulomb scattering out of the mirrors. Justification for neglecting cold ions from ionization is discussed.

The plasma potential ϕ and also, aside from normalization, the energy distributions are found to depend only on the ion injection energy and the fraction of "burnout" of the neutrals and not directly on absolute magnitudes of neutral pressure

or ion injection current. Results are combined with equations governing neutrals to obtain a new DCX-2 performance curve relating injection current to ion density achieved. Enhancement of the charge-exchange loss rate due to collisional cooling of the ions on electrons, neglected in earlier calculations, is found to increase (by a factor <2) the critical injection current required to reach densities limited only by mirror losses.

PHENOMENOLOGICAL NUCLEAR POTENTIALS FOR CLOSED-SHELL NUCLEI

J. L. Fowler

Perhaps the simplest and most straightforward example of the shell model is the case of a nucleon interacting with a doubly closed shell nucleus, such as He^4 , O^{16} , or Pb^{208} . Van der Spuy, in 1956, explained the available information on neutron scattering from He^4 in terms of the shell model. For the neutron- O^{16} system, the $d_{5/2}$ ground state, the $s_{1/2}$ excited state, and the s - and d -wave phase shifts can be fitted by the Woods-Saxon potential shown on the left side of Fig. 1.¹ The velocity dependence of the potential is included by changing the depth of the potential for the d states relative to that of the s states. This procedure for empirically fitting the data by changing the well depth, though simple, is not completely satisfactory. For example, the radial wave functions obtained are not orthogonal. A more satisfactory procedure for including the velocity dependence is by use of the reduced mass formalism

$$m = \frac{m_0}{[1 + KV(r)]}$$

The wave equation is

$$\left[p \frac{1}{2m(r)} p + V(r) \right] \psi = E\psi,$$

with, of course, $p = -i\hbar\nabla$. Now with the substitution of $M/r[\sqrt{1 + KV(r)}]$ for R (the radial wave

function), the radial part of the equation can be put in the form

$$\frac{d^2 M}{dr^2} = F(r) M(r),$$

as shown on the right side of Fig. 1. The solution of this equation is somewhat more involved than the solution of the state-dependent case. The parameters one adjusts are: the radius R , the boundary diffuseness constant A , the well depth V_0 , the constant multiplying Thomas spin-orbit term γ , and the constant K . The constants which fit all of the experimental data are given in Fig. 1. With $K = 1.25/V_0$, the effective mass at the center of the well is 44% of the real neutron mass. This is in agreement with the estimates of the effective mass in infinite nuclear matter from 40 to 60%.

In the upper part of the figure are the $2s_{1/2}$ and $1d_{5/2}$ wave functions for the velocity-dependent potential and also for the state-dependent potential. As one can see, in the former case there is relatively less probability of finding the $2s_{1/2}$ neutron near the center of the nucleus. As a matter of fact, the value of $\langle r^2 \rangle$ taken between the two states differs by 7% - in the reduced mass case (right side), $\langle r^2 \rangle = 13.4$ sq fermis; in the latter case it is 12.5 sq fermis.

Recently, Blomqvist and Wahlborn² in fitting the bound-state levels of nuclei around lead arrived at a Woods-Saxon potential with parameters as

¹J. L. Fowler, E. G. Corman, and E. C. Campbell, p 474 in *Proceedings of International Conference on Nuclear Structure* (ed. by D. A. Bromley and E. W. Vogt), University of Toronto Press, Canada, 1960.

²J. Blomqvist and S. Wahlborn, *Arkiv Fysik* 16, 545 (1960).

follows: $R = 7.52$ fermis, $A = 0.67$ fermi, $V_0 = 44$ Mev, and $\gamma = 32$ (see state-dependent equations in Fig. 1). As in the case of O^{16} , one would like to extend this analysis to the virtual-state region and calculate scattering phase shifts. At low enough energies, ~ 50 kev, scattering should be predominantly s wave, so that the s phase shift should be given by $\sin^2 \delta_{s_{1/2}} = \sigma_T / 4\pi\lambda^2$. At 50 kev, Good, Muenzer, and Nishimura³ find $\sigma_T = 9.8$ barns for Pb^{208} . Figure 2 shows the result of this measurement, interpreted in terms of phase shift. Wilenzick *et al.*⁴ have made a

phase-shift analysis of total-cross-section data up to ~ 700 kev for neutrons scattered from Pb^{208} . The figure shows the results of this analysis also; its uncertainty is at least $\pm 5^\circ$. The dashed curve is the $\delta_{s_{1/2}}$ phase shift calculated with essentially the potential of Blomqvist and Wahlborn.⁵ The solid curve shows how this phase shift is altered by a compound-nucleus s resonance at 0.5 Mev and 130 kev wide. There is good agreement with experiment.

³W. M. Good, H. Muenzer, and K. Nishimura, ORNL, private communication.

⁴R. M. Wilenzick *et al.*, *Phys. Rev.* **121**, 1150 (1961).

⁵Mary Jo Mader and J. L. Fowler, paper presented at the 71st meeting of the Tennessee Academy of Science, Martin, Tenn., November 1961. To be published in *Journal of the Tennessee Academy of Science*, April 1962.

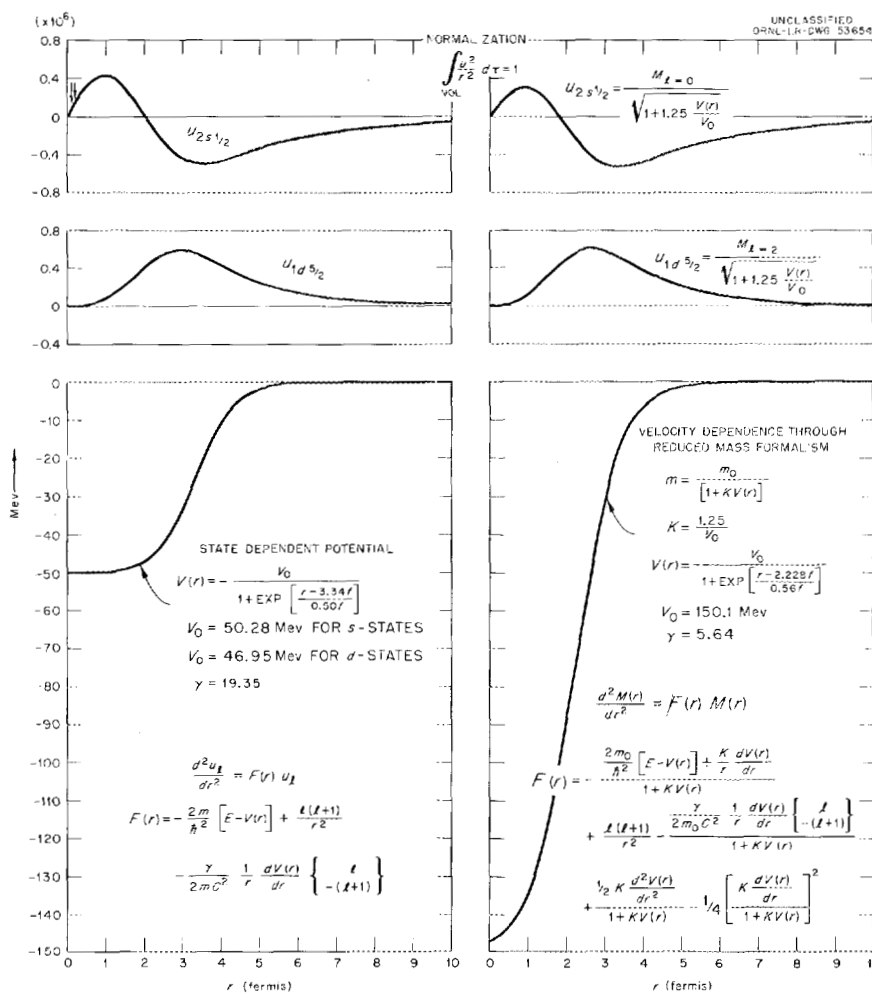


Fig. 1. Phenomenological Potentials Which Fit Single-Particle Properties in the Neutron- O^{16} System. Also shown are $2s_{1/2}$ and $1d_{5/2}$ bound-state wave functions.

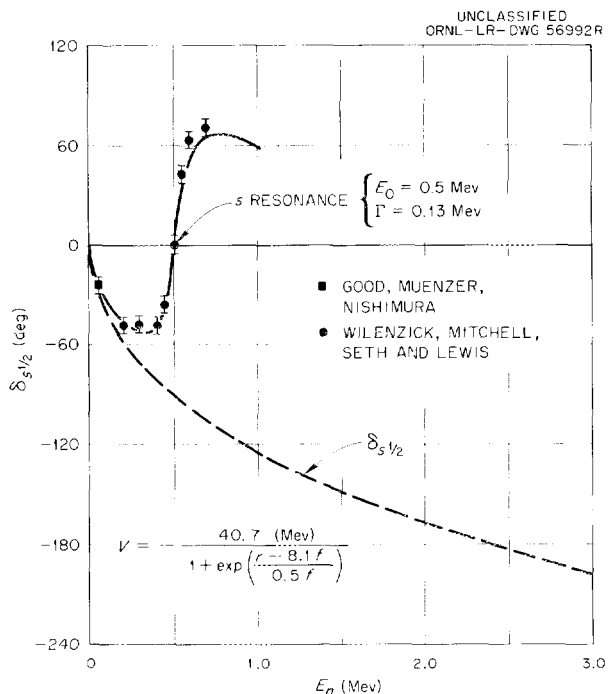


Fig. 2. Comparison with Experimental Information on Neutron Scattering of Neutrons from Pb^{208} of s -Wave Phase Shifts Calculated, with the Potential Well Indicated.

Since the $2g_{7/2}$ state in Pb^{209} has not been positively identified, and since total neutron cross sections of Pb^{208} show $J = 7/2$ levels,⁶ it is of interest to check whether these $J = 7/2$ levels could

⁶J. L. Fowler and E. C. Campbell, *Bull. Am. Phys. Soc.* 6, 251 (1961).

be associated with the $2g_{7/2}$ state. With a suitable choice of well-depth (42 Mev) and spin-orbit terms used with the Woods-Saxon potential given in Fig. 2, one finds a $2g_{9/2}$ state at -3.80 Mev and calculates the phase shifts due to a $2g_{7/2}$ state at 1.75 Mev, as shown in Fig. 3.⁵ The calculated width of a single-particle $2g_{7/2}$ state at 1.75 Mev is ~ 8 times the observed width of the $J = 7/2$ level. Furthermore, the constant multiplying the Thomas spin-orbit term, 66, is somewhat larger than usual. If the observed $7/2$ level turns out to be a g level, then its reduced width indicates that it has considerable single-particle character. Angular distributions of scattered neutrons at 1.75 Mev will be measured to determine whether the $J = 7/2$ level is in fact a g state.

This set of calculations has also been performed⁵ with the diffuseness constant = 0.5 fermi (the constant used for O^{16} plus a neutron) instead of 0.67 fermi as chosen by Blomqvist and Wahlborn.² The $4s_{1/2}$ experimental information is reproduced, but the single-particle $2g_{7/2}$ level is reduced in width by 13%.

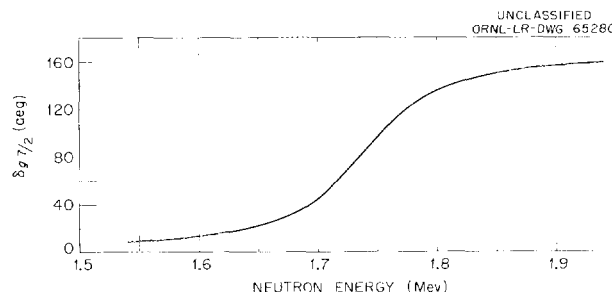


Fig. 3. Phase Shifts for $2g_{7/2}$ Waves Calculated from Potential Well Shown in Fig. 2.

CHARGED-PARTICLE NUCLEAR CROSS-SECTION COMPILATION

F. K. McGowan

M. R. Patterson¹

About 1955, a program was instituted at Los Alamos Scientific Laboratory to assemble a compilation of nuclear cross sections for charged-particle-induced reactions. The first two volumes

of this series, which covered the elements hydrogen through chromium, were published in two Los Alamos reports^{2,3} distributed in 1957 and

¹Consultant and graduate student at the University of Tennessee, Knoxville.

²Nelson Jermie and J. C. Seagrave, *Charged Particle Cross Sections: Hydrogen Through Fluorine*, LA-2014 (March 1956).

³D. B. Smith, *Charged Particle Cross Sections: Neon Through Chromium*, LA-2424 (June 1960).

1961. Near the end of 1960 this compiling program was discontinued at Los Alamos.

A group in the Physics Division at ORNL is being organized to continue the compilation of nuclear cross sections for charged particles. At present the plans are to finish the first cycle of this compilation, that is, the region from manganese through uranium. The cross sections will be presented in graphical form with the grid lines reproduced.

In many cases of early data, the only source of information is from the small figures in the journals or from reprints of the published papers. A Moseley model 2S X-Y point plotter has been modified to read data points from small published

figures. Helipot has been coupled to the cables which drive the pen and carriage of the plotter. The coordinates of the data points are displayed in analog form on an automatic dc digital voltmeter which will drive a digital recorder. The X and Y ranges may be adjusted to yield 2000 increments of information in analog form for any size figure. Data points from a figure 2×2 in. in a journal are read to an accuracy within $\pm 1\%$.

A literature search of charged-particle-induced reactions for the years 1959, 1960, and 1961 is 90% complete. Requests for either reprints, tabular data, or larger graphs of results for the elements manganese through zinc have been mailed to the authors of the published papers.

LEVEL STRUCTURE IN Ne^{22} AND Si^{30} FROM THE REACTIONS $\text{O}^{18}(\alpha, n)\text{Ne}^{21}$ AND $\text{Mg}^{26}(\alpha, n)\text{Si}^{29}$ ¹

J. K. Bair

H. B. Willard

Compound states of high excitation in Ne^{22} and Si^{30} have been observed in the total neutron yield from the reactions $\text{O}^{18}(\alpha, n)\text{Ne}^{21}$ and $\text{Mg}^{26}(\alpha, n)\text{Si}^{29}$. In the case of Ne^{22} , 25 resonances were observed, varying in width from 5 to 150 keV for alpha bombarding energies from 2.5 to 5 MeV (excitation energy from 11.7 to 13.8 MeV). The reaction $\text{Mg}^{26}(\alpha, n)\text{Si}^{29}$ showed 40 resonances

varying in width from less than 10 to 60 keV for alpha energies from 3 to 5.3 MeV (excitation energy from 13.3 to 15.3 MeV). Absolute cross sections were measured for both reactions. A statistical analysis of the area under the excitation curves gives an alpha-particle strength function $\bar{S}_\alpha = 0.05$ for $\text{O}^{18} + \alpha$ and $\bar{S}_\alpha = 0.03$ for $\text{Mg}^{26} + \alpha$. Analysis of the individual resonances in $\text{O}^{18} + \alpha$ give a value of $\langle \gamma_\alpha^2 \rangle / D = 0.04$, in agreement with the \bar{S}_α obtained by the statistical analysis.

¹Abstract of paper submitted to *Physical Review*.

ANGULAR CORRELATION STUDY OF THE $\text{Be}^9(\alpha, n)\text{C}^{12}(\gamma_{4.43})\text{C}^{12}$ REACTION¹

J. Kjellman²

T. Dazai³

J. H. Neiler

The angular correlation between the neutrons to the 4.43-MeV state and the gamma rays from this level to the ground state in C^{12} for the reaction $\text{Be}^9(\alpha, n)\text{C}^{12}$ has been studied at a bombarding energy of 3.55 MeV. The correlations were meas-

ured both in the reaction plane and in the azimuthal plane at four different neutron detector angles, $\theta_n = -10, -20, -75, \text{ and } -135^\circ$. The correlation for a certain θ_n was first measured in

²Visiting investigator from the Research Institute of National Defense, Stockholm, Sweden.

³Visiting investigator from the Tokyo Institute of Technology, Tokyo, Japan.

¹Abstract of published paper: *Nuclear Phys.* 30, 131 (1962).

the reaction plane, and the correlations in the azimuthal plane were then measured around and parallel to the symmetry axis found in the reaction

plane. The symmetry axis for the different θ_n 's was found to be $\theta_{sym} = -5, -15, -50, \text{ and } -85^\circ$ respectively.

A STUDY OF THE REACTIONS $\text{Be}^9(\text{He}^3, n)\text{C}^{11}$, $\text{Li}^7(\text{He}^3, n)\text{B}^9$, AND $\text{C}^{13}(\text{He}^3, n)\text{O}^{15}$ ¹

J. L. Duggan²P. D. Miller³R. F. Gabbard⁴

Time-of-flight techniques with time resolution capabilities of 4 μsec for neutrons have been used to study (He^3, n) reactions with the targets Be^9 , Li^7 , and C^{13} . The angular distributions of neutrons from the ground state and the first four excited states (1.99, 4.26, 4.75, and 6.50 Mev) of C^{11} have been measured for the reaction $\text{Be}^9(\text{He}^3, n)\text{C}^{11}$ at an incident He^3 energy of 2.1 Mev. Excitation functions were measured for these states for E_{He^3} from 1 to 2.7 Mev at 0 and 81.5° . For the $\text{Li}^7(\text{He}^3, n)\text{B}^9$ reaction an angular

distribution was measured at $E_{\text{He}^3} = 2.1$ Mev for the ground-state neutron group from B^9 , and the yield curve was measured for this group from 1 to 2.7 Mev at 0° . For the $\text{C}^{13}(\text{He}^3, n)\text{O}^{15}$ reaction, resolved neutron groups were seen for the ground and the third excited states (6.15 Mev) in O^{15} . Excitation functions were measured at 0 and 90° for this reaction for E_{He^3} from 1 to 2.7 Mev, and angular distributions were measured at $E_{\text{He}^3} = 2.66$ Mev. Distorted-wave calculations have been made in an attempt to describe the reactions. In general, the calculations can be made to fit the angular distributions quite well in the forward direction, but the back-angle cross sections predicted by the calculations are usually much lower than the measured values. Tentative spin and parity assignments are given for the resolved groups.

¹Abstract of paper to be submitted to *Nuclear Physics*.

²ORINS graduate fellow from LSU; now at the University of Georgia, Athens.

³On leave to AERE, Harwell, England.

⁴Summer research participant from the University of Kentucky, Lexington.

COULOMB EXCITATION OF THE FIRST 2^+ STATE OF EVEN-EVEN NUCLEI WITH $58 \leq A \leq 82$ ¹

P. H. Stelson

F. K. McGowan

The yields of gamma rays resulting from Coulomb excitation have been measured for 15 even-even nuclei of nickel, zinc, germanium, and selenium. Coulomb excitation was produced by variable-energy alpha particles (3 to 10 Mev). In favorable cases the absolute gamma-ray yields are deter-

mined to an accuracy within $\pm 4\%$. The reduced electric quadrupole transition probabilities, $B(E2)$, are generally determined to an accuracy within $\pm 9\%$. The observed values for $B(E2)$ are larger than the single-particle estimate by factors ranging from 11 for Ni^{58} to 51 for Se^{76} . The 2^+ energies and $B(E2)$ values are interpreted in terms of the collective vibrational model.

¹Abstract of paper to be published in *Nuclear Physics*.

COULOMB EXCITATION OF SECOND 2^+ STATES IN Ge^{74} , Ge^{76} , Se^{76} , Se^{78} , AND Se^{80} ¹

F. K. McGowan

P. H. Stelson

The location of a second 2^+ state has been established for five even-even nuclei by means of Coulomb excitation produced by 6-, 7-, and 8-Mev alpha particles. The relatively weak excitation of these states is detected by a coincident measurement of the cascade gamma rays. The $B(E2)$'s for decay of the second 2^+ state to the ground state by the crossover transition are rather small, being about single-particle value or a little less. For Ge^{74} , Se^{76} , and Se^{78} , the cascade/crossover

ratio for the decay of the second 2^+ state is known from radioactive decay measurements. The upper cascade $B(E2, 2' \rightarrow 2)$'s exhibit enhancements comparable to those for the lower cascade $B(E2, 2 \rightarrow 0)$'s. The ratios of the $B(E2)$'s for the decay of the first and second 2^+ states are comparable to the predictions of several collective models. The $B(M1, 2' \rightarrow 2)$ values for Ge^{74} and Se^{76} are small, being about 10^{-3} times the single-particle estimate. This result is in qualitative agreement with the collective models for vibrational excitations.

¹Abstract of paper submitted to *Physical Review*.

COULOMB EXCITATION OF LEVELS IN Se^{77} ¹

R. L. Robinson

F. K. McGowan

P. H. Stelson

An investigation has been made of the gamma rays which de-excite levels of Se^{77} that have been Coulomb-excited by means of variable-energy alpha particles (2.1 to 8.0 Mev). The energies (in keV), spins and parities, and $B(E2)_{\text{ex}}$'s (in units of $e^2 \text{ cm}^4 \times 10^{-50}$) found for the levels are: 242 ± 2 , $\frac{3}{2}^-$, and 18.2 ± 1.6 ; 248 ± 5 , $\frac{5}{2}^-$, and 0.37 ± 0.09 ; 440 ± 4 , $\frac{5}{2}^-$, and 25.9 ± 1.7 ; 515 ± 8 , $\frac{3}{2}^-$, and 1.0 ± 0.2 . New evidence for the two close-lying levels at 242 and 248 keV has been provided by coincidence studies. A comparison of the

$B(E2)_{\text{ex}}$'s with the $B(E2)_{\text{sp}}$ suggests that the 242- and 440-keV levels result from collective excitations of the ground-state configuration and that the 248- and 515-keV levels result from changes in the ground-state configuration. Besides the ground-state transitions from these Coulomb-excited levels, gamma rays with energies of 87, 161, 203, and 283 keV were observed. Excitation curves of the 87- and 161-keV transitions indicate that they cascade from the 248-keV level. From the measurements of the gamma-ray angular distributions, values for $(E2/M1)^{1/2}$ of 0.18 ± 0.03 and 0.05 ± 0.03 were obtained, respectively, for the 242-keV gamma ray and for the 203-keV gamma ray, which originates at the 440-keV level.

¹Abstract of paper to be published in *Physical Review*.

COULOMB EXCITATION OF OSMIUM AND CHROMIUM NUCLEI¹

F. K. McGowan

P. H. Stelson

R. L. Robinson

Coulomb excitation measurements have been made by alpha-particle bombardment of metallic targets enriched in the different isotopes of osmium and chromium. Some of the results obtained are summarized in Table 1. Lemberg's² value of the $B(E2)_{ex}$ for the first 2^+ state of Cr^{54} is about a factor of 2 lower than our value. The other values of $B(E2)_{ex}$ for 2^+ states listed in

Table 1 agree reasonably well with other published information. In particular, there is good agreement for Cr^{52} with the resonance fluorescence result of Ofer and Schwarzschild.³ Two states in Os^{189} at 69 and 219 kev are directly Coulomb-excited. Angular-distribution measurements lead to a unique spin assignment of $7/2$ for the 219-kev state. The 30-kev isomeric state in Os^{189} is found to be indirectly excited via the 219-kev state.

¹Abstract of published paper: *Proceedings of Conference on Electromagnetic Lifetimes and Properties of Nuclear States*, Gatlinburg, Tenn., Oct. 5-7, 1961.

²Lemberg, p 112 in *Reactions Between Complex Nuclei* (ed. by A. Zucker, F. T. Howard, and E. C. Halbert), Wiley, New York, 1960.

³S. Ofer and A. Schwarzschild, *Phys. Rev. Letters* 3, 384 (1959).

Table 1. Coulomb Excitation Measurements

Nucleus	Energy (kev)	$B(E2)_{ex}$ (cm^4)	$T_{1/2}$ (sec)
Os^{192}	206	$(2.34 \pm 0.23) \times 10^{-48}$	$(2.49 \pm 0.25) \times 10^{-10}$
Os^{190}	187	$(2.72 \pm 0.27) \times 10^{-48}$	$(3.16 \pm 0.32) \times 10^{-10}$
Os^{188}	155	$(3.19 \pm 0.32) \times 10^{-48}$	$(5.36 \pm 0.54) \times 10^{-10}$
Cr^{50}	782 ± 8	$(1.15 \pm 0.08) \times 10^{-49}$	$(8.4 \pm 0.7) \times 10^{-12}$
Cr^{52}	1433	$(7.3 \pm 0.7) \times 10^{-50}$	$(6.4 \pm 0.7) \times 10^{-13}$
Cr^{53}	565 ± 6	$(1.18 \pm 0.08) \times 10^{-50}$	
Cr^{54}	838	$(1.06 \pm 0.07) \times 10^{-49}$	$(6.4 \pm 0.5) \times 10^{-12}$

COULOMB EXCITATION OF Br^{79}

R. L. Robinson

F. K. McGowan

P. H. Stelson

As part of a program to study the properties of the low-lying levels of even-odd medium-weight nuclei by means of the Coulomb excitation process, an investigation of Br^{79} has been undertaken. For these studies a thick target of $PbBr_2$ in which the bromine had been enriched to 95.1% Br^{79} was used. To effect Coulomb excitation the target was bombarded with doubly ionized helium ions that

were obtained from the 5.5-Mv Van de Graaff generator. The beam intensity was kept below $0.02 \mu a$ to prevent damage of the target.

The gamma-ray spectra which resulted from the bombardment of $PbBr_2^{79}$ with eight different alpha-particle energies between 2.5 and 7.1 Mev have been measured with a 3×3 in. NaI scintillation spectrometer. One of these spectra is illustrated

in Fig. 1. Several of the peaks are not due to transitions of Br^{79} . The peak at 77 keV is assumed to be the K x ray of lead. Since the target contained 5% Br^{81} , the weak 0.28-Mev gamma ray is explained as the transition from the 0.278-Mev level of that nucleus.¹ Failure to observe the 0.67-Mev gamma ray in any other spectrum suggests that it is not from Br^{79} . The peak at 527 keV is too wide to be explained by a single gamma ray. Its shape indicates the presence of a weak transition on the high-energy side. The gamma-ray yields have been determined in each spectrum. Those found from the spectrum observed when the target was bombarded with 7.02-Mev alpha particles are given in Table 1.

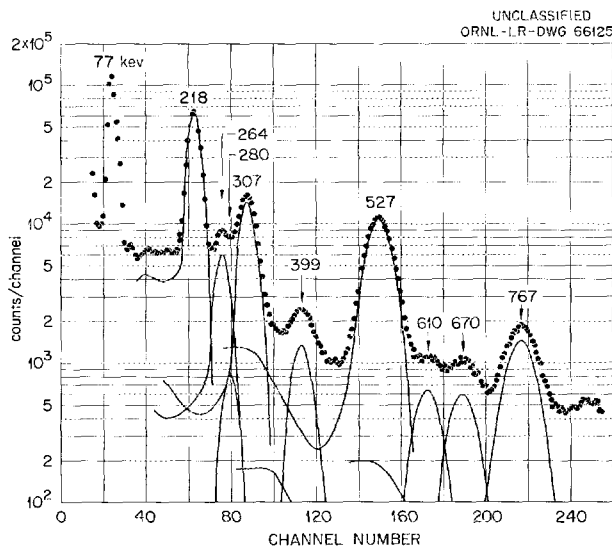


Fig. 1. Gamma-Ray Spectrum for 7.02-Mev Alpha Particles on Br^{79} .

The spectra in coincidence with the 218- and 307-keV gamma rays were also investigated for four alpha-particle energies. Representative spectra are given in Figs. 2 and 3. In Fig. 2 the peak at 218 keV is due to coincidences with Compton-scattered higher-energy gamma rays. The 545-keV gamma ray (see Fig. 2) accounts for the unusual width of the 527-keV gamma-ray peak in the singles spectra. The gamma-ray yields from the coincidence spectra obtained for 7.02-Mev alpha-particle excitation of Br^{79} are included in Table 1.

¹E. A. Wolicki, L. W. Fagg, and E. H. Geer, *Phys. Rev.* 105, 238 (1957).

Table 1. Gamma Rays per Microcoulomb of Doubly Ionized 7.02-Mev Helium Ions on a Thick Target of PbBr_2^{79}

E_γ (keV)	Singles Spectrum	Gating Gamma Ray	
		218 keV	307 keV
	$\times 10^3$	$\times 10^3$	$\times 10^3$
218 ± 2	319 ± 23		18.5 ± 2.6
264 ± 4	41 ± 6		
302 ± 5	121 ± 11		6.1 ± 0.8
307 ± 3			
308 ± 4		20.1 ± 2.7	
393 ± 6	18 ± 3	4.3 ± 1.0	
399 ± 6			
527 ± 5	244 ± 17	58 ± 6	
545 ± 7			
609 ± 9	16 ± 4		
767 ± 9	46 ± 5		

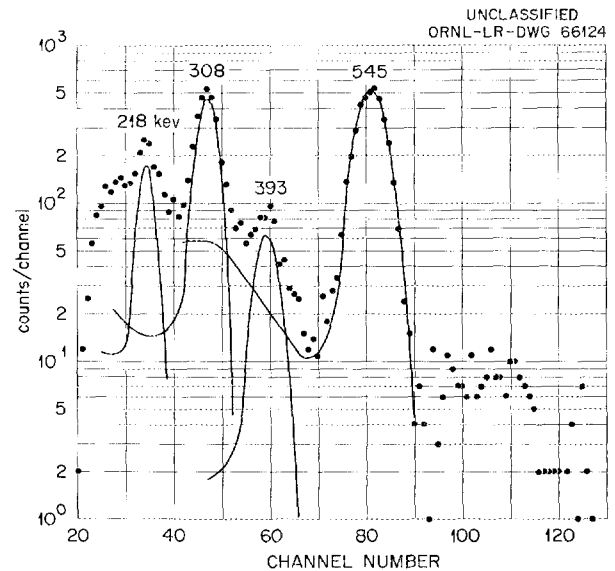


Fig. 2. Gamma-Ray Spectrum in Coincidence with the 218-keV Gamma Ray for 7.02-Mev Alpha Particles on Br^{79} .

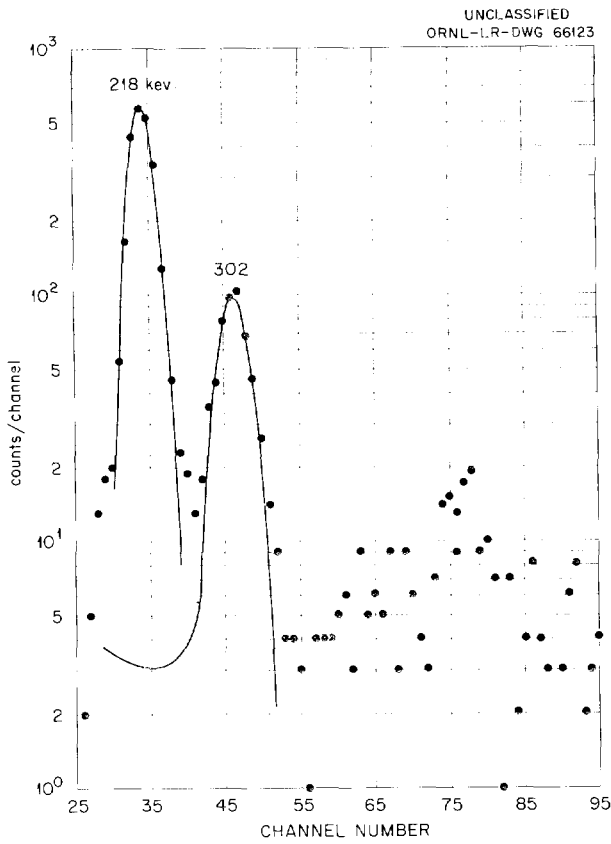


Fig. 3. Gamma-Ray Spectrum in Coincidence with the 307-keV Gamma Ray for 7.02-MeV Alpha Particles on Br⁷⁹.

Levels and transitions which are consistent with the results of the singles and coincidence spectra are shown in Fig. 4. The pair of numbers associated with each gamma ray gives its energy in keV and the relative intensity as deduced from the spectra which were observed for $E_\alpha = 7.02$ Mev. It was necessary to include three gamma rays with very similar energies between 302 and 308 keV to explain (1) the presence of peaks in this energy range in all coincidence spectra, and (2) the fact that their intensities in these coincidence spectra were insufficient to account for the intensities of the 307-keV transition in the singles spectra. The levels at 218, 264, 307, 399, and 610 keV have been suggested previously from the investigation of Kr⁷⁹.²

The decay scheme is borne out by the gamma-ray yields determined as a function of the alpha-particle energy. These are given in Figs. 5 (for the single spectra) and 6 (for the coincidence spectra). The yields of the 218- and 307-keV gamma rays in Fig. 5 have been corrected for the yields of gamma rays which cascade into the levels of these energies. The curves in Figs. 5 and 6 give the energy dependence predicted for the yields of gamma rays from electric quadrupole (E2) Coulomb-excited levels with energies ΔE above the ground state of Br⁷⁹. The agreement between the experimental points and the theoretical curves indicates that each of the levels in Fig. 4 is populated by the E2 Coulomb excitation process. Since the ground-state spin of Br⁷⁹ is $\frac{3}{2}$,³ the possible spins of the excited levels are $\frac{1}{2}$, $\frac{3}{2}$, $\frac{5}{2}$, or $\frac{7}{2}$. Their parities are the same as the parity of the ground state.

From the gamma-ray yields the reduced E2 transition probabilities for excitation, $B(E2)_{ex}$'s, have been determined. The procedure for this determination has been described previously.⁴ The $B(E2)_{ex}$'s are given in Table 2. They have not been corrected for the internal-electron conversion of the transitions. The $B(E2)_{ex}$ for the 218-keV level is higher than the value of $(2.3 \pm 0.5) \times 10^{-50} e^2 cm^4$ reported by Wolicki *et al.*¹ The prediction of the single-particle model for the reduced transition probability is $1.01 \times 10^{-50} e^2 cm^4$. This was obtained from the equation

$$B(E2)_{sp} = \frac{5e^2}{4\pi} \left| \frac{3}{5} R_0^2 \right|^2,$$

with $R_0 = 1.2 \times 10^{-13} A^{1/3} cm$. Thus the $B(E2)_{ex}$'s of the Br⁷⁹ levels range from 0.07 to 12 times that predicted by the single-particle

²S. Thulin, J. Moreau, and H. Atterling, *Arkiv Fysik* 8, 229 (1954).

³S. Tolansky, *Proc. Roy. Soc. (London)* 136, 585 (1932).

⁴F. K. McGowan and P. H. Stelson, *Phys. Rev.* 116, 154 (1959).

model. If all the strong $E2$ transitions from the low-lying levels of Br^{79} have been detected, the sum of the $B(E2)_{\text{ex}}$'s, which is $27.7 \times 10^{-50} e^2 \text{cm}^4$, should be approximately the same as that of the $B(E2)_{\text{ex}}$'s of the first 2^+ levels of neighboring even-even nuclei.⁵ Values of $(38.5 \text{ and } 28.3) \times 10^{-50} e^2 \text{cm}^4$ have been reported for the $B(E2)_{\text{ex}}$'s of the first 2^+ levels in Se^{78} and Se^{80} (ref 6) respectively. The four levels with large $B(E2)_{\text{ex}}$'s may result from the coupling of the first core excitation to the odd nucleon in its lowest state.⁷

Table 2. The $B(E2)_{\text{ex}}$'s of Levels in Br^{79}

Level (kev)	$B(E2)_{\text{ex}}/e^2 (\text{cm}^4)$
	$\times 10^{-50}$
218	3.91 ± 0.33
264	0.069 ± 0.006
307	0.209 ± 0.018
399	0.37 ± 0.05
526	9.7 ± 0.9
610	1.49 ± 0.23
765	11.9 ± 1.1

⁵K. Alder et al., *Revs. Modern Phys.* 28, 432 (1956).

⁶P. H. Stelson and F. K. McGowan, *Phys. Div. Ann. Progr. Rept. Feb. 10, 1960*, ORNL-2910, p 12.

⁷A. de-Shalit, *Phys. Rev.* 122, 1530 (1961).

UNCLASSIFIED
ORNL-LR-DWG 66122

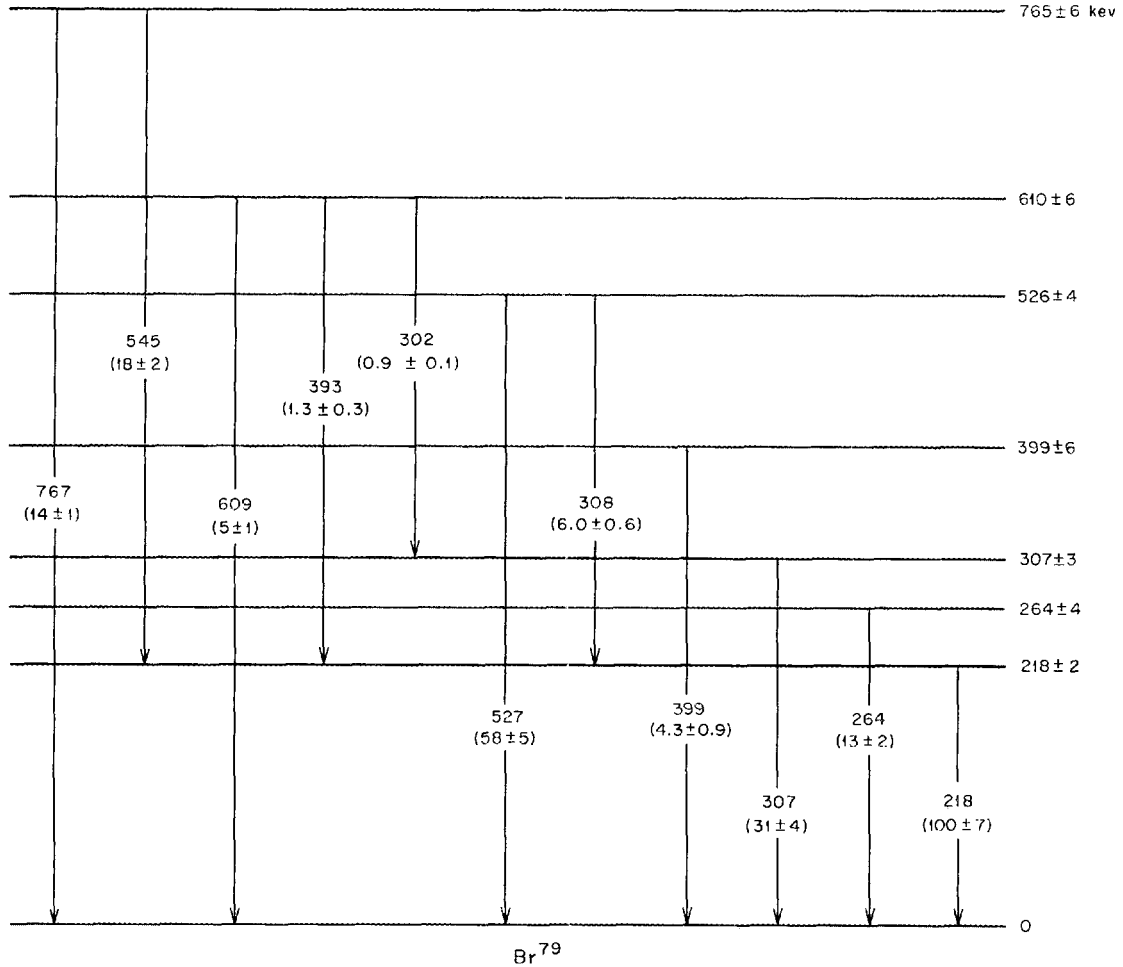


Fig. 4. Energy-Level Diagram of Br^{79} .

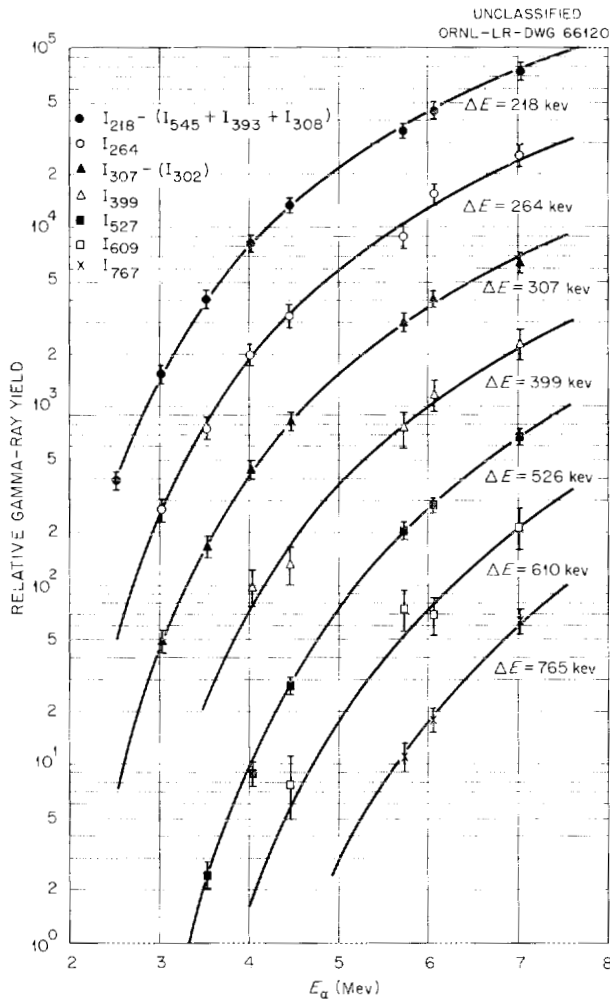


Fig. 5. Relative Yields of the Gamma Rays in the Singles Spectra as a Function of the Alpha-Particle Energy.

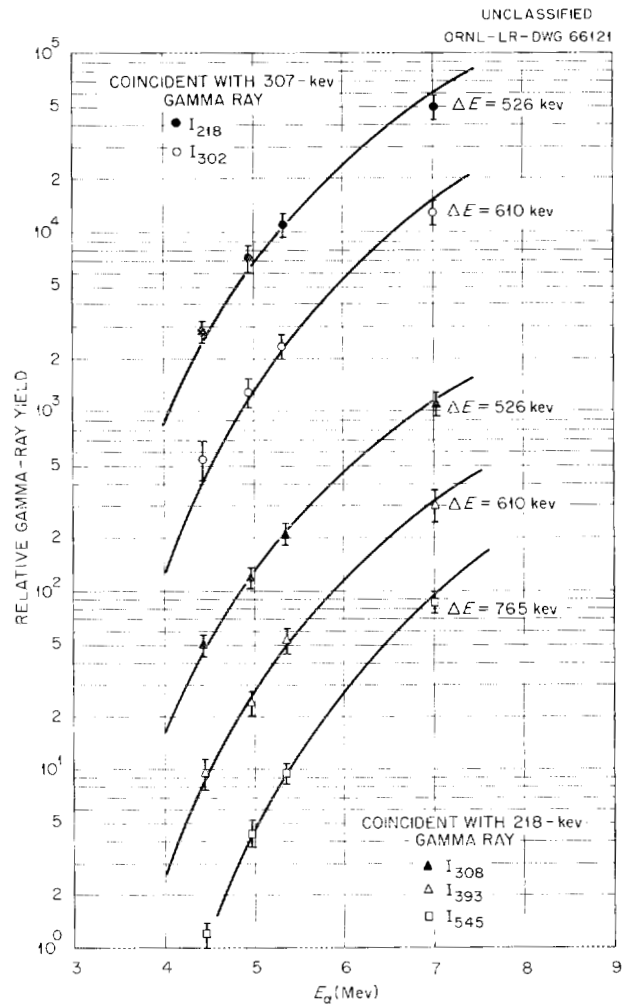


Fig. 6. Relative Yields of the Gamma Rays in the Coincidence Spectra as a Function of the Alpha-Particle Energy.

DECAY OF $Rh^{102} \rightarrow Ru^{102}$ ¹

F. K. McGowan

P. H. Stelson

The singles and coincident spectra of the gamma rays from the decay of Rh^{102} , which was produced by the (p,n) reaction on ruthenium containing 97.2% Ru^{102} , have been measured with scintillation spectrometers. The energies (in keV) of the gamma

rays are: 415 ± 4 , 475 ± 5 , 630 ± 6 , 695 ± 7 , 745 ± 8 , 765 ± 8 , 1050 ± 10 , 1105 ± 8 , 1110 ± 11 , 1365 ± 10 , 1565 ± 13 , 1795 ± 15 , 2040 ± 14 , and 511 (annihilation gamma rays). Spins of the levels in Ru^{102} which are consistent with the directional angular correlations of gamma-ray cascades are: $475 (2^+)$, $1105 (2^+ \text{ and } 4^+, \text{ doublet})$, $1525 (3)$, $1840 (0^+)$, $1870 (3, 4, 5, \text{ or } 6)$, $2040 (2^+)$, $2220 (3)$,

¹Abstract of published paper: *Phys. Rev.* 123, 2131 (1961).

and 2270 (?). A value of $E2/M1 \geq 225$ for the 630-keV transition ($2^+ \rightarrow 2^+$) was deduced from the composite correlation of the 630-475-keV cascades. The branching ratio of cascade to crossover transitions from the decay of the second 2^+ state is 1.5 ± 0.3 . The intensity of the annihilation

gamma rays decays with a half-life of 205 ± 10 days. Gamma-ray spectra have been measured as a function of time for 920 days, and a change in the relative population of the states is observed. From this we infer the existence of a long-lived isomeric state in Rh^{102} .

NUCLEAR LEVELS OF Ge^{74} ¹

E. Eichler² G. D. O'Kelley² R. L. Robinson
 J. A. Marinsky³ N. R. Johnson²

Radiations from Ga^{74} and As^{74} were studied by using gamma-ray scintillation spectrometry. By means of coincidence techniques, previous level

assignments were confirmed and new states were indicated. A decay scheme consistent with most of the results is proposed with levels at 0.598, 1.20, 1.47, 1.71, 2.18, 2.53, 2.95, 3.05, 3.16, 3.33, 3.41, 3.57, and 3.83 MeV. A measurement of the angular correlation between the 0.598- and 0.60-MeV gamma rays confirmed the predominantly E2 character of the 0.60-MeV ($2^+ \rightarrow 2^+$) transition.

¹Abstract of paper submitted to *Nuclear Physics*.

²Chemistry Division.

³Permanent address, Department of Chemistry, University of Buffalo, Buffalo, N. Y.

DECAY OF Cs^{132}

R. L. Robinson N. R. Johnson¹ E. Eichler¹

A previous investigation of 2.3-hr I^{132} by this group established many of the properties for nine low-lying levels in Xe^{132} .² Since a study of Cs^{132} , which decays principally by orbital electron capture to Xe^{132} , would be expected to disclose additional information about levels of Xe^{132} , the gamma rays of Cs^{132} have been investigated. Such information provides a test of the numerous nuclear models that have been proposed to explain the properties of low-lying levels of even-even nuclei. It should also prove useful in the future development of these models.

For this study, Cs^{132} was prepared with the Oak Ridge 86-in. cyclotron by means of the nuclear

reaction $\text{Cs}^{133}(p, pn)\text{Cs}^{132}$. The gamma rays were detected with 3×3 in. NaI crystals which were coupled to 6363 Du Mont photomultiplier tubes. The singles gamma-ray spectra are illustrated in Figs. 1 and 2. Intensities of the Cs^{132} gamma rays obtained from these spectra are given in Table 1. No values are listed for the 1.21- and 1.84-MeV gamma rays, since the peaks at these energies in the figures can be explained as a result of summing in the crystal of lower-energy gamma rays. Half-lives of the gamma rays shown in Fig. 1 were determined from the analysis of four spectra taken with the same Cs^{132} source over a period of two months. From the intense 669-keV gamma ray the half-life of Cs^{132} was computed to be 6.54 ± 0.06 days. Half-lives of > 170 days and 26 days found for the 795- and 883-keV gamma rays, respectively, demonstrate that they are not transitions of Cs^{132} .

¹Chemistry Division.

²R. L. Robinson, E. Eichler, and N. R. Johnson, *Phys. Rev.* **122**, 1863 (1961).

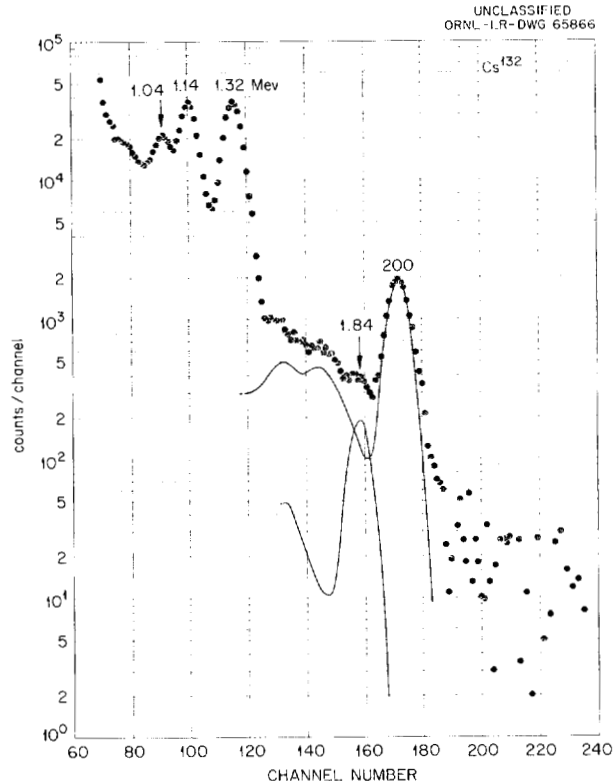
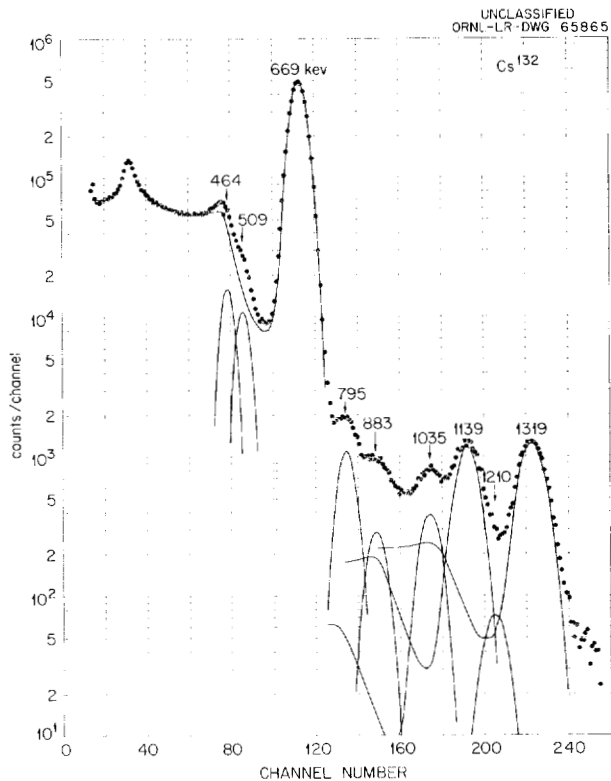


Fig. 1. Low-Energy Gamma-Ray Spectrum for Cs¹³².

Fig. 2. High-Energy Gamma-Ray Spectrum for Cs¹³².

Table 1. Cs¹³² Gamma-Ray Energies and Relative Intensities
 Intensities are normalized to a value of 1000 for the 669-keV gamma-ray intensity

E_γ (keV)	Singles Spectrum	Spectra in Coincidence with Gamma Rays of Energies (keV):				
		464	509 ^a	669	1139	1319
464 ± 5	21 ± 5					
509 ± 7	17 ± 4			18 ± 4	0.1	0.31 ± 0.16 ^b
569 ± 6		2.7 ± 0.8				
631 ± 8			5.6 ± 1.9	8.5 ± 1.8		
669 ± 4	1000 ± 30		16 ± 5		4.8 ± 0.8	4.6 ± 1.5
1035 ± 12	1.6 ± 0.3					
1139 ± 11	5.2 ± 0.5			5.0 ± 0.6		
1304 ± 20	6.5 ± 0.6		0.58 ± 0.20			
1319 ± 10	6.5 ± 0.6			6.6 ± 0.7		
2000 ± 30	0.53 ± 0.06					

^aThe intensities are for the spectrum taken with $\theta = 90^\circ$.

^bThis gamma ray is believed to result from coincidences with the 1304-keV gamma ray.

The spectra in coincidence with the 464-, 509-, 669-, 1139-, and 1319-keV gamma rays have also been investigated. Representative coincidence spectra are shown in Figs. 3 and 4. The intensities of the gamma rays in these spectra have been determined and are included in Table 1. Corrections have been applied for the angular correlation between the coincident gamma rays when known and for coincidences with Compton-scattered higher-energy gamma rays. The spectrum in coincidence with the 509-keV gamma ray was observed for $\theta = 90^\circ$ (illustrated in Fig. 4) and $\theta = 180^\circ$, where θ is the angle between the two detectors. In the spectrum with $\theta = 180^\circ$, a strong peak was present at 0.51 MeV. From this peak the intensity of annihilation radiation was estimated to be 11 ± 5 in the units used in Table 1.

Energy levels and transitions of Xe^{132} and Ba^{132} compatible with the results in Table 1 are illustrated in Fig. 5. Levels of Xe^{132} with energies less than 2.0 MeV populated by I^{132} have been included in Fig. 5 for comparison. The numbers shown with each gamma ray in this figure give its energy and relative intensity. Those shown for the decay by electron capture, positron emission, and beta-ray emission are the relative intensities and $\log ft$ values. Since the 464- and 1035-keV gamma rays are not in coincidence with

the 669-keV gamma ray and since their half-lives associate them with the decay of Cs^{132} , they are given as transitions in Ba^{132} . The energy of the 464-keV transition is consistent with the energy value of 470 ± 7 keV established for the first 2^+ level of Ba^{132} by the Coulomb excitation studies of Fagg.³

From earlier gamma-gamma angular correlation studies, the 1300- and 1988-keV levels have each been assigned spin 2.⁴ A remeasurement of the correlation of the 1139-669-keV gamma-ray cascade has yielded values of $+0.134 \pm 0.019$ and $+0.049 \pm 0.033$ for the A_2 and A_4 correlation coefficients. These are in good agreement with the spin sequences $2(98\% D + 2\% Q)2(Q)0$ and $3(92\% D + 8\% Q)2(Q)0$. The angular correlation of the 569-464-keV gamma-ray cascade has also been measured. The coefficients A_2 and A_4 are

³L. W. Fagg, *Phys. Rev.* **109**, 100 (1958).

⁴R. L. Robinson, E. Eichler, and N. R. Johnson, *Phys. Div. Ann. Progr. Rept.* Feb. 10, 1961, ORNL-3085, p. 61.

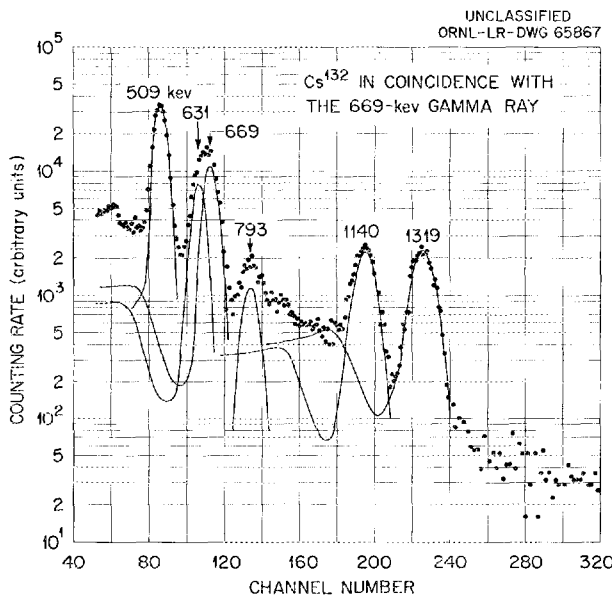


Fig. 3. Cesium-132 Gamma-Ray Spectrum with a 110-keV Window Set at 669 keV.

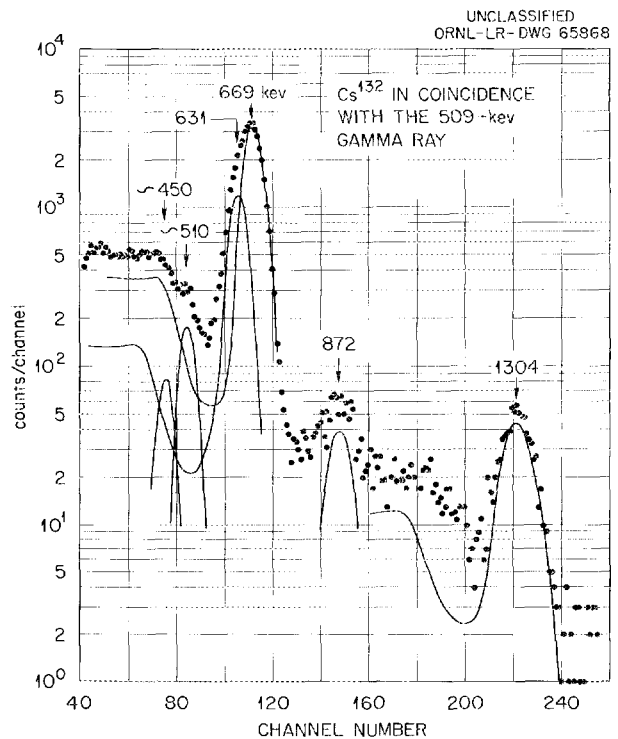


Fig. 4. Cesium-132 Gamma-Ray Spectrum with a 35-keV Window Set at 509 keV.

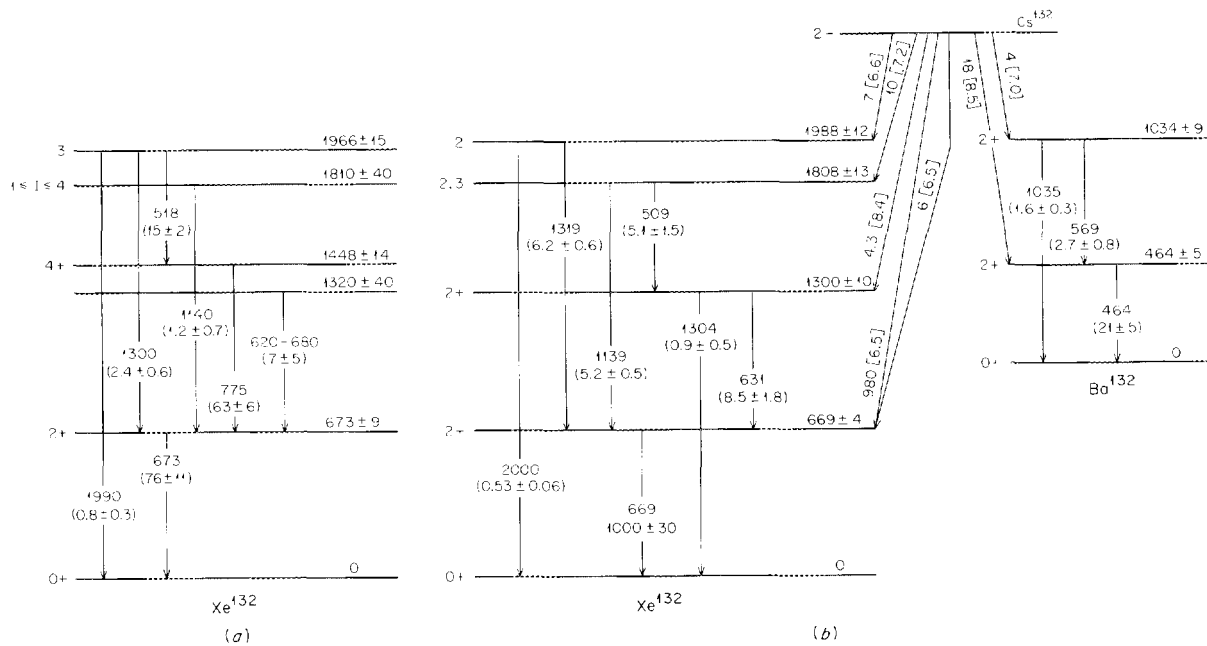


Fig. 5. Levels and Transitions of (a) Xe^{132} Below 2.0 Mev Which Occur in the Decay of I^{132} as Reported in Reference 2 and of (b) Xe^{132} and Ba^{132} Which Occur in the Decay of Cs^{132} .

-0.069 ± 0.045 and $+0.39 \pm 0.09$. They establish that the spin of the 1034-keV level in Ba^{132} is 2 and that the ratio of quadrupole to dipole radiation for the 569-keV transition is ≥ 200 .

The lowest three levels of Xe^{132} excited by Cs^{132} are probably the same as those observed at 673 ± 9 , 1320 ± 40 , and 1810 ± 40 keV in our study of I^{132} .² Although the energies of the (1988 ± 12) -keV level populated by Cs^{132} and the (1966 ± 15) -keV level populated by I^{132} are in reasonable agreement, their spins and the branching ratios of gamma rays from them are different. Therefore it is concluded that they are not the same level. The 1300-keV level in Xe^{132} and the 1034-keV level in Ba^{132} are assigned even parity, since many even-even nuclei are known to have second 2^+ levels with energies approximately twice those of the first 2^+ levels. These parity assignments are supported by the typically predominant quadrupole character of the transitions between the second and first spin-2 levels. The strong $E2$ character of these transitions is attributed to the collective behavior of the nuclei.

From the ratio of decay by electron capture and by positron emission to the 669-keV level, the

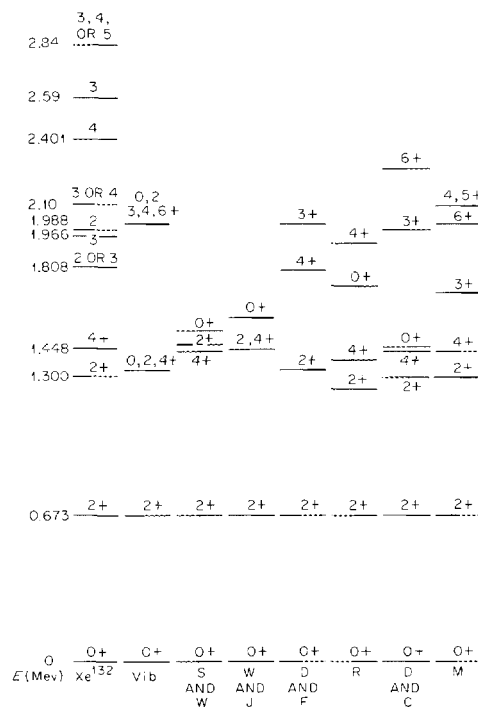


Fig. 6. Comparison of the Xe^{132} Levels with Levels Predicted by Several Nuclear Models.

total energy separation between Cs^{132} and Xe^{132} was estimated to be 2.15 Mev.⁵ For this energy the log ft values for decay to the Xe^{132} levels have been determined. They are given in Fig. 5. The log ft values of the beta-ray groups in this figure are for an energy separation of 1.2 Mev between Cs^{132} and Ba^{132} . This energy has been predicted by beta-decay energy systematics.⁶

We have previously compared the levels of Xe^{132} populated by I^{132} with levels predicted by various

⁵E. Feenberg and G. Trigg, *Revs. Modern Phys.* **22**, 399 (1950).

⁶*Nuclear Data Sheets*, National Academy of Sciences - National Research Council, Washington, D.C.

nuclear models.² These predicted levels are reproduced in Fig. 6 along with the Xe^{132} levels found in the studies of Cs^{132} and I^{132} . As pointed out before, the second 2^+ and first 4^+ levels can be explained by all models except that of Davydov and Filippov.⁷ However, none of the models can account for all four levels between 1.8 and 2.1 Mev. It is possible that a low-lying 0^+ level as predicted by several of the models does exist. Neither Cs^{132} nor I^{132} would be expected to populate a level of this spin with sufficient intensity to be observed.

⁷A. S. Davydov and G. F. Filippov, *Nuclear Phys.* **8**, 237 (1958).

TOTAL NEUTRON CROSS SECTION OF Pb^{208} ¹

J. L. Fowler

E. C. Campbell

Measurements are reported on the total neutron cross section of isotopically enriched Pb^{208} (99.75%) for neutron energy in the range 720 to 1890 keV with an energy spread of about 3 keV. In this region at least 85 resonances are observed, of which 24 are analyzed to give tentative spin

assignments and reduced widths. For the $J = \frac{5}{2}$ levels at 723 and 821 keV, the reduced-width estimates furnish evidence that these are even-parity resonances. Differential cross sections of normal lead measured with a 50-keV energy spread at 1.2, 2.2, and 3.2 MeV were used in estimating the in-scattering correction for the total cross-section data and are included in this paper.

¹Abstract of paper submitted to *Physical Review*.

CHANNEL ANALYSIS OF FISSION: INTERPRETATION OF SOME EXPERIMENTAL DATA ACCORDING TO THE THEORY OF A. BOHR¹

R. W. Lamphere

Formulas have been derived to facilitate the comparison of experimentally measured fission-fragment angular distributions with theory. They are of especial significance near threshold and have been applied to neutron-induced fission of U^{234} , one of the few cases where adequate data exist which make possible the identification of individual fission channels.

Neutron emission competes strongly with fission and can affect the angular distribution of the fragments. Although exact calculations of the nature of this effect cannot now be carried out, a very rough approximative treatment has been made based on a modified Hauser-Feshbach² (H-F) analysis.

¹A. Bohr, *Proc. Intern. Conf. Peaceful Uses Atomic Energy, Geneva, 1955*, paper P/911.

²W. Hauser and H. Feshbach, *Phys. Rev.* **87**, 366 (1952).

Through the courtesy of F. G. Perey,³ machine calculations have been done by use of the nonlocal optical potentials of Perey and Buck (P-B potentials)⁴ for cases of fast neutrons of 500, 850, and 1050 kev incident on a U²³⁴ target, and for 1600-kev neutrons incident on Th²³². In addition to total, scattering, and reaction cross sections, these calculations yielded the scattering matrices. From these, neutron transmission factors $T(l)$, which contain a spin-orbit force dependence, were calculated and were used in the computation of fission channel strengths.

Individual fission bands are identified, and estimates are made for the approximate strengths of the levels within each band for fission of U²³⁴ bombarded with neutrons of 500, 850, and 1050 kev. At 1050 kev, however, the fragment angular distribution differs markedly from what would be expected on the basis of theory. For Th²³² bombarded by 1600-kev neutrons, the analysis of Willets and Chase,⁵ assigning fission predominantly to the $K = \frac{3}{2}$ -band, is confirmed.

Differential Cross Sections for Formation of States in Spheroidally Deformed Compound Nuclei

The following is a derivation of relations pertinent to the analysis of fission-fragment angular distributions, particularly for fission of heavy nuclei near threshold. It has been specialized to the case of neutrons incident on even-even targets. A similar development was made by Hittmair,⁶ who, however, expressed his results somewhat differently. The notation used herein is that of Blatt and Weisskopf⁷ except where noted.

Consider a plane wave of monoenergetic neutrons (neglect the neutron spin for the moment) traveling in the z direction to be incident on a heavy, fissionable even-even target:

$$e^{ikz} = \sum_l A_l(r) Y_{l,0}(\theta) \xrightarrow{kr \gg l} \frac{1}{kr} \sum_l \sqrt{\pi(2l+1)} i^{l+1} \left\{ \exp \left[-i \left(kr - \frac{l\pi}{2} \right) \right] - \exp \left[+i \left(kr - \frac{l\pi}{2} \right) \right] \right\} Y_{l,0}(\theta) \equiv \frac{1}{kr} \sum_l \sqrt{\pi(2l+1)} i^{l+1} \{A - B\}. \quad (1)$$

The outgoing wave is modified by the target, so for $kr \gg l$,

$$\psi_r = \frac{1}{kr} \sum_l \sqrt{\pi(2l+1)} i^{l+1} \{A - \eta_l B\}. \quad (2)$$

³Neutron Physics Division.

⁴F. G. Perey and B. Buck, to be published in *Nuclear Physics*.

⁵L. Willets and D. M. Chase, *Phys. Rev.* **103**, 1292 (1956).

⁶O. Hittmair, *Nuclear Phys.* **18**, 346 (1960).

⁷J. M. Blatt and V. F. Weisskopf, *Theoretical Nuclear Physics*, Wiley, New York, 1952.

Let total incident flux be $N = v = \hbar/m\lambda$ and the absorbed flux be N_r . Then

$$\sigma_r(\theta) = \frac{m\lambda}{\hbar} N_r(\theta), \quad (3)$$

$$\begin{aligned} d\sigma(\theta) &= -\frac{m\lambda}{\hbar} \frac{\hbar}{2mi} \left(\frac{\partial\psi_r}{\partial r} \psi_r^* - \frac{\partial\psi_r^*}{\partial r} \psi_r \right) r^2 d\Omega \\ &= \pi\lambda^2 \sum_l (2l+1) |Y_{l,0}(\theta)|^2 (1 - |\eta_l|^2) d\Omega. \end{aligned} \quad (4)$$

Interference terms between different l waves will not arise because parity considerations and the fact that there is only one channel spin, $J = 1/2$, are sufficient to ensure that not more than a single channel contributes to the formation of any compound state ($I\pi$). Interference effects are absent from the fission-fragment angular distribution but for a different reason. Each fission exit channel, as defined here by what a simple ion chamber measures, contains many modes (spin, mass ratios, excitation) which are summed over, and this washes out the effects of interference from decay of close-lying $I\pi$ levels and leads to the symmetry about 90° which is characteristic of fission-fragment angular distributions. Consequently, only even powers of the Legendre polynomials ($x = \text{even integers}$) occur in the expansion. Since neither beam nor target is polarized there will be no ϕ dependence:

$$d\sigma(\theta = 0) = \frac{\lambda^2}{4} \sum_l (2l+1)^2 (1 - |\eta_l|^2) d\Omega, \quad (5)$$

$$d\sigma(\theta = \theta') = \frac{\lambda^2}{4} \sum_{lm} (2l+1)^2 (1 - |\eta_l|^2) D_{MK}^I(\alpha, \theta', \gamma) D_{MK}^{*I}(\alpha, \theta', \gamma), \quad (6)$$

where α, θ', γ are Euler angles between space-fixed and body-fixed coordinates, the new body-fixed set is taken as fixed in the deformed compound nucleus, with z' coinciding with the major symmetry axis, and K is the projection of the total angular momentum, l , on this axis. Henceforth, drop the primes on θ and consider θ to mean the angle between neutron beam and the major symmetry axis of the compound nucleus, or in accordance with the theory of Bohr, the angle between beam and fission fragments in those cases where fission follows neutron capture.

Now

$$D_{MK}^{*I} = (-1)^{M-K} D_{-M-K}^I,$$

so

$$D^*D = (-1)^{M-K} D_{-M, -K}^I D_{MK}^I = (-1)^{M-K} \sum_x C_{-MM0}^{Ix} C_{-KK0}^{Ix} P_x(\cos \theta).$$

Therefore

$$d\sigma(\theta) = \frac{\chi^2}{4} \sum_{lMx} \int (2l+1)^2 (-1)^{M-K} (1 - |\eta_l|^2) C_{-KK0}^{llx} C_{-MM0}^{llx} P_x, \quad (7)$$

$$\begin{aligned} 1 - |\eta_l|^2 &= 1 - |S_l|^2 = \sum_{ljm} |\langle IKM(R)jlm0 \rangle|^2 \\ &= \sum_{lJM} |\langle IK(R)jJ \rangle C_{m0M}^{jJl}|^2 \\ &= \sum_{ljm} \frac{2l+1}{(2j+1)(2l+1)} T(l) |C_{m0m}^{jJl}|^2. \end{aligned} \quad (8)$$

The existence of neutron spin has been neglected so far in order to simplify the calculations. Its effect has been introduced in an admittedly somewhat ad hoc manner in Eq. (8). If the spin functions had been carried along in the work preceding Eq. (8), it would have been more cumbersome, but the end result would not have been affected.

$$\sigma(\theta) = \frac{\chi^2}{4} \sum_m \frac{(2l+1)(2l+1)}{2j+1} (-1)^{-K} T(l) C_{-KK0}^{llx} P_x \sum_m (-1)^m |C_{m0m}^{jJl}|^2 C_{-mm0}^{llx}. \quad (9)$$

Now

$$\sum_m (-1)^m C_{m0m}^{jJl} C_{m0m}^{jJ'l} C_{-mm0}^{llx} = (-1)^{x-j} (2l+1) C_{000}^{ll'x} W(l'l, xj). \quad (10)$$

The proof of this is rather lengthy, so it is not included here. By use of this relation,

$$\sigma(\theta) = \frac{\chi^2}{4} \sum_m (-1)^{x-j-K} (2l+1)^2 \frac{2l+1}{2j+1} T(l) C_{000}^{llx} W(l'l, xj) C_{-KK0}^{llx} P_x. \quad (11)$$

Now

$$\begin{aligned} C_{000}^{ll'x} W(l'l, xj) &= [(2l+1)(2l'+1)(2l+1)^2]^{-1/2} \bar{Z}(ll'l, jx) \\ &= (-1)^{1/2(x+l'-l)} Z(ll'l, jx) [(2l+1)(2l'+1)(2l+1)^2]^{-1/2}. \end{aligned} \quad (12)$$

For $l = l'$ and $x \equiv$ even integers only, as for neutrons on an even-even target,

$$\sigma(\theta)_K = \frac{\chi^2}{8} (-1)^{-K-1/2} \sum_{xll} (-1)^{x/2} (2l+1) T(l) C_{-KK0}^{llx} Z(lll, \frac{1}{2}x) P_x, \quad (13)$$

where

$$j = \text{channel spin} = \vec{s} + \vec{i} = \frac{1}{2} + 0,$$

$s =$ neutron spin,

$i =$ target spin.

In the above the differential cross section has been expressed in terms of the ordinary Z functions as tabulated, for example, in a previous report;⁸ but the Huby⁹ correction for phase has been included as shown above, so that results are invariant under time reversal. Define

$$W(KI) \equiv \frac{(-1)^{-K-1/2}}{2} \sum_x (-1)^{x/2} C_{-KK0}^{Ix} Z(III, \frac{1}{2}x) P_x(\cos \theta). \quad (14)$$

Then

$$\sigma(\theta)_{K\pi} = \frac{\kappa^2}{4} \sum_I (2I+1) T(I) W(KI), \quad (15)$$

which is the cross section for formation of a compound nucleus with total angular momentum I , component K along its major symmetry axis, and with that axis oriented at an angle θ with the neutron beam. The significance to fission is that it provides a framework within which any analysis of fragment angular distribution made according to the picture of A. Bohr must fit. It cannot by itself predict the angular distribution because:

1. Some of the compound nuclei will decay by neutron or gamma emission, so that the population decaying by fission will, in general, differ from the formation population of states $W(KI\pi)$ given by the formula.

2. The availability and the spacing of the $(K\pi)$ bands near the saddle point are not yet known.

The framework offered by the theory may, however, serve to tie together experimental data from fission near threshold and inelastic scattering of neutrons. Define

$$T_I^\pm \equiv T(I, I = I \pm \frac{1}{2}).$$

⁸L. C. Biedenharn, *Tables of the Racah Coefficients*, ORNL-1098 (Mar. 21, 1952).

⁹R. Huby, *Proc. Phys. Soc. (London)* **67A**, 1103 (1954).

The expressions pertinent to fission-fragment analyses near threshold may be written in an easily remembered array which brings out the significance of the quantities with clarity:

$$\begin{aligned}
 \sigma(\theta)_{1/2-} &= \frac{\chi^2}{2} \left[T_1^- W(\frac{1}{2} \frac{1}{2}) + 2T_1^+ W(\frac{1}{2} \frac{3}{2}) + 3T_3^- W(\frac{1}{2} \frac{5}{2}) + 4T_3^+ W(\frac{1}{2} \frac{7}{2}) + \dots \right], \\
 \sigma(\theta)_{1/2+} &= \frac{\chi^2}{2} \left[T_0 W(\frac{1}{2} \frac{1}{2}) + 2T_2^- W(\frac{1}{2} \frac{3}{2}) + 3T_2^+ W(\frac{1}{2} \frac{5}{2}) + \dots \right], \\
 \sigma(\theta)_{3/2-} &= \frac{\chi^2}{2} \left[\phantom{T_0 W(\frac{1}{2} \frac{1}{2})} 2T_1^+ W(\frac{3}{2} \frac{3}{2}) + 3T_3^- W(\frac{3}{2} \frac{5}{2}) + 4T_3^+ W(\frac{3}{2} \frac{7}{2}) + \dots \right], \\
 \sigma(\theta)_{3/2+} &= \frac{\chi^2}{2} \left[\phantom{T_0 W(\frac{1}{2} \frac{1}{2})} 2T_2^- W(\frac{3}{2} \frac{3}{2}) + 3T_2^+ W(\frac{3}{2} \frac{5}{2}) + \dots \right], \\
 \sigma(\theta)_{5/2-} &= \frac{\chi^2}{2} \left[\phantom{T_0 W(\frac{1}{2} \frac{1}{2})} \phantom{2T_1^+ W(\frac{3}{2} \frac{3}{2})} 3T_3^- W(\frac{5}{2} \frac{5}{2}) + 4T_3^+ W(\frac{5}{2} \frac{7}{2}) + \dots \right], \\
 \sigma(\theta)_{5/2+} &= \frac{\chi^2}{2} \left[\phantom{T_0 W(\frac{1}{2} \frac{1}{2})} \phantom{2T_1^+ W(\frac{3}{2} \frac{3}{2})} \phantom{3T_3^- W(\frac{5}{2} \frac{5}{2})} 3T_2^+ W(\frac{5}{2} \frac{5}{2}) + \dots \right], \\
 \sigma(\theta)_{7/2-} &= \frac{\chi^2}{2} \left[\phantom{T_0 W(\frac{1}{2} \frac{1}{2})} \phantom{2T_1^+ W(\frac{3}{2} \frac{3}{2})} \phantom{3T_3^- W(\frac{5}{2} \frac{5}{2})} \phantom{4T_3^+ W(\frac{5}{2} \frac{7}{2})} 4T_3^+ W(\frac{7}{2} \frac{7}{2}) + \dots \right].
 \end{aligned} \tag{16}$$

The $W(KI)$ are positive definite functions of θ symmetrical about 90° . They have been tabulated up to $K = I = \frac{7}{2}$ by Nancy M. Dismuke.¹⁰ Figure 1 shows a plot of these functions, and numerical values are listed in Table 1. They may also be expressed simply in terms of the Legendre polynomials, $P_x(\cos \theta)$; the more common ones are given in Table 2.

The $W(KI)$ as defined above are automatically normalized so that

$$\int_{-1}^{+1} W(KI) d(\cos \theta) = 1.$$

Consequently, the integrated cross section becomes

$$\sigma_{K\pi} = \pi\chi^2 [\text{sum of coefficients of the } W(KI)], \tag{17}$$

$$\sigma_r \equiv \text{reaction cross section} = \sigma_{1/2+} + \sigma_{1/2-} = \frac{\pi\chi^2}{2} \sum_{II} (2I+1)T(II)\delta(II \frac{1}{2} = \Lambda) = \pi\chi^2 \sum_I (2I+1)\tau_I, \tag{18}$$

where

$$\tau_I \equiv \sum_l \frac{(2I+1)T(II)}{(2j+1)(2I+1)} = \left[\frac{(I+1)T_I^+ + IT_I^-}{2I+1} \right]_{j=1/2}.$$

¹⁰Mathematics Panel.

UNCLASSIFIED
CRNL-LR-DWG 56677

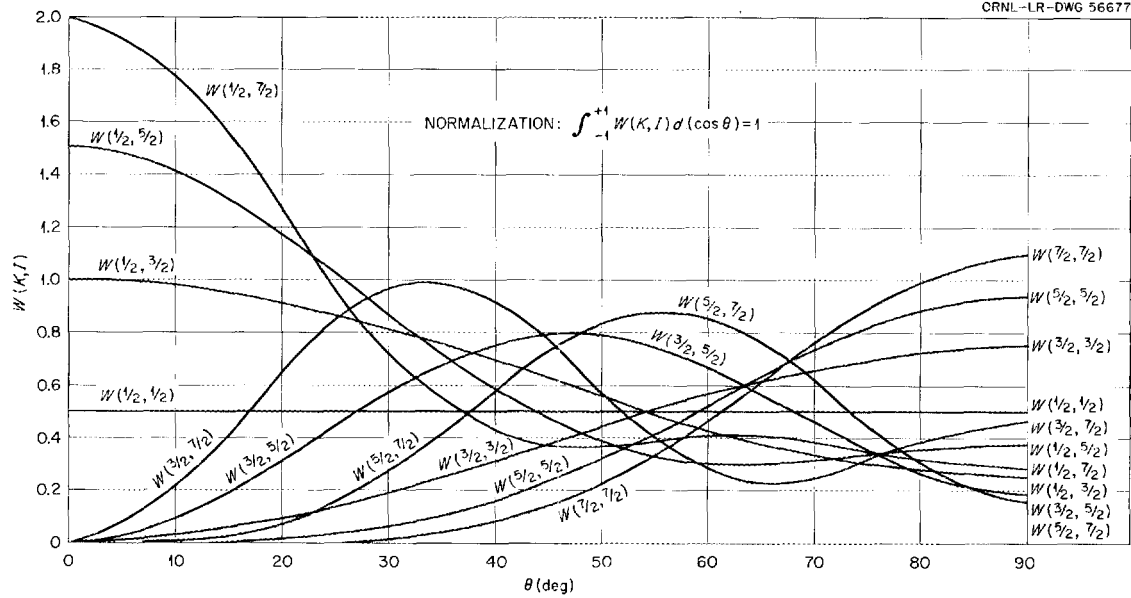


Fig. 1. Theoretical Fission Fragment Angular Distributions for Fission Through Pure Rotational States, $W(K,I)$.

Table 1. Values of $W(KI)$

$$W(KI) \equiv \frac{(-1)^{-K-1/2}}{2} \sum_x (-1)^{x/2} C_{-KK0}^{Ix} Z(III, \frac{1}{2}x) P_x(\cos \theta)$$

θ (deg)	$W(\frac{1}{2}, \frac{3}{2})$	$W(\frac{1}{2}, \frac{5}{2})$	$W(\frac{1}{2}, \frac{7}{2})$	$W(\frac{3}{2}, \frac{3}{2})$	$W(\frac{3}{2}, \frac{5}{2})$	$W(\frac{3}{2}, \frac{7}{2})$	$W(\frac{5}{2}, \frac{5}{2})$	$W(\frac{5}{2}, \frac{7}{2})$	$W(\frac{7}{2}, \frac{7}{2})$
0	1.0000	1.5000	2.0000	0	0	0	0	0	0
5	0.9943	1.4773	1.9437	0.0057	0.0226	0.0560	0.0001	0.0003	0.0000
10	0.9774	1.4112	1.7839	0.0226	0.0879	0.2111	0.0009	0.0050	0.0000
15	0.9498	1.3075	1.5464	0.0502	0.1883	0.4296	0.0042	0.0236	0.0003
20	0.9123	1.1747	1.2679	0.0877	0.3124	0.6622	0.0128	0.0682	0.0018
25	0.8660	1.0240	0.9882	0.1340	0.4461	0.8573	0.0299	0.1483	0.0062
30	0.8125	0.8672	0.7427	0.1875	0.5742	0.9741	0.0586	0.2661	0.0171
35	0.7533	0.7160	0.5555	0.2467	0.6826	0.9915	0.1015	0.4141	0.0389
40	0.6901	0.5806	0.4360	0.3099	0.7594	0.9123	0.1600	0.5745	0.0771
45	0.6250	0.4688	0.3789	0.3750	0.7969	0.7617	0.2344	0.7227	0.1367
50	0.5599	0.3852	0.3678	0.4401	0.7920	0.5793	0.3228	0.8319	0.2210
55	0.4967	0.3312	0.3805	0.5033	0.7467	0.4086	0.4221	0.8804	0.3304
60	0.4375	0.3047	0.3960	0.5625	0.6680	0.2856	0.5273	0.8569	0.4614
65	0.3840	0.3009	0.3991	0.6160	0.5666	0.2303	0.6325	0.7644	0.6061
70	0.3377	0.3129	0.3839	0.6623	0.4561	0.2423	0.7310	0.6206	0.7531

Table 1 (continued)

θ (deg)	$w(\frac{1}{2} \frac{3}{2})$	$w(\frac{1}{2} \frac{5}{2})$	$w(\frac{1}{2} \frac{7}{2})$	$w(\frac{3}{2} \frac{3}{2})$	$w(\frac{3}{2} \frac{5}{2})$	$w(\frac{3}{2} \frac{7}{2})$	$w(\frac{5}{2} \frac{5}{2})$	$w(\frac{5}{2} \frac{7}{2})$	$w(\frac{7}{2} \frac{7}{2})$
75	0.3002	0.3332	0.3540	0.6998	0.3507	0.3028	0.8161	0.4549	0.8883
80	0.2726	0.3541	0.3191	0.7274	0.2641	0.3810	0.8818	0.3021	0.9978
85	0.2557	0.3694	0.2916	0.7443	0.2073	0.4446	0.9233	0.1948	1.0690
90	0.2500	0.3750	0.2813	0.7500	0.1875	0.4688	0.9375	0.1563	1.0938

Note: $w(\frac{1}{2} \frac{1}{2}) = 0.5000$ for all angles; the values of $w(KI)$ are automatically normalized by its definition so that

$$\int_{-1}^{+1} w(KI) d(\cos \theta) = 1.$$

Table 2. The $w(KI)$ Expressed in Terms of the Legendre Polynomials

$w(KI)$	Coefficients of:			
	P_0	P_2	P_4	P_6
$(\frac{1}{2} \frac{1}{2})$	0.5			
$(\frac{1}{2} \frac{3}{2})$	0.5	0.5		
$(\frac{3}{2} \frac{3}{2})$	0.5	-0.5		
$(\frac{1}{2} \frac{5}{2})$	0.5	0.571	0.429	
$(\frac{3}{2} \frac{5}{2})$	0.5	0.144	-0.644	
$(\frac{1}{2} \frac{7}{2})$	0.5	0.597	0.527	0.379
$(\frac{3}{2} \frac{7}{2})$	0.5	0.359	-0.176	-0.682

A partial cross section, $\sigma(\theta)_{K\pi}$, would yield a fission-fragment angular distribution directly only in the unlikely situation where all capture decayed by fission through the $K\pi$ band. Then the coefficients of the $w(KI)$ would give the relative probabilities of fission via the various $KI\pi$ levels within that band. The same would still be true if two bands differing in parity coexisted. If two bands of like parity coexisted, then the coefficients of the $w(KI)$ of this common parity would equal the sum of the fission probabilities through the two levels of the same $I\pi$.

Actually, however, neutron emission always competes very strongly ($\Gamma_n/\Gamma_f > 1$ usually) with fission and with unequal strengths for different levels. Accurate predictions of fission-fragment angular distribution could, in theory, be made, providing the locations of the first few K bands near saddle point were known, along with the signs of the decoupling constants in the case of $K = \frac{1}{2}$ bands, and if all levels open to neutron decay in the target nucleus were known, as well as the laws governing decay to such

levels. Turning the thing about, experimental measurements of some of these things may yield information about others. For example, fission measurements may provide information on inelastic neutron scattering processes as well as on the relative locations of $K\pi$ bands in highly distorted nuclei.

Decay by Neutron Emission

Neutron emission, by proceeding more readily from some compound states than from others, causes the relative level strengths for fission through a given K band to differ from the relative formation strengths. To make an estimate of this effect, a modified H-F analysis was carried out to find the relative ease of neutron emission, $P(I\pi)$, from each of the $I\pi$ levels. This was done for incident neutron energies of 500, 850, and 1050 keV:

$$P(I\pi) = \sum_{i'} T_{l'}(E_n')$$

summed over all possible decay channels and, hopefully, to all available levels, i' , in U^{234} . Table 3 shows these levels. Note that four have been postulated on the basis of nuclear systematics. Decay to these four is comparatively light, due either to their high spin or energy. Decay to the ground state gives rise to the so-called compound-elastic scattering. The $P(I\pi)$ include this, of course, but the relative probabilities of decay to the ground level were also separated out and used with other factors to compute σ_{ce} , the compound-elastic scattering cross section, a quantity which cannot be directly measured. The $P(I\pi)$ obtained are listed in Table 4. The transmission factors used in their computation were those of Emmerich,¹¹ since the P-B factors are not yet available as functions of energy. For lack of better information, decays to the beta and octupole levels were treated on the same basis as decays to the ground-state band.

¹¹W. S. Emmerich, Westinghouse Research Laboratory Report 6-94511-R19, Pittsburgh, Pa. (Apr. 29, 1958).

Table 3. Energy Levels in U^{234} ^a

E (keV)	K	$I\pi$	Type of Level	Comments
984	0	5-	Octupole	Postulated
952	0	4+	Beta	Postulated
858	0	3-	Octupole	Postulated
854	0	2+	Beta	Observed
812	0	0+	Beta	Observed
788	0	1-	Octupole	Observed
290	0	6+	Ground-state rotational band	Postulated
143	0	4+	Ground-state rotational band	Observed
43	0	2+	Ground-state rotational band	Observed
0	0	0+	Ground-state rotational band	

^aC. J. Gallagher, Jr., and T. D. Thomas, *Nuclear Phys.* 14, 1 (1959).

Table 4. Summation of Transmission Factors for Neutron Emission in Compound Nucleus U^{235} to the Levels Listed in Table 3

Compound Level, $l\pi$	$P(l\pi)$		
	$E_n = 500$ kev	$E_n = 850$ kev	$E_n = 1050$ kev
$\frac{1}{2}+$	0.39	0.97	2.04
$\frac{3}{2}+$	0.46	1.10	2.78
$\frac{5}{2}+$	0.49	1.06	2.81
$\frac{1}{2}-$	1.56	2.33	3.61
$\frac{3}{2}-$	2.35	3.50	5.54
$\frac{5}{2}-$	2.25	3.45	5.67
$\frac{7}{2}-$	2.15	3.47	5.75

Table 5 lists a few nuclear parameters determined from a combination of theory and the experimentally evaluated fission cross sections. The capture cross section is assumed to be negligible, compared with fission and neutron emission. The total, scattering, and reaction cross sections have been obtained from machine calculations by use of the P-B potentials through the courtesy of F. G. Perey. The cross section for neutron emission, σ_n , is taken as the difference between this reaction cross section, σ_r , and the measured fission cross section, σ_f . Then Γ_n/Γ_f , a function pertinent to fission-fragment angular distribution analysis, is simply σ_n/σ_f . This is, of course, the average over all channels; σ_{c_e} is obtained, then, from the H-F analysis and σ_n .

One can see by inspection that neutron emission should not appreciably affect the *relative* intensities of fission from levels within any given K band except the two $\frac{1}{2}$ bands. For these, the ground-state levels would be expected to have higher Γ_f/Γ_n than the average over all levels within the band. At 500 kev, since $(\overline{\Gamma_n/\Gamma_f}) \gg 1$, the individual $\Gamma_f/\Gamma_t = \Gamma_f/(\Gamma_f + \Gamma_n)$ may be taken as very nearly in inverse proportion to the $P(l\pi)$. At the higher energies a somewhat more accurate but still quite approximate method is used.

The major sources of error are believed to lie with the assumptions. For example, it has been assumed that inelastic neutron scattering probability is independent of whether the daughter state is a ground-state rotational level or one built on a beta or octupole vibration. Intuitively, one would not expect this to be so.

Decay by Fission

The Bohr theory states that near saddle point most of the energy of excitation is tied up in potential energy of deformation, and that under these circumstances a level structure made up of various K bands

Table 5. Cross Sections Deduced from Calculations for Neutrons Incident on U²³⁴

Capture cross sections assumed negligible

	E_n (kev)		
	500	850	1050
σ_t	9.80	8.05	7.51
σ_s	5.52	4.18	3.68
σ_r	4.27	3.87	3.83
σ_f	0.50	1.26	1.10
σ_n	3.77	2.61	2.73
σ_{ce}	1.41	0.62	0.43
Γ_n/Γ_f	7.5	2.1	2.5

should exist and fission should take place via these bands. Measurements of fragment angular distribution can lead to assignments of the relative ordering of these bands and in some simple cases to a crude estimate of the level strengths within the bands. Such studies are meaningful only near threshold, since the number of bands contributing to fission increases rapidly with increasing excitation, and one is forced to use statistical methods. Many such statistical analyses have been made, but almost no individual channel analyses of the type undertaken here. There is one other such analysis known, that of Willets and Chase.¹² Experimental data are very difficult to obtain, due to not only the low fission cross sections, but also to the lower yield of monoenergetic neutrons available at the lower energies and finer resolutions required. Following is part of an analysis of U²³⁴ data taken at ORNL. Figure 2 is a plot of that data.

Analysis at 500 kev. - At this energy, maximum sidewise peaking occurs with a fragment intensity ratio $\sigma_f(0/90)^\circ = 0.50$. The fission cross section is 0.5 barn, and the calculated reaction cross section is given in Table 5 as 4.27 barns. Substituting the transmission factors obtained from the P-B scattering matrix in Eqs. (16), one obtains

$$\begin{aligned}
 \sigma(\theta)_{1/2+} &= 0.210 \left[0.361 w(\frac{1}{2} \frac{1}{2}) + 0.154 w(\frac{1}{2} \frac{3}{2}) + 0.207 w(\frac{1}{2} \frac{5}{2}) \right], \\
 \sigma(\theta)_{1/2-} &= 0.210 \left[0.702 w(\frac{1}{2} \frac{1}{2}) + 1.620 w(\frac{1}{2} \frac{3}{2}) + 0.054 w(\frac{1}{2} \frac{5}{2}) + 0.128 w(\frac{1}{2} \frac{7}{2}) \right], \\
 \sigma(\theta)_{3/2+} &= 0.210 \left[\begin{array}{c} 0.154 w(\frac{3}{2} \frac{3}{2}) + 0.207 w(\frac{3}{2} \frac{5}{2}) \end{array} \right] \\
 \sigma(\theta)_{3/2-} &= 0.210 \left[\begin{array}{c} 1.620 w(\frac{3}{2} \frac{3}{2}) + 0.054 w(\frac{3}{2} \frac{5}{2}) + 0.128 w(\frac{3}{2} \frac{7}{2}) \end{array} \right].
 \end{aligned}
 \tag{19}$$

¹²L. Willets and D. M. Chase, *Phys. Rev.* 103, 1292 (1956).

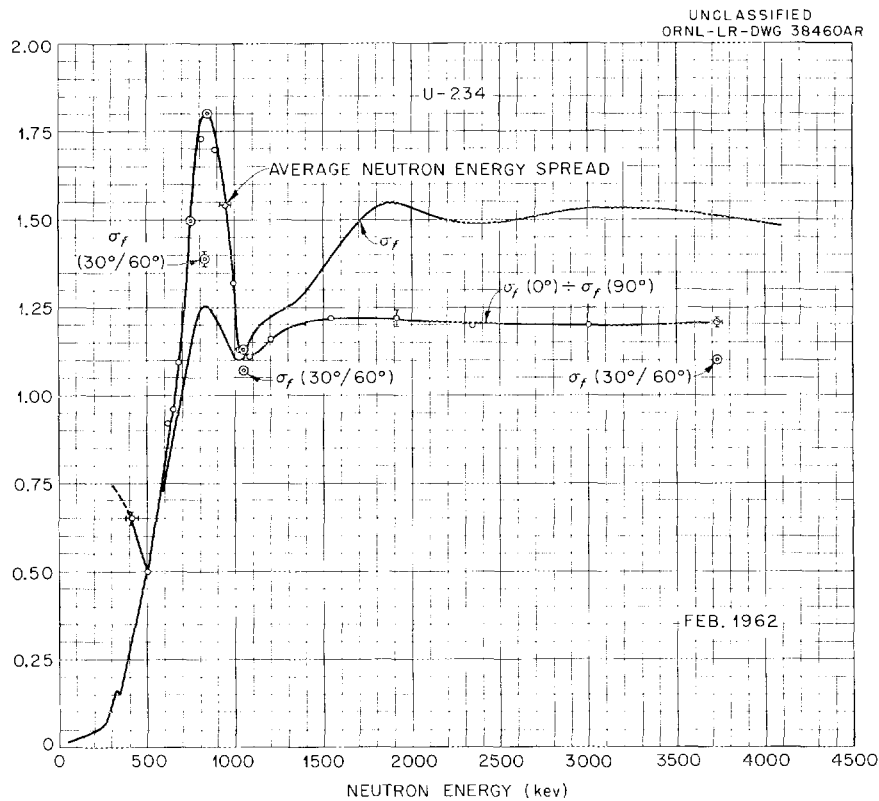


Fig. 2. Total Neutron-Induced Fission Cross Section and Ratio of Fragments Emitted at 0° to Those Emitted at 90° to Neutron Beam Axis. The three points so marked are the ratios of fragments emitted at 30° to those emitted at 60°.

The sidewise peaking makes it clear that a $K = \frac{3}{2}$ band is dominant, bands with higher K having too small formation cross sections. The value $\sigma_{3/2+} = 0.48$ barn with $(\bar{\Gamma}_f/\bar{\Gamma}_i) = 0.117$ is clearly ruled out, and the value of $\sigma_{3/2-}$ is 2.38 barns, so clearly the $\frac{3}{2}-$ band is the major contributor. Since there is some fragment intensity at 0°, either one must say that the K axis is wobbling (K a poor quantum number) or that a $\frac{1}{2}$ band is also contributing. The trend away from sidewise peaking below 500 keV favors the latter hypothesis, and one is obliged to select the $\frac{1}{2}+$ band, because if it were the $\frac{1}{2}-$ it would override the $\frac{3}{2}-$ and lead to forward peaking. Therefore, for U^{235} near saddle point, the lowest band is a $\frac{1}{2}+$ and the next one is a $\frac{3}{2}-$, and the spacing is probably of the order of a few hundred kilovolts.

Individual level weights within the bands can be estimated only roughly. Neglect the two higher members of the $\frac{3}{2}-$ band, modify the $\frac{1}{2}+$ band by dividing each term by the appropriate $P(I\pi)$, and reduce the two upper terms a bit more by factors of 0.93 and 0.82, respectively, to take into account the loss in available energy for deformation due to the higher rotation (assuming a decoupling constant of zero and $\hbar^2/2d = 5$ keV at saddle point). This last correction is very crude, as in reality the decoupling constant would be expected to be either ± 1 , but there is no way to predict which. Then one can write

$$\sigma(\theta) = aW(\frac{1}{2} \frac{1}{2}) + bW(\frac{1}{2} \frac{3}{2}) + cW(\frac{3}{2} \frac{3}{2}) + dW(\frac{1}{2} \frac{5}{2}), \quad (20)$$

$$b = \left(\frac{0.154}{0.361} \right) \left(\frac{0.39}{0.46} \right) (0.93) a = 0.336a, \quad (21)$$

$$d = \left(\frac{0.207}{0.361} \right) \left(\frac{0.39}{0.49} \right) (0.82) a = 0.374a, \quad (22)$$

$$a + b + c + d = \sigma_f / 2\pi = 0.0796. \quad (23)$$

From Table 1,

$$\sigma_f \left(\frac{0}{90} \right)^\circ = \frac{1}{2} = \frac{0.5a + b + 0c + 1.5d}{0.5a + 0.25b + 0.75c + 0.375d}. \quad (24)$$

These four simultaneous equations yield

$$\sigma_f(\theta, 500 \text{ kev}) = 0.210 \left[0.234 W(\frac{3}{2} \frac{3}{2}) + 0.085 W(\frac{1}{2} \frac{1}{2}) + 0.029 W(\frac{1}{2} \frac{3}{2}) + 0.032 W(\frac{1}{2} \frac{5}{2}) \right]. \quad (25)$$

For those individual levels which fission, this gives $\gamma(I\pi) \equiv (\Gamma_f / \Gamma_t) (I\pi)$ of

$$\begin{aligned} \gamma(\frac{1}{2}+) &= 0.085 \div 0.361 = 0.24, \\ \gamma(\frac{3}{2}+) &= 0.029 \div 0.154 = 0.19, \\ \gamma(\frac{5}{2}+) &= 0.032 \div 0.207 = 0.15, \\ \gamma(\frac{3}{2}-) &= 0.234 \div 1.620 = 0.14, \\ \overline{(\Gamma_f / \Gamma_t)} &= 0.50 \div 4.27 = 0.12 \quad \text{for all fission.} \end{aligned} \quad (26)$$

These results look reasonable, bearing in mind that other compound levels decay only by neutron emission. Alternatively, one could neglect the possible presence of the last two levels and make a two-parameter fit to the data wholly from experiment, but this involves an assumption at greater variance with theory than the one chosen in arriving at Eqs. (21) and (22).

Analysis at 850 kev. — At this energy a least-squares fit to the fragment distribution, after correction for angular resolution, is

$$\sigma_f(\theta) = 0.100 [(1 \pm 0.0054)P_0 + (0.419 \pm 0.011)P_2 + (0.083 + 0.017)P_4] \quad \text{barns/steradian,}$$

and a force fit through all four points

$$\sigma_f(\theta) = 0.100 [P_0 + 0.426 P_2 + 0.079 P_4 - 0.018 P_6]. \quad (27)$$

The drastic change to strong forward and backward peaking points unambiguously to the appearance of a $K = \frac{1}{2}-$ band. Substituting transmission factors obtained from the P-B potential into Eq. (16) gives, for the three bands contributing to fission at this energy,

$$\begin{aligned}\sigma(\theta)_{1/2+} &= 0.125 \left[0.431 w(\frac{1}{2} \frac{1}{2}) + 0.342 w(\frac{1}{2} \frac{3}{2}) + 0.474 w(\frac{1}{2} \frac{5}{2}) \right] , \\ \sigma(\theta)_{1/2-} &= 0.125 \left[0.871 w(\frac{1}{2} \frac{1}{2}) + 1.894 w(\frac{1}{2} \frac{3}{2}) + 0.303 w(\frac{1}{2} \frac{5}{2}) + 0.632 w(\frac{1}{2} \frac{7}{2}) \right] , \\ \sigma(\theta)_{3/2-} &= 0.125 \left[1.894 w(\frac{3}{2} \frac{3}{2}) + 0.303 w(\frac{3}{2} \frac{5}{2}) + 0.632 w(\frac{3}{2} \frac{7}{2}) \right] .\end{aligned}\quad (28)$$

Write

$$\sigma_f(\theta) = a w(\frac{1}{2} \frac{1}{2}) + b w(\frac{1}{2} \frac{3}{2}) + c w(\frac{3}{2} \frac{3}{2}) + d w(\frac{1}{2} \frac{5}{2}) + e w(\frac{3}{2} \frac{5}{2}) + f w(\frac{1}{2} \frac{7}{2}) + g w(\frac{3}{2} \frac{7}{2}) . \quad (29)$$

The barrier heights for the $\frac{1}{2}+$ and $\frac{3}{2}-$ bands are probably well under 850 kev, but the $\frac{1}{2}-$ band is estimated to be only about 70% open, based on a very rough comparison of data from the H-F analysis and the curve of σ_f vs E_n .

For a first-order estimate of the level strengths contributing to fission, neglect the effects of neutron competition in obtaining the following equations:

$$c/e/g = 1.894/0.303/0.632 , \quad (30)$$

$$\frac{f+g}{d+e} = \frac{4T_3^+}{3(T_2^+ + T_3^-)} = 0.813 . \quad (31)$$

From these relations and the four obtainable from matching P coefficients with the measured angular distribution, one finds

$$\begin{aligned}\sigma_f(\theta) &= 0.10 \left[0.70 w(\frac{1}{2} \frac{1}{2}) + 0.72 w(\frac{1}{2} \frac{3}{2}) + 0.22 w(\frac{3}{2} \frac{3}{2}) + 0.16 w(\frac{1}{2} \frac{5}{2}) \right. \\ &\quad \left. + 0.04 w(\frac{3}{2} \frac{5}{2}) + 0.09 w(\frac{1}{2} \frac{7}{2}) + 0.07 w(\frac{3}{2} \frac{7}{2}) \right] \quad \text{barns/steradian} .\end{aligned}\quad (32)$$

To account very approximately for the effects of neutron competition on the distribution, define

$\alpha(I\pi) \equiv$ formation cross section for compound state $I\pi$,

$$\bar{P} \equiv \frac{\sum \alpha(I\pi) P(I\pi)}{\sum \alpha(I\pi)} , \quad (33)$$

$$\gamma(I\pi) \equiv \Gamma_f / \Gamma_t = \Gamma_f / (\Gamma_f + \Gamma_n) \quad \text{for state } I\pi . \quad (34)$$

$n(I\pi) \equiv$ number of fission channels open for state $I\pi$.

$\beta(KI\pi) \equiv$ reduction factor applied to terms in a given $K\pi$ band due to spin effects. Taken as unity for ground state level in each band.

Set

$$\Gamma_f(I\pi) \propto \Sigma(n\beta)_{I\pi} . \quad (35)$$

Then

$$\overline{\Gamma}_f \propto \frac{\Sigma(n\beta) \text{ over all states}}{\text{number of states}} \equiv \overline{\Sigma(n\beta)} , \quad (35a)$$

$$\overline{\Gamma}_f = \frac{1}{7} [1 + 1 + 1 + 0.7 + (1 + 0.7 \times 0.98) + (1 + 0.7 \times 0.95) + (1 + 0.7 \times 0.90)] = \frac{1}{0.806} .$$

The quantities in the brackets are $\Sigma n\beta$ for the $1/2+$, $3/2+$, $5/2+$, $1/2-$, $3/2-$, $5/2-$, and $7/2-$ states respectively. Now

$$\gamma(I\pi) = \frac{\Gamma_f / \overline{\Gamma}_f}{\Gamma_f / \overline{\Gamma}_f + \Gamma_n / \overline{\Gamma}_f} = \frac{0.806 \Gamma_f(I\pi)}{0.806 \Gamma_f(I\pi) + \Gamma_n(I\pi) / \overline{\Gamma}_f} . \quad (34a)$$

But

$$\Gamma_n(I\pi) / \overline{\Gamma}_n = P(I\pi) / \overline{P} . \quad (36)$$

So

$$\Gamma_n(I\pi) / \overline{\Gamma}_f = \frac{\overline{\Gamma}_n P(I\pi)}{\Gamma_f \overline{P}} = 2.1 \frac{P(I\pi)}{2.67} = 0.787 P(I\pi) .$$

Therefore

$$\gamma(I\pi) = \frac{\Sigma(n\beta)_{I\pi}}{\Sigma(n\beta)_{I\pi} + 0.975 P(I\pi)} , \quad (35b)$$

$$\gamma(5/2+) = 0.492 , \quad \gamma(5/2-) = 0.331 , \quad \gamma(7/2-) = 0.325 ,$$

$$\frac{f+g}{d+e} = \frac{\alpha(7/2-)\gamma(7/2-)}{\alpha(5/2+)\gamma(5/2+) + \alpha(5/2-)\gamma(5/2-)} = \frac{0.632(0.325)}{0.474(0.492) + 0.303(0.331)} = 0.616 . \quad (37)$$

By using this relation in place of Eq. (31), together with Eq. (30) (since neutron emission proceeds with equal facility from all the $K = 3/2-$ levels) and the same four equations from matching P coefficients, one obtains for the fission-fragment angular distribution in terms of level strengths

$$\sigma_f(\theta) = 0.10 \left[0.78 w(1/2 \ 1/2) + 0.71 w(1/2 \ 3/2) + 0.19 w(3/2 \ 3/2) + 0.17 w(1/2 \ 5/2) \right. \\ \left. + 0.03 w(3/2 \ 5/2) + 0.06 w(1/2 \ 7/2) + 0.06 w(3/2 \ 7/2) \right] . \quad (38)$$

Comparison of Eqs. (38) and (32) shows that at this energy neutron emission produces only small effects on the *relative level strengths for fission*. From (38) one finds the following values for $\gamma(I\pi)$:

$$\begin{aligned}\gamma(\frac{1}{2}) &= 0.48 \text{ (average for both parities) ,} \\ \gamma(\frac{3}{2}) &= 0.32 \text{ (average for both parities) ,} \\ \gamma(\frac{5}{2}) &= 0.21 \text{ (average for both parities) ,} \\ \gamma(\frac{7}{2}^-) &= 0.15 .\end{aligned}\tag{39}$$

All of the above are reasonable in view of a value of 0.33 (from Table 5) for $\bar{\gamma}$.

Analysis at 1050 kev. — The partial cross-section formulas obtained by use of transmission factors derived from the P-B potential are

$$\begin{aligned}\sigma(\theta)_{1/2+} &= 0.100 \left[0.460 W(\frac{1}{2} \frac{1}{2}) + 0.442 W(\frac{1}{2} \frac{3}{2}) + 0.621 W(\frac{1}{2} \frac{5}{2}) \right] , \\ \sigma(\theta)_{1/2-} &= 0.100 \left[0.916 W(\frac{1}{2} \frac{1}{2}) + 1.954 W(\frac{1}{2} \frac{3}{2}) + 0.567 W(\frac{1}{2} \frac{5}{2}) + 1.076 W(\frac{1}{2} \frac{7}{2}) \right] , \\ \sigma(\theta)_{3/2+} &= 0.100 \left[\phantom{0.916 W(\frac{1}{2} \frac{1}{2})} 0.442 W(\frac{3}{2} \frac{3}{2}) + 0.621 W(\frac{3}{2} \frac{5}{2}) \right] , \\ \sigma(\theta)_{3/2-} &= 0.100 \left[\phantom{0.916 W(\frac{1}{2} \frac{1}{2})} 1.954 W(\frac{3}{2} \frac{3}{2}) + 0.567 W(\frac{3}{2} \frac{5}{2}) + 1.076 W(\frac{3}{2} \frac{7}{2}) \right] .\end{aligned}\tag{40}$$

From experiment, the actual fission-fragment angular distribution normalized and corrected for finite angular resolution is:

From least-squares fit:

$$\sigma_f(\theta) = 0.100 [(0.874 \pm 0.003)P_0 + (0.0724 \pm 0.0271)P_2 + (0.0018 \pm 0.0061)P_4] \text{ barns/steradian} .\tag{41}$$

From force fit through all four points:

$$\sigma_f(\theta) = 0.100 [0.877P_0 + 0.0754P_2 + 0.004P_4 - 0.006P_6] \text{ barns/steradian} .\tag{41a}$$

The almost complete disappearance of the two higher harmonics indicates that either very special relations exist between the $W(KI)$ for $I > \frac{3}{2}$ or that these levels make negligible contributions to fission. An investigation of the special relations necessary for the existence of significant contributions to σ_f from these higher spin levels shows that the relative proportions required would be at complete variance with theory and would also force constraints on the terms of lower spin, so as to lead to most improbable assignments for their weights also. Consequently, it appears more likely that the higher terms really are negligible and that one can write with good accuracy

$$\sigma_f(\theta) = 0.100 [0.877P_0 + 0.075P_2] = aW(\frac{1}{2} \frac{1}{2}) + bW(\frac{1}{2} \frac{3}{2}) + cW(\frac{3}{2} \frac{3}{2}) .\tag{41b}$$

Since there are only two P coefficients to match, and three unknowns, it is necessary to introduce an assumption based on theory to supply the third equation. Now theory does not predict the sharp break in

the anisotropy between 850 and 1050 kev. The drop in fission cross section between these two energies can be understood in the light of data in Tables 3 and 4, which show the hefty increase in competition from neutron emission to the newly available vibrational levels in U^{234} . Since the extrema in the angular distribution coincide exactly energywise with those in the cross section, one *suspects* that they arise from the same cause, namely, neutron emission to the new levels. A glance at the results of the H-F analysis given in Table 4, however, would lead one to predict no drastic change in the angular distribution. This is indeed borne out. Calculations similar to those in the preceding section still lead to strong forward peaking, although not quite as strong as at 850 kev. Consequently, it appears that either the H-F analysis does not properly represent the nature of scattering to beta and octupole levels, or that the K quantum number in this energy region, at least, has lost most of its stability.

Since the high-spin terms are at greatest variance with theory, it is perhaps safest to introduce as the third criterion some function of the lowest spin term. At 1050 kev the $\frac{1}{2}-$ band should be completely open, so let

$$\gamma(\frac{1}{2}, 1050 \text{ kev}) = (2/1.7)\gamma(\frac{1}{2}, 850 \text{ kev}) = (2/1.7)(0.48) = 0.57 . \quad (42)$$

This leads to

$$\sigma_f(\theta) = 0.100 \left[0.79 w(\frac{1}{2} \frac{1}{2}) + 0.56 w(\frac{1}{2} \frac{3}{2}) + 0.40 w(\frac{3}{2} \frac{3}{2}) \right] \quad (43)$$

and a value of 0.40 for $\gamma(\frac{3}{2})$. From Table 5, $\bar{\gamma} = 0.29$, so these values of $\gamma(\frac{1}{2})$ and $\gamma(\frac{3}{2})$ are reasonable, since the other levels decay almost entirely by neutron emission.

Equation (43) accounts adequately for the experimentally observed quantities, but the disappearance of the higher spin levels from fission is not at all explained. The substantial increase in the contribution from the $w(\frac{3}{2} \frac{3}{2})$ level over that at 850 kev could be due in part to the appearance of a $\frac{3}{2}+$ band, although from the relative formation cross sections a much more modest increase would be expected.

Conclusions

The measured angular distribution of the fragments is consistent with the Bohr theory for neutron bombarding energies up to 850 kev. At 1050 kev the measured distribution is at variance with what would be expected from theory, but the theory now of necessity includes an analysis of compound nucleus decay to beta and octupole levels in U^{234} . The anomaly could be explained if decay to these states can occur from high-spin parent levels with greatly enhanced probabilities relative to decay from low-spin states.

If K remains a good quantum number remote from saddle point in regions of low nuclear deformation where neutron emission is thought to occur, one might suspect the operation of some sort of K selection rule retarding neutron emission for $\partial K > \frac{1}{2}$. This could account for the increased strength of the $w(\frac{3}{2} \frac{3}{2})$ level at 1050 kev.

Alternatively, the possibility exists that K loses stability over a narrow energy region, regaining some or all of it at higher energies. A wobbling of the K axis would certainly smear out the higher-order

harmonics much more drastically than the second order. Possibly the top of the barrier for the dominant fissioning band is a region of K instability.

It is of interest to note that a somewhat analogous, although in a way a reverse, situation exists for Th^{232} bombarded by 1.6-Mev neutrons.¹³ At this energy there is a peak in σ_f and a maximum *sidewise* peaking in $\sigma_f(\theta)$. At higher energy, σ_f drops and $\sigma_f(\theta)$ tends toward isotropy. The dominant fissioning band here was found to be a $\frac{3}{2}$ - by the analysis of Wilets and Chase,¹⁴ and this was also borne out by an analysis using the methods outlined here. The significant thing is that in both cases, Th^{232} and U^{234} , following a maximum in σ_f the angular distribution of the fragments tends toward isotropy. This would clearly be true if K becomes unsettled in a narrow region of energy near the top of the dominant fission barrier. Possibly neutron decay could also explain it, but more needs to be known about the types of levels available and the physical laws governing decay to levels involving collective vibrations.

¹³J. E. Brolley, Jr., and W. C. Dickinson, *Phys. Rev.* **94**, 640 (1954).

¹⁴L. Wilets and D. M. Chase, *Phys. Rev.* **103**, 1292 (1956).

CAPTURE CROSS SECTIONS FOR 30-keV NEUTRONS

R. L. Macklin

T. Inada¹

A novel counter for neutron capture gamma-ray detection has been developed recently at the Harwell Linac.² It is an analog of the thick-walled Geiger counter, the counting gas being replaced by a thin plastic scintillator. While its overall efficiency is low, its inherently good time resolution and low background make it attractive for pulsed Van de Graaff application. By use of the design of Moxon and Rae² (1-in. graphite walls and four 5-in. photomultipliers), the time resolution was about 15 nanoseconds (see Fig. 1).

This resolution was sufficient to resolve 30-keV neutrons from $\text{Li}^7(p,n)$ at 19.7 cm (see Fig. 2). Several elements were compared, and the capture cross sections are given in Table 1. The results are normalized to the silver capture cross section found in earlier work here.³ The values for elements with several isotopes are uncertain because the detector efficiency depends on the binding energy (plus the 30-keV incident neutron energy),

which varies appreciably. (In the case of the silver isotopes, the separate isotopic cross sections are known.) The item of chief interest is the gold cross section, about $\frac{1}{2}$ barn, which agrees with the earlier large liquid scintillator and spherical-shell transmission measurements, but not with the gold activation results.

A code has been written for computer calculation of the efficiency of Moxon-Rae-type detectors as a function of gamma-ray energy. For independence of capture-gamma cascade details, the efficiency should be simply proportional to the energy. This condition appears most nearly fulfilled for elements near tin. To avoid capture of scattered neutrons, possible wall materials are restricted to graphite and perhaps lead. Calculated efficiency curves (Compton and pair processes only) are shown in Fig. 3.

With improved time resolution, measurements on most of the separated stable isotopes should be possible. Initial attention is being directed to isotopes formed in stellar interiors by the s process.⁴

¹Visiting scientist from NIRS, Japan.

²M. C. Moxon and E. R. Rae, *A New Detector for Neutron Capture Cross Section Measurements, Neutron Time of Flight Methods* (ed. by J. Spaepen), EURATOM, Brussels, 1961.

³J. H. Gibbons *et al.*, *Phys. Rev.* **122**, 182 (1961).

⁴D. D. Clayton and W. A. Fowler, *Ann. Phys.* **16**, 51 (1961); and many earlier references.

UNCLASSIFIED
ORNL-LR-DWG 66168R

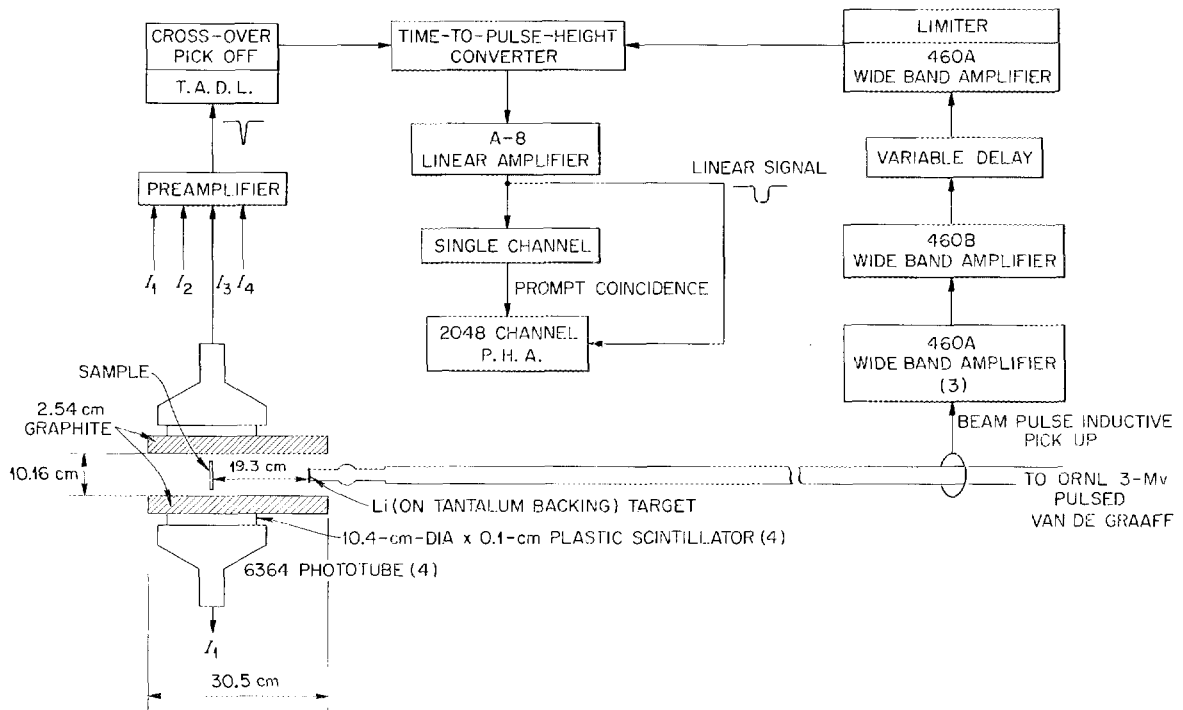


Fig. 1. The 30-keV Neutron Capture Experiment; Block Diagram.

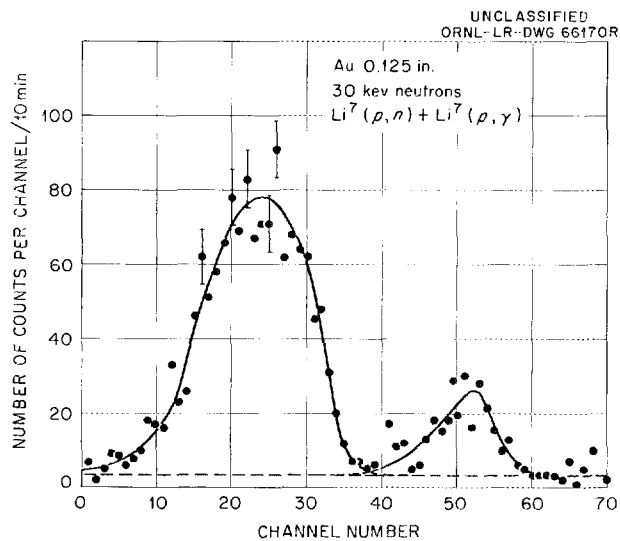


Fig. 2. Typical Time Spectrum Example.

Table 1. Comparison of Capture Cross Sections

Z	Element	Capture Cross Sections for 30-keV Neutrons (mb)	
		Present Work	Gibbons, Macklin, Miller, and Neiler
42	Mo	141 ($\pm 23\%$)	140 ($\pm 10\%$)
47	Ag	(951)	951 ($\pm 10\%$)
48	Cd	343 ($\pm 21\%$)	330 ($\pm 10\%$)
50	Sn	124 ($\pm 24\%$)	88 ($\pm 15\%$)
73	Ta	630 ($\pm 20\%$)	735 ($\pm 10\%$)
74	W	184 ^a ($\pm 21\%$)	270 ($\pm 10\%$)
78	Pt	321 ($\pm 23\%$)	330 ($\pm 10\%$)
79	Au	513 ($\pm 20\%$)	515 ($\pm 10\%$)

^a Approximately 300 by using peak counts only.

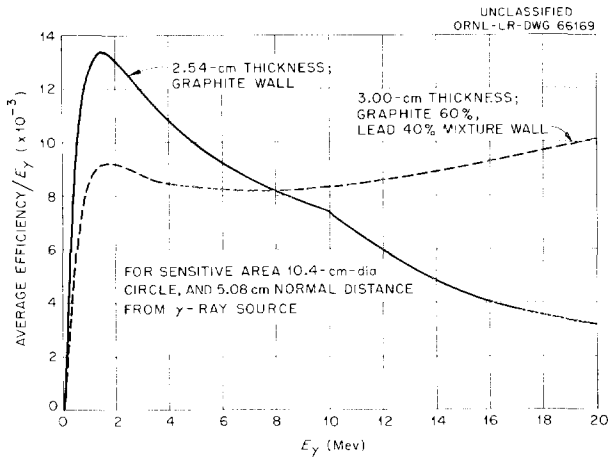


Fig. 3. Calculated Efficiency Curves (Compton and Pair Processes Only).

DIRECT COMPARISON OF GAMMA-RAY SPECTRA OBTAINED FROM CAPTURE OF THERMAL AND (30 ± 10) -keV NEUTRONS¹

F. W. K. Firk²

J. H. Gibbons

The spectra of gamma rays observed with a 9×6 in. NaI(Tl) crystal have been compared directly for radiative capture of thermal and (30 ± 10) -keV neutrons in Au, Cu, Fe, and Ni. Two sets of measurements were made by using neutron time-of-flight techniques on both the ORNL neutron chopper and the 3-MeV pulsed Van de Graaff. Identical geometries were used for the NaI(Tl) gamma-ray spectrometer in the two experiments. In the Van

de Graaff experiment, nanosecond time-of-flight techniques were used for triple-event discrimination, namely, a time separation of gamma rays from (1) the lithium target of the machine, (2) the sample under investigation, and (3) capture by iodine of 30-keV neutrons elastically scattered from the sample into the crystal. For gold and iron the spectra of gamma rays above 3 MeV due to capture of thermal or (30 ± 10) -keV neutrons do not differ significantly. However, for copper and nickel the gamma-ray spectra are significantly different at the two neutron energies investigated. There is evidence that a direct capture process contributes to the thermal-neutron capture in copper.

¹Abstract of published paper: pp 213-19 in *Proceedings of the Symposium on Neutron Time-of-Flight Methods*, Session II, Saclay, France, July 24-27, 1961.

²Visiting ORNL from AERE, Harwell, England.

GAMMA-RAY SPECTRA FROM 30-keV NEUTRON CAPTURE

J. R. Bird¹

J. H. Gibbons

W. M. Good

A preliminary report of the extension of the study of neutron capture gamma rays up to the keV range was given a year ago.² The motivations for this study are, briefly:

1. dependence of capture spectra upon J^π of capturing state,
2. variation of partial radiative widths from resonance to resonance for a given J^π ,
3. possible energy-dependent effects such as "direct" capture vs "compound" capture.

A new detector has been obtained³ which has improved characteristics from the viewpoint of both time and energy resolution. The neutron source (pulsed Van de Graaff accelerator) has also been significantly modified, resulting in considerably enhanced operational characteristics. Bursts of 30-keV neutrons are produced via the $\text{Li}^7(p,n)\text{Be}^7$ reaction by bombarding a lithium metal target with

protons 2.0 keV above the reaction threshold at 1881 keV.

The experimental arrangement is given in Fig. 1. The neutron flight path (15 cm) was adjusted to produce separation of the capture gamma-ray peak from the prompt gamma-ray peak (Fig. 2). The overall time resolution is about 10 nanoseconds. The kinematically collimated neutron beam at the target position (about $2\frac{1}{2}$ -in. diameter) is small enough to allow measurements with enriched isotope samples. Gamma-ray pulses arriving at the crystal are gated into the analyzer according to their arrival time. Thus "foreground" and "background" can be taken simultaneously, a very important feature of the experiment.

Samples are normally metal disks about 1 in. thick and 3 in. in diameter. However, it is quite feasible to use samples $\frac{1}{16}$ in. thick by 2 in. in diameter if $\sigma_c \geq 100$ mb. The lower limit of sensitivity of the experiment is dependent upon many factors but apparently ranges as low as 1 mb.

Some examples of results are given in Figs. 3-8; they are discussed in order below.

¹ Visiting ORNL from AERE, Harwell, England.

² F. W. K. Firk and J. H. Gibbons, *Phys. Div. Ann. Progr. Rept. Feb. 10, 1961*, ORNL-3085, pp 54-56.

³ Loaned by Neutron Physics Division.

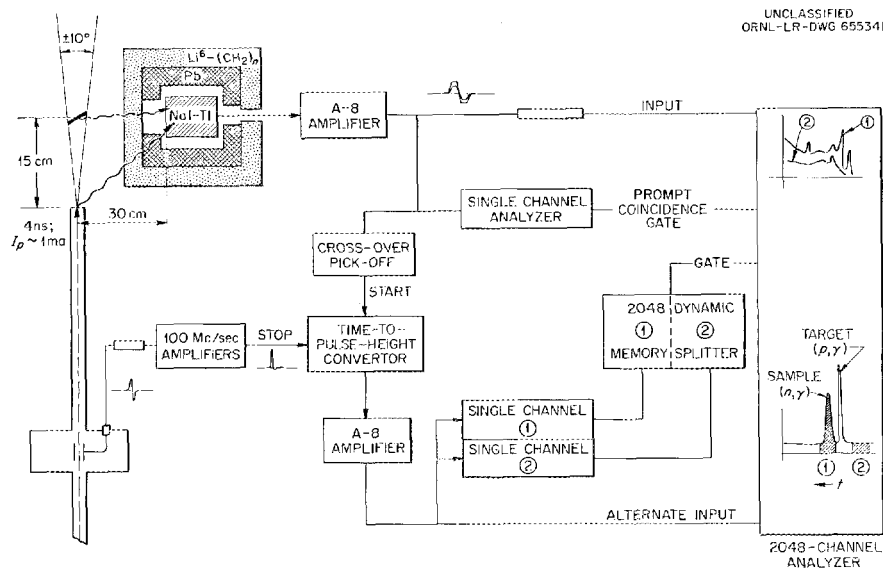


Fig. 1. Block Diagram of Experimental Apparatus. Proton target gamma rays and natural background are discriminated against (in comparison with neutron capture gamma rays) by means of pulsed beam time-of-flight. Both "foreground" and "background" are measured simultaneously.

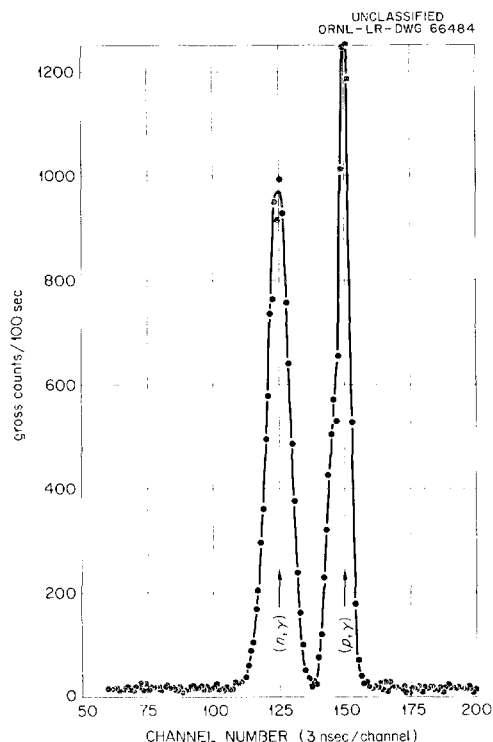


Fig. 2. Time Spectrum, Showing Natural Background, Proton Target Gamma Rays, and Neutron Capture Gamma Rays. Time is measured from right to left.

Fluorine. - The total cross section for neutrons exhibits a strong resonance at 27 keV. This has been identified as $J^\pi = 2^- (l = 1)$. It is not surprising that the spectrum (Fig. 3) is markedly different from that observed with thermal neutrons, since the thermal capture is assigned to a $J^\pi = 0^+$ or $1^+ (l = 0)$ character. The relative intensities observed in the two cases are given in Table 1. In terms of simple multipolarity rules, one would expect the ground-state gamma ray to be much stronger for the 30-keV capture [$2^- \rightarrow (2^+, 3^+)$] than for thermal capture [$(0^+, 1^+) \rightarrow (2^+, 3^+)$]. In fact, just the opposite effect is observed. The 30-keV results indicate a strong preference for cascade transitions through levels near 1.31 and 1.97 MeV. These results in comparison with thermal results may be indicative of "direct" capture effects or of strong collective-motion selection rules operating in this deformed nucleus.

Aluminum. - The capture observed with 30-keV neutrons in aluminum (Fig. 4) is due to the $J^\pi = 2^+$ ($l = 0$) resonance at 27 keV. The thermal capture is characterized by $J^\pi = 2^+$ or $3^+ (l = 0)$, so it is

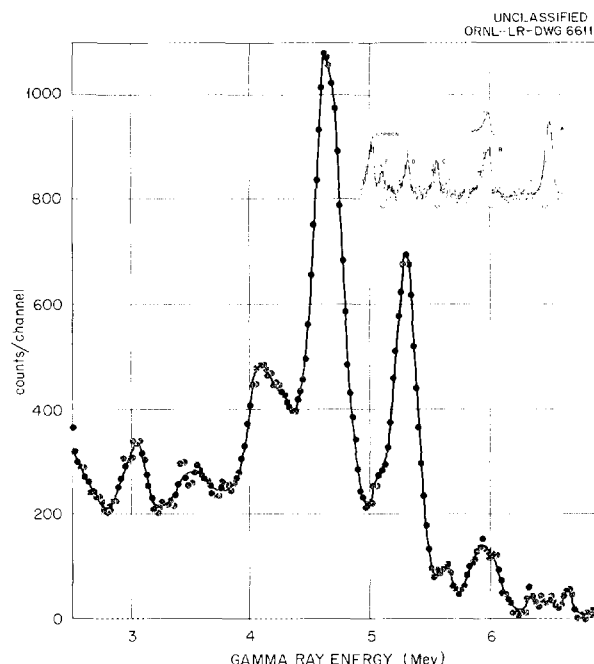


Fig. 3. Capture Gamma-Ray Spectrum for Fluorine.

Table 1. Capture Gamma-Ray Energies and Relative Intensities in Fluorine: A Comparison Between Results Obtained with Thermal and 30-keV Neutrons

Thermal Capture ^a		30-keV Capture	
Energy (Mev)	Relative Intensity	Energy (Mev)	Relative Intensity
6.60	20	6.64 ± 0.03	≤ 2
		6.3-6.5	≤ 2
6.01	10	5.91-6.05	6
		5.66	2
5.55	16		
5.28	20	5.30	24
5.10	14	5.07	2
		4.62-4.64	36
4.50	15		
		4.25	≤ 2
		3.45-3.7	6
		2.95-3.07	6
		2.4-2.7	6

^aFrom Groshev's Atlas.

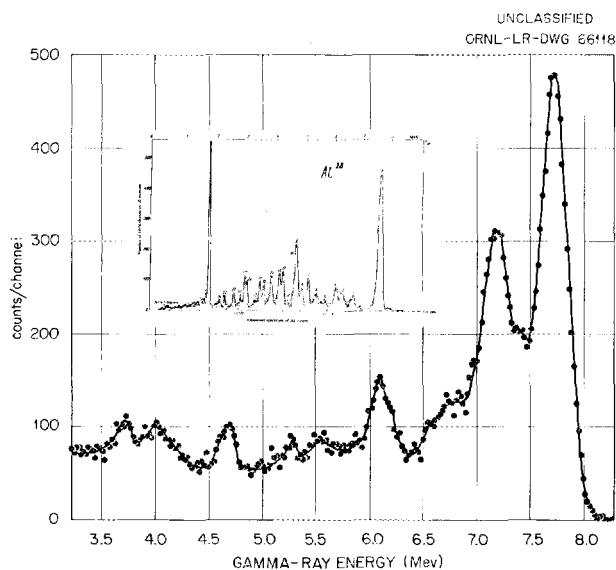


Fig. 4. Capture Gamma-Ray Spectrum for Aluminum.

not surprising that the results are very similar. The observed spectrum for $E_\gamma > 6.5$ Mev is accounted for in detail by a single gamma ray of 7.72 ± 0.03 Mev. A ground-state transition should correspond to 7.757 Mev, and a transition to the first excited state (31 keV) would occur at 7.726 Mev. While this latter energy corresponds more exactly to the observed gamma ray, the ground-state transition energy is within the limit of error. Strong transitions to either the ground (3^+) or first excited state (2^+) from capture by either thermal (2^+ , 3^+) or the 35-keV resonance (2^+) would not be expected from considerations of multipolarity. Other lines seen in the spectrum correspond to cascade through excited states at 0.97, 1.02, and 1.63 Mev. The peaks at lower energies correspond to unresolved groups of excited states. In general, the spectrum for 30-keV capture differs from that due to thermal capture only in that cascades through intermediate states (compared with the high-energy transition) are weaker for 30-keV capture.

Iron. — The $J^\pi = 1/2^+$ ($l = 0$) resonance in Fe^{56} at 29 keV is predominantly responsible for the capture observed with 30-keV neutrons (Fig. 5). Thermal capture is characterized by the same spin and parity. The ground state of Fe^{57} is $1/2^-$. The peak at 7.68 Mev, when fitted for line shape, indicates the presence of a 7.3-Mev gamma

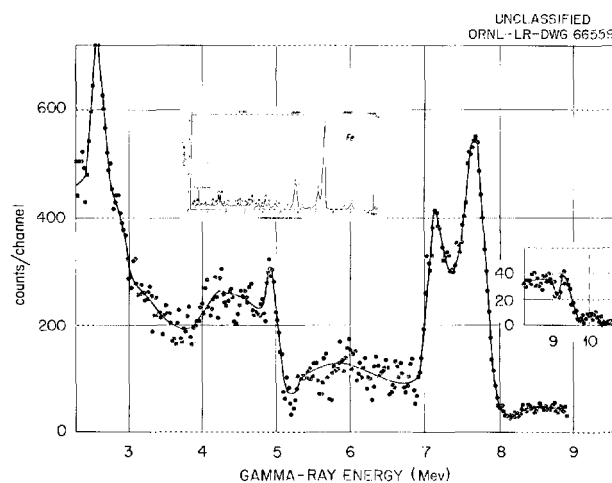


Fig. 5. Capture Gamma-Ray Spectrum for Iron.

ray in approximately the same intensity ratio relative to the 7.68-Mev gamma ray as observed by thermal capture. For gamma-ray energies less than 5 Mev, however, the intensities are in general much stronger than for thermal capture. This is particularly true for the gamma ray at 4.93 Mev, which is an order of magnitude weaker for thermal capture.

The energy range above 7.68 Mev is particularly interesting. Gamma rays observed near 9.35 and 10.2 Mev correspond to ground-state transitions from capture in Fe^{54} and Fe^{57} respectively. The strength of these lines compared with the Fe^{56} line at 7.68 Mev is surprisingly large (the three line intensities are in a ratio directly proportional to isotopic abundance) and indicates that capture must be present near 30 keV for both isotopes and also that (as in the case of Fe^{56}) ground-state transitions must also be dominant.

Copper. — In order to help eliminate possible effects due to the presence of two isotopes, a run was made with a sample of pure Cu^{63} (Fig. 6). Resonance-level spacing in copper is an order of magnitude closer than spacing in Fe, Al, or Fe. The energy spread of the 30-keV neutron beam thus produces, in the case of copper, capture in *at least* ten resonances. Therefore 30-keV capture is characterized by $J^\pi = 1^-$ or 2^- ($l = 0$), identical with the character of thermal capture. The ground-state spin and parity of Cu^{64} is 1^+ , thus allowing E1 transitions to the ground state. While strong transitions to and near the ground

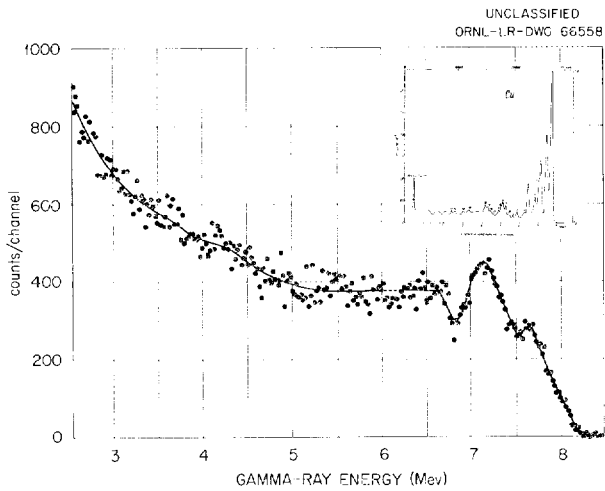


Fig. 6. Capture Gamma-Ray Spectrum for Separated Cu^{63} .

state dominate the thermal results, these transitions are weak at best in the case of 30-keV capture. This striking difference has been predicted in this range of atomic weight on the basis of the mechanism of "direct" capture.

Nickel. — The gamma-ray spectrum from 30-keV capture in natural nickel is dominated by the two major isotopes Ni^{58} (68%) and Ni^{60} (26%), with known resonances at (17 and 65) and (15, 30, and 67) keV respectively. All of these resonances are characterized by $J^\pi = 1/2^+$, which is the value for thermal capture. Measurements were made with samples of pure isotopes of Ni^{58} and Ni^{60} and for natural nickel (Fig. 7). The results are similar to those for copper in that the principal difference observed between 30-keV and thermal capture is a marked suppression of the highest-energy gamma rays with respect to cascade transitions.

Lead. — Only Pb^{207} has an identified resonance in the 30-keV range ($J^\pi = 1^-, l = 0$, at 45 keV). It is probable that unobserved *p*-wave resonances exist in this region in mass numbers 204, 206, 207, and possibly 208; Pb^{204} also probably has *s*-wave resonances in this region.

The observed spectrum from normal lead for 30-keV capture (Fig. 8) is much more complicated than that observed by using thermal neutrons. In the thermal case two lines appear, corresponding to ground-state transitions from capture in Pb^{207} ,

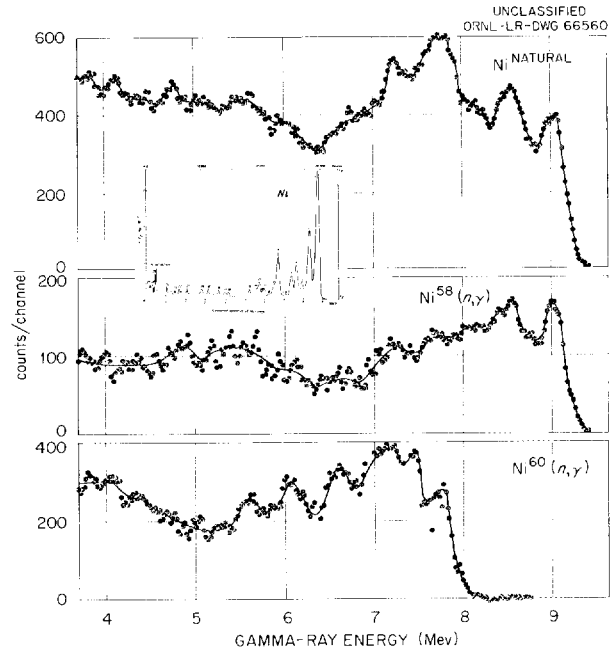


Fig. 7. Capture Gamma-Ray Spectrum for Ni^{58} , Ni^{60} , and Natural Nickel.

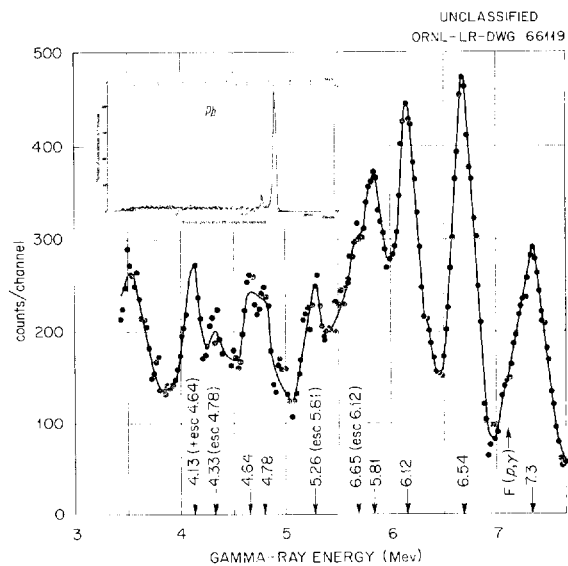


Fig. 8. Capture Gamma-Ray Spectrum for Lead.

Pb^{204} , and/or Pb^{206} . In the case presented here, several additional lines appear. Similar to the thermal results, it is not yet possible to clearly distinguish between capture in mass numbers 204 and 206, since their binding energies and low-lying level structure are so similar. However, the prominent lines indicate ground-state gamma rays from capture in mass numbers 207, 204,

and/or 206. Further, there are gamma rays corresponding to transitions to the first and second excited states of $Pb^{205,207}$ as well as a gamma ray whose energy is consistent with a ground-state transition from capture in Pb^{208} . The strong ground-state transition observed for Pb^{207} capture ($J^\pi = 1^-$) is compatible with an $E1$ character, since Pb^{208} has a ground-state spin $J^\pi = 0^+$.

GENERAL SURVEY ON RADIATIVE CAPTURE MEASUREMENTS BY TIME-OF-FLIGHT¹

J. H. Gibbons

A general review is given of techniques for radiative capture cross-section measurements, with particular emphasis given to 4π liquid scintillator

systems. Experiments with both "white" and "monoenergetic" neutrons are discussed, with reference to optimum source types at various energies. Some typical experimental results are presented and used to illustrate presently attained capabilities as well as to point out areas where improvements or changes in technique are called for.

¹Abstract of published paper: pp 151-66 in *Proceedings of the Symposium on Neutron Time-of-Flight Methods*, Session II, Saclay, France, July 24-27, 1961.

PARAMETERS OF NEUTRON RESONANCES IN Pa^{231}

J. R. Patterson¹

J. A. Harvey

The ORNL fast-chopper time-of-flight spectrometer has been utilized in measuring the total neutron cross section of Pa^{231} from 0.04 to 200 ev. Transmission measurements were made with the 45-m flight-path spectrometer from 0.04 to 50 ev with an energy resolution of $\sim 1.5\%$. By use of the 180-m flight-path spectrometer, measurements were made from 2.5 to 200 ev with an energy resolution of $\sim 0.3\%$.

The sample used was 59.40 g of Pa_2O_5 , which had been sent to ORNL from Harwell for irradiation in the ORR to produce U^{232} . The powder was screened as it was inserted into the sample holder, which had inside dimensions of $0.619 \times 1.127 \times 3.130$ in. The thickness of the protactinium was 0.00579 atom/barn.

The transmission data were analyzed by use of the resonance analysis programs² written for the

IBM 7090, and include resolution and Doppler broadening. The area analysis program was used for all resonances up to 100 ev. The shape analysis program was used for the first eight resonances up to 3.5 ev, since both the resolution and the Doppler widths are less than the natural widths of these resonances. The results of the analysis are summarized in Table 1. The parameters are in good agreement with those measured by Simpson *et al.*,³ who determined parameters for the resonances up to 11 ev. The errors on the radiation widths in Table 1 include an estimated uncertainty

¹Summer research participant from Clemson College; now at Rockford College, Rockford, Ill.

²S. E. Atta and J. A. Harvey, *Numerical Analysis of Neutron Resonances*, ORNL-3205 (1961).

³F. B. Simpson *et al.*, *Nuclear Sci. and Eng.* 12, 243 (1962).

Table 1. Resonance Parameters of ${}_{91}\text{Pa}^{231}$

E_0 (ev)	Γ_γ (mv)	$g\Gamma_n^0$ (mv)	Error (\pm) (mv)	E_0 (ev)	Γ_γ (mv)	$g\Gamma_n^0$ (mv)	Error (\pm) (mv)
0.40		0.067	0.003	25.97		0.105	0.005
0.50		0.0060	0.0010	26.85		0.015	0.002
0.743	38 ± 2	0.00393	0.00006	27.32		0.053	0.004
1.238	47 ± 2	0.0119	0.0002	28.23		0.019	0.002
1.405		0.0007	0.0003	28.69		0.025	0.002
1.960	46 ± 4	0.00252	0.00005	29.62		0.155	0.010
2.787	39 ± 5	0.00295	0.00008	30.22		0.0050	0.0015
3.480	47 ± 5	0.0126	0.0002	31.73		0.30	0.02
4.12		0.0208	0.0006	32.2		0.005	0.002
4.35		0.0141	0.0006	32.80		0.016	0.002
4.53		0.0045	0.0003	33.39		0.012	0.002
5.07		0.106	0.005	35.15		0.017	0.002
5.28		0.0195	0.0010	36.14		0.032	0.003
5.64		0.0099	0.0004	36.65		0.12	0.02
5.82		0.0118	0.0003	36.8		0.03	0.01
6.55		0.0090	0.0004	37.53		0.080	0.005
6.88		0.047	0.002	38.26		0.016	0.003
7.58		0.0164	0.0004	39.73		0.083	0.005
7.83		0.0304	0.0008	41.27		0.035	0.008
8.74		0.130	0.005	42.08		0.050	0.008
9.27		0.0083	0.0004	43.34		0.115	0.012
9.72		0.039	0.002	44.54		0.014	0.003
10.34		0.119	0.005	44.91		0.008	0.003
10.77		0.054	0.002	45.64		0.090	0.012
11.26		0.054	0.002	46.39		0.024	0.005
11.67		0.100	0.009	47.22		0.075	0.012
12.08		0.0031	0.0004	48.60		0.021	0.004
13.26		0.11	0.02	50.12		0.009	0.004
13.38		0.15	0.02	50.85		0.060	0.006
14.10		0.077	0.004	51.25		0.034	0.005
15.06		0.0141	0.0008	51.92		0.068	0.007
15.57		0.0255	0.0010	52.54		0.150	0.010
16.02		0.041	0.002	53.91		0.055	0.006
16.66		0.028	0.002	54.45		0.092	0.007
16.99		0.037	0.002	55.20		0.63	0.05
18.29		0.177	0.010	56.05		0.145	0.010
18.74		0.080	0.004	56.52		0.055	0.006
19.25		0.020	0.003	57.16		0.094	0.009
19.55		0.009	0.003	60.16		0.016	0.004
20.3		0.0045	0.0010	61.35		0.18	0.02
20.6		0.110	0.006	61.77		0.05	0.02
21.3		0.06	0.02	62.35		0.014	0.006
21.45		0.07	0.02	63.38		0.087	0.009
22.12		0.050	0.003	64.40		0.018	0.005
24.75		0.028	0.002	65.30		0.067	0.009
25.45		0.009	0.002	66.43		0.007	0.005

Table 1 (continued)

E_0 (ev)	Γ_γ (mv)	$g\Gamma_n^0$ (mv)	Error (\pm) (mv)	E_0 (ev)	Γ_γ (mv)	$g\Gamma_n^0$ (mv)	Error (\pm) (mv)
67.35		0.058	0.009	79.2		0.025	0.008
68.21		0.013	0.006	80.1		0.056	0.010
69.09		0.11	0.02	81.0		0.043	0.011
70.07		0.016	0.006	83.5		0.18	0.06
70.64		0.050	0.008	84.7		0.11	0.03
71.33		0.09	0.02	85.7		0.11	0.03
72.03		0.032	0.007	87.7		0.11	0.03
73.8		0.040	0.009	90.0		0.06	0.02
74.9		0.071	0.011	91.5		0.06	0.02
75.7		0.021	0.007	92.8		0.025	0.014
76.6		0.030	0.009	93.9		0.031	0.014
77.8		0.049	0.010	95.8		0.20	0.04
78.5		0.019	0.008	99.0		0.11	0.02

of 10% in the Doppler and resolution broadenings. Accurate values for radiation widths could not be obtained for three of these low-energy resonances, since the sample was much too thick for the large resonances at 0.40 and 0.50 ev and too thin for the small resonance at 1.405 ev. The area analysis was based on a Γ_γ of 45 mv, but the values of Γ_n^0 are quite insensitive to reasonable changes in Γ_γ . The values of the resonance parameters are the averages of at least two measurements and in many cases two with each flight path. The errors are obtained from the statistical accuracy of a single measurement and the agreement between different measurements.

A total of 118 resonances were analyzed from 0 to 100 ev. A plot of the number of resonances against neutron energy up to 72 ev is shown in Fig. 1. Considering the energy range from 0 to 12.5 ev, the observed level spacing for both spin states was computed to be 0.45 ± 0.07 ev. Assuming the $(2J + 1)$ law for the average level density for the two spin states gives a value of 0.72 ± 0.15 ev for $D_{I+1/2}$ for states of spin 2 and a value of 1.2 ± 0.3 ev for $D_{I-1/2}$ for states of spin 1. Above 13 ev, it is obvious that many resonances are being missed, since the Doppler width increases with neutron energy and equals Γ at ~ 5 ev. The s-wave strength function was obtained

from a plot of the sum of $g\Gamma_n^0$ against neutron energy, as shown in Fig. 2. Even though many resonances are "missed" at the higher energies, the data can be used, since the "missed" resonances are either small or have been included with other resonances. The s-wave strength function per spin state obtained was $(0.85 \pm 0.10) \times 10^{-4}$, which is in good agreement with other experimental values in this mass region but somewhat lower than the value calculated from the deformed-nucleus, diffuse-edge, nuclear model.

The distribution of the 44 reduced neutron widths up to 23 ev is plotted in Fig. 3 and compared to a Porter-Thomas distribution. The agreement is obvious. Finally, the distribution of the 26 observed spacings between resonances up to 13 ev are plotted in Fig. 4, where D' is the average of the 26 spacings. Three computed curves are also shown: a Wigner distribution for a single spin state, a random distribution of two Wigner distributions of the same level density, and a random distribution of two Wigner distributions with the $(2J + 1)$ law for level density. The Wigner distribution for a single spin state appears to be the best fit to the data. However, it must be noted that no correction was made for "missed" resonances, which would increase the number of small spacings and, hence, produce better agreement with the curves for the two spin states.

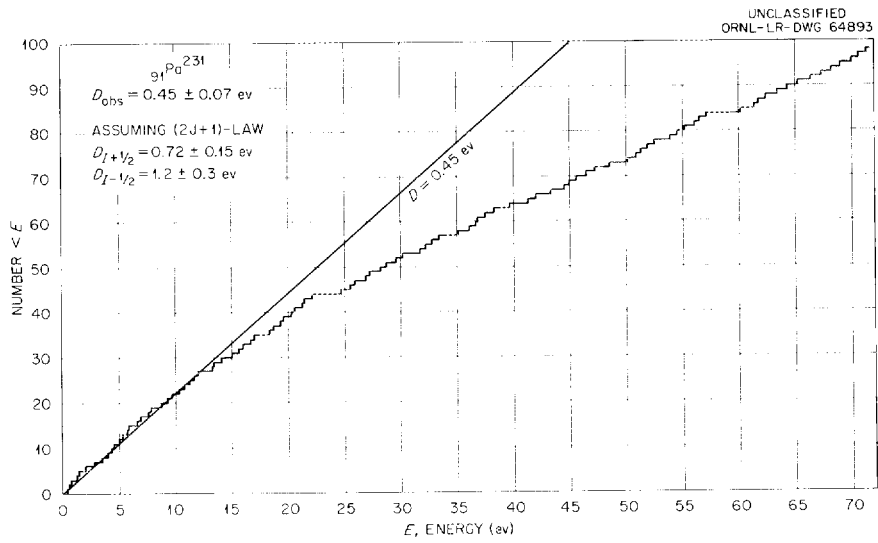


Fig. 1. Number of Resonances Observed in Pa^{231} as a Function of Neutron Energy.

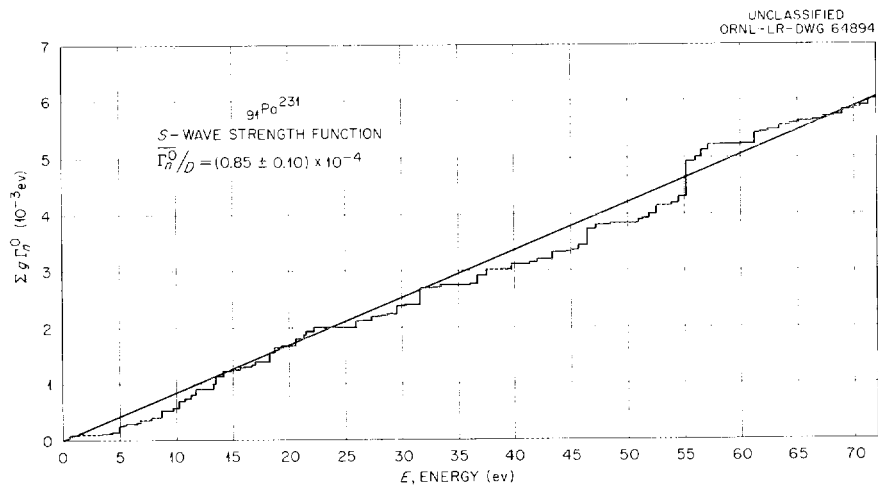


Fig. 2. Sum of the Reduced Neutron Widths ($g_{1,n}^0$) of the Resonance of Pa^{231} as a Function of Neutron Energy.

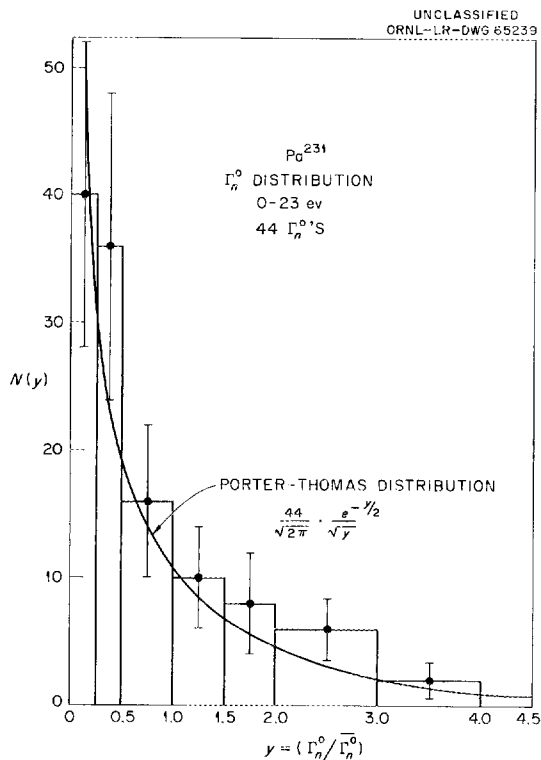


Fig. 3. Reduced Neutron Width Distribution of the 44 Resonances up to 23 ev in Pa^{231} Compared with the Porter-Thomas Distribution.

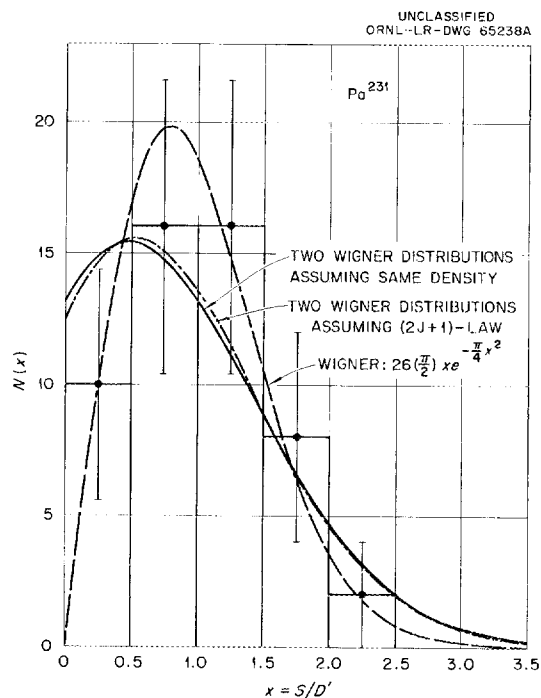


Fig. 4. Level Spacing Distribution of Pa^{231} from the 26 Observed Spacings Between Resonances up to 13 ev Compared with Three Theoretical Curves.

PARAMETERS OF NEUTRON RESONANCES IN W^{184} F. A. Khan¹

J. A. Harvey

Since tungsten has such a high melting point, it has been seriously considered for use in nuclear space reactors, which must operate at high temperatures. Experimental data on the fabrication of tungsten fuel elements at NASA have been very encouraging. Normal tungsten consists of four abundant isotopes: W^{182} (26.4%), W^{183} (14.4%), W^{184} (30.6%), and W^{186} (28.4%), which have thermal cross sections of 20 ± 2 , 11 ± 1 , 2.0 ± 0.3 , and 35 ± 3 barns respectively. Because of the low thermal cross section and expected low resonance radiative capture of W^{184} , this isotope looked very promising as a fuel-bearing material for rocket and satellite reactors.

Total neutron cross-section measurements had been made on the tungsten isotopes to several hundred electron volts. Parameters² for several resonances in the isotopes W^{182} , W^{183} , and W^{186} had been determined. The infinitely dilute resonance radiative-capture integrals for W^{182} , W^{183} , and W^{186} were computed from the resonance parameters to be 550, 400, and 550 barns respectively. Only one resonance had been observed in W^{184} at 185 ev, which gave a resonance radiative-capture integral of only ~ 5 barns. Hence there was a need for information on the parameters of resonances in W^{184} up to 1 or 2 kev for calculations of reactors using tungsten fuel elements enriched in W^{184} . Information on the resonance cross section along with the thermal absorption cross section of W^{184} would also set desirable limits on the composition of the enriched tungsten.

Transmission measurements were made with the ORNL fast-chopper spectrometers on an 8.4-g sample enriched to 95% in W^{184} and upon normal tungsten samples. The W^{184} metal powder had been pressed into three pieces $0.044 \times 0.330 \times 0.946$ in. The M1 rotor with the 45-m flight path was used for measurements from 2 kev to 44 ev with a resolution of $0.06 \mu\text{sec/m}$ and from 45 to 2.5 ev with a resolution of $0.2 \mu\text{sec/m}$. A comparison of the transmissions of the W^{184} and normal tungsten samples showed that there were many large resonances in W^{184} above the only previously known resonance at 185 ev, and also possibly a small resonance at 102 ev. In order to obtain better data at the higher energies, high-resolution measurements by use of the M11 rotor and the 180-m flight path were made from 2 kev to 105 ev with a resolution of 10 nanoseconds/m. The thickness (0.0160 atom/barn) of the normal tungsten sample (30.6% W^{184}) was selected to have approximately the same number of atoms per barn of W^{184} as the sample enriched to 95% W^{184} , which contained 0.00453 atom/barn. The thicknesses of the other isotopes in the enriched W^{184} sample were less by factors > 50 than their thicknesses in the natural tungsten sample.

The transmission data were analyzed up to 2 kev with the area analysis program written for the IBM 7090 by Atta and Harvey.³ The resonance at 185 ev was the only one analyzed with the shape-analysis program, since the energy resolution was not sufficiently good for the higher energy resonances.

¹On leave from AEC, Pakistan.

²D. J. Hughes, B. A. Magurno, and M. K. Brussel, *Neutron Cross Sections*, BNL-325, 2d ed, suppl No. 1.

³S. E. Atta and J. A. Harvey, *Numerical Analysis of Neutron Resonances*, ORNL-3205 (1961).

Nine resonances were assigned to W^{184} and were analyzed to obtain neutron widths for the resonances, assuming a value for Γ_γ of 0.047 ev. Since the values of Γ_n are $\gg \Gamma_\gamma$, the accuracy on Γ_n is quite independent of the value chosen for Γ_γ . The parameters of the resonances are given in Table 1. The average level spacing computed from these data is 133 ± 27 ev. These data give an s-wave strength function, $(\bar{\Gamma}_n^0)/D$, of $(3.7 \pm 1.8) \times 10^{-4}$, which is in reasonable agreement with theoretical predictions.

 Table 1. Parameters of Resonances in W^{184}

E_n (ev)	Γ_n (ev)	Γ_n^0 (ev)	Contribution to I_γ (barns)
184.9	1.13 ± 0.13	0.083 ± 0.010	5.38
311.9	0.109 ± 0.017	0.0062 ± 0.0010	1.39
425.3	0.116 ± 0.020	0.0056 ± 0.0010	0.75
687.0	0.75 ± 0.09	0.029 ± 0.003	0.39
805.0	2.01 ± 0.16	0.071 ± 0.006	0.29
964.0	1.35 ± 0.22	0.043 ± 0.007	0.20
1093	3.8 ± 0.3	0.113 ± 0.009	0.16
1142	0.47 ± 0.16	0.014 ± 0.004	0.13
1271	1.3 ± 0.3	0.037 ± 0.008	0.11

The contributions of the resonances to the infinitely dilute radiative-capture integral, I_γ , have been computed from the formula

$$I_\gamma = \frac{\pi}{2} (2.6 \times 10^6) \sum_{\lambda=1}^N \left(\frac{\Gamma_\gamma^\lambda}{E_\lambda^2} \right) \frac{1}{1 + (\Gamma_\gamma^\lambda / \Gamma_n^\lambda)},$$

where I_γ is in barns, E_λ and Γ_γ^λ are in ev, and a value of 0.047 ev for Γ_γ is assumed. The contributions of the various resonances to the radiative-capture integral are given in Table 1. The estimated contribution of resonances above 1271 ev was computed to be 1.1 barns. The epithermal resonance radiative-capture integral, including this contribution and a 1-barn contribution from the $1/v$ thermal tail, equals 11 ± 2 barns. Hence the radiative-capture integral of W^{184} is about 40 times smaller than those of W^{182} , W^{183} , and W^{186} . It is clear from the above formula that a more precise value of Γ_γ is needed in order to decrease the error in the radiative-capture integral. The assumed value for Γ_γ of 0.047 ± 0.010 ev is the average of the average radiation widths of W^{182} and W^{186} , which are 0.047 ± 0.009 and 0.046 ± 0.010 ev respectively. To improve the value of Γ_γ for W^{184} , it would be necessary to make accurate measurements of the radiation widths of the resonances, particularly the 185-ev resonance.

The contribution to the thermal absorption cross section from the resonances in Table 1 has been computed with the formula

$$\sigma_{th} = \frac{2.6 \times 10^6}{4\sqrt{0.0253}} \sum_{\lambda=1}^N \frac{\Gamma_n^0 \Gamma_\gamma^\lambda}{E_\lambda^2},$$

where σ_{th} is in barns. Assuming a Γ_γ of 0.047 ± 0.010 ev, a value of 0.5 ± 0.1 barn was obtained, which is only 25% of the measured thermal cross section. The remaining 75% must arise from contributions from bound levels. This is quite reasonable, since a level with a reduced neutron width equal to the average reduced neutron width and bound by 76 ev (about one-half the average level spacing) would account for the remainder of the thermal cross section.

MANGANESE-BATH MEASUREMENTS OF η OF Pu^{239} ¹

R. L. Macklin

G. deSaussure²J. D. Kington²W. S. Lyon³

Manganese-bath relative measurements for Pu^{239} , similar to those reported earlier⁴ for U^{233} and U^{235} , are presented. The value of eta averaged over a thermal spectrum, for a black sample, is

2.058 ± 0.010 . Correction to a 2200-m/sec value introduces additional uncertainties because of unmeasured details of the thermal-spectrum shape.

The 2200-m/sec value found is $2.143 \pm \begin{matrix} 0.010 \\ 0.020 \end{matrix}$.

¹Abstract of paper submitted to *Nuclear Science and Engineering*.

²Neutron Physics Division.

³Analytical Chemistry Division.

⁴R. L. Macklin *et al.*, *Nuclear Sci. and Eng.* **8**, 210-20 (1960).

FISSION FRAGMENT CORRELATION EXPERIMENTS

F. J. Walter

J. H. Neiler

R. J. Silva

H. W. Schmitt

Measurements of the correlated energy spectra of fission fragment pairs were continued with Cf^{252} spontaneous fission and were extended to the thermal-neutron-induced fission of U^{235} . The results, together with a discussion of the present state of experimental techniques, will be reviewed; brief descriptions of the experimental apparatus, electronics, and correlation analyzer are included. The results of studies of surface barrier diode response to fission fragments, which were performed as a necessary adjunct to this work, are described in another report.¹

Experience gained from the californium work has provided guide lines for requirements on detectors to be used in fission work. Detector size should be as large as possible to allow use of fairly-large-area sources and neutron beams without excessive loss of geometric efficiency. The detectors should operate reliably at bias voltages large enough to ensure good "charge collection." Silicon resistivity should be optimized based on the following factors:

1. Too low a resistivity requires excessive bias voltage to obtain a barrier (sensitive) depth exceeding the fission fragment ranges. For example, if the resistivity is less than 25 ohm-cm the maximum internal electric field will exceed the critical breakdown field in silicon before the

barrier depth exceeds the range of fission fragments.

2. For large-area counters the shallow barrier depth resulting from low-resistivity material leads to large detector capacitance and therefore to poorer signal-to-noise ratios.

3. Too high a resistivity requires excessive bias voltage to obtain electric fields large enough to ensure saturation of "charge collection."

4. For high-resistivity material the large barrier depth resulting from the required bias leads to increased sensitivity to gamma-ray- and fast-neutron-induced "noise" broadening of the resolution. For any resistivity a long carrier lifetime is considered important for minimizing loss of charge by recombination along the densely ionized track of the fission fragment.

Following these criteria, surface-barrier detectors for U^{235} thermal-neutron-induced fission measurements at the ORR were made from 600-ohm-cm *n*-type silicon. A float-zone-purified silicon ingot having less than $\pm 10\%$ resistivity variation over the entire length and a charge carrier lifetime of 1.0 to 1.8 msec was used. Slices 1 mm thick were cut radially, adjacent slices being used to provide uniformity in each pair of detectors. The crystal wafers were lapped in No. 1800 Lappmaster compound and then etched

¹See "Response of Silicon Surface-Barrier Detectors to Fission Fragments," this report.

for 5 min on both sides in a modified CP-4 etch.² In order to minimize neutron spectrum distortion and reduce background counts from knock-on protons, a minimum quantity of amine-cured epoxy resin was used to mount the detectors in ceramic rings similar to those developed by R. J. Fox.³ After curing the epoxy, the front electrode was applied by vacuum evaporation of a 40- $\mu\text{g}/\text{cm}^2$ gold film and the rear electrode by vacuum evaporation of a film of aluminum. The finished detectors have an active area of 4 cm^2 . The pulse-height response of these detectors to fission fragments was found to saturate satisfactorily – that is, to give the same pulse-height and peak-to-valley ratio – at bias voltages between 50 and 150 v. At 200 v bias there was an indication of distortion (probably caused by a multiplication phenomenon) of the high-energy tail of the light fragment peak. Rounded collimators made of aluminum and located close to the detectors prevented fragments from reaching the edges of the detectors.

The source-detector chamber used for the neutron-induced fission is shown in Fig. 1. (The californium work was done with a somewhat simpler arrangement.) Several features of the chamber were found to be very useful. The shutter arrangement, by which the detectors may be shielded from the source, is a virtual necessity when alpha-active sources are used. This arrangement allows monitoring of the root mean square noise from the detector and electronics, and allows stability checks through periodic measurements of the overall gain of the system by injecting a known amount of charge into the detector circuit. The rack and pinion adjustments of the counter positions are convenient for measuring the effect of source backing thickness on energy resolution; in addition, the effect of spacing on the amount of excess noise introduced into the detectors from scattered neutrons and gamma rays from the reactor beam could be measured. By means of this series of measurements, the source-to-detector spacings could be optimized. The rotatable rod on which the source is mounted provides a convenient method for measuring the

shift in the fission fragment energy spectrum caused by the finite thickness of the source backing. The lead shielding was added to reduce noise from gamma and beta backgrounds arising from neutron capture in the beam collimator and chamber walls and from scattering out of the collimated beam.

A block diagram of the electronics used for the two-detector correlation measurements is given in Fig. 2. The preamplifier, main amplifier, and biased amplifier blocks are a single unit – the Q-2069C amplifier system developed by Blankenship⁴ from the original design by Fairstein.⁵ The pulse-height selectors, which are discriminators taken from ORNL A-1 amplifiers, are necessary to provide the coincidence-enabling signal to the correlated pulse-amplitude recorder. This device consists of a pair of analog-to-digital converters (ADC's), utilizing the standard lengthener, ramp generator, comparator, and oscillator countdown technique. Upon receipt of a coincident event the ADC units provide (to a paper-tape punch control) outputs in binary code representing the channel numbers into which each of the coincident pulse amplitudes fell. The tape punch-control unit translates the parallel information into serial hexadecimal code which is then recorded on paper tape. The tape format is such that the analyzer may be converted from 128 \times 128 to 256 \times 256 channels, and a third dimension containing a maximum of 16 channels may be added.

During the U^{235} experiment more than 10^6 events were recorded. The detectors were operated at 50 v bias, and maximum source-to-detector spacings resulted in a geometric efficiency of approximately 3%. The counting rate in the detectors at this geometry was approximately 60 counts/sec, and the correlated data acquisition rate, which was limited by the punch speed, was 7 to 8 counts/sec. The overall gain stability, which was checked every 2×10^4 events, varied less than $\pm \frac{1}{2}$ channel (± 0.3 Mev) during the run. The noise broadening of the resolution was completely dominated by the beam-induced noise and was approximately 70 kev full

²Composition by volume: 4½ parts glacial acetic acid, 5 parts 70% HNO_3 , 3 parts 48% HF.

³J. W. T. Dabbs and F. J. Walter (eds.), *Semiconductor Nuclear Particle Detectors*, NAS-NRC 32, pp 270–72 (1961).

⁴*Low Noise Amplifiers for Use with Solid State Detectors*, TID-6119 (1960).

⁵N. W. Hill and C. C. Courtney, *Instrumentation and Controls Div. Ann. Progr. Rept. July 1, 1960*, ORNL-3001, p 18.

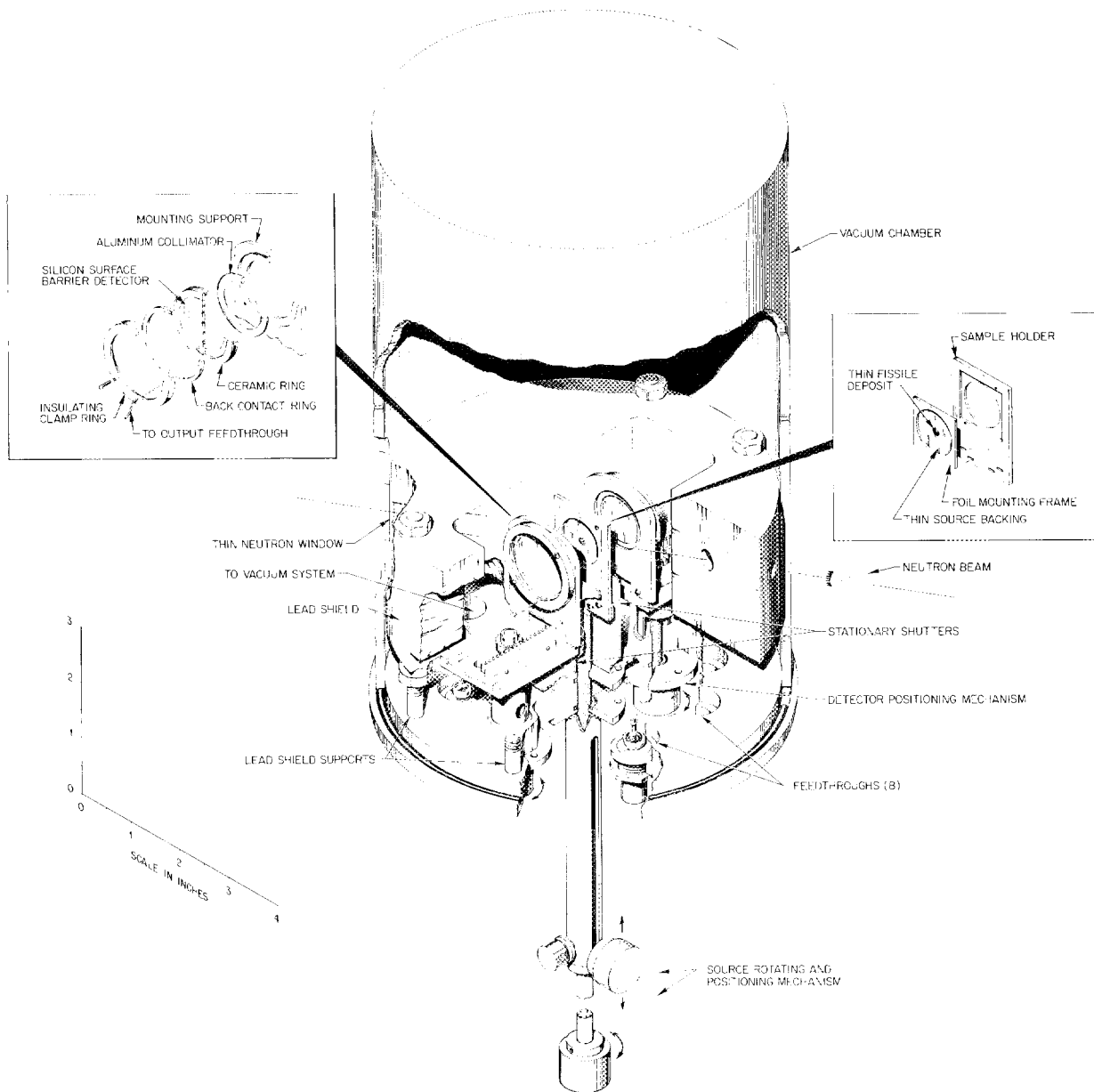


Fig. 1. Schematic Diagram of the Source-Detector Chamber Employed in U^{235} Thermal-Neutron-Induced Fission Correlation Experiments.

width at half maximum (compared with approximately 35 keV with the beam off).

The U^{235} source⁶ was made by vacuum evaporation onto a thin nickel foil. The observed peak-

⁶The authors gratefully acknowledge the U^{235} source preparation by R. M. Johnson.

to-valley ratio in the uncorrelated energy spectrum was 20/1 for both sides of the source, and the fission fragment energy loss in the source backing was 2.5 ± 0.3 MeV for the heavy fragment peak and 2.8 ± 0.3 MeV for the light fragment peak. Additional measurements of the alpha-particle energy resolution from both sides of similar sources and of the variation of alpha-particle

UNCLASSIFIED
ORNL-LR-DWG 52264R

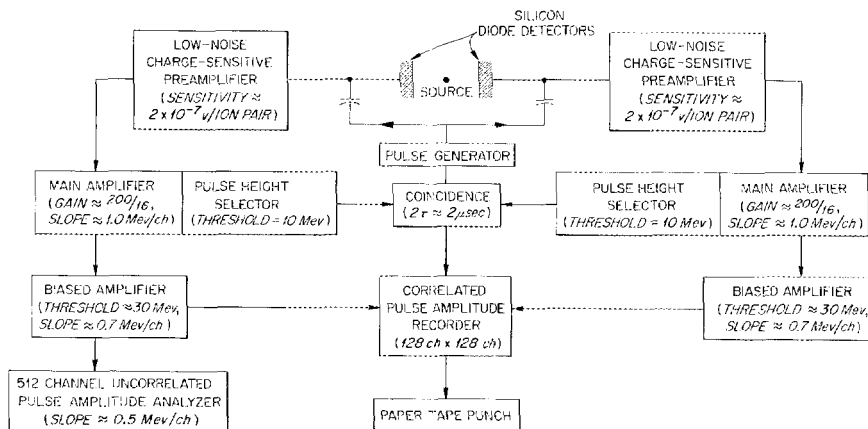


Fig. 2. Block Diagram of Instrumentation for Fission Correlation Experiments.

energy loss in these thin nickel films as a function of position on the film⁷ have also shown that these sources are quite uniform.

The pulse-height spectrum from detector No. 2 is shown in Fig. 3. The U²³⁵ deposit was facing this detector; thus the unperturbed spectrum is shown. The pulse-height spectrum in detector No. 1 appeared almost identical, but was slightly shifted as indicated above. Each point of the spectrum shown in Fig. 3 was obtained directly from the correlation data by summing events in all channels of side 1 corresponding to a given channel of side 2.

The correlation data are shown in Fig. 4. These data represent approximately 10⁶ events, recorded in a period of ~50 hr on 10.4 miles of paper tape. Sorting and summing of the data were performed on the Oracle; further analyses yielding mass distributions, mass-energy correlations, etc., are in progress with the aid of the IBM 7090. Detectors, amplifier gains, and post-amplifier biases were matched; thus the responses of the two sides were nearly identical. The width of each channel corresponds to about 0.6 Mev for both sides. Energies shown are based on comparisons with the energy spectrum obtained by Milton and Fraser from double time-of-flight measurements.⁸

⁷The authors gratefully acknowledge the carrying out of these tests by A. Chetham-Strode and J. S. Eldridge.

⁸J. C. D. Milton, private communication, 1962 (to be published).

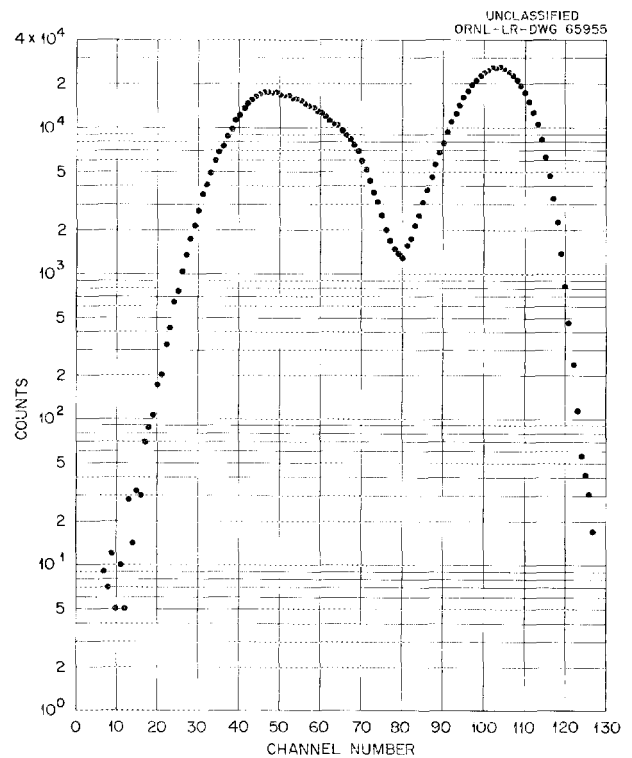


Fig. 3. Pulse-Height Spectrum for Thermal-Neutron-Induced Fission of U²³⁵ (Detector 2). Fragments incident on detector 1 produced a nearly identical spectrum, but shifted to slightly lower energies ($\Delta E = 2.5 - 2.8$ Mev) as a result of passage through the thin nickel backing.

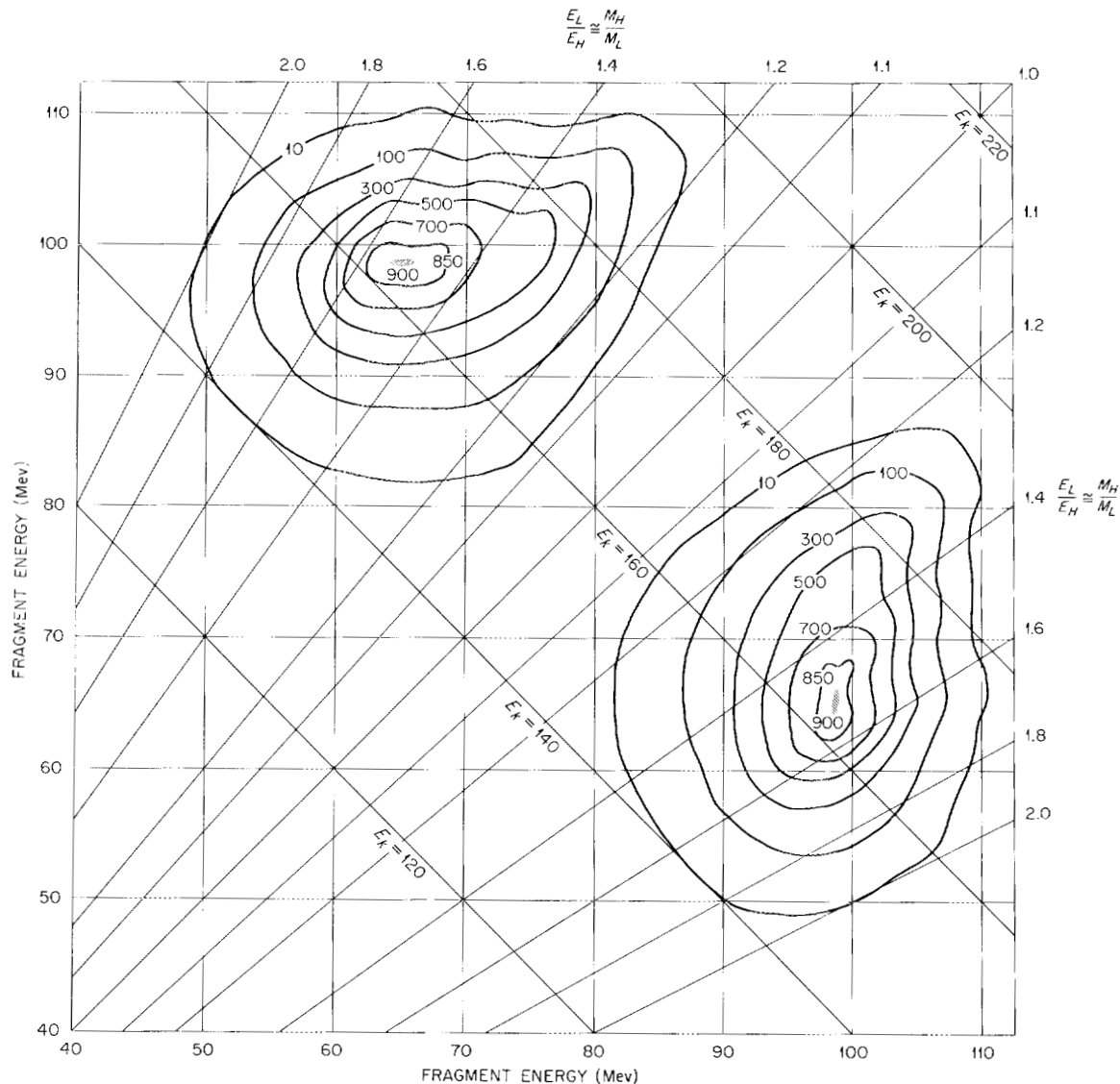


Fig. 4. Contour Diagram Representing the Correlation of Fragment Energies in the Thermal-Neutron-Induced Fission of U^{235} . Lines corresponding to constant mass ratio and constant total kinetic energy are indicated.

Features of the contours are in general agreement with those obtained by Gibson, Thomas, and Miller⁹ in a similar experiment. A preliminary

⁹W. M. Gibson, T. D. Thomas, and G. L. Miller, *Phys. Rev. Letters* 7, 65 (1961).

analysis of our data also indicates agreement with the appearance of fine structure in the calculated mass distribution. A few lines of constant mass are shown in Fig. 4, to indicate the much cleaner separation in masses of the two fragment groups relative to the separation in

energies. Preliminary analysis of these data indicates a peak-to-valley ratio in the mass distribution of about 300.

A similar experiment, in which about 10^5 events were recorded, was performed for the spontaneous fission of Cf^{252} . The preparation of a very thin and uniform source of Cf^{252} on a thin backing has, however, presented a major difficulty in these measurements. Since nearly all the locally available material (a few hundredths of a microgram) was required to make the source, it was not possible to use the desirable but low-yield methods of vacuum evaporation or electrostatic collection of recoil californium atoms from a second thin but very active source. The fragility of the thin backing material precluded the method of electrodeposition. The method finally employed consisted in drop-by-drop evaporation of a liquid solution of californium – a method which usually results in a source of nonuniform thickness consisting of rings and clumps. Considerable effort was put into obtaining reagents as free as possible from inert material and in trying different spreading agents. The source used in the present experiment was prepared by dropwise evaporation of a solution of californium in 0.05 M HCl and ethyl alcohol (20%) on a thin carbon film (approximately $20 \mu\text{g}/\text{cm}^2$). This source had an effective thickness corresponding to about a 40-keV energy loss by the 6.11-MeV alpha of Cf^{252} .

The integral pulse-height spectra are shown in Fig. 5. In this experiment, performed earlier than the U^{235} experiment, the main amplifier gains and postamplifier biases were not identical for the two sides – a condition which does not detract from the experiment but which explains the slightly broader (higher gain) appearance of the spectrum from side 1 relative to that from side 2. The peak-to-valley ratio is about 2.7. Preliminary analysis of the data does not indicate fine structure in the mass distribution, although deviations up to 10% from the smooth mass-yield curve may not be observed because of statistical limitation.

There is some tailing toward lower energies in the Cf^{252} experiment; this is probably a result of two conditions: (1) the fragments were not

collimated, and hence some fragments were incident on the detectors very near the edges where the pulse-height response might have been reduced, and (2) there was evidence of some slight clumping of the source material. Neither of these conditions existed for the U^{235} experiment described above; further work may be done with Cf^{252} as more source material becomes available.

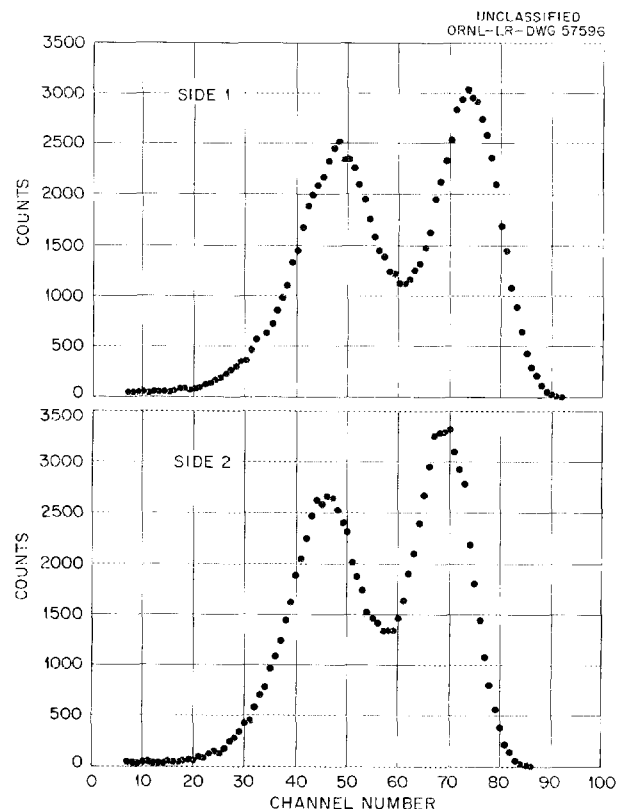


Fig. 5. Pulse-Height Spectra Obtained in the Cf^{252} Spontaneous Fission Fragment Correlation Experiment.

A PRECISION MEASUREMENT OF THE LONGITUDINAL POLARIZATION OF BETAS FOLLOWING P^{32} DECAY¹

A. R. Brosi²A. I. Galonsky³B. H. Ketelle²

H. B. Willard

The method of Mott-scattering has been used to determine the longitudinal polarization of 616-kev betas from the allowed Gamow-Teller decay of P^{32} . After rotation of the spin from longitudinal to transverse by a spherical electrostatic analyzer, the up-down asymmetry was measured over a wide range of gold target thickness. Source depolarization, plate scattering depolarization, multiple and plural scattering in gold and aluminum targets, and instrumental asymmetry effects were carefully investigated experimentally. Corrections were made for various backgrounds, wall scattering, finite geometry, and fringing fields. The final value of

$$P = (-0.990 \pm 0.009) v/c$$

¹Abstract of paper submitted to *Nuclear Physics*.

²Chemistry Division.

for $v/c = 0.891$ depends upon a calculated value of the Mott-scattering function, $S(\theta)$, which has not been corrected for screening, inelastic scattering, Schwinger radiative loss, or finite nuclear size effects. These are estimated to be of the order of 2% or less. Neglecting these effects and small theoretical corrections to the polarization which result from such effects as Δ -forbiddenness and finite nuclear size, this experimental result can be interpreted in terms of the beta-decay coupling constants. If time-reversal invariance and the two-component neutrino theory are assumed, the ratio $C_T/C_A = 0.011 \pm 0.010$ is computed from the measured polarization. On the other hand, assuming time-reversal invariance and $C_T = C_T' = 0$, then the ratio C_A'/C_A is limited to the range $+0.82$ to $+1.22$ by the result reported here.

³Midwestern Universities Research Association, Madison, Wisconsin.

HALF-LIFE OF He^6

J. K. Bienlein¹

Frances Pleasonton

A determination of the half-life of He^6 has been made in conjunction with experimental studies of internal bremsstrahlung in the beta decay of He^6 .

The source gas was produced by the same techniques that were used in earlier recoil and charge spectrometer studies² of He^6 , but an additional stage of purification with a titanium pump was included to remove contaminants known to be present in small concentrations. A Lucite cylinder, 6 in. long by $2\frac{1}{2}$ -in. ID and terminated by 0.002-in. aluminum windows, served as the source volume. The beta particles were counted by a plastic scintillator, together with a Du Mont 6363 photomultiplier tube and a DD2 Fairstein-

type amplifier. The data were recorded by a movie camera, operating at a rate of 12 to 15 frames/sec, which took pictures of two decade scalars. One of these registered the integral counts from the beta detector; the other, working on a 60-cps signal, served as a clock.

After the He^6 gas flow in the source volume had reached a steady state, the camera started recording the counts as they accumulated on the scalars. Three seconds later, the source volume was isolated from the rest of the system by shutting a valve. The camera, however, continued to run for another 12 sec while the gas decayed. The initial counting rate was about 6000 counts/sec above a background rate of about 115 counts/sec. In order to accumulate enough counts for good statistical accuracy after the first few half-lives, 34 separate runs were made.

¹University of Erlangen, Erlangen, Germany.

²C. H. Johnson, Frances Pleasonton, and A. H. Snell, *Phys. Div. Ann. Rept. Mar. 10, 1959*, ORNL-2718, p 5.

During the time required for these runs, the background was measured seven times, with a statistical accuracy of 0.4% for each measurement.

In obtaining the data from the films, the following readings were made:

1. the first frame of each run;
2. the last frame before the valve was closed, as well as one intermediate frame;
3. the first frame visible after closing the valve (this act was noted by temporarily covering the lens of the camera);
4. at time intervals after step 3 of 0.25, 0.50, 1.00 sec and at every second thereafter, interpolating between frames as necessary.

The counts accumulated between successive readings were tabulated vs time, at the midpoint of each time interval. We thus established the existence of an equilibrium counting rate (steps 1 and 2), the isolation of the source volume (steps 2, 3, and 4), and the continued decay through step 4. Since the timing of the "break," while shutting the valve, varied from one run to another, least-squares fits were made to the data, both including and excluding the value tabulated at 0.375 sec. The two results agreed within their limits of error, thus confirming that the decay was well established by 0.25 sec after the "break."

A preliminary value of the half-life was obtained from five particular runs which were chosen because they immediately preceded background measurements and were also more extended in time than the others. They were

corrected for dead time ($1.0 \pm 0.1 \mu\text{sec}$) and background. They were then added together, giving an average counting rate of about 2500 counts/sec at 1.00 sec on our arbitrary time scale. When plotted, the data showed the presence of contaminants to the extent of 10 counts/sec, after 10 sec. Two separate least-squares fits were then made to the first 7 sec of the run which contained the statistically reliable points. In one case a correction for contamination was made by using a slope which was compatible with the half-life of N^{16} (7.3 sec), since it was known to be present in the gas. The second fit assumed an essentially constant contribution, during the decay of He^6 , from a much longer lived contaminant. In each case the computing machine³ was asked to find the best values for the constants N_{bkg} , N_0 , and λ in the function $N = N_{bkg} + N_0 e^{-\lambda t}$. Using the data corrected for N^{16} contamination, we obtained a value of $T_{1/2} = 0.781 \pm 0.010$ sec, while the fit obtained by use of a constant correction gave $T_{1/2} = 0.786 \pm 0.010$ sec.

These values are definitely lower than those previously published. Strominger, Hollander, and Seaborg⁴ list values ranging from 0.799 to 0.85 sec, while Ajzenberg-Selove and Lauritsen⁵ give a weighted mean value of 0.813 ± 0.007 .

³Courtesy of Dr. Nuding and co-workers from the Reactor Engineering Division, Siemens, Erlangen, Germany.

⁴D. Strominger, J. M. Hollander, and G. T. Seaborg, *Revs. Modern Phys.* 30, 603 (1958).

⁵F. Ajzenberg-Selove and T. Lauritsen, *Nuclear Phys.* 11, 17 (1959).

AN ABSOLUTE DETERMINATION OF THE He^6 BETA-DECAY ENERGY¹

C. H. Johnson

Frances Pleasonton

T. A. Carlson

The end point of the energy spectrum of recoils from beta decay of He^6 was observed with a spectrometer which is calibrated in terms of a

standard voltage cell. The average of two essentially independent measurements gives a maximum beta energy of 3.507 ± 0.004 Mev. Addition of the maximum recoil energy, 1.4 kev, gives a decay energy corresponding to an $\text{He}^6\text{-Li}^6$ atomic mass difference of 3.768 ± 0.004 micro-mass units.

¹Abstract of paper to be submitted to *Nuclear Physics*.

RECOIL ENERGY AND CHARGE SPECTRA FOR THE Na^{23} IONS FORMED FROM THE β^- DECAY OF Ne^{23}

T. A. Carlson

Recoil Energy

Precise measurements of the recoil energy and charge spectra following the β^- decay of He^6 have been previously reported.¹ By use of the same equipment as described in detail in those reports, similar measurements have been carried out on Ne^{23} (see Fig. 1). The Ne^{23} is produced in the center of the ORR by an (n,p) reaction on Na^{23} , which is in the form of sodium aluminum silicate. The radioactive gas is carried into a source volume, where, upon the decay of Ne^{23} , the sodium ions thus formed are analyzed for both their recoil energy and charge by means of a magnetic and an electrostatic analyzer in tandem.

The purpose of measuring the recoil-energy spectrum is to establish the angular correlation

between the β^- particle and neutrino. The decay scheme for Ne^{23} is shown in Fig. 2.² Both the principal and secondary branches involve β^- transitions which require Gamow-Teller selection rules. The contribution of Fermi interactions is negligible because of isotopic-spin selection rules. This means that either tensor or axial vector interaction or a mixture of the two can be expected. In Fig. 3 the experimentally determined recoil-energy spectrum is given, together with the theoretically predicted shapes for complete axial vector and complete tensor interaction. The theoretically calculated curves are based on the formulas given by Rose.³ The calculation includes considerations of both the primary and

¹C. H. Johnson, Frances Pleasonton, and T. A. Carlson, *Phys. Div. Ann. Progr. Rept.* Mar. 28, 1961, ORNL-3085; *Bull. Am. Phys. Soc.* 6, 277 (1961).

²J. R. Penning and F. H. Schmidt, *Phys. Rev.* 105, 647 (1957).

³M. E. Rose, *The Beta-Decay Interaction and the Analysis of Recoil Experiments*, ORNL-1593 (Sept. 15, 1953).

UNCLASSIFIED
ORNL-LR-DWG 3466OR2

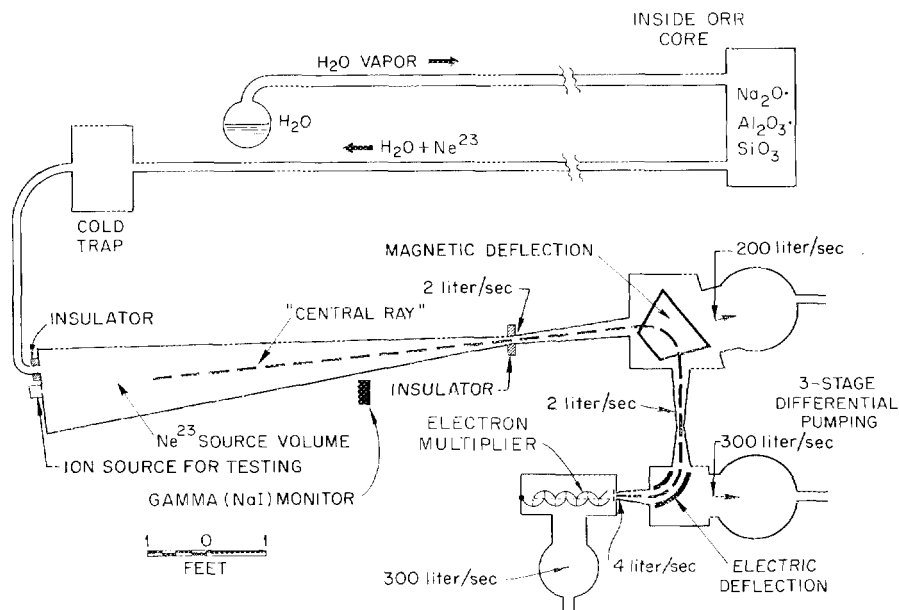


Fig. 1. Neon-23 Recoil Experiment.

the secondary branches, the 0.439-Mev gamma considered as being emitted isotropically. The usual Coulomb correction is included, but consideration of β^- transitions to the higher energy states is omitted.

Figure 3 shows not only that the principal interaction is axial vector but that there is no apparent admixture of tensor. In fact, experimentation has reached the point that we may assume

the validity of the two-component theory and say that there is indeed no admixture; the spectrum can now be evaluated for second-order effects.

Morita⁴ and Gell-Mann⁵ have discussed second-order effects which might change a recoil-energy spectrum, and Greuling and Rose⁶ have suggested that such effects might alter the recoil spectrum of Ne^{23} by about 1%. Figure 4 shows a plot of experimental values vs theoretical predictions, assuming no second-order effects, and no deviation is noted within 0.5% over the entire measured

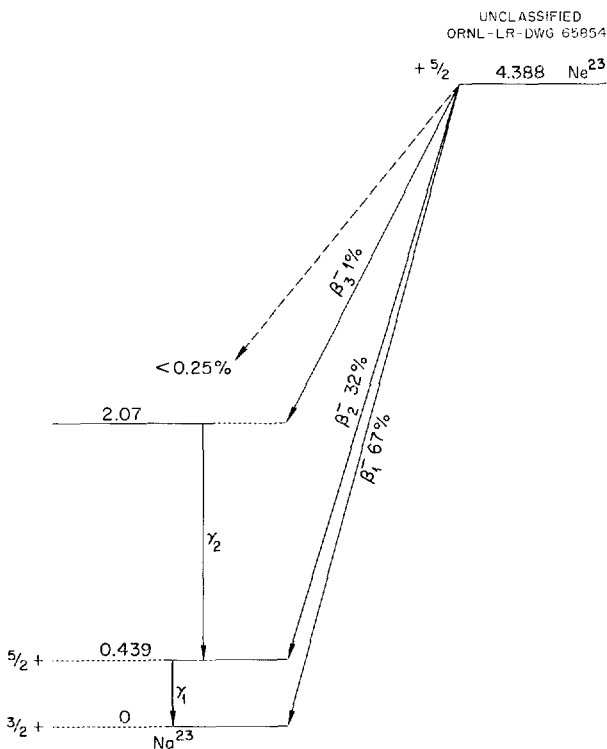


Fig. 2. Decay Scheme Proposed for Ne^{23} .

- ⁴M. Morita, *Nuclear Phys.* 14, 106 (1959-60).
- ⁵M. Gell-Mann, *Phys. Rev.* 111, 362 (1958).
- ⁶E. Greuling and M. E. Rose, private communication.

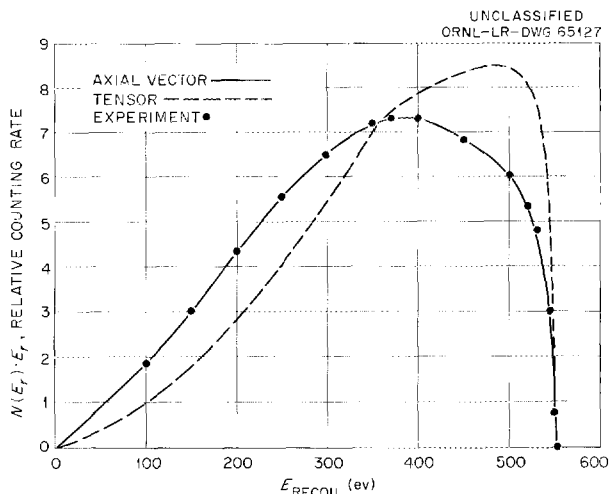


Fig. 3. Recoil Spectrum of $(\text{Na}^{23})^+$ Following the β^- Decay of Ne^{23} .

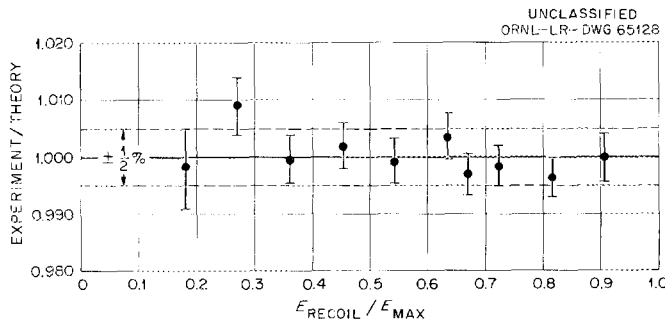


Fig. 4. Comparison with Theory of the Experimentally Determined Recoil Spectrum of $(\text{Na}^{23})^+$ from the β^- Decay of Ne^{23} , Where Theory Assumes $\lambda = -1/2$.

spectrum. Final conclusion, however, must await complete calculation of the second-order terms and a final evaluation of the experimental error, particularly with regard to the role that the accuracy of the decay scheme plays.

Charge Spectrum

Following β^- decay there is a sudden change in the nuclear charge which causes the atomic electrons to experience a new Coulombic field. This gives rise to excitation which may result in the loss of one or more electrons.

The charge spectrum of the sodium ions formed following decay of Ne^{23} has been measured in the same field-free source volume used for determining the recoil spectrum. Measurements were also made in a source volume containing a series of field rings which collect, focus, and accelerate the ions.⁷ This procedure destroys the versatility of measuring the recoil energy as well as the charge, but greatly enhances the collection efficiency. Agreement within counting statistics between the two sets of data adds confidence to the experimental procedures. Weighted averages of the results are given in Table I.

⁷For description of this piece of equipment, see A. H. Snell and Frances Pleasonton, *Phys. Rev.* **107**, 740 (1957).

Table I. Charge Spectrum of Na^{23} Ions Following β^- Decay of Ne^{23}

Charge	Experiment	Theory	
		Migdal	Semiempirical
1	79.08	79.5	79.6
2	17.49 ± 0.09	18.2	18.4
3	2.85 ± 0.06	2.1	1.7
4	0.49 ± 0.02	0.19	0.22
5	0.076 ± 0.007	0.013	0.016
6	0.006 ± 0.002	0.0007	0.0008
7	0.0007 ± 0.0007	0.00003	0.00004

Singly charged sodium ions represent the cases in which no electrons are shaken off following β^- decay, the charge arising simply from the difference in nuclear charge, while doubly charged ions represent the loss of one electron. There are essentially two main methods for removing more than one electron. One involves the removal of an inner orbital electron followed by one or more Auger processes, which in turn require the removal of one extra electron for each process. The probability of there being at least one Auger process following the removal of an inner electron is nearly unity, and in some cases a large vacancy cascade can occur, resulting in an ion of very high charge. The second method of removing more than one electron is simply the multiplicity of electron shake-off at the time of the β^- decay. A feature unique to the Ne^{23} study is that the spectrum of the multicharged ions can be nearly interpreted solely in terms of the multiplicity of electron shake-off, since the only inner orbital in neon is the 1s level, in which a hole will result in only one Auger process and for which the probability of shake-off is less than 1%.⁸⁻¹⁰ On the other hand, in the more complex atoms of argon, krypton, and xenon, Auger processes seem to play a large if not dominant role in producing multicharged ions.

Calculations of the expected charge spectrum from the decay of Ne^{23} have been made on the assumption that the probability of multiple shake-off of N or more electrons is the summation of all possible sets where N electrons are removed. The probability of each set is approximated by the product of N factors, where each factor is made up of the probability of removing a single electron from an nl orbital, (P_{nl}), times the number of ways in which electrons can be removed. That is,

$$P(N) = \sum_{\alpha} P_{\alpha}$$

and α is the set of numbers $M_{nl}^{(\alpha)}$, where $M_{nl}^{(\alpha)}$ is the number of electrons shaken out of the nl

⁸A. Migdal, *J. Phys. U.S.S.R.* **4**, 449 (1941).

⁹J. S. Levinger, *Phys. Rev.* **90**, 11 (1953).

¹⁰H. M. Schwartz, *J. Chem. Phys.* **21**, 45 (1953).

shell, with the restrictions that

$$\sum_{nl} M_{nl}^{(\alpha)} = N \text{ and } M_{nl}^{(\alpha)} \leq N_{nl},$$

where N_{nl} is the number of electrons originally in the orbital. P_{α} is thus expressed as

$$P_{\alpha} = \pi_{nl} N_{nl} (N_{nl} - 1) \dots$$

$$[N_{nl} - M_{nl}^{(\alpha)} + 1] (P_{nl})^{M_{nl}^{(\alpha)}} \cdot \frac{1}{[M_{nl}^{(\alpha)}]!}.$$

The probability of shaking off just N electrons and no more is equal to $P(N) - P(N + 1)$. Care is also taken in noting that removal of $1s$ electrons will be followed by an Auger process which will lead to the loss of one additional electron. The P_{nl} 's for the neon decay have been obtained from Migdal.⁸ The agreement of the calculations

based on Migdal with experiment is probably fortuitous, since Migdal's results for the L -shell electrons are at large variance with Schwartz¹⁰ and Levinger,⁹ and all three theories claim to be only approximate. Evaluation of the shake-off from the L shell has also been determined empirically by summing the total number of ions observed and subtracting the small effect of shaking off only K electrons, which from all three authors is about 0.6%. The calculations on the charge spectrum are obtained by using the same assumptions above for multiplicity of shake-off and also assuming that all the L electrons are indistinguishable from each other. A more specific and better calculation of the initial shake-off probabilities is needed and contemplated, but it already seems that at least qualitatively the multiplicity of shake-off can be correlated in a rather simple fashion.

ELECTRON SHAKE-OFF FOLLOWING THE β^- DECAY OF Ar^{41}

T. A. Carlson

Measurement of the charge spectrum of the K^+ ions formed from the decay of Ar^{41} completes a series of similar studies on the five rare gases from helium to xenon, begun by Snell and Pleasonton several years ago.¹⁻⁵ The experimental equipment and procedures have been described more fully elsewhere³ and consist mainly of allowing the radioactive gas, formed by bombarding potassium aluminum silicate [$\text{K}^{41}(n,p)\text{Ar}^{41}$] in the core of the ORR, to decay in a specially designed source volume. The Ar^{41} is purified so that the

pressure in the source volume is approximately 4×10^{-7} mm Hg, and the ions that are formed following β^- decay are collected, focused, and accelerated into a mass spectrometer which analyzes their charge.

The charge spectrum for the decay of Ar^{41} is given in Table I and graphically displayed in comparison with the studies on the other rare gases in Fig. 1. The argon work is seen to fit

Table 1. Charge Spectrum for Potassium Ions Formed from the Decay of Ar^{41}

Charge	Abundance (%)
1	82.3
2	12.6 ± 0.8
3	3.0 ± 0.2
4	1.4 ± 0.1
5	0.44 ± 0.06
6	0.16 ± 0.04
7	0.06 ± 0.02
8	0.016 ± 0.009

¹He⁶: T. A. Carlson, Frances Pleasonton, and C. H. Johnson, *Phys. Div. Ann. Progr. Rept. Mar. 28, 1961*, ORNL-3085; *Bull. Am. Phys. Soc.* **6**, 277 (1961).

²Ne²³: T. A. Carlson, "Recoil Energy and Charge Spectra for the Na^{23} Ions Formed from the β^- Decay of Ne^{23} ," this report; *Bull. Am. Phys. Soc.* **7**, 33 (1962).

³Kr⁸⁵: A. H. Snell and Frances Pleasonton, *Phys. Rev.* **107**, 740 (1957).

⁴Xe¹³³: A. H. Snell and Frances Pleasonton, *Phys. Rev.* **111**, 1338 (1958).

⁵T. A. Carlson *et al.*, pp 155-60 in *Chemical Effects of Nuclear Transformation* (Proceedings of a Symposium, Prague, October 1960), vol 1, IAEA.

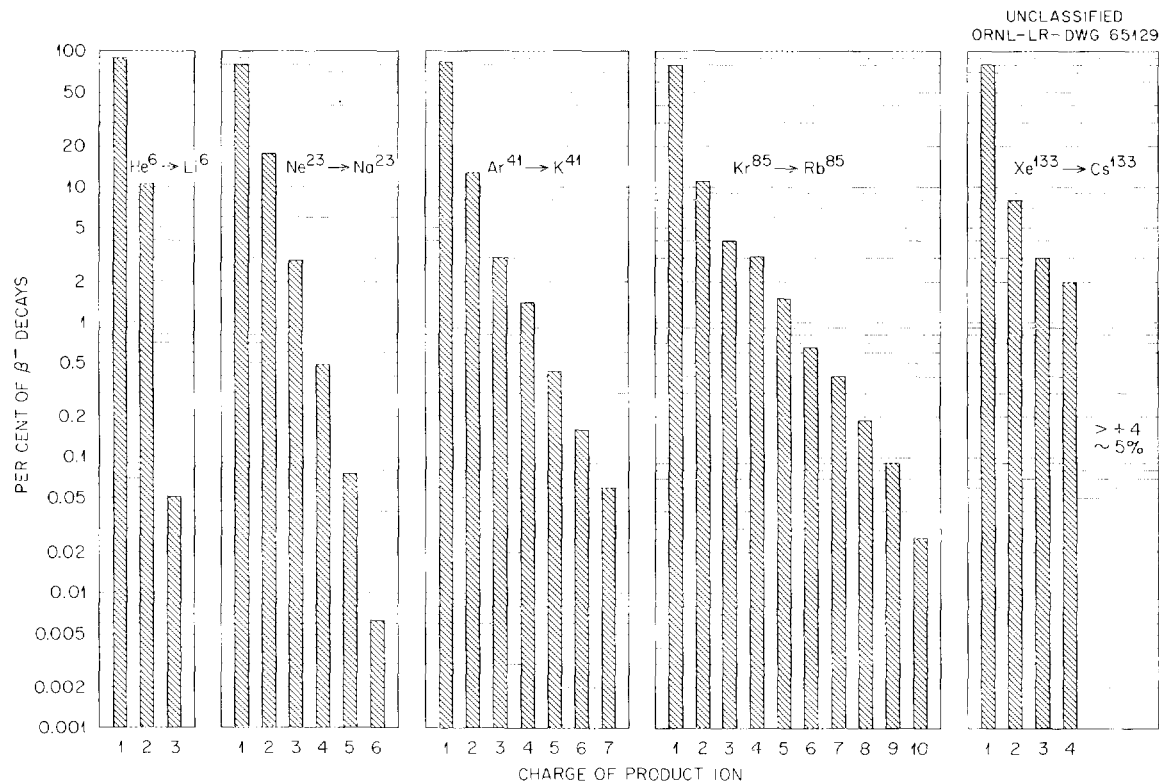


Fig. 1. Charge Spectra of Ions Formed as a Result of Beta Decay.

into the general pattern, which can be summarized by noting (1) that charge 1 is present in about 80% of the decays, indicating that most beta decays do not result in shaking off extra electrons, and (2) that the remainder of the spectrum decreases monotonically with charge, the rate of decrease becoming smaller as the atom becomes more complex.

To explain these observed generalizations, it is useful to consider the intensities of the doubly charged ion and the sum of the intensities of ions with charges greater than 2. The first generalization may be rephrased to state that the intensity of the charge 2 ion decreases slightly with Z from argon to xenon, but that this decrease is compensated by an increase in the total intensity for ions of charge greater than 2. The reason for concentrating attention on charge 2 is that it represents the shake-off of a single electron from the outermost octet of electrons which forms the structure of the rare gases from argon to xenon. The theoretically calculated probability for electron shake-off⁶⁻⁹ has the form $P = \alpha/(Z_{\text{eff}})^2$, where α is a constant associated with

a given orbital, and Z_{eff} is the effective charge. It is interesting to note that the experimental values for charge 2 from argon to xenon times $1/Z_{\text{eff}}$ are nearly constant, suggesting that the alpha's for the outer orbitals are independent of the rare gas. If the Ne²³ spectrum is considered as a "base-line" for shake-off not involving Auger processes,² it also seems apparent that the increase in the intensity for ions of charge greater than 2 is due principally to shake-off followed by multiple Auger processes.

In confirmation of the above discussion, a comparison is made between the experimental results and various theoretical predictions (Table 2). The calculations made from Schwartz⁶ and Migdal⁷ are based on generalized and approximate treatments; those of Winther⁸ and Green⁹ are specific and should be more reliable.

⁶H. M. Schwartz, *J. Chem. Phys.* **21**, 45 (1953).

⁷A. Migdal, *J. Phys. (U.S.S.R.)* **4**, 449 (1941).

⁸A. Winther, *Kgl. Danske Videnskab. Selskab, Mat.-fys. Medd.* **27**, 2 (1952).

⁹A. E. S. Green, *Phys. Rev.* **107**, 1646 (1957).

Table 2. Comparison of the Abundance of Charge 2 with Theoretical Predictions for Electron Shake-Off
(No. of Electrons Shaken Off/No. of β^- Decays)

Parent Atom	Experiment		Theory		Author
	% of +2	>+2	Shake-Off for Outermost Electrons (%)	Shake-Off for Inner Electrons (%)	
He ⁶	10.6	0.05	10.5		Winther
Ne ²³	17.5	3.4	6.6	0.7	Schwartz Migdal
			19.6	0.6	
Ar ⁴¹	12.6	5.1	4.8	1.4	Schwartz Migdal
			16.1	3.7	
Kr ⁸⁵	10.9	9.9	9.0	4.4	Green
Xe ¹³³	8	~12			

DECOMPOSITION OF $(\text{CH}_3\text{Xe}^{131})^+$ FOLLOWING THE NUCLEAR DECAY OF $\text{CH}_3\text{I}^{131}$ ¹

T. A. Carlson

R. M. White²

The charged fragments resulting from the decay of $\text{CH}_3\text{I}^{131}$ have been measured by a specially designed mass spectrometer. In 70% of the decays, the parent ion CH_3Xe^+ remained intact, in

direct contrast to the decay of CH_3T in which hardly any CH_3He^+ was found.³

More than 20 other ions were also detected, including the doubly charged methyl xenon, $(\text{CH}_3\text{Xe})^{2+}$. Their relative abundances are discussed in terms of excitation resulting from the sudden change in nuclear charge, and from multiple Auger processes in cases where internal conversion accompanies the decay.

¹Abstract of paper to be published in *Journal of Chemical Physics*.

²1961 summer research participant.

³A. H. Snell and Frances Pleasonton, *J. Phys. Chem.* **62**, 1377 (1958).

MÖSSBAUER PARITY EXPERIMENT

F. E. Obenshain

H. H. Wegener¹

The Mössbauer nucleus Ni^{61} has been investigated.^{2,3} The ratio of the magnetic moments of the first excited state to the ground state is known. The relative sign of the magnetic moments

is also known, but the general sign of either the excited state or the ground state is unknown. To determine the absolute sign of one moment, for example μ_g , a beta-gamma coincidence experiment (Mössbauer parity experiment) has been designed.

¹University of Erlangen, Erlangen, Germany.

²F. E. Obenshain and H. H. Wegener, *Phys. Rev.* **121**, 1344 (1961).

³H. H. Wegener and F. E. Obenshain, *Z. Physik* **163**, 17 (1961).

The experimental arrangement is shown in Fig. 1. The source, Co^{61} in metallic nickel, is located in a "field-free" region and is moved by a cam and follower mechanism. The Mössbauer scatterer is

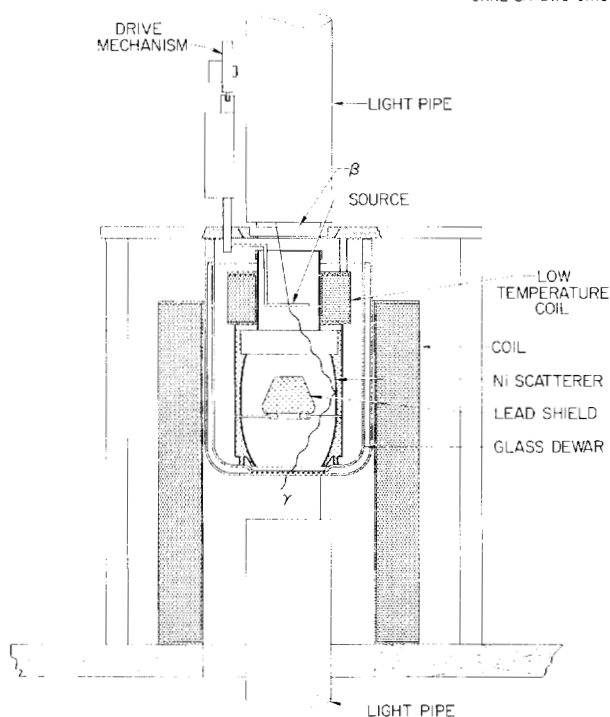
UNCLASSIFIED
ORNL-LR-DWG 6110

Fig. 1. Cross Section of Mössbauer Scattering Chamber. The external coil serves to magnetize the nickel scattering foil, and the small coil effectively cancels the external magnetic field at the source.

a nickel cylinder which is magnetized by an external magnetic field. The source and scatterer are maintained at 80°K by a liquid-nitrogen bath. The beta counter is located at the top of the apparatus, the gamma counter at the bottom. The beta from the Co^{61} decay is counted in coincidence with the scattered gamma from the decay of the Ni^{61} .

The beta is polarized because of parity violation, and as a result the excited Ni^{61} nucleus will be partially polarized. This polarization is then passed on to the gamma radiation and is manifest by a certain degree of circular polarization of the gamma. A theoretical⁴ treatment has been done to obtain the emission spectrum of the Mössbauer gamma. The calculation involves the Co^{61} ground state A , the Ni^{61} excited state B , and the Ni^{61} ground state C . Because of the magnetic field in the nickel metal, these states will be split into

⁴This calculation was done in cooperation with M. E. Rose; only the results will be reported here.

$(2J + 1)$ sublevels due to the $(\mu \cdot H)$ interaction. Let the magnetic quantum numbers of the three levels be designated by M_A , M_B , and M_C ; then consider the beta-gamma cascade $M_A \rightarrow M_B \rightarrow M_C$. If M_A and M_C are fixed, there will be, in general, several different values of M_B that are possible. Therefore, interference between adjacent sublevels of the excited state will occur,⁵ provided that there is sufficient overlap of the neighboring levels, which is the case for Ni^{61} . The frequency dependence of the emitted gamma radiation is not, in this case, a simple sum of Lorentz-shaped lines with different relative intensities, but has a more complicated shape because of the interference terms.

To calculate the emission spectrum of the gammas which are in coincidence with the preceding beta, it was possible to apply the resonance scattering theory developed by Weisskopf.⁶ It is only necessary to replace the photon-absorption Hamiltonian occurring in Weisskopf's formulation by the beta-decay Hamiltonian. The final expression for the spectrum is obtained by a straightforward application of angular correlation technique, and for numerical results by the use of the IBM 7090 computer.

The results of this calculation are shown in Fig. 2. The upper curves represent the gamma spectra for the case when the beta and gamma go off in opposite directions and the beta has a velocity of $v = 0.87c$. The distinction must be made between the two circular polarizations $P = \pm 1$. The intensities of the two polarizations are different because of parity violation.

The lower curves of Fig. 2 give the probability for Mössbauer scattering in the presence of an external magnetic field. The direction of the magnetic field is along the direction of propagation of the gamma. The curves shown are for the two possible polarizations P . In addition to P the sign of μ_g becomes important, as is indicated in the figure.

The velocity dependence (Mössbauer spectrum) of the beta-gamma coincidence rate is obtained in

⁵G. Felsner and M. E. Rose, *Resonance Scattering of Linearly Polarized Gamma Rays on Nuclei*, ORNL-3042 (1961).

⁶V. Weisskopf, *Ann. Phys.* **9**, 23 (1931).

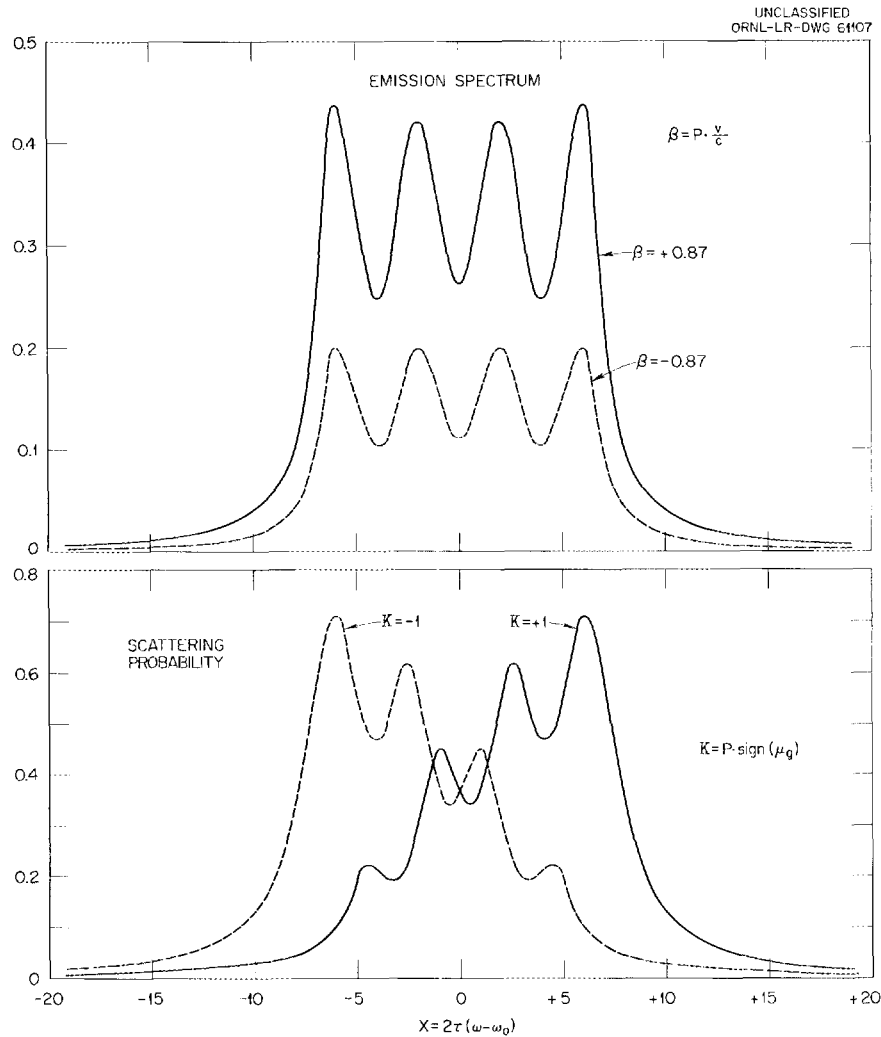


Fig. 2. Form of Gamma-Emission Spectrum in Coincidence with the Preceding Beta (Upper Curves). The intensities are different for the two possible polarizations $P = \pm 1$. The lower curves give the scattering probabilities for the two polarizations. Here the sign of the magnetic moment μ_g becomes important.

the usual way by folding the emission and scattering probabilities. The result is shown in Fig. 3. The solid curve is not symmetrical to $v_s = 0$. A 30% lower coincidence rate is expected for $v_s = +1.6$ mm/sec than for $v_s = -1.6$ mm/sec; for this case the sign of μ_g is taken to be positive. If this is not the proper sign, the mirror image of this curve would be obtained. The dashed curve of Fig. 3 represents the Mössbauer spectrum for the single gamma rate, which is, of course, symmetrical to $v_s = 0$. A measurement of this

curve gives a check on the symmetry of the apparatus.

The effect in coincidence is diluted by a background of scattered annihilation radiation, and the apparatus is being modified slightly in order to reduce this background. However, preliminary results show that the Mössbauer effect in the scattering position, that is, single gamma rate, may be obtained with this apparatus. The result is approximately what is expected from absorption experiments.²

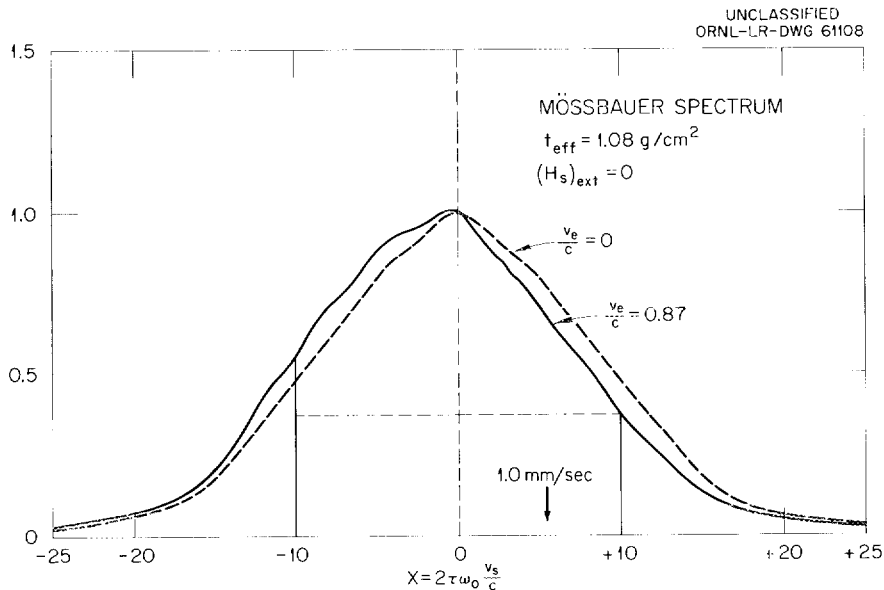


Fig. 3. Emission Spectrum and Scattering Probability of Fig. 2 Folded Together in the Usual Way (Solid Curve). The Mössbauer spectrum for this case is not symmetrical to $v_s = 0$. The effect for $x = +1$ is about 30% less than for $x = -1$. The Mössbauer spectrum for the singles rate (dashed curve) is symmetrical to $v_s = 0$ and serves as a check on the symmetry of the equipment. The effective thickness of the scattering foil is $t_{\text{eff}} = 1.08 \text{ g/cm}^2$.

A MÖSSBAUER STUDY OF THE 77-keV GAMMA TRANSITION OF Au^{197} IN A SERIES OF FERROMAGNETIC ALLOYS. THE MAGNETIC MOMENT OF THE FIRST EXCITED STATE OF Au^{197}

L. D. Roberts

J. O. Thomson¹

The copper-nickel alloy system has often been investigated experimentally and theoretically. This solid-solution system has the interesting property that the ferromagnetic moment and curie temperature fall linearly with increasing copper content, becoming zero at about 60 at. % copper. This behavior has been described theoretically² as due to a partial transfer of electron charge from the copper s -state to the nickel d -state, gradually filling the latter as the copper percentage is increased, and thus attenuating the ferromagnetic properties of the substance. In a theoretical discussion of this alloying process using the rigid-band model,² Wohlfarth gave a prediction of the

behavior of the s -state density on the copper atoms. In the understanding of the magnetic behavior of the alloy, the s -state density on the copper is clearly of comparable importance to the d -band filling. Until the advent of the Mössbauer method, however, no experimental technique was available to measure the amplitude of the s -state wave function. The Mössbauer method does this nicely for suitable nuclei, the isomer shift being proportional within an additive term to the s -state density at the Mössbauer nucleus.

Unfortunately, there is no copper nucleus suitable for Mössbauer-effect studies. However, the 77-keV gamma of Au^{197} gives a conveniently measurable Mössbauer effect, and the gold-nickel alloy system has magnetic properties which are very similar to those of copper-nickel. A study of the gold-nickel system has been made for a series of 11 gold-nickel alloy compositions.

¹Summer 1961 visitor and consultant from the University of Tennessee, Knoxville.

²E. P. Wohlfarth, *Proc. Roy. Soc. (London)* **A195**, 434 (1949).

The gamma-ray source used in these studies was a metallic sample of platinum enriched in Pt^{196} . This was neutron activated in the ORR to produce Pt^{197} , which beta-decays to Au^{197} . The absorbers that have been studied are pure gold and a series of gold alloys and compounds. The 77-keV gamma originates from the first excited state of Au^{197} of spin $\frac{1}{2}$ and with a previously unmeasured magnetic moment. The ground state has a spin of $\frac{3}{2}$ and a magnetic moment of $+0.14$ mm. The measurements were made at 4.2°K . In the nonferromagnetic materials a single Mössbauer absorption line is observed, while in ferromagnetic materials a hyperfine structure consisting of two well-resolved lines is seen. Each of these lines is a triplet. Some progress (not reported here) has been made toward resolving the triplet structure.

Mössbauer Effect in Pure Gold

Figure 1 shows the Mössbauer absorption line for pure gold. The solid line drawn is the Lorentz curve corresponding to the lifetime $\tau_{1/2} = 1.9 \times 10^{-9}$ sec, previously measured by Sunyar.³ It is seen that our results are in good agreement with those of Sunyar, and that the natural width

³A. Sunyar, *Phys. Rev.* **98**, 653 (1955).

is thus obtained. This is one of the few instances in which the Mössbauer absorption is found to have the natural width. It should be noted that the isomer shift is negative, -1.3 ± 0.2 mm/sec.

Gold-Nickel Alloys

When gold is alloyed with nickel, the Mössbauer line for gold may be expected to shift and to broaden. The shift corresponds to the change of the s -state density at the gold nucleus. The broadening arises from magnetic effects (Zeeman splitting) and from a variation of s -state density from atom to atom. In the most simple rigid-band picture, there would be no broadening of the latter type. These effects are illustrated in the data in Fig. 1 along with Figs. 2-5.

Here, with increasing atomic percentage of nickel the line is seen to shift and broaden and finally to resolve into two peaks. Figure 6 shows the isomer shift as a function of alloy composition for the 11 alloys studied. The results are seen to fall nicely on a straight line. This strongly departs from the predictions of the rigid-band picture.² Figure 7 shows the broadening of the line as a function of composition. It is seen that the increase in width above the natural width remains moderate compared with the total shift with composition from 0 to 100% nickel over a

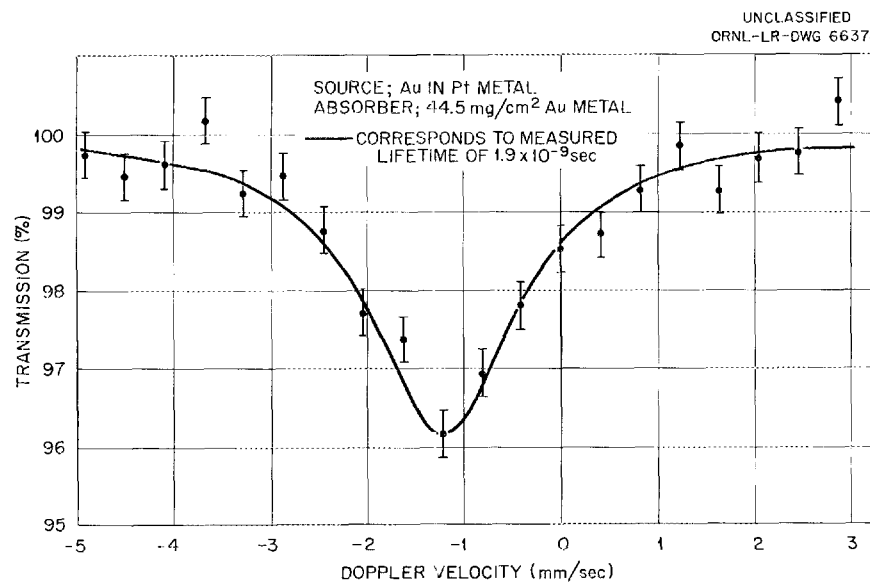


Fig. 1. Mössbauer Absorption and Lifetime Measurement for Pure Gold.

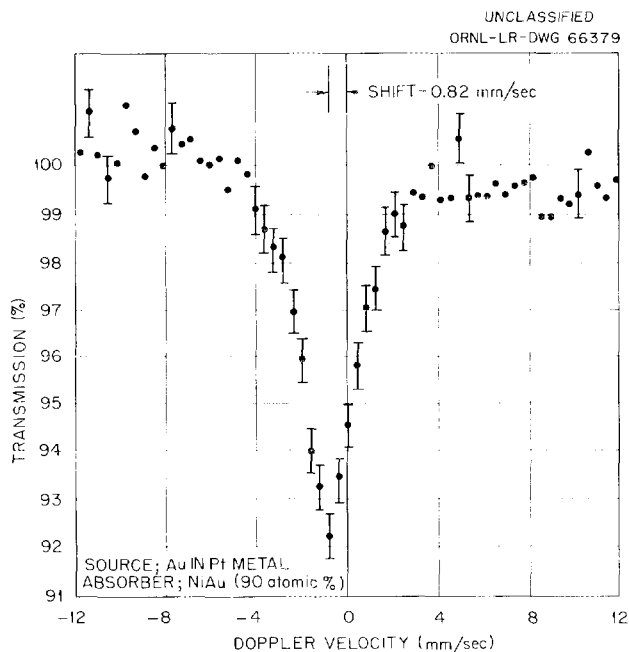


Fig. 2. Mössbauer Absorption Line for a Gold-Nickel Alloy with 90 at. % Gold.

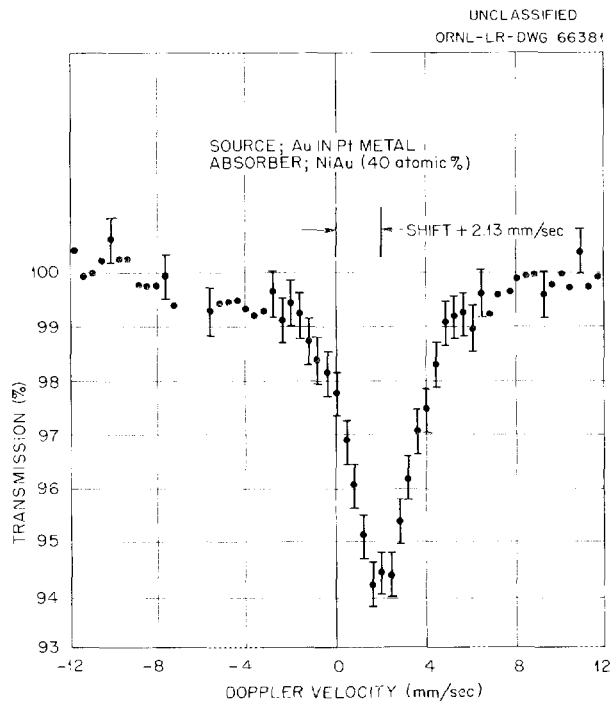


Fig. 4. Mössbauer Absorption for a Gold-Nickel Alloy with 40 at. % Gold.

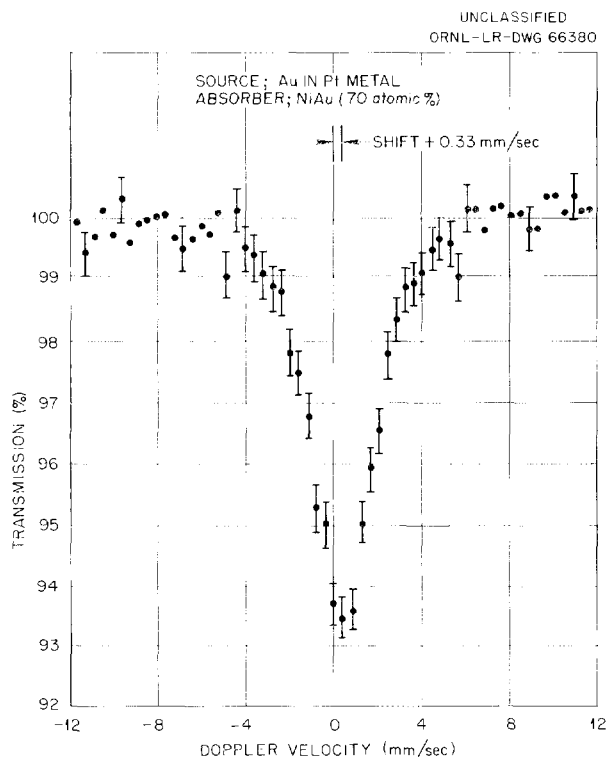


Fig. 3. Mössbauer Absorption for a Gold-Nickel Alloy with 70 at. % Gold.

fair composition range at the gold-rich end, reflecting in a degree the rigid-band picture. On the other hand, the width increases most rapidly with composition here. It should be possible to correlate these observations in the gold-rich region with the theoretical treatment of the Knight shift in alloys given by Blandin and Daniel.⁴ The results over the whole composition range disagree with the rigid-band model. It seems remarkable that neither the *s*-state density on the gold nor the line width shows any abrupt change in behavior in the composition region at which the alloys become ferromagnetic.

Magnetic Moment of the First Excited State of Au¹⁹⁷

Measurements have been reported previously⁵ of the hyperfine splitting in the Mössbauer spectrum for 1 at. % alloys of gold in iron and cobalt. Figure 5 shows this result for 1 at. % gold in nickel.

⁴A. Blandin and E. Daniel, *J. Phys. Chem. Solids* 10, 126 (1959); E. Daniel, *J. Phys. Chem. Solids* 10, 174 (1959).

⁵L. D. Roberts and J. O. Thomson, *Bull. Am. Phys. Soc.* 6, 230 (1961); *Bull. Am. Phys. Soc.* 6, 462 (1961).

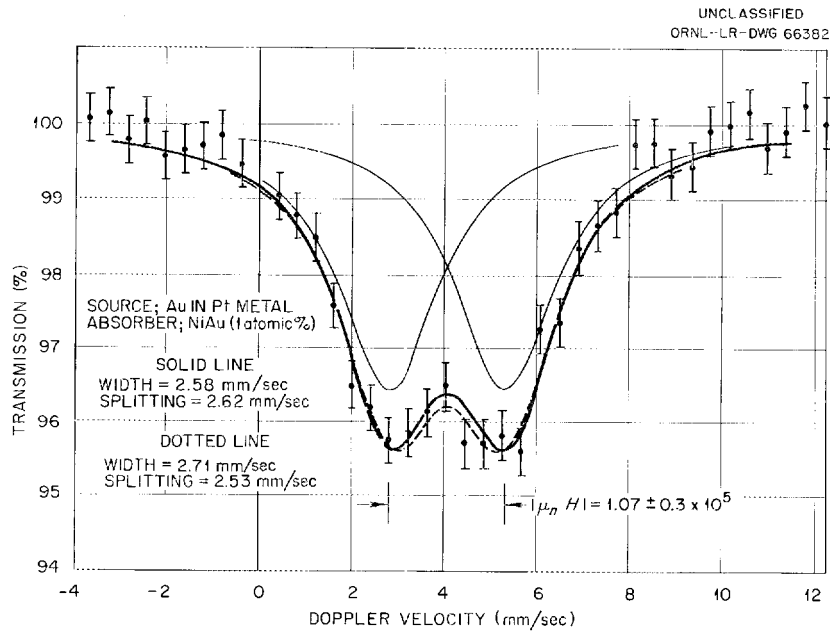


Fig. 5. Mössbauer Absorption for a Gold-Nickel Alloy with 1 at. % Gold Showing Splitting into Two Peaks.

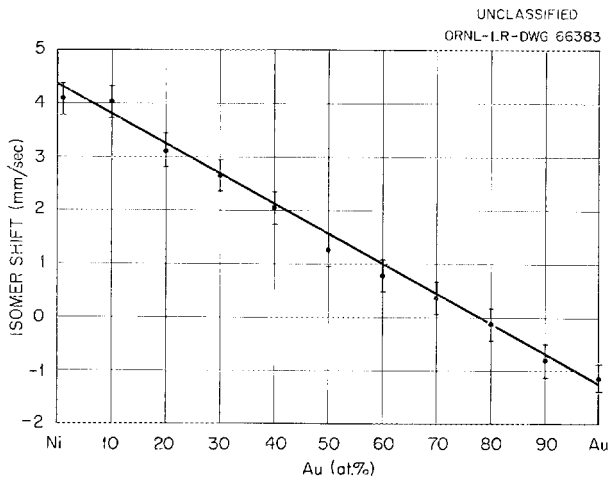


Fig. 6. Isomer Shift of the Au^{197} Mössbauer Absorption Line as a Function of Composition for the Gold-Nickel Alloy System.

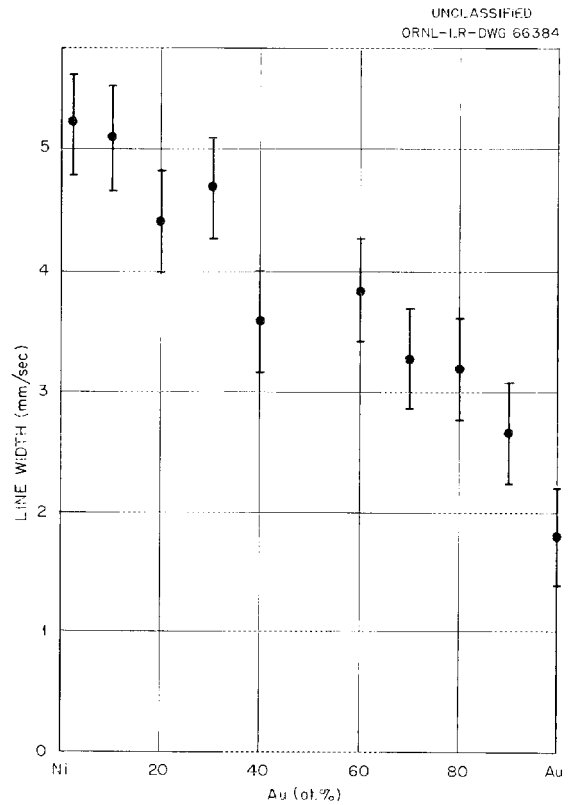


Fig. 7. Width of Mössbauer Absorption Line for Gold-Nickel Alloys as a Function of Composition.

In Fig. 8 our measured value of $|\mu_n H|$ is plotted as the magnetic moment of the host material: 2.22, 1.72, and 0.61 for iron, cobalt, and nickel. Here H is the effective magnetic field at the nucleus. In some nuclear orientation experiments with Au¹⁹⁸, Samoilov⁶ and co-workers have measured this field for gold in iron and nickel. Their results, plotted as (o) in Fig. 8, are seen to be in good agreement with our measurements within a normalization factor, that is, μ_n . If their field values are accepted, the magnetic moment of the first excited state of gold may be calculated as $\mu_n = |0.45|$. This is a remarkably small moment. The simple shell model would assign this state as having s -character, and for such an odd proton spin $\frac{1}{2}$ state the shell-model moment would be much larger. The above result thus would seem to indicate a strong configuration mixing with the adjacent $d_{3/2}$ state.

The linear behavior of the effective field H with magnetic moment of the host seems natural enough, but this is the only system for which this simple behavior has been observed.

⁶V. N. Samoilov, V. V. Sklyarevskii, and V. D. Gorobachenko, *J. Exptl. Theoret. Phys. (U.S.S.R.)* 41, 1783-86 (1961).

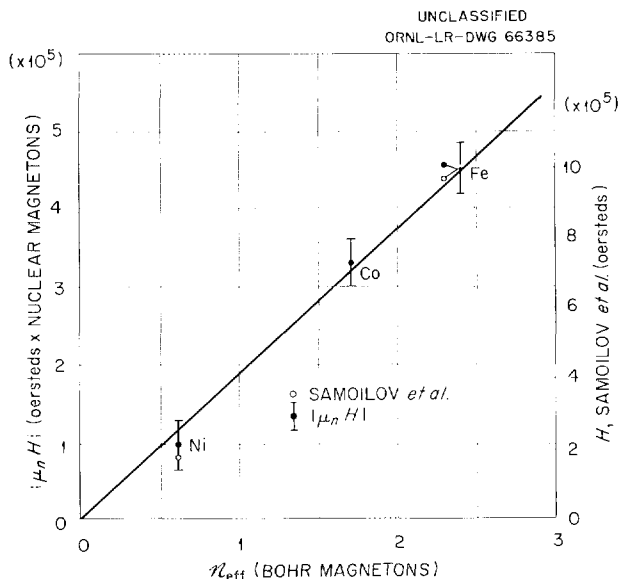


Fig. 8. The Value of $|\mu_n H|$ for 1 at. % Gold Dissolved in Iron, Cobalt, and Nickel.

ISOMER SHIFT OF GOLD IN A NUMBER OF ALLOYS AND COMPOUNDS

J. O. Thomson¹ H. Pomerance C. F. Dam² L. D. Roberts

The isomer shift in a Mössbauer experiment gives information about the s -state density at the Mössbauer nucleus times the change of nuclear size when the gamma ray is emitted or absorbed. In recent nuclear model studies on Au¹⁹⁷, configurations have been proposed for which the nuclear volume may increase, decrease, or change virtually not at all. The fact that a large isomer

shift is observed for gold³ demonstrates that the nuclear volume does change appreciably. Measurements of the isomer shift for gold for a number of environments are reported here. The purpose is to obtain a conclusion about the sign of the nuclear volume change which will be as well documented as possible. The new as well as some earlier results are given in Fig. 1. Note that the isomer shift is positive relative to pure gold for all the materials studied.

¹Summer 1961 visitor and consultant from the University of Tennessee, Knoxville.

²Summer 1961 research participant from Cornell College, Mount Vernon, Iowa.

³L. D. Roberts and J. O. Thomson, *Bull. Am. Phys. Soc.* 6, 230 (1961); *Bull. Am. Phys. Soc.* 6, 462 (1961).

UNCLASSIFIED
ORNL-LR-DWG 61918A

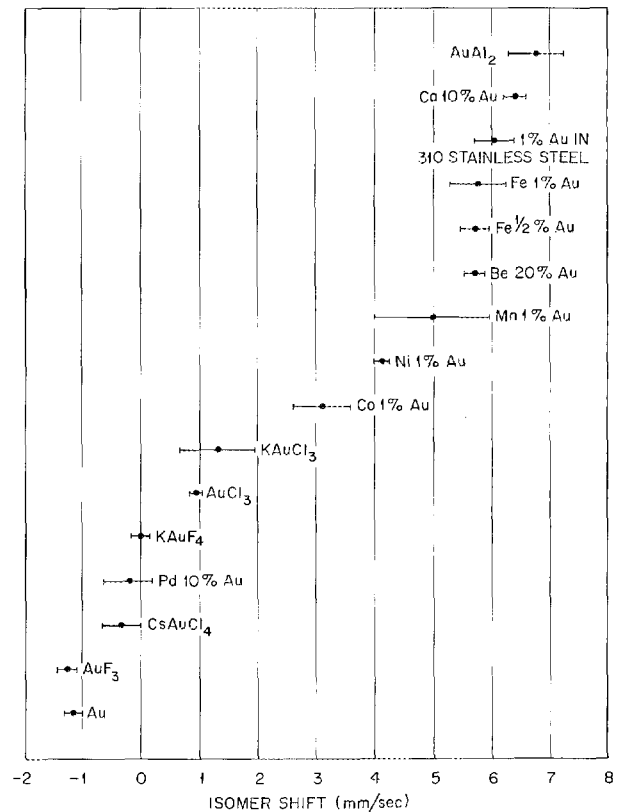


Fig. 1. Summary of Measured Isomer Shifts for Gold in a Number of Alloys and Compounds.

NEUTRON DIFFRACTION STUDY OF ANTIFERROMAGNETIC FeCl_3 ¹

J. W. Cable

M. K. Wilkinson

E. O. Wollan

W. C. Koehler

Neutron diffraction measurements were made on polycrystalline and single-crystal samples of anhydrous FeCl_3 at sample temperatures from 298 to 1.3°K. Antiferromagnetic reflections were observed which indicate a complicated magnetic structure with a Néel temperature of $15 \pm 2^\circ\text{K}$. In this structure the magnetic moments of near-neighbor atoms in the *c*-axis direction are oppo-

sitely oriented, but superimposed on this order there is a modulation of the moment distribution in the $[\bar{1}450]$ direction. From the absence of satellite reflections other than first order and from the relative intensities of the first-order satellites, it is concluded that the modulation is of the helical type in which the moments lie within $(1\bar{4}50)$ planes and rotate by $2\pi/15$ in successive planes along the $[\bar{1}450]$ direction. Absolute-intensity measurements yield a moment of $4.3 \pm 0.4 \mu_B$ per Fe^{3+} ion and indicate a slight distortion of the helix.

¹Abstract of paper to be submitted to the *Physical Review*.

THE MAGNETIC STRUCTURES OF THULIUM¹

W. C. Koehler

J. W. Cable

E. O. Wollan

M. K. Wilkinson

Neutron diffraction studies on polycrystalline and single-crystal specimens of thulium have been made at temperatures ranging from room temperature to 1.3°K. The results are interpreted by means of a method which exhibits explicitly the Fourier components of the distribution of magnetic moments on the lattice sites. At about 56°K, the Néel temperature, a simple oscillating z -component type of antiferromagnetic structure is developed. At approximately 40°K, nonzero Fourier coefficients of overtones of the fundamental observed at higher temperatures are first detected. At 4.2°K

the magnetic structure of thulium is a type of antiphase domain structure in which several layers of moments parallel to the $+a_3$ direction are followed by several layers in which the moments are oppositely directed. The sequence in thulium is $-4, +3, -4, +3, \dots$, etc. Each atom has, within the precision of the experiments, an ordered moment of $7\mu_B$, and the ferrimagnetic structure has a net moment, parallel to the c -axis, of $1\mu_B$ per atom. The fundamental period of the modulation remains constant over the whole range of temperatures at a value corresponding to $3.5 a_3$ periods. In the course of this study the scattering amplitude of thulium was determined to be $b_{Tm} = 0.69 \pm 0.02 \times 10^{-12}$ cm.

¹Abstract of paper submitted to the *Physical Review*.

INVESTIGATIONS OF PARAMAGNETIC NEUTRON SCATTERING FROM METALLIC CHROMIUM

M. K. Wilkinson

E. O. Wollan

W. C. Koehler

J. W. Cable

Following the discovery by neutron diffraction¹ that chromium is antiferromagnetic at low temperatures, numerous investigations have been performed in recent years to determine the magnetic behavior of this metal. These investigations have revealed some very unusual magnetic properties, which are not understood, and it appears that a complete explanation of chromium may be the key to a better understanding of magnetism in the $3d$ metals.

Neutron diffraction experiments²⁻⁵ have indicated that single-crystal chromium samples have a Néel temperature near 310°K, but in some powdered specimens this transition is near 450°K.

Since careful studies have revealed anomalies in electrical resistivity,⁶ Hall effect,⁷ magnetic susceptibility,⁸ and specific heat⁹ near the lower temperature, this value is believed to correspond to the antiferromagnetic transition in pure strain-free chromium. The antiferromagnetic structure has been found to correspond to a complicated type of magnetic order in which there is a long-range modulation of the moment distribution. This long-range periodicity was first discovered by Corliss, Hastings, and Weiss,² and they interpreted the structure as one with periodic antiphase domains. Alternative possibilities for the antiferromagnetic order are a spiral-spin arrangement and a model in which the amplitude of the magnetic moment experiences a sinusoidal modulation.

¹C. G. Shull and M. K. Wilkinson, *Revs. Modern Phys.* 25, 100 (1953).

²L. Corliss, J. Hastings, and R. Weiss, *Phys. Rev. Letters* 3, 211 (1959).

³V. N. Bykov *et al.*, *Soviet Phys. "Doklady"* 4, 1070 (1960).

⁴G. E. Bacon, *Bull. Am. Phys. Soc.* 5, 455 (1960).

⁵M. K. Wilkinson, E. O. Wollan, and W. C. Koehler, *Bull. Am. Phys. Soc.* 5, 456 (1960).

⁶H. Pursey, *J. Inst. Metals* 86, 362 (1958).

⁷G. de Vries and G. W. Rathenau, *J. Phys. Chem. Solids* 2, 339 (1957).

⁸E. W. Collings, F. T. Hedgcock, and A. Siddiqi, *Phil. Mag.* 6, 155 (1961).

⁹R. H. Beaumont, H. Chihara, and J. A. Morrison, *Phil. Mag.* 5, 188 (1960).

Since these possible antiferromagnetic structures involve different values for the atomic magnetic moments, it was of interest to determine the moment value from investigations of the paramagnetic scattering from chromium. These investigations were also important, because there was no evidence from other types of experiments for the existence of localized atomic moments in the so-called paramagnetic region. If the moment values in the ordered magnetic lattice are induced in the cooperative ordering process, then the properties of chromium would not be typical of the majority of metals found to be antiferromagnetic.

Because of the small moment value, any possible paramagnetic scattering from chromium would be very weak, and other types of diffuse scattering had to be reduced to a minimum. The shielding on the diffractometer was modified to eliminate as much background scattering as possible, Soller slits were used to define the scattered beam, and radiation shields within the cryostat were reconstructed to minimize the observed scattering from these shields and any condensation on them at low temperatures. Furthermore, an isotopic sample containing 99.6% Cr⁵² was used to eliminate the isotopic incoherent scattering and nuclear-spin incoherent scattering which are observed from normal chromium. Twenty-six grams of this isotopic sample was used in the investigations, and spectrochemical analyses showed that the sample was very pure, with only traces of metallic impurities. The neutron diffraction pattern was found to be very sensitive to the presence of oxides, and, in fact, the first diffraction pattern showed diffraction peaks corresponding to 1.25% Cr₂O₃. The sample was then heated¹⁰ in a hydrogen atmosphere at 1000°C for 72 hr, and the absence of detectable oxide reflections in the diffraction pattern limited the maximum possible oxide impurity to 0.1%.

The usual antiferromagnetic properties were observed from this isotopic specimen (see Fig. 1). The group of three magnetic reflections observed at 140°K and at room temperature in the angular region near the (001) reflection are characteristic of the complex magnetic structure, and the presence of only one magnetic reflection at 90°K is the result of a change in the moment direction

near 110°K. The total normalized integrated intensities (for three reflections above 110°K and one reflection below 110°K) are shown at the bottom of the figure, and it is seen that there is no discontinuity at the spin-flip transition. Most of the scattered intensity follows a Brillouin-type dependence toward the Néel temperature obtained in single-crystal measurements, while a smaller amount exists up to a temperature corresponding to the Néel point observed in some powdered specimens. The value of jF^2 , extrapolated to absolute zero, is in good agreement with values obtained in previous neutron diffraction investigations. This value corresponds to an atomic moment of about 0.4 μ_B for the simple body-centered-cubic antiferromagnetism, and models with a long-range modulation of the moment distribution would require a somewhat larger moment value.

The analyses of the diffuse scattering are shown in Fig. 2. The points plotted in the top figure represent absolute intensity measurements of the diffuse scattering from Cr⁵² at the indicated angles for a sample temperature of 510°K. The points have been corrected for background scattering and for thermal diffuse scattering by using the Debye theory of independent oscillators. For the latter corrections, the Debye temperature was established from observations of the coherent reflections between 706 and 86°K, and the determined value of 485°K is in good agreement with the value of 480°K previously established by other methods.¹¹ The absolute values of the diffuse scattering are very small, and rough calculations show that they could be due entirely to multiple scattering. These values certainly do not agree with the curve giving the expected differential paramagnetic cross section for an atomic moment, which corresponds to 0.4 μ_B /atom in the ordered lattice. The calculated curve, which is proportional to $g^2 S(S+1)j^2$, was obtained for an average S value of 0.2. Similar calculations of the paramagnetic scattering, assuming that 40% of the chromium atoms have an S value of 0.5 and the other atoms have zero spin, show an even greater discrepancy with the observed values.

Since there is some doubt concerning the applicability of the paramagnetic-scattering cross-section expression for metallic systems, it was

¹⁰We are indebted to D. E. LaValle of the Analytical Chemistry Division for purifying the chromium.

¹¹B. B. Argent and G. J. C. Milne, *J. Less-Common Metals* 2, 154 (1960).

UNCLASSIFIED
ORNL-LR-DWG 61753

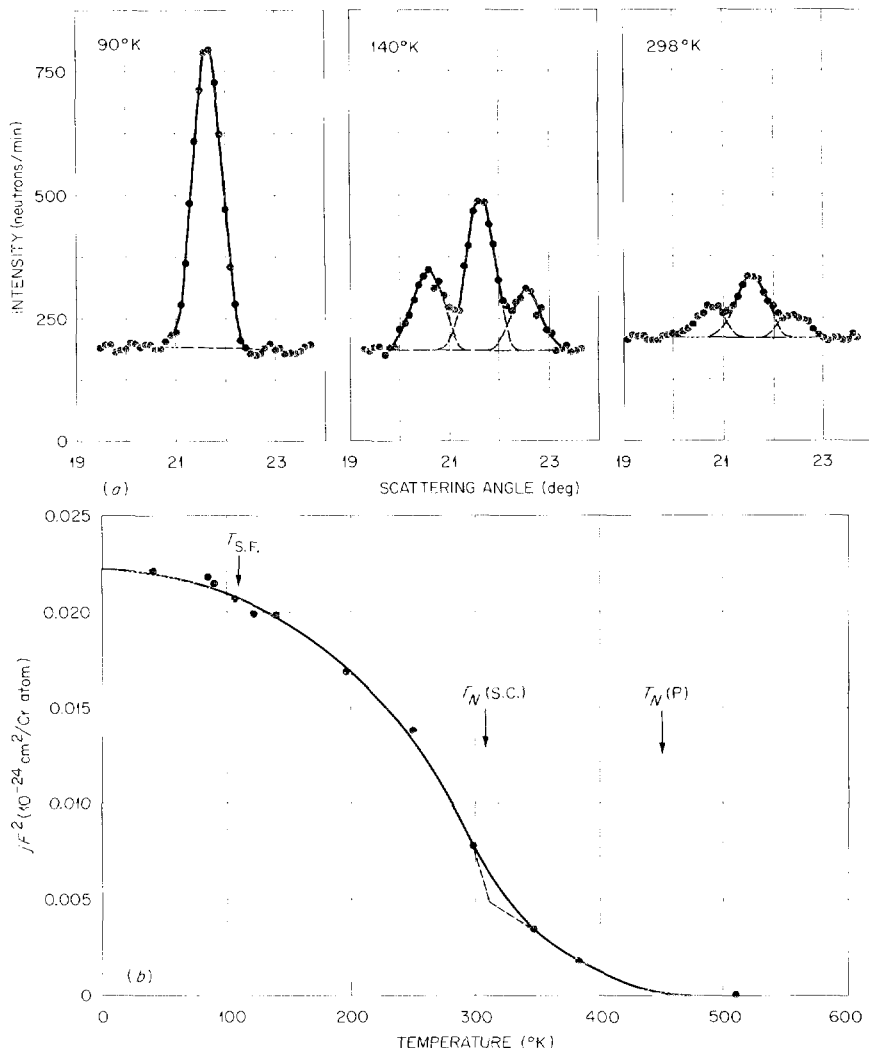


Fig. 1. Temperature Variation of Antiferromagnetic Reflections from Cr⁵². (a) Partial powder diffraction patterns in the angular region near the position of the (001) reflection; (b) normalized integrated intensities for the total coherent scattering near the position of the (001) reflection.

also of interest to determine if the S^2 contribution was present in the diffuse scattering. It is this part of the paramagnetic scattering which goes into the magnetic reflections below the ordering transition. As suggested in the top figure, it is

not possible to determine accurately the presence of this contribution in the diffuse scattering above the transition temperature. If it is present, however, there should be a decrease in the diffuse scattering by this amount as the magnetic lattice

UNCLASSIFIED
ORNL-LR-DWG 61755

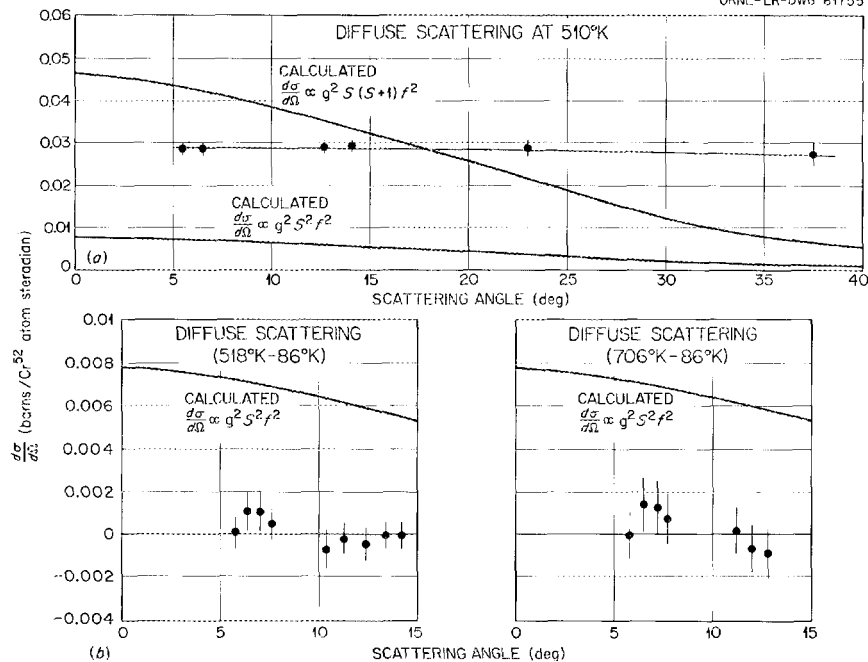


Fig. 2. Diffuse Scattering from Polycrystalline Cr^{52} . (a) Absolute values of the total diffuse scattering from Cr^{52} (corrected for background and thermal diffuse scattering) at $510^\circ K$ compared with calculated curves for the expected total paramagnetic scattering and the expected S^2 contribution to the paramagnetic scattering; (b) results of two experiments showing the differences in diffuse scattering between 518 and $86^\circ K$ and between 706 and $86^\circ K$; corrections have been applied to the data for changes in the thermal scattering.

becomes ordered. Since the calculated S^2 contribution in the low-angle region corresponded to about 18% of the total diffuse scattering from the sample and background, such a decrease should be readily observable. The lower part of the figure shows results from two experiments which measured the difference in diffuse scattering at temperatures above and below the Néel point. The experimental points, which have been corrected for changes in the thermal diffuse scattering, represent average values of several determinations in which the sample was cycled between the indicated temperatures, and the (110) nuclear reflection was carefully monitored at each temperature to ensure that there were no changes in the scattering conditions. In the experiment between 518 and $86^\circ K$, a direct comparison of the data was possible, because both temperatures

could be obtained with the sample mounted in the cryostat. For temperatures above $518^\circ K$, the sample was placed in a small furnace, and the data at $706^\circ K$ were compared with those at $86^\circ K$ by normalizing both sets of results to room-temperature measurements under similar conditions. Both experiments show that there is essentially no difference in the diffuse scattering from chromium above and below the antiferromagnetic transition.

The results of this investigation indicate that there is little or no localized atomic magnetic moment associated with chromium above the Néel temperature. Consequently, the magnetic moment which is observed in the ordered antiferromagnetic structure must be induced in the ordering process.

MAGNETIC ORDERING IN HoN

H. R. Child

M. K. Wilkinson

J. W. Cable

E. O. Wollan

W. C. Koehler

Neutron diffraction investigations^{1,2} performed on rare-earth nitrides with the rock-salt structure have indicated that many of these compounds become ferromagnetic at low temperatures. However, the diffraction patterns obtained for these nitrides in the ferromagnetic state always showed a very pronounced small-angle scattering and a large increase in diffuse scattering in the angular regions of the ferromagnetic reflections. Such effects, which are indicative of short-range ferromagnetic correlations, were found to exist at temperatures well below the magnetic transition temperatures. In fact, experiments on the small-angle scattering from HoN showed that it occurred at temperatures slightly above the Curie point and that the intensity increased with decreasing temperatures down to 1.3°K, which was the lowest temperature obtained. Consequently, this scattering does not have the characteristics associated with critical magnetic scattering, and the mechanism for producing it has not been understood. This large variation in the diffuse scattering has caused considerable uncertainty in the cal-

culaton of the ferromagnetic moments in the nitrides and the consequent correlation of these values with the crystal-field calculations of Trammell.³ If the background near the magnetic reflections in HoN is drawn so that the long-range ferromagnetic order produces reflections with a resolution comparable to the nuclear reflections, then the long-range ferromagnetic moment corresponds to about $6.0 \mu_B$ per holmium ion. However, if the short-range order scattering is included in the magnetic reflections, a moment value of about $8.9 \mu_B$ per ion is obtained. Of course, both possible extreme values are less than the maximum ordered moment ($10.0 \mu_B$) associated with the Ho^{3+} ion, and this indicates that crystal-field interactions affect the energy levels in this compound.

Recent experiments at the ORR, in which HoN samples were placed in external magnetic fields applied in a direction perpendicular to the scattering vector, have indicated that the larger value of the ferromagnetic moment ($8.9 \mu_B$) is correct. Figure 1, which shows the scattered intensity near the (111) and (200) magnetic reflections in zero field and with 16 kilo-oersteds applied

¹M. K. Wilkinson *et al.*, *J. Appl. Phys.* **31**, 3585 (1960).

²H. R. Child *et al.*, *Phys. Div. Ann. Progr. Rept. Feb. 10, 1961*, ORNL-3085, p 73.

³G. T. Trammell, private communication.

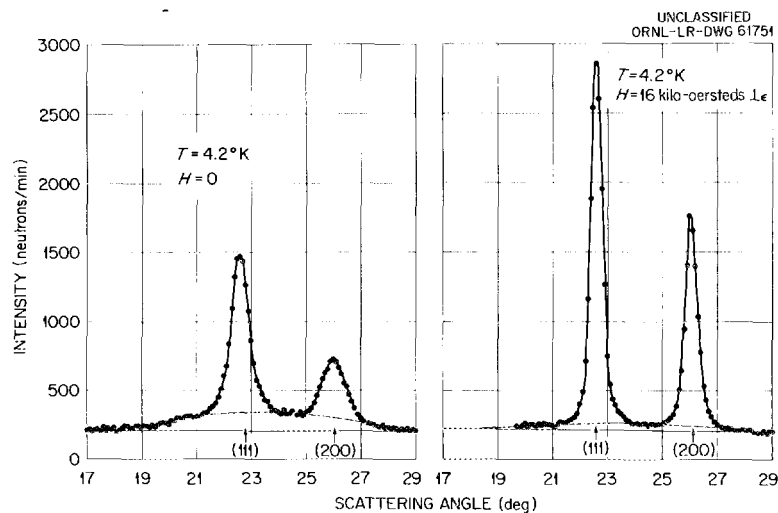


Fig. 1. Comparison of Magnetic Reflections from HoN in Zero Magnetic Field and in a Magnetic Field of 16 kilo-oersteds Applied in a Direction Perpendicular to the Scattering Vector.

perpendicular to the scattering vector, shows the observed effects. The intensity of the background hump decreases with the applied field, while the reflections become sharper and their intensity increases. These effects were observed as a function of the magnetic field up to 21 kilo-oersteds, and the results indicate that saturation would occur at about 25 kilo-oersteds. The magnetic intensities of the (111) and (200) reflections, extrapolated to the saturation value, can be explained on the basis of complete ferromagnetic long-range order with atomic moments of $8.9 \mu_B$ directed along the edge of the cubic unit cell. This is the moment direction which was predicted from crystal-field calculations and verified in earlier experiments with magnetic fields applied in a direction parallel to the scattering vector. Consequently, the results of these investigations indicate that the crystal-field interactions are large when compared with 25 kilo-oersteds, that these interactions reduce the moment value to $8.9 \mu_B$, and that weaker forces prevent these moments from obtaining complete ferromagnetic alignment in zero magnetic field.

Many ordered magnetic structures have been investigated in an attempt to explain the observed

diffraction patterns from HoN below the magnetic ordering temperature. The only type of model that has been found to satisfactorily predict the observed effects is shown in Fig. 2. In this model the atomic moments have the value dictated by the crystal field, and they are arranged in small ferromagnetic bands with the moment direction always along one of the cube edges. These bands are perpendicular to the cube diagonal, and in the model shown in the figure the band width is composed of seven layers of moments. Such a structure gives a net ferromagnetism along the cube diagonal and also predicts many satellite reflections around the regular ferromagnetic reflections. At the lower part of the figure, the calculated intensities for a polycrystalline specimen are compared with the experimental data, and it is seen that the envelope of the predicted reflections is in satisfactory agreement with the observed results. This particular model, of course, is not a unique structure determination, and single-crystal experiments would be necessary to establish the exact structure. However, it is certainly possible that magnetic ordering of this type could be responsible for the unusual patterns that are observed.

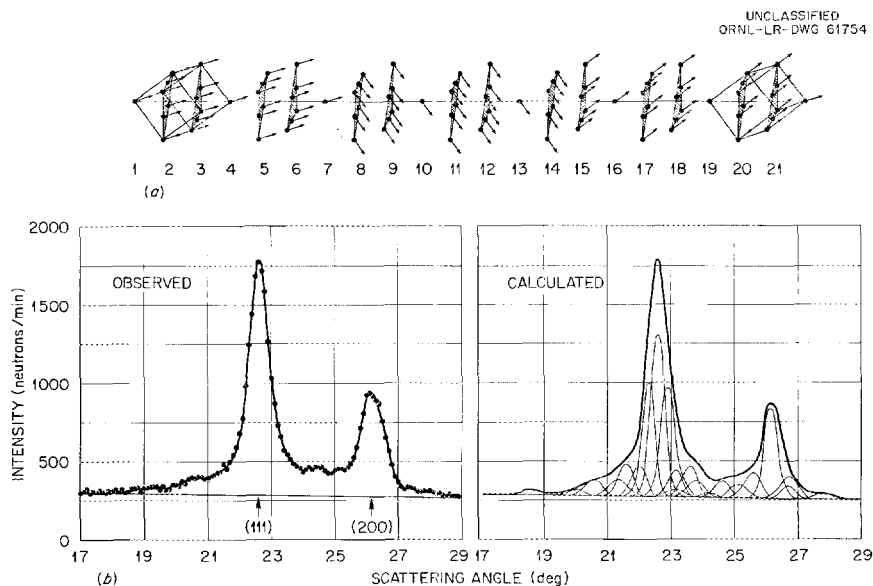


Fig. 2. (a) Possible Magnetic Structure of HoN Below 18°K ; (b) Comparison of Observed Magnetic Reflections from Polycrystalline HoN with Those Calculated on the Basis of the Possible Magnetic Structure Shown Above.

MAGNETIC COUPLING IN Pd-DILUTE IRON GROUP ALLOYS¹

E. O. Wollan

The magnetic properties of palladium and its alloys with iron group elements are discussed in terms of the splitting of the d orbitals. The paramagnetic properties of pure palladium are accounted for on the basis that the holes in the d shell are associated with the nonoverlapping e orbitals,

whereas the ferromagnetic coupling in the face-centered $3d$ elements and their alloys is associated primarily with holes in the overlapping t orbitals. On this basis and on the basis of a change in the splitting when palladium is alloyed with $3d$ metals, it is possible to account for the paramagnetic and ferromagnetic properties of the palladium-dilute iron group alloys. Because of the larger amount of available data, attention is given primarily to the palladium-iron system.

¹Abstract of published paper: *Phys. Rev.* **122**, 1710 (1961).

NEUTRON DIFFRACTION INVESTIGATIONS OF FERROMAGNETIC PALLADIUM AND IRON GROUP ALLOYS¹

J. W. Cable

E. O. Wollan

W. C. Koehler

M. K. Wilkinson

In order to account for the magnetic properties of alloys, it becomes important to determine the individual magnetic moments of the constituent atoms. This determination can be accomplished by the combination of neutron diffraction and

magnetic induction measurements. Such measurements were made on the following ferromagnetic alloys: Pd_3Fe , PdFe , Pd_3Co , PdCo , Ni_3Co , and NiCo . The average moment values were obtained from magnetic induction measurements, while the differences in the atomic moments were determined from either the ferromagnetic diffuse scattering of the disordered alloys or the superlattice reflections of the ordered alloys.

¹Abstract of paper to be published in *Journal of Applied Physics* (suppl).

MAGNETIC MOMENT DISTRIBUTION IN PALLADIUM AND IRON GROUP ALLOYS¹

E. O. Wollan

J. W. Cable

W. C. Koehler

M. K. Wilkinson

Neutron diffraction measurements have been made on the magnetic properties of a number of palladium-iron group alloys. The individual mag-

netic moments of the palladium and of the iron group atoms have been determined in both ordered and disordered states of the alloy systems. These results and the considerable body of other magnetic data available on these systems are used in the interpretation of the magnetic properties of palladium and its alloys in terms of the occupation and overlap properties of the d orbitals.

¹Abstract of paper presented at International Conference on Magnetism and Crystallography, Kyoto, Japan, Sept. 25-30, 1961; published in *Intern. Conf. Magnetism and Crystallography (Kyoto, Japan)* **4**, 314 (1961).

PHENOMENOLOGICAL DISCUSSION OF MAGNETIC ORDERING IN THE HEAVY RARE-EARTH METALS¹

R. J. Elliott²

The rare-earth metals gadolinium-thulium have similar crystal structures, and their magnetic properties have been partially evaluated by a number of techniques. The magnetic order is complicated, showing several phases in some cases and differing considerably in the various elements. These various orderings can be explained on a molecular field (Bragg-Williams) model if a long-range oscillatory exchange interaction whose minimum Fourier component $J(\vec{q})$ is at

$q \neq 0$, small quadrupole-quadrupole interaction, and anisotropy are included. A crystal-field calculation gives axial and hexagonal anisotropies which vary along the series in a way which accounts for the observed structures. In terbium, dysprosium, and holmium the moment is forced into the basal plane, and the order is a spiral at high T , becoming ferromagnetic at low T because of the hexagonal anisotropy. The quadrupole-quadrupole interaction determines the change of pitch with T . In erbium and thulium the moment is forced along the c axis, and the observed order with sinusoidal variation of this moment is found to have lowest free energy at high T . As T is lowered, transitions to an antiphase domain structure and then to ferromagnetism are predicted.

¹Abstract of published paper: *Phys. Rev.* 124, 346 (1961).

²Present address: Physics Department, University of California, Berkeley; permanent address: Clarendon Laboratory, Oxford, England.

NEUTRON DIFFRACTION BY HELICAL-SPIN STRUCTURES¹

W. C. Koehler

A method is described for predicting the intensities of magnetic reflections from helical-spin structures. The computation is based on a generalization of the theory of x-ray diffraction by disordered crystals. Applications to more complex structures are indicated.

¹Abstract of published paper: *Acta Cryst.* 14, 535 (1961).

RECENT PROGRESS IN MAGNETIC STRUCTURE DETERMINATIONS OF RARE-EARTH METALS¹

W. C. Koehler

J. W. Cable

E. O. Wollan

M. K. Wilkinson

Results of recent neutron diffraction investigations of single crystal terbium and thulium and of extended studies of single crystal holmium are summarized.

¹Abstract of published paper: *Intern. Conf. Magnetism and Crystallography (Kyoto, Japan)* 4, 312 (1961).

RECENT MAGNETIC NEUTRON SCATTERING INVESTIGATIONS AT
OAK RIDGE NATIONAL LABORATORY¹

M. K. Wilkinson H. R. Child W. C. Koehler
J. W. Cable E. O. Wollan

A brief summary is given of recent magnetic neutron scattering investigations of rare earth metals and rare earth intermetallic compounds.

¹Abstract of published paper: *Intern. Conf. Magnetism and Crystallography (Kyoto, Japan) 4*, 311 (1961).

NEUTRON DIFFRACTION¹

M. K. Wilkinson E. O. Wollan W. C. Koehler

This is a summary article giving a rather broad view of neutron diffraction research relating to nuclear physics, crystal structure and magnetic problems. The article contains about 200 references to the work in this field.

¹Abstract of published chapter: *Ann. Rev. Nuclear Sci.* 11, 303 (1961).

OPTICAL PHYSICS

G. W. Charles H. W. Morgan P. A. Staats T. A. Welton
P. M. Griffin¹ O. B. Rudolph K. L. Vander Sluis G. K. Werner¹

An Optical Physics Group has been formed to exploit the rapidly expanding field of optical masers. The interest of the group has been primarily in the development of a device generally similar to the helium-neon maser first described by Javan, Bennett, and Herriott,² which utilizes a method for obtaining population inversion first suggested by Javan.³ In this inversion method a tube containing two gases (*A* and *B* in the following) sustains an electrodeless discharge. The discharge acts primarily to maintain some fraction, ϕ , of the species *A* in an excited state A_1 , which differs in energy from the ground state A_0 by an amount ν_A (cm^{-1}).

The species *B* is supposed to possess an excited state B_1 , whose energy exceeds that of the ground state by an amount ν_B (cm^{-1}), which is assumed to differ from ν_A by an amount less than the mean thermal energy of a gas atom in the discharge tube. Under these conditions an equilibrium is rapidly established by collisional transfer of excitation between the two species such that the population of the states B_1 and B_0 also are in the ratio ϕ , if the various relaxation processes are ignored. If these relaxation processes are now turned on (spontaneous emission from B_1 to a lower state B_2 , spontaneous emission and wall collisions from B_2 to B_0), we may be left with an inverted population for the $1 \rightarrow 2$ transition. In that event, amplification can be obtained at the frequency ν_1 , and it is assumed that optical feedback is supplied to permit the intensity of coherent light to build up to some saturation level. The

¹On loan from Thermonuclear Division.

²A. Javan, W. R. Bennett, Jr., and D. R. Herriott, *Phys. Rev. Letters* 6, 106 (1961).

³A. Javan, *Phys. Rev. Letters* 3, 87 (1959).

resulting induced relaxation rate from B_1 to B_2 may overbalance the spontaneous rate, and this will be assumed for simplicity in the following.

An approximate description of such a system can be given in terms of a few simple parameters. Let the populations (number of atoms per cm^3 , averaged over the active volume of the amplifier or oscillator) of the various states be denoted by the symbols used above to designate the states themselves. Then, for the time derivatives of the B populations,

$$\dot{B}_1 = \nu\sigma(A_1B_0 - A_0B_1) - \frac{1}{h\nu_1} I, \quad (1)$$

$$\dot{B}_2 = \frac{1}{h\nu_1} I - \frac{1}{T} B_2, \quad (2)$$

$$\dot{B}_0 = \frac{1}{T} B_2 - \nu\sigma(A_1B_0 - A_0B_1), \quad (3)$$

where

$\nu\sigma$ = Maxwell average of the product of the relative A - B velocity and the energy transfer cross section,

$h\nu_1$ = energy of one quantum of the induced radiation,

I = intensity of induced radiation in $\text{ergs cm}^{-3} \text{sec}^{-1}$ averaged over the active volume of the system,

T = mean lifetime of the state B_2 against relaxation to state B_0 by all processes.

We assume that the net effect of the electrodeless discharge is to maintain a definite ratio of A_1 to A_0 . If it is now assumed that balance has been achieved, with a steady value of I , then

$$B_1 = \phi B_0 - \frac{1}{A_0\nu\sigma} \frac{I}{h\nu_1}, \quad (4)$$

$$B_2 = T \frac{I}{h\nu_1}. \quad (5)$$

We now seek the largest value of I , consistent with the maintenance of the population inversion required for the amplification which supports the coherent oscillation. From (4) and (5),

$$B_1 - B_2 = \phi B_0 - \left(T + \frac{1}{A_0\nu\sigma}\right) \frac{I}{h\nu_1} \geq 0. \quad (6)$$

If the inequality is solved for I , we obtain

$$I \leq \frac{h\nu_1 \phi B_0}{T + 1/A_0\nu\sigma}. \quad (7)$$

This simple formula suffices to describe the essential features of gas optical masers of the He-Ne type. For the device described by Javan, Bennett, and Herriott,² $\phi = 10^{-5}$ to 10^{-6} , B_0 corresponds to a pressure of 0.1 mm Hg of neon, while A_0 corresponds to a pressure of 1.0 mm Hg of helium. The mean molecular velocity $v \approx 10^5$ cm/sec, and σ was measured to be approximately $3.5 \times 10^{-17} \text{ cm}^2$. Under these conditions, T is principally due to diffusion of excited atoms to the tube wall and is equal to 10^{-4} to 10^{-5} sec for a tube diameter of 1 cm. We then see that $T > 1/A_0\nu\sigma$ by about one order of magnitude. It seems probable that T will always dominate $1/A_0\nu\sigma$, except for tube radii which are impractically small, T varying inversely as the square of the radius. Under these conditions, the performance of an optical amplifier or oscillator is seen to depend critically on the values of ϕ , B_0 , and T which can be achieved.

A survey has been made of the various two-component systems which seem likely to yield amplification, without undue materials problems, and one system, consisting of krypton and mercury vapor, has been singled out for careful study. It appears to offer performance which is at least as good as the He-Ne system, and in addition should produce coherent visible light. Two excited krypton states are involved, namely, the 2^- and 1^- states, which are 79973 and 80918 cm^{-1} , respectively, above ground. These are the lowest excited states and can be populated with good efficiency. The two possible upper mercury states are 9^1P_1 and 10^3P_1 , at 79964 and 80917 cm^{-1} , respectively, above ground. It appears likely that the 10^3P_1 level will be more strongly populated, in which case a yellow line, $10^3P_1 \rightarrow 7^1S_0$ at 16989 cm^{-1} , may be amplified.

A very considerable amount of diagnostic work is necessary before construction of an oscillator becomes possible, the main problem being the determination of the optimum pressures and excitation conditions, as well as the gain per unit length which will be available. The principal diagnostic tool must be a device for measuring

the absorption (or amplification) of various relevant spectral lines by a gas discharge of suitable composition. The principal experimental problem is the necessity in the absorption measurements for discriminating against a large amount of background radiation emitted by the discharge. For this purpose an "optical bridge" has been designed (see Fig. 1) and constructed, and it is in the process of being checked out by conducting experiments in which comparison with known data may be made. The bridge consists of four mirrors, two totally reflecting and two beam splitting (partially transmitting half-silvered mirrors), placed in a rectangular array. Light from an external source is rendered parallel and divided into two separate beams by the first half-silvered mirror. One beam traverses a leg of the bridge in which is placed the gas discharge cell. The other beam traverses an equivalent leg of the bridge without the gas discharge cell, and subsequently the two beams are recombined by the second half-silvered mirror and focused onto the slit of a monochromator. The function of the monochromator is to isolate the light of the wavelength corresponding to a transition that terminates on the level whose population is to be measured. Inasmuch as the levels of interest are excited levels of the atom, there will be light of the same wavelength emitted by the gas discharge cell as is originating from the external source. Discrimination is achieved by chopping the light from the external source at 450 cps. The chopping is done after the splitting into sample beam and reference beam, and light is transmitted alternately through the two legs. The recombined chopped light at the wavelength of interest, along with the steady-state light originating in the sample cell, is detected by a photomultiplier tube which feeds

a narrow-band phase-sensitive amplifier. Only the 450-cps signal is amplified and represents the difference in light transmission between the two legs of the bridge. A neutral-density filter in the form of a rotatable disk, having an optical density at any point which is proportional to the angular setting, is located in the reference leg of the bridge. By proper setting of the neutral-density filter, a null signal is obtained. The optical density of the sample discharge is proportional to the difference in angular setting of the filter as measured with the discharge on and the discharge off and is directly related to the product Nf , where N is the population of the state in question, and f is the oscillator strength of the line observed.

The accuracy of measurement with this light bridge is being tested by measuring the relative oscillator strengths (f values) for transitions in neon, which had been previously measured by Ladenburg⁴ by an entirely different method. These measurements indicate substantial agreement with Ladenburg (see Table I). The discrepancies for the larger Nf products are qualitatively attributable to incorrectly assumed line contours for the external light source which probably arise from the fact that the external source is not "optically thin" for the strong lines.

Since it was established that it is possible to measure an Nf product accurately in a self-luminous gas, these products can be used in conjunction with calculated f values to yield measurements of the population of excited levels in a gas discharge. Preliminary measurements have been made with krypton and with mercury, and it is anticipated that the essential questions can be answered with this apparatus.

⁴R. Ladenburg, *Revs. Modern Phys.* 5, 243 (1933).

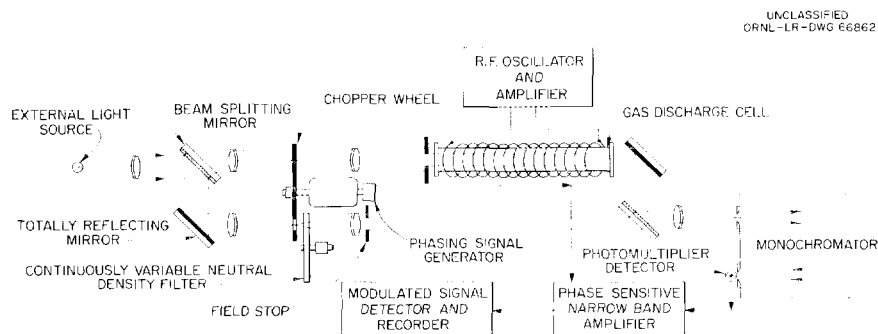


Fig. 1. Optical Bridge for Measurement of Absorption or Amplification in a Self-Luminous Gas.

Table 1. Relative f Values of the $1s_5-2p$ Lines of Neon

Neon transition	5881	5945	5975	6143	6217	6334	6402	7032
Source	$1s_5-2p_2$	$1s_5-2p_4$	$1s_5-2p_5$	$1s_5-2p_6$	$1s_5-2p_7$	$1s_5-2p_8$	$1s_5-2p_9$	$1s_5-2p_{10}$
Shortly ^a (theoretical)	0.044	0.150	0.020	0.099	0.022	0.106	0.500 (assumed)	0.137
Ladenburg ^b (experimental)	0.06 ₇	0.09	~0.03	0.18 ₅	0.05	0.12 ₅	0.500 (assumed)	0.14 ₅
ORNL (experimental)	0.067 (assumed)	0.10 ₂	0.02 ₇	0.15 ₃	0.05 ₀	0.12 ₉	0.18 ₅	0.13 ₉
Average deviation	0.000	0.004	0.001	0.019	0.002	0.006	0.026	0.012

^aG. H. Shortley, *Phys. Rev.* 47, 295 (1935).

^bR. Ladenburg, *Revs. Modern Phys.* 5, 243 (1933).

INFRARED SPECTRA OF DILUTE SOLID SOLUTIONS¹

H. W. Morgan

P. A. Staats

The infrared spectra of polyatomic ions in dilute solid solution reflect interactions of the vibrational modes with the lattice environment. The spectra are usually characterized by very narrow band widths, and by frequency shifts and changes in absorption intensities which depend upon the host lattice. We have examined the spectra of a number of ions in solid solution in alkali halides. From this data, conclusions have been drawn relative to the symmetries of the ions and the lattice sites

which they occupy. The ultimate goal is the use of complex ions as "probes" to yield information on crystal lattices.

Certain of the ions produced in fused alkali halides are characteristic of chemical equilibria at high temperatures and have not previously been studied. We have identified several impurities found in the spectra of single crystals from commercial sources. The infrared absorption offers the possibility of determining the types and concentrations of trace impurities in single crystals.

The spectra of the metaborate ion, BO_2^- , and of carbonate-metal ion pairs in solid solution are discussed briefly.

¹Abstract of published paper: *J. Appl. Phys. (suppl)* 33, 364 (1962).

SOLID-SOLUTION INFRARED SPECTRA. THE METABORATE ION, BO_2^- ¹

H. W. Morgan

P. A. Staats

The metaborate ion, BO_2^- , is produced by the addition of any boron-oxygen compound to a fused alkali halide. The infrared spectra of this ion in solid solution in NaCl, NaBr, KCl, and KBr have

been observed at 300 and 77°K, in single crystals and in pressed disks. Frequencies of ions containing B^{10} and B^{11} , O^{16} , O^{17} , and O^{18} have been measured, and the ion was shown to have a linear OBO configuration, of symmetry $D_{\infty h}$. Selection rules for the ion symmetry are observed. The frequencies ν_2 and ν_3 are infrared-active, and ν_1 is determined from combination bands.

¹Abstract of paper to be submitted to *Journal of Chemical Physics*.

FRAGMENT AND CHARGE SPECTRA OF THE IONS FORMED FOLLOWING RADIOACTIVE DECAY OF $\text{C}_2\text{H}_5\text{I}^{131}$ AND $\text{CH}_3\text{I}^{130}$

T. A. Carlson

R. M. White¹

Three principal areas of interest arose from the study on $\text{CH}_3\text{I}^{131}$ (ref 2); (1) the stability, following β^- decay, of the parent species, which is a rather unique xenon-hydrocarbon ion, (2) the hydrocarbon fragment spectrum, and (3) the charge spectrum of xenon.

Two companion studies were chosen to shed more light on the problems raised by the investigation of $\text{CH}_3\text{I}^{131}$. Data on $\text{C}_2\text{H}_5\text{I}^{131}$ should yield information on the importance of the hydrocarbon with regard to the stability of the xenon-hydrocarbon ion, while $\text{CH}_3\text{I}^{130}$ is important because I^{130} receives a maximum recoil energy which is six times that of I^{131} and affords an opportunity to evaluate the role that recoil energy plays in the decomposition. Experimental procedures and the preparation of high-specific-activity methyl and ethyl iodides are similar to those discussed for $\text{CH}_3\text{I}^{131}$ (ref 2). The I^{130} is prepared by a (p,n) reaction on Te^{130} , by use of the Oak Ridge 86-in. cyclotron. The radioactive gas is allowed to decay in a source volume that contains a set of field rings, which collects and accelerates the ions into a mass spectrometer where they are analyzed for their mass-over-charge ratios.

The analyses of the ions formed from the decay of $\text{C}_2\text{H}_5\text{I}^{131}$ and $\text{CH}_3\text{I}^{130}$ are presented in Table I along with the data from $\text{CH}_3\text{I}^{131}$ for comparison. The only notable difference found on comparing the results in the study on $\text{CH}_3\text{I}^{130}$ with those from $\text{CH}_3\text{I}^{131}$ is that the intensity of CH_3^+ is 20 times greater in the case of $\text{CH}_3\text{I}^{130}$, with a corresponding decrease in the intensity of the parent ion $(\text{CH}_3\text{Xe}^{130})^+$. This points out that the principal role of recoil energy in the decomposition of the CH_3Xe^+ is the breaking of the $\text{CH}_3\text{-Xe}$ bond without the subsequent production of other ions. The results on $\text{CH}_3\text{I}^{130}$ also confirm that when CH_3Xe^+ breaks apart the charge goes with the CH_3^+ as expected, since xenon has a greater ionization potential than CH_3 . Thus the explanation for the relatively large amount of Xe^+ noted following the β^- decay of $\text{CH}_3\text{I}^{131}$ cannot be found by supposing that the xenon carries away the charge when CH_3Xe^+ decomposes, but might rather be sought in the conjecture that following the shake-off of an electron from the parent ion, the resulting $(\text{CH}_3\text{Xe})^{2+}$ generally decomposes into CH_3^+ and Xe^+ . Because of the lighter weight of the CH_3^+ , the hydrocarbon will receive the greater share of the Coulombic repulsion between the two ions and will be collected with poorer efficiency.

The most interesting piece of information to be gained from the data on $\text{C}_2\text{H}_5\text{I}^{131}$ is that the

¹Summer research participant, 1961.

²T. A. Carlson and R. M. White, to be published in *Journal of Chemical Physics*.

Table 1. Comparison of the Fragment and Charge Spectra of Ions Resulting from the Radioactive Decay of $\text{CH}_3\text{I}^{131}$, $\text{CH}_3\text{I}^{130}$, and $\text{C}_2\text{H}_5\text{I}^{131}$

Ion	Abundance (%)		
	$\text{CH}_3\text{I}^{131}$	$\text{CH}_3\text{I}^{130}$ (normalized to 97.5%)	$\text{CH}_3\text{CH}_2\text{I}^{131}$
$\text{C}_2\text{H}_5\text{Xe}^+$			1.4 ± 0.3
CH_3Xe^+	69.4	34.1	0.17 ± 0.5
C_2H_5^+			87.2
C_2H_4^+			0.09 ± 0.2
C_2H_3^+			1.1 ± 0.1
C_2H_2^+			1.9 ± 0.4
C_2H^+			0.32 ± 0.07
C_2^+			0.18 ± 0.06
CH_3^+	2.0 ± 0.2	39.0 ± 5.0	0.36 ± 0.07
CH_2^+	2.4 ± 0.3	3.3 ± 0.7	0.27 ± 0.09
CH^+	2.2 ± 0.4	3.4 ± 0.7	0.2 ± 0.1
C^+	1.9 ± 0.3	3.9 ± 0.6	0.4 ± 0.3
C^{2+}	0.07 ± 0.04	0.1 ± 0.07	0.0 ± 0.01
H_2^+	0.0 ± 0.07		0.0 ± 0.04
H^+	1.4 ± 0.2		0.22 ± 0.04
Xe^+	14.6 ± 0.6	9.6 ± 0.6	2.3 ± 0.3
Xe^{2+}	2.7 ± 0.3	2.0 ± 0.4	0.44 ± 0.07
Xe^{3+}	0.9 ± 0.1	1.4 ± 0.3	0.17 ± 0.03
Xe^{4+}	0.37 ± 0.07	0.29 ± 0.06	0.10 ± 0.03
Xe^{5+}	0.40 ± 0.10		0.14 ± 0.08
Xe^{6+}	0.24 ± 0.04	0.3 ± 0.1	0.20 ± 0.03
Xe^{7+}	0.23 ± 0.04		0.27 ± 0.08
Xe^{8+}	0.32 ± 0.06	0.24 ± 0.07	0.23 ± 0.07
Xe^{9+}	0.25 ± 0.06	0.20 ± 0.05	0.13 ± 0.03
Xe^{10+}	0.22 ± 0.06		0.11 ± 0.04
Xe^{11+}	0.14 ± 0.05	0.11 ± 0.07	0.10 ± 0.04
Xe^{12+}	0.07 ± 0.02	0.0 ± 0.02	0.04 ± 0.01
Xe^{13+}	0.06 ± 0.02		0.011 ± 0.004
Xe^{14+}	0.023 ± 0.008		0.02 ± 0.01
Xe^{15+}	0.017 ± 0.008		0.009 ± 0.004
Xe^{16+}	0.008 ± 0.004		0.006 ± 0.004

substitution of CH_3 for H has greatly reduced the stability of the xenon-hydrocarbon complex, as seen by the small amount of $\text{C}_2\text{H}_5\text{Xe}^+$ and the large amount of C_2H_5^+ . This may be caused by the relatively greater nucleophilic character of CH_3 as compared with a hydrogen atom, but it seems also possible that the substitution of CH_3 for H involves a distortion of the bond structure of the xenon-hydrocarbon ion. There remains a large area for speculation as to the generally lower intensities of ions found with $\text{C}_2\text{H}_5\text{I}^{131}$ as compared with $\text{CH}_3\text{I}^{131}$. However, the carry-over from atomic phenomena for the expected excitation is still valid in a qualitative sense. That is, the hydrocarbon spectrum needs to be interpreted in terms of the amount of energy received from a sudden change in the nuclear charge of an iodine atom, and the charge spectrum for xenon ions is that expected for atomic ionization resulting from β^- decay followed by vacancy cascades in the

few percent of decays also undergoing internal conversion.³

Finally, as pointed out above, the collection efficiency of an ion is strongly dependent on its kinetic energy.^{2,4} This variable must always be kept in mind, particularly in molecular decay. The argument brought to bear in the study on $\text{CH}_3\text{I}^{131}$ – that if the initial recoil energy were large enough the importance of the subsequent Coulombic repulsion would be minimized – is substantiated in Table 2, because it can be seen that $\text{CH}_3\text{I}^{130}$ with a much larger recoil energy yields a more satisfactory agreement for the intensity of ions arising from internal conversion.

³A. H. Snell and Frances Pleasonton, *Phys. Rev.* **111**, 1338 (1958).

⁴T. A. Carlson, *J. Chem. Phys.* **32**, 1234 (1960).

Table 2. Comparison of Recoil Energy, Collection Efficiency, and Internal Conversion Associated with $\text{CH}_3\text{I}^{131}$, $\text{CH}_3\text{I}^{130}$, and $\text{C}_2\text{H}_5\text{I}^{131}$

Parent Molecule	Maximum Recoil Energy (ev)	Relative Collection Efficiency	Internal Conversion (% of decays)	
			From Nuclear Chemical Data ^a	From Spectrum of Xenon Ions
$\text{CH}_3\text{I}^{131}$	6.8	1	6.2	2.0
$\text{CH}_3\text{I}^{130}$	41.8	$\frac{1}{3}$	1.8	1.5
$\text{C}_2\text{H}_5\text{I}^{131}$	6.2	$1\frac{1}{2}$	6.2	1.5

^aD. Strominger, J. M. Hollander, and G. T. Seaborg, *Revs. Modern Phys.* **30**, 707 (1958).

A 7090 PROGRAM FOR BUBBLE-CHAMBER TRACK RECONSTRUCTION

H. O. Cohn

W. M. Bugg¹

R. D. McCulloch²

Reduction of data from bubble-chamber photographs is most efficiently done with the aid of digital computers. A program was written for the IBM 7090 computer to reconstruct spatial geometrical data and calculate momenta of single tracks from coordinate information meas-

ured on stereo photographs. The program is based in part on PANG,³ an angle and momenta reconstruction program developed at LRL, but draws heavily on techniques employed in manual data processing. Coordinate measurement is done with a Hermes⁴ precision film reader. The data and

¹University of Tennessee.

²Central Data Processing Group.

³UCRL, Physics Notes, Memo 111.

⁴Manufactured by Itek Laboratories, Lexington, Mass.

other pertinent information are punched on paper tape.

Flexibility of the Hermes output was increased by the addition of a hexadecimal keyboard. A letter followed by one or two digits is used to identify tracks and fiducials and give special orders to the computer. A letter specifies whether or not a track stopped in the chamber, and the numbers identify the particle and the vertex from which it came.

A track is measured on each of three stereo views with the Hermes, and three fiducial marks are measured in each view. The program selects the best two views for track reconstruction. In general, the best two views are those for which the line joining the lenses makes an angle closest to 90° with the track direction. Reconstruction is done by superimposing the positions of two fiducial marks. The third measured mark is used only as a check.

Coordinates for the orthogonal projection of a point are obtained by finding the point of intersection of straight lines drawn between corresponding points on the superimposed stereo photographs and the projection of the lens positions. End points of stopping short tracks are measured as corresponding points; however, all other corresponding points along a track are constructed. A curve is fitted to the constructed points, and values for an azimuth angle, dip angle, end coordinates, arc length, and curvature (and, hence, momentum) are calculated for each end of the track.

Error assignments to each quantity are carried through the calculation. Neither optical nor magnetic-field distortions are at present considered by the program, which is now used to analyze data from the helium bubble chamber.⁵ The magnetic field over the area of this chamber can be considered uniform, and the distortion of a straight line by the glass plates through which the camera photographs the chamber is negligible, corresponding at worst to 70 m radius of curvature.

The computer program may be broken into three parts: the input program, the main program, and the output program. The punched paper tape from the Hermes measuring machine is written as card images on magnetic tape. The input program accepts these data, reads one card image at a time,

decodes the information, and stores the information in the common storage region so that it will be available for further manipulation and calculation. Storage locations have been allocated for nine tracks in each of the views. A maximum number of 50 points may be measured for each track. An attempt has been made to incorporate error detection and correction into the input program.

The main program shown on the simplified flow chart, Fig. 1, first checks the data as stored by the input program to ensure that enough information is available to proceed with the calculations. Any tracks that may have been measured in reverse order are rearranged in correct order. The subroutine FIDO is entered with fiducial data for each of the three views. This subroutine uses the two fiducials that have the greatest separation to construct the bubble-chamber coordinate system. The position of a third fiducial is calculated and compared with the measured coordinates of this fiducial. If the calculated and measured positions differ by more than some preset distance, the view is rejected. The magnification for each view is also calculated. All track data are translated and rotated into the coordinate system as constructed by FIDO. The main program selects a track and the best two views in which this track was measured. The data for this track are presented to a subroutine, SPACE. A least-squares polynomial is fit through the points in one (auxiliary) view. A line is constructed through each point, as measured in the other (principal) view, parallel to the line joining the cameras, with which these two views were obtained, and the intersections of these lines with the polynomial are computed. With these calculated corresponding points, the X, Y, and Z coordinates of the points, as they were in the bubble chamber, are calculated.

The subroutine POLFIT is entered with the calculated X, Y, and Z coordinates, and the least-square polynomials are fit in the X-Y plane and the X-Z plane. The order of polynomial is under parametric control. With the two expressions $Y = F(X)$ and $Z = G(X)$, an integration is made in subroutine ARC to compute the arc length. The projected arc length is also computed. The dip angles and azimuthal angles, with errors, are calculated at the end points of the track. The projected curvature at the center of the track is

⁵M. M. Block *et al.*, *Proc. Intern. Conf. High-Energy Accelerators and Instrumentation, Geneva, 1959*, p 461.

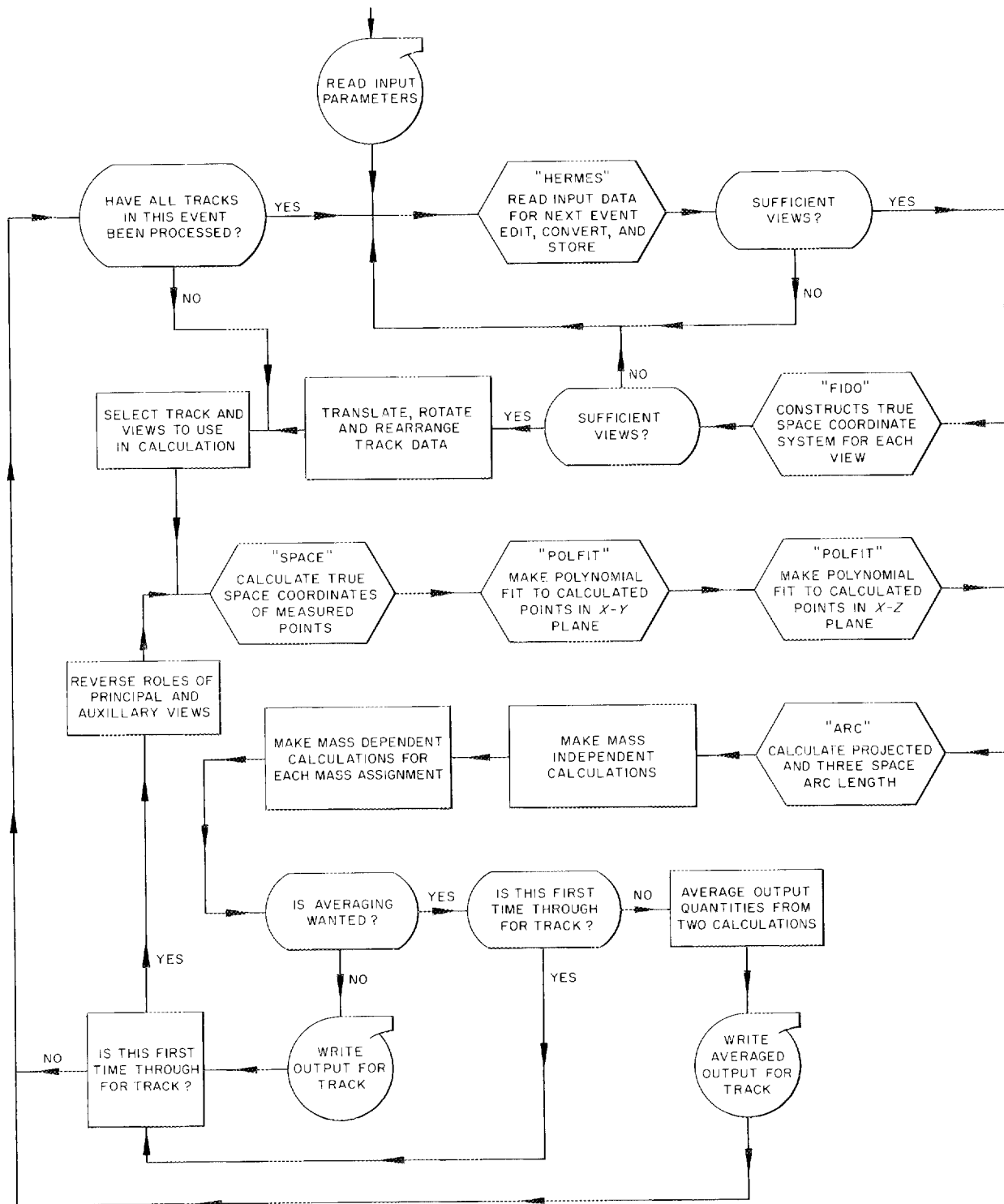


Fig. 1. Program Flow Chart.

calculated, and the momentum of the particle at the center of the track is computed. By means of a range-momentum subroutine PRANG, the momentum at the end points of the track is calculated. Error assignments are also made for these momenta. Since the momentum calculation is mass-dependent, this calculation is made for each mass assignment for the track. At this point the roles of the two views are interchanged, and the entire calculation is done as before. Provisions have been made so that one may average or have separate output for each of these calculations. Each track is processed in turn until

all tracks have been processed. The input program is then re-entered, and the data for the next event are read into the computer for processing. Selected track parameters are available as punched-card output for processing by an auxiliary program. An example is shown in Fig. 2, where a histogram of K^- momenta was directly obtained.

The program as well as the operation of the Hermes have been tested in several ways. A number of events and tracks, which had previously been measured by the old and tedious methods, were measured and processed by the program. Agreement was found to be within quoted errors

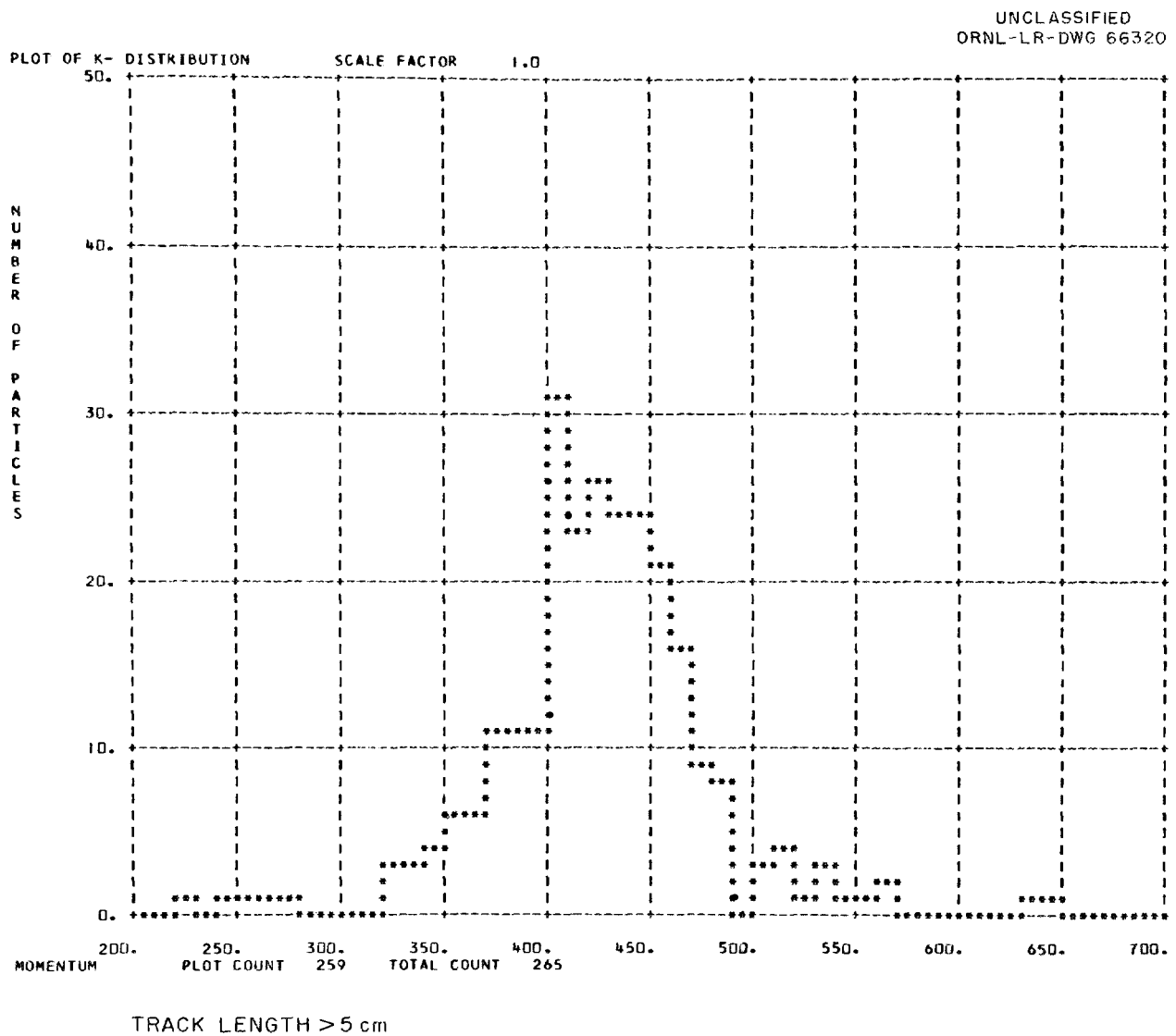


Fig. 2. The K^- Meson Momentum Distribution.

of measurement. The errors are similar in magnitude for both methods. The coordinates of ten available fiducial marks were repeatedly measured in this manner. The average of the measurements employing the two methods agreed to within 0.1 mm for the X and Y coordinates, while the Z (depth) coordinate differed by only 0.7 mm. Due to the geometry of the chamber, the error in Z determination is expected to be about six times that of the X and Y coordinate uncertainty. Meas-

urements of complete events also agreed very satisfactorily. A number of τ decays were measured, with the resulting momenta and angles kinematically overdetermined. The results showed that the program and the Hermes operated very well. The program has to date been used successfully to reconstruct several hundred tracks.

We gratefully acknowledge the assistance of J. L. Gabbard, Jr., in preparing the program.

RESPONSE OF SILICON SURFACE-BARRIER DETECTORS TO FISSION FRAGMENTS

H. W. Schmitt

J. H. Neiler

F. J. Walter

R. J. Silva

Investigation of the response of silicon surface-barrier detectors to fission fragments was continued. The methods of measurement and analysis have been discussed in previous reports;^{1,2} it is found that the pulse height and energy are related through the equation

$$E = a \times PH + \delta, \quad (1)$$

where δ has been termed the "pulse-height defect" or "energy defect" for fission fragments.

Figure 1 shows a typical pulse-height spectrum from the spontaneous fission of Cf^{252} . The seven points identified for pulse height vs energy are as follows: the valley, the two peaks, the points at half-maximum on the low- and high-energy edges, and the extrapolations to zero counts of the low- and high-energy edges. The pulse heights corresponding to these points were obtained from a pulser calibration made under the same conditions that prevailed in the fission run. Energies corresponding to these points were obtained from the data of Milton and Fraser³ and Stein and Whetstone.⁴

Figure 2 shows a typical plot of pulse height vs energy for the two sets of time-of-flight data.

Closed circles were obtained for the energies of Stein and Whetstone, open circles for the energies of Milton and Fraser. Note the large difference in values of δ (the intercept on the energy axis). It was found that this difference remained essentially constant, independent of the values of δ , for a wide variety of detectors.

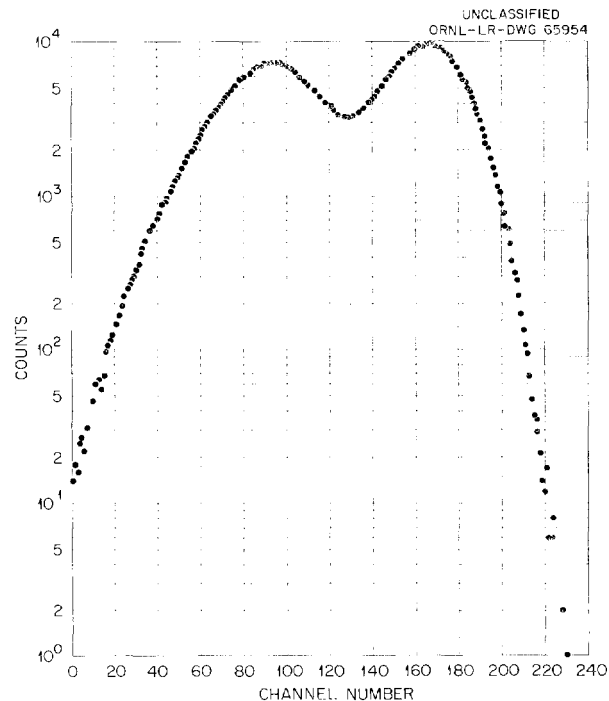


Fig. 1. Typical Cf^{252} Spontaneous Fission Fragment Pulse-Height Spectrum. The thin Cf^{252} source was deposited on a platinum backing and fired.

¹H. W. Schmitt *et al.*, *Phys. Div. Ann. Progr. Rept.* Feb. 10, 1961, ORNL-3085, p 91.

²H. W. Schmitt *et al.*, *Bull. Am. Phys. Soc.* **6**, 240 (1961).

³J. C. D. Milton and J. S. Fraser, *Phys. Rev.* **111**, 877 (1958).

⁴W. E. Stein and S. L. Whetstone, *Phys. Rev.* **110**, 476 (1958).

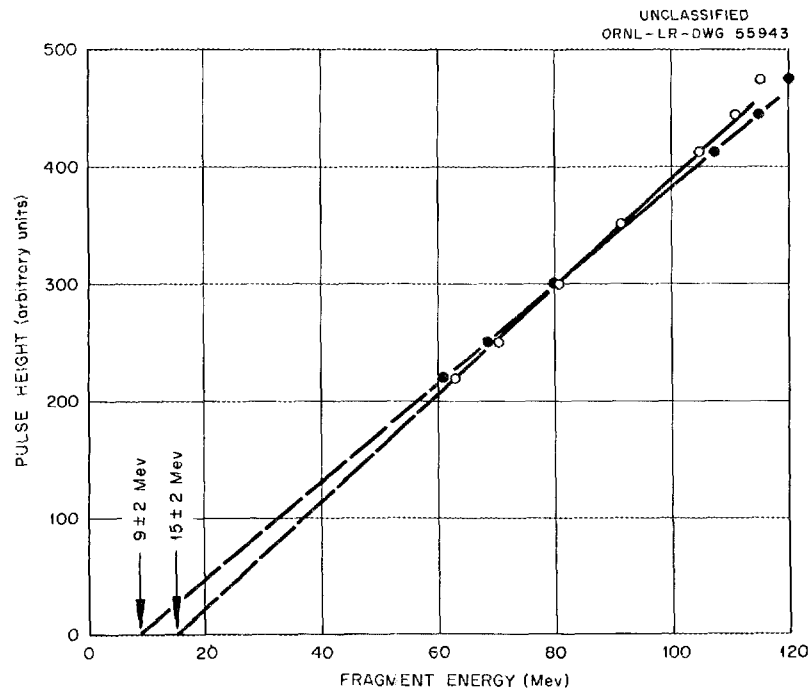


Fig. 2. Pulse Height vs Fragment Energy. Open circles are results obtained with the energies of Milton and Fraser; closed circles are results obtained with the energies of Stein and Whetstone.

Figure 3 shows δ , obtained from data as shown in Fig. 2, plotted as a function of E_0 , the maximum electric field in the barrier. Energies were those of Stein and Whetstone, although the choice was arbitrary and a similar plot, with all points displaced upward by 6 or 7 Mev, was obtained when the Milton and Fraser energies were used. The maximum field in v/cm in silicon is given by the expression

$$E_0 = 4.2 \times 10^4 \sqrt{V/\rho}, \quad (2)$$

where V is the detector bias in volts (i.e., the applied bias plus 0.6 v), and ρ is the resistivity in ohm-cm. Note that δ is essentially constant, independent of E_0 , and independent of all detectors, except for the anomalous 3600-ohm-cm detector. This detector was tested again later, after further aging, and δ was still found to be decreasing toward the lower values; on this basis it was concluded that the surface treatment of this detector had not been satisfactory in the beginning, and that indeed the data obtained from the 3600-ohm-cm detector should be considered anomalous. The gold thickness on all detectors

was $100 \mu\text{g}/\text{cm}^2$ or less, corresponding to fragment energy losses of 2 Mev or less — small compared with the measured values of δ .

Figure 4 shows the slope, $1/a$, of the pulse-height-vs-energy relation as a function of maximum electric field E_0 . Again, energies are those of Stein and Whetstone. Values of a , energy loss in ev per ion pair formed, are shown at the right; calibration for this scale was obtained from measurements in which natural alpha particles were used. If we ignore the anomalous behavior of the 3600-ohm-cm detector (see previous paragraph), then a more or less consistent qualitative picture will explain these data. Thus, as the field E_0 approaches the critical field in silicon (6×10^4 v/cm), multiplication may set in; thus the slope $1/a$ would be expected to increase with increasing E_0 , as indicated for the 30-ohm-cm detector. In the case of the 120-ohm-cm detector, the slope $1/a$ tends to decrease with decreasing field below about 1.3×10^4 v/cm; this occurs because the barrier depth is less than the fragment range for the lower fields, and indeed the barrier depth becomes a smaller fraction of the total range, giving rise to smaller amounts of charge collected,

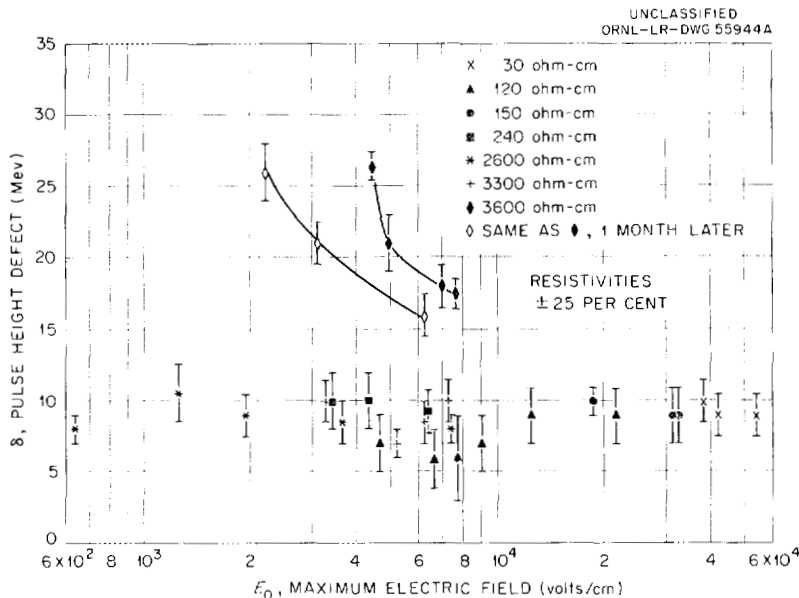


Fig. 3. "Pulse-Height Defect," Sometimes Called "Energy Defect," for Cf^{252} Fission Fragments as a Function of Maximum Electric Field in the Detector. Reference energies are those of Stein and Whetstone. Similar results, with values of δ approximately 6 Mev higher, are obtained when reference energies of Milton and Fraser are used.

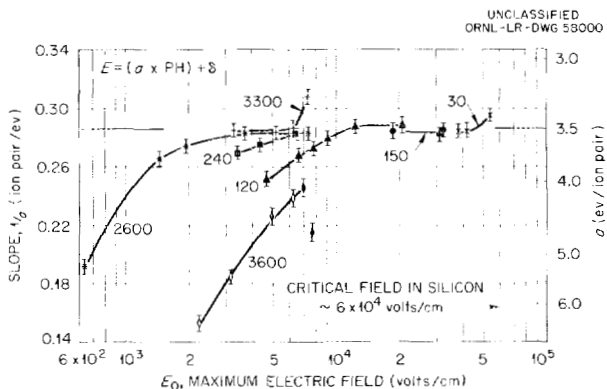


Fig. 4. Slope, $1/a$, of Pulse-Height-vs-Energy vs Maximum Electric Field, E_0 . Silicon surface-barrier detectors. Number labels indicate silicon resistivity. Energy reference data from Stein and Whetstone.

of the amplifier. In the case of the 2600-ohm-cm detector, the barrier depth is always greater than the fragment range; thus the decrease below fields of about 4×10^3 v/cm is attributed simply to decreased efficiency for "charge collection" at the lower fields, reasons for which are not at present understood. The one high point obtained with the 3300-ohm-cm counter remains unexplained.

It is interesting that the plateau in Fig. 4 occurs at $a = 3.5$ ev/ion pair, in agreement with the value obtained by other investigators for alpha particles. The possibility that the time-of-flight data are in error, at least at the present time, should not be ignored, particularly in view of the large discrepancy in the present results depending on which set of data is used. No theoretical studies of possible carrier loss mechanisms have been undertaken in connection with this work. However, if the energy scale is correct, the form of the empirical relation suggests that more than one loss mechanism may be involved.

Figure 5 shows the slope $1/a$ as a function of maximum field E_0 , where the reference energies are those of Milton and Fraser. Qualitative results for the slope $1/a$ are much as indicated in

the previous discussion, although quantitatively there are significant differences, as seen in a comparison of Figs. 4 and 5. Resolution of the discrepancies in the time-of-flight measurements for Cf²⁵² spontaneous fission is required in order to discuss quantitatively the results presented in this paper.

A single determination of δ was made for U²³⁵ thermal-neutron-induced fission fragments. Energies used for comparison with the pulse-height spectrum were those of Milton and Fraser.⁵ The value of δ in this case was found to be 11 ± 2 Mev, compared with an average for the above series of detectors of 14 ± 2 for the Cf²⁵² source and the reference energies of Milton and Fraser.³

⁵J. C. D. Milton, private communication, 1962, to be published.

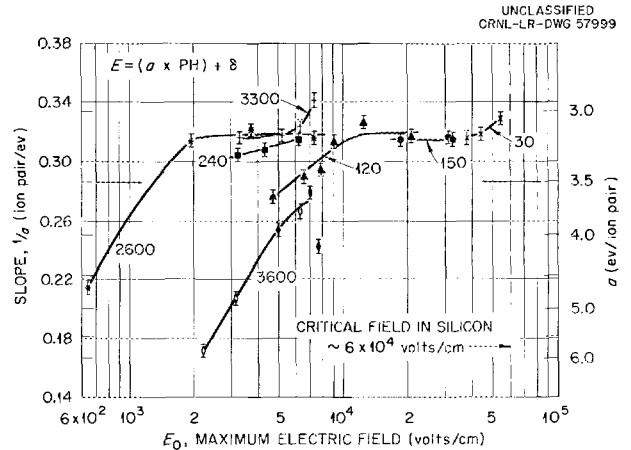


Fig. 5. Slope, $1/a$, of Pulse-Height-vs-Energy vs Maximum Electric Field, E_0 . Silicon surface-barrier detectors. Number labels indicate silicon resistivity. Energy reference data from Milton and Fraser.

BEHAVIOR OF SEMICONDUCTOR NUCLEAR-PARTICLE DETECTORS¹

F. J. Walter

J. W. T. Dabbs

L. D. Roberts

Experimental and theoretical studies of the behavior of semiconductor nuclear-particle detectors have been carried out over the temperature range 0.2 to 300°K. A simple theoretical model which describes the detector behavior over a wide range of parameters is presented. The importance of semiconductor purity and bias voltage in connection with pulse height, pulse rise time, and detector area is discussed.

Empirical studies of noise and energy resolution indicate that for alpha particles the smallest peak widths observed are substantially larger than those expected on the basis of electrical noise from the detector and the amplifier. Equivalent noise values ≤ 3 kev full width at half maximum were found for a 40-mm² silicon surface-barrier detector at 77°K.

Semiconductor detectors exhibit a "pulse-height defect" for fission fragments. There is evidence that this defect is not caused by a "dead layer." If electric fields insufficient to ensure complete

"collection" are responsible for the defect, the necessary minimum field (at the surface) is $> 3 \times 10^4$ v/cm for fission fragments, compared with the value of $\sim 2 \times 10^3$ v/cm found necessary in the case of alpha particles in germanium and silicon.

Detailed considerations regarding pulse rise time at the amplifier have shown that in high-resistivity material both the "dielectric" relaxation time and the resistance associated with the undepleted base material can play an important role. A quantitative description of the effect of detector and amplifier parameters on the shapes and rise times associated with the pulse is presented.

The advantages and problems associated with the use of surface-barrier detectors in several unique low-temperature nuclear-alignment experiments are discussed. The experiments involved fission-fragment angular distributions and resolution of alpha fine structure with long-term stability. Matched-expansion-coefficient fabrication techniques that have been successfully used to make detectors up to 8 cm² in active area are also described.

¹Abstract of paper to be published in *Proceedings of a Conference on Nuclear Electronics*, Belgrade, 1961.

A SUPERCONDUCTING MAGNET STUDY¹

L. D. Roberts

R. W. Boom

A superconducting solenoid ($\frac{1}{2}$ -in. ID, 2-in. OD, 1.25-in. length) containing 1800 ft of 0.010-in.-diam wire (75% Nb-25% Zr) was fabricated with an open construction such that the turns within the magnet were well exposed to liquid helium. The behavior of this magnet was studied in the temperature range 1.5 to 4.2°K as a function of magnet current. The maximum current in the superconducting state was somewhat temperature dependent, and the rate of the transition to the normal state was strongly temperature dependent. At the lower temperatures, the transition was faster, and the maximum field was about 10% higher. Near 4.2°K the transition rate was in the millisecond region, whereas at the lowest temperatures maximum transition rates of the order of 0.1 μ sec were observed. The maximum

current was near 20 amp, and the maximum field was about 33 kilogauss.

The very high speed of the superconducting-to-normal transition near 1.5°K and the corresponding rapid collapse of the magnetic field produced quite high voltages in the vicinity of the coil. A simple mathematical model of the transition process has been considered in which it is assumed that the superconducting wire goes normal at some point and that the normal-state region then spreads along the wire.

In a first calculation we assumed that length of the normal section and thus the coil resistance increased linearly with time, that is, as $R = at$. Taking the other circuit constants as those used in actual measurements on the coil, and assuming a set of a values over a suitable range, the time dependence of the magnet current and the voltage during the transition were calculated. The calculated curves agree fairly well with oscillograph studies of the coil behavior.

¹Other aspects of this work are more fully reported by R. W. Boom and L. D. Roberts in the annual progress reports of the Electronuclear Division.

GENERAL SURVEY ON PULSED ELECTROSTATIC ACCELERATORS AS SOURCES OF PULSED NEUTRONS¹

W. M. Good

This paper is mainly devoted to the production of neutrons having energies between 2 and 100 kev by means of positive ions (from an electrostatic accelerator) bombarding a thin Li⁷ target. A description is given of the pulsed ion source,

and some computations are made, giving the resolution now available and the expected improvements of the resolution. It is shown that the method described is particularly valuable with small samples. Moreover, the energy resolution is maintained constant from 2 to 50 kev. A transmission measurement with an Se⁸⁰ sample is provided to illustrate one application of the technique.

¹Abstract of published paper: pp 309-19 in *Proceedings of the Symposium on Neutron Time-of-Flight Methods, Session III, Saclay, France, July 24-27, 1961*.

NAPHTHALENE DERIVATIVE SCINTILLATORS AND GLASS LOADING POSSIBILITIES¹

R. L. Macklin

Naphthalene derivatives have been found to provide a base for scintillators that cover a range of refractive indices overlapping those of the lead optical glasses. Included in the discussion

are considerations that indicate the feasibility of making scintillation gamma detectors having several times the stopping power of organic scintillators. A mixture of glass powder and liquid scintillator is used, and the proportions are near 1:1 by volume.

¹Abstract of published report: AERE-R 3744 (June 1961).

PULSE-SHAPE CALCULATIONS FOR A LARGE LIQUID SCINTILLATOR

R. L. Macklin

J. H. Gibbons

Earlier neutron capture measurements¹ involved extrapolation to zero pulse height in order to obtain areas proportional to total capture. To provide guidance in such extrapolation an extensive computational program has been pursued.

First, the Zerby-Moran code was applied to get the pulse-height distributions corresponding to single gamma rays up to 10 Mev at the sample position in the 1.2-m liquid scintillator. These results were empirically fitted to permit interpolation and were then incorporated in a Monte Carlo cascade code which found the pulse-height distributions that corresponded to model neutron-capture gamma cascades.

The model chosen as a rough representation gave a predetermined Maxwellian distribution to the cascade gammas, except the last, which was chosen to ensure energy conservation. The model can be parameterized by the binding energy and either the temperature of the Maxwellian distribution or the average resulting multiplicity of the cascades.

In addition to the model representation, we included specially favored transitions to or through specified levels (unique cascades) and a resolution broadening code (courtesy of M. C. Taylor) in order to permit direct comparison with the experimental data. The spectrum distortion produced by the attenuation of weak gamma rays in the thicker samples was corrected for empirically, using thick-vs-thin-sample results.

The results are much as expected, giving, for instance, finite intercepts at zero pulse height. A measure of the agreement is illustrated in Fig. 1. The dashed curve is the result of the empirical extrapolations¹ and falls in the expected range of multiplicities, 3 to 5.

Detailed fits to most of the capture spectra are possible with the Maxwellian model alone. Figure 2 shows such a fit for a thin sample of silver. The slight departure at the high-energy toe can be attributed to the effect of the slightly higher binding energy of Ag¹⁰⁷. The multiplicities found range from the 3.17 for silver to 4.7 for tantalum.

It should be emphasized that several more gamma rays of very low energy (say, 0.1 Mev), while raising the multiplicity, would not appreciably influence our pulse spectra.

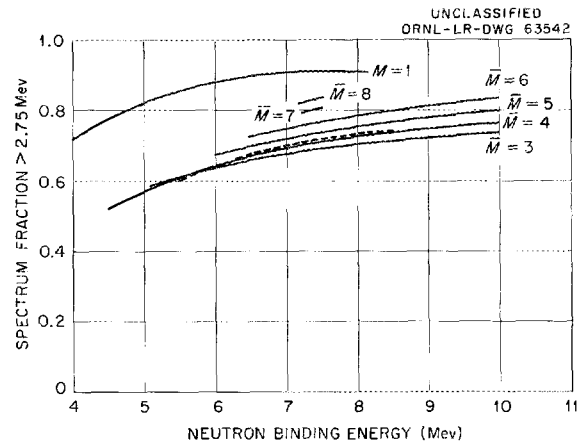


Fig. 1. The 1.2-m Liquid-Scintillator Spectrum Fractions for Maxwellian Cascades and Single Gamma Rays.

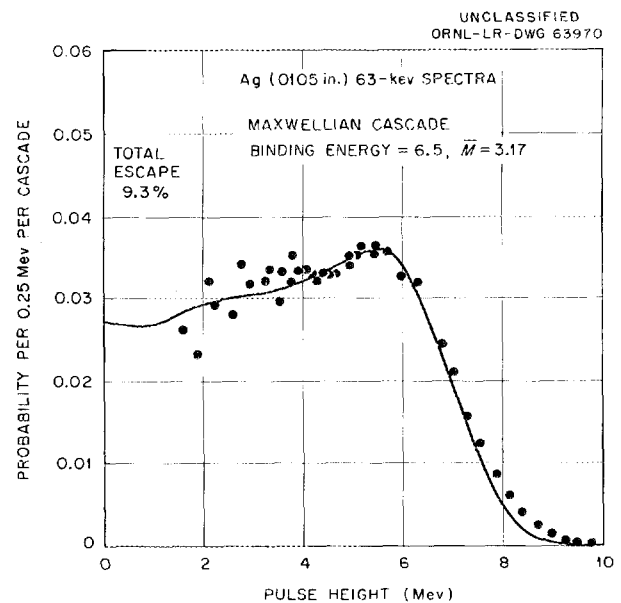


Fig. 2. The 1.2-m Liquid-Scintillator Pulse-Height Distribution.

¹J. H. Gibbons, R. L. Macklin, P. D. Miller, and J. H. Neiler, *Phys. Rev.* 122, 182 (1961).

Several rare-earth samples (A near 160) show a remarkable double-humped structure. This necessitated the addition of favored transitions through a band of levels near one-half the binding energy in order to produce fits. The spectrum from Tb^{159} (Fig. 3) shows the effect most strongly. The competition of the favored band with the Maxwellian distribution decreases to half maximum near $A = 152$ and $A = 166$, though the decrease may be overemphasized by the decreased sensitivity of the spectra when the band is displaced from the half-binding-energy position.

It is suggestive that the single-particle level responsible for the p -wave strength function peak near $A = 100$ is predicted to lie at half the binding energy near $A = 150$. This could provide favored dipole transitions from s -wave initial capture levels to the enhanced p -wave levels.

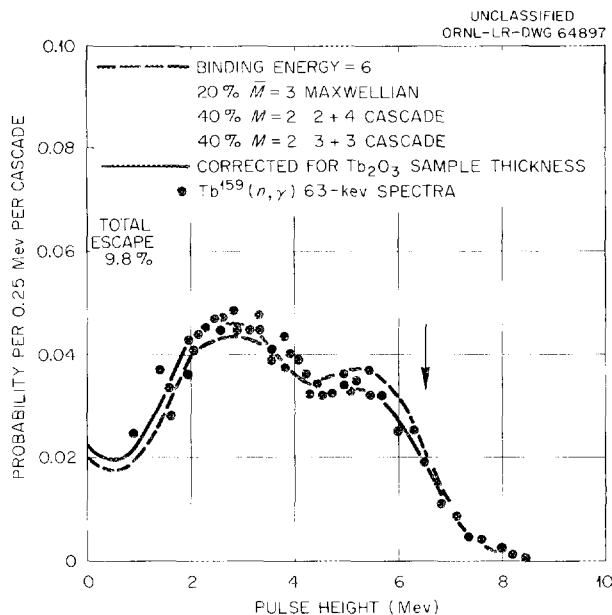


Fig. 3. The 1.2-m Liquid-Scintillator Pulse-Height Distribution.

IMPROVED BEAM PULSER FOR 3-Mv VAN DE GRAAFF ACCELERATOR

C. D. Moak R. F. King H. E. Banta¹ J. W. Johnson

A new pulser built for the duoplasmatron ion source has been installed in the terminal of the 3-Mv accelerator. Larger currents, shorter pulse duration, and increased reliability were the objectives.

The new pulser is able to deliver peak currents of several milliamperes, with pulse durations

variable down to 2 nanoseconds. Gas consumption is comparable with that of earlier, less efficient systems. The system has run for more than 700 hr without overhaul; the rf ion-source pulser previously used required overhaul every 200 hr. The use of heavier currents brought about the need for liquid cooling of various electrodes. This is accomplished through the use of a new heat transfer fluid that has sufficiently high electrical strength to permit it to be pumped up and back along the accelerator column in Teflon tubes.

¹Now at the Oak Ridge Institute of Nuclear Studies.

COUNTDOWN CIRCUITS FOR PULSED VAN DE GRAAFF ACCELERATOR

R. F. King

W. H. Du Preez¹

Each experiment designed for pulsed-accelerator work will in general require a different optimum pulse-repetition rate; beyond a certain point compromises cannot be made. For capture-tank experiments or for experiments with very slow neutrons, it is necessary to reduce the pulse-

repetition rate to avoid background effects from previous pulses.

In order to avoid further complication of the accelerator terminal assembly, a synchronized countdown system has been built in order to effectively reduce the repetition rate from the basic 10^6 pulses per second to $\frac{1}{8}$ this value. With this arrangement, a set of electrostatic deflector plates is used to allow only one pulse out of eight to reach the target, while the remaining seven pulses are discarded.

¹Visiting investigator from South Africa Atomic Energy Board, Pretoria, South Africa.

RELIABILITY IN HELIUM LIQUEFACTION¹

J. W. T. Dabbs

A dual-liquefier arrangement was recently established at the Oak Ridge National Laboratory in order to improve the reliability of helium liquefaction. Two Collins liquefiers,² only slightly modified, were used. Four compressors are connected in parallel; gasholders and traps are duplicated. The valving (with associated electrical safety switches) permits any combination of components to be used. Simultaneous operation of both liquefiers is, however, not provided in the present arrangement. The compressors are mounted on individual stands spaced 1.5 m apart so that repairs can proceed on one compressor

while its neighbors are in operation. Thus the arrangement essentially eliminates downtime caused by single mechanical failures.

The problem of contamination of the helium gas in the circuit also received attention. A major difficulty in the past has been air leakage into the crankcases of the compressors. This was virtually eliminated by operating the entire low-pressure side of the system above atmospheric pressure. Larger crankcase breather piping was used, and lead weights were introduced into the gasholders.

The production capability of the system is estimated to be about 1000 liters/month; present usage is about 400 liters/month. (In January 1962, about 700 liters was used.) No downtime from mechanical failure has occurred since the system was made operative.

¹Abstract of paper to be published in *Proceedings of a Conference of l'Institute International du Froid*, London, September 20-22, 1961.

²Manufactured by the Arthur D. Little Co., Cambridge, Mass.

PUBLICATIONS

- Bair, J. K., "Levels in N^{14} at 11.74 and 11.82 Mev," *Phys. Rev.* **122**, 897 (1961).
- Biedenharn, L. C., and G. R. Satchler, "Polarization Phenomena in Deuteron Stripping Reactions," *Proc. Intern. Symposium Polarization Phenomena of Nucleons, Basel, 1960* [*Helv. Phys. Acta, Suppl. VI*, pp 372-401 (1960)].
- Block, M. M., E. B. Brucker, R. Gessaroli, T. Kikuchi, A. Kovacs, C. M. Meltzer, R. Kraemer, M. Nussbaum, A. Pevsner, P. Schlein, R. Strand, H. O. Cohn, E. M. Harth, J. Leitner, L. Lendinara, L. Monari, and G. Puppi, " K^- Absorption in He^4 - I. The Hyperon-Pion Resonance," *Nuovo cimento* **20**, 724 (1961).
- Block, R. C., G. G. Slaughter, L. W. Weston, and F. C. VonderLage, "Neutron Radiative Capture Measurements Utilizing a Large Liquid Scintillator Detector at the ORNL Fast Chopper," pp 203-11 in *Proc. Symposium Neutron Time-of-Flight Methods, Saclay, 1961* (ed. by J. Spaepen), European Atomic Energy Community (Euratom), Brussels, 1961.
- Cable, J. W., M. K. Wilkinson, and E. O. Wollan, "Neutron Diffraction Investigation of Antiferromagnetism in $CrCl_3$," *Phys. and Chem. Solids* **19**, 29 (1961).
- Cable, J. W., E. O. Wollan, W. C. Koehler, and M. K. Wilkinson, "Neutron Diffraction Study of Metallic Erbium," *Proc. Sixth Symposium Magnetism and Magnetic Materials, New York, 1960* [*J. Appl. Phys. Suppl.* **32**, 49S (1961)].
- Carlson, T. A., A. H. Snell, Frances Pleasonton, and C. H. Johnson, "Electron Shake-Off Following Beta Decay," *Proc. IAEA Symposium Chemical Effects of Nuclear Transformations, Prague, 1960*, I, 155-60 (1961).
- Charles, G. W., "Intermediate Coupling in Atomic Spectra," p 894 in *Encyclopaedic Dictionary of Physics* (ed. by J. Thewlis), vol 3, Pergamon, New York, 1961.
- Clegg, A. B., and G. R. Satchler, "Gamma-Rays from Inelastic Scattering of High Energy Nucleons," pp 143-44 in *Proc. Rutherford Jubilee Intern. Conf., Manchester, England, 1961* (ed. by J. B. Birks), Heywood, London, 1961; *Nuclear Phys.* **27**, 431 (1961).
- Cohn, H. O., J. K. Bair, and H. B. Willard, "Carbon-13 Neutron Total Cross Section," *Phys. Rev.* **122**, 534 (1961).
- Dabbs, J. W. T., S. H. Hanauer, L. D. Roberts, F. J. Walter, and G. W. Parker, "Alpha-Particle Emission from Oriented Np^{237} ," pp 177-80 in *Proc. 7th Intern. Conf. Low Temperature Physics, Toronto, 1960* (ed. by G. M. Graham and A. C. H. Hallet), University of Toronto Press, Toronto, 1961.
- Elliott, R. J., "Phenomenological Discussion of Magnetic Ordering in the Heavy Rare Earth Metals," *Phys. Rev.* **124**, 346 (1961).
- Felsner, G., and M. E. Rose, "Effect of Inelastic Scattering on Polarization Asymmetry," *Nuovo cimento* **20**, 509 (1961).
- Firk, F. W. K., and J. H. Gibbons, "A Direct Comparison of Gamma-Ray Spectra Obtained from the Capture of Thermal and (30 ± 10) keV Neutrons," pp 213-19 in *Proc. Symposium Neutron Time-of-Flight Methods, Saclay, 1961* (ed. by J. Spaepen), European Atomic Energy Community (Euratom), Brussels, 1961.
- Firk, F. W. K., G. G. Slaughter, and R. J. Ginther, "An Improved Li^6 -Loaded Glass Scintillator for Neutron Detection," *Nuclear Instr. & Methods* **13**, 313 (1961).
- Fowler, J. L., "The Neutron as a Probe of Nuclear Matter," *J. Tem. Acad. Sci.* **36**(2), 109 (1961).

- Gibbons, J. H., "General Survey on Radiative Capture Measurements by Time-of-Flight," pp 151-65 in *Proc. Symposium Neutron Time-of-Flight Methods, Saclay, 1961* (ed. by J. Spaepen), European Atomic Energy Community (Euratom), Brussels, 1961.
- Gibbons, J. H., R. L. Macklin, P. D. Miller, and J. H. Neiler, "Average Radiative Capture Cross Sections for 7 to 170 keV Neutrons," *Phys. Rev.* **122**, 182 (1961).
- Good, W. M., "General Survey on Pulsed Electrostatic Accelerators as Sources of Pulsed Neutrons," pp 309-19 in *Proc. Symposium Neutron Time-of-Flight Methods, Saclay, 1961* (ed. by J. Spaepen), European Atomic Energy Community (Euratom), Brussels, 1961.
- Halbert, E. C., R. M. Drisko, G. R. Satchler, and N. Austern, "Finite-Range Distorted-Waves Calculation of Direct Reactions," pp 555-56 in *Proc. Rutherford Jubilee Intern. Conf., Manchester, England, 1961* (ed. by J. B. Birks), Heywood, London, 1961.
- Hanauer, S. H., J. W. T. Dabbs, L. D. Roberts, and G. W. Parker, "The Angular Distribution of Alpha Particles Emitted by Oriented Np^{237} Nuclei," *Phys. Rev.* **124**, 1512 (1961).
- Harvey, J. A., "General Survey on Time-of-Flight Measurements Applied to Nuclear Physics," pp 23-56 in *Proc. Symposium Neutron Time-of-Flight Methods, Saclay, 1961* (ed. by J. Spaepen), European Atomic Energy Community (Euratom), Brussels, 1961.
- Harvey, J. A., "Chopper, Fast or Slow, for Neutrons," pp 677-78 in *Encyclopaedic Dictionary of Physics* (ed. by J. Thewlis), vol 1, Pergamon, New York, 1961.
- Harvey, J. A., "Cross-Section Measurement," p 197 in *Encyclopaedic Dictionary of Physics* (ed. by J. Thewlis), vol 2, Pergamon, New York, 1961.
- Harvey, J. A., and S. E. Atta, "Shape and Area Analysis of Low Energy Neutron Resonances Using an IBM-7090 Computer," pp 555-60 in *Proc. Symposium Neutron Time-of-Flight Methods, Saclay, 1961* (ed. by J. Spaepen), European Atomic Energy Community (Euratom), Brussels, 1961.
- Johnson, J. W., and W. M. Good, "Gas Leak Valve with Improved Characteristics," *Rev. Sci. Instr.* **32**, 219 (1961).
- Koehler, W. C., "Neutron Diffraction by Helical Spin Structures," *Proc. Sixth Symposium Magnetism and Magnetic Materials, New York, 1960* [*J. Appl. Phys. Suppl.* **32**, 20S-21S (1961)].
- Koehler, W. C., "Neutron Diffraction by Helical Spin Structures," *Acta Cryst.* **14**, 535 (1961).
- Koehler, W. C., E. O. Wollan, M. K. Wilkinson, and J. W. Cable, "Magnetic Structure Properties of Rare Earth Metals," pp 149-57 in *Arrowhead (Rare Earth) Research Conf., Lake Arrowhead, California, 1960* (ed. by E. V. Kleber), Macmillan, New York, 1961.
- Leitner, J., L. Gray, E. Harth, S. Lichtman, J. Westgard, M. Block, B. Brucker, A. Engler, R. Gessaroli, A. Kovacs, T. Kikuchi, C. Meltzer, H. O. Cohn, W. Bugg, A. Pevsner, P. Schlein, M. Meer, N. T. Grinellini, L. Lendinara, L. Monari, and G. Puppi, "Helicity of the Proton from Λ Decay," *Phys. Rev. Letters* **7**, 264 (1961).
- McGowan, F. K., and P. H. Stelson, "Coulomb Excitation of the Second 2^+ States in W, Os, and Pt Nuclei," *Phys. Rev.* **122**, 1274 (1961).
- McGowan, F. K., and P. H. Stelson, "Decay of $\text{Rh}^{102} \rightarrow \text{Ru}^{102}$," *Phys. Rev.* **123**, 2131 (1961).
- Morgan, H. W., "Vibrational Spectrum of the NCSe^- Ion," *J. Inorg. & Nuclear Chem.* **16**, 367 (1961).
- Obenshain, F. E., and H. H. F. Wegener, "Mössbauer Effect with Ni^{61} ," *Phys. Rev.* **121**, 1344 (1961).
- Pinkston, W. T., and G. R. Satchler, "Collective Effects in Inelastic Scattering from Nuclei," *Nuclear Phys.* **27**, 270 (1961).

- Roberts, L. D., and J. W. T. Dabbs, "Nuclear Orientation," *Ann. Rev. Nuclear Sci.* **11**, 175 (1961).
- Roberts, L. D., J. W. T. Dabbs, and G. W. Parker, "Nuclear Orientation Experiments with Oriented U^{233} , U^{234} , U^{235} , and Np^{237} Isotopes," *Intern. J. Appl. Radiation and Isotopes* **9**, 176 (1960).
- Roberts, L. D., J. W. T. Dabbs, F. J. Walter, S. H. Hanauer, and G. W. Parker, "Nuclear Orientation Experiments with U^{233} , U^{234} , U^{235} , and Np^{237} Isotopes," pp 329-40 in *Proc. Conf. Use of Radioisotopes in Physical Sciences and Industry, Copenhagen, 1960*, International Atomic Energy Agency, Vienna, 1962.
- Roberts, L. D., F. J. Walter, J. W. T. Dabbs, G. W. Parker, and J. O. Thomson, "Fission Fragments from Oriented U^{233} and U^{235} ," pp 174-77 in *Proc. 7th Intern. Conf. Low Temperature Physics, Toronto, 1960* (ed. by G. M. Graham and A. C. H. Hallett), University of Toronto Press, Toronto, 1961.
- Robinson, R. L., E. Eichler, and N. R. Johnson, "Decay of I^{132} ," *Phys. Rev.* **122**, 1863 (1961).
- Rose, M. E., "Analysis of Internal Conversion Data," pp 834-51 in *Nuclear Spectroscopy, Part B* (ed. by Fay Ajzenberg-Selove), Academic Press, New York, 1961.
- Rose, M. E., "Analysis of Beta Decay Data," pp 811-33 in *Nuclear Spectroscopy, Part B* (ed. by Fay Ajzenberg-Selove), Academic Press, New York, 1961.
- Rose, M. E., and R. L. Carovillano, "Coherence Effects in Resonance Fluorescence," *Phys. Rev.* **122**, 1185 (1961).
- Satchler, G. R., "Direct Nuclear Reactions with Polarized Targets," pp 545-46 in *Proc. Rutherford Jubilee Intern. Conf., Manchester, England, 1961* (ed. by J. B. Birks), Heywood, London, 1961.
- Schmid, E. W., and K. Wildermuth, "Phase Shift Calculations on α - α Scattering," *Nuclear Phys.* **26**, 463 (1961).
- Schmitt, H. W., and J. Halperin, " $Al^{27}(n,\alpha)Na^{24}$ Cross Section as a Function of Neutron Energy," *Phys. Rev.* **121**, 827 (1961).
- Slaughter, G. G., F. W. K. Firk, and R. J. Ginther, "A Li^6 -Loaded Glass Scintillator for Neutron Detection," pp 425-29 in *Proc. Symposium Neutron Time-of-Flight Methods, Saclay, 1961* (ed. by J. Spaepen), European Atomic Energy Community (Euratom), Brussels, 1961.
- Snell, A. H., Frances Pleasonton, and T. A. Carlson, "Techniques of Radioactive Recoil Spectrometry and Charge Spectrometry; The Atomic Consequences of Internal Conversion and Electron Capture," *Proc. IAEA Symposium Chemical Effects of Nuclear Transformations, Prague, 1960*, **1**, 147-54 (1961).
- Tracy, J. W., N. W. Gregory, E. C. Lingafelter, J. D. Dunitz, H. C. Mez, R. E. Rundle, Christian Scheringer, H. L. Yakel, and M. K. Wilkinson, "The Crystal Structure of Chromium(II) Chloride," *Acta Cryst.* **14**, 927 (1961).
- Trammell, G. T., "Gamma-Ray Diffraction by Resonant Nuclei," *Proc. IAEA Symposium Chemical Effects of Nuclear Transformations, Prague, 1960*, **1**, 75-85 (1961).
- Walter, F. J., J. W. T. Dabbs, and L. D. Roberts, "Behavior of Semiconductor Nuclear Particle Detectors," *Proc. IAEA Conf. Nuclear Electronics, Belgrade, 1961*, pp 391-401 (1962).
- Wegener, H. H. F., and F. E. Obenshain, "Mössbauer Effect for Ni^{61} with Applied Magnetic Fields," *Z. Physik* **163**, 17 (1961).
- Welton, T. A., "System Kinetics," *Proc. Symposia Appl. Math. XI (Nuclear Reactor Theory, 1959)*, 309-26 (1961).

- Welton, T. A., "Reactor Stability Theory," *Nuclear Safety* 3, 23 (1961).
- Wildermuth, Karl, and R. L. Carovillano, "Optical Giant Resonances in Nuclear Reactions," *Nuclear Phys.* 28, 636 (1961).
- Wilkinson, M. K., H. R. Child, C. J. McHargue, W. C. Koehler, and E. O. Wollan, "Neutron Diffraction Investigations of Metallic Cerium at Low Temperatures," *Phys. Rev.* 122, 1409 (1961).
- Wilkinson, M. K., W. C. Koehler, E. O. Wollan, and J. W. Cable, "Neutron Diffraction Investigation of Magnetic Ordering in Dysprosium," *Proc. Sixth Symposium Magnetism and Magnetic Materials, New York, 1960* [*J. Appl. Phys. Suppl.* 32, 48S (1961)].
- Wilkinson, M. K., E. O. Wollan, and W. C. Koehler, "Neutron Diffraction," *Ann. Rev. Nuclear Sci.* 11, 303 (1961).
- Willard, H. B., "Detection of Deuteron Alignment with S-Wave Reactions," *Proc. Intern. Symposium Polarization Phenomena of Nucleons, Basel, 1960* [*Helv. Phys. Acta, Suppl.* VI, pp 175-80 (1960)].
- Wollan, E. O., "Magnetic Coupling in Pd-Dilute Iron Group Alloys," *Phys. Rev.* 122, 1710 (1961).
- Zeidman, B., J. L. Yntema, and G. R. Satchler, "Energy Dependence of the $B^{10}(d,p)B^{11}$ Angular Distribution," pp 515-16 in *Proc. Rutherford Jubilee Intern. Conf., Manchester, England, 1961* (ed. by J. B. Birks), Heywood, London, 1961.

PAPERS PRESENTED AT SCIENTIFIC AND TECHNICAL MEETINGS

American Physical Society, Monterey, California, March 20-23, 1961

- M. K. Wilkinson (invited paper), "Magnetic Ordering in Rare Earth Metals and Compounds."
 G. Felsner and M. E. Rose, "Resonance Scattering of Linearly Polarized Gamma-Rays on Nuclei."

Southeastern Section of the American Physical Society, Louisville, Kentucky, March 30-April 1, 1961

- M. E. Rose (invited paper), "The Theory of Internal Conversion."
 P. H. Stelson (invited paper), "Vibrational States in Nuclei."
 H. H. F. Wegener (invited paper), "The Mössbauer Effect."
 J. W. T. Dabbs and F. J. Walter, "Pulse Rise Times in Semiconductor Particle Detectors."
 T. Dazai, J. U. Kjellman, and J. H. Neiler, " (n,γ) Angular Correlations from $Be^9(\alpha,n)C^{12*}$."
 J. L. Fowler, "Phenomenological Nuclear Potentials for Closed Shell Nuclei."
 W. M. Good and R. F. King, "Post Acceleration Pulsar for the Oak Ridge Pulsed Van de Graaff."
 C. H. Johnson, Frances Pleasonton, and T. A. Carlson, "An Absolute Determination of the He^6 Beta-Decay Energy."
 R. C. Ritter, P. H. Stelson, F. K. McGowan, and R. L. Robinson, "Coulomb Excitation of States in V^{51} , Zn^{67} , Fe^{57} , Ge^{73} , and Ni^{61} ."
 L. D. Roberts and J. O. Thomson, "Measurement of the Lifetime of the 77 keV Excited State of Au^{197} by the Mössbauer Method."
 F. J. Walter, J. W. T. Dabbs, and L. D. Roberts, "Resolution, Stability and Noise in Si Nuclear Particle Detectors."

American Physical Society, Washington, D.C., April 24-27, 1961

C. H. Johnson (invited paper), "A Detailed Study of the Recoil Ions from the Beta-Decay of He^6 ."

G. R. Satchler (invited paper), "The Distorted Wave Theory of Direct Nuclear Reactions."

R. L. Becker, "Fluctuation-Dissipation Relations for Neutron Diffraction."

R. C. Block, F. C. VonderLage, and L. W. Weston, "Neutron Radiative Capture Measurements."

T. A. Carlson, Frances Pleasonton, and C. H. Johnson, "Electron Shake-Off Following $\text{He}^6 \xrightarrow{\beta^-} \text{Li}^6$."

E. Eichler, R. L. Robinson, G. D. O'Kelley, and N. R. Johnson, "Decay of As^{74} ."

F. W. K. Firk and J. H. Gibbons, "Spectra of Gamma-Rays from Capture of (30 ± 10) keV Neutrons."

J. L. Fowler and E. C. Campbell, "Neutron Total Cross Section of Pb^{208} with 3 keV Resolution."

C. H. Johnson, Frances Pleasonton, and T. A. Carlson, "Recoil Energy Spectrum for the Beta-Decay of He^6 ."

H. Muenzer, K. Nishimura, and W. M. Good, "Total Neutron Cross Section of the Isotopes of Selenium."

L. D. Roberts and J. O. Thomson, "A Study by the Mössbauer Method of the HFS Splitting of Au^{197} Alloyed in Cobalt and Nickel."

R. L. Robinson, F. K. McGowan, and P. H. Stelson, "Coulomb Excitation of Levels in Se^{77} ."

E. Rost, N. Austern, and G. R. Satchler, "Collective Enhancement in $\text{Mg}^{24}(p,p')$."

H. W. Schmitt, J. H. Neiler, F. J. Walter, and R. J. Silva, "Response of Silicon Surface Barrier Detectors to Fission Fragments."

J. E. Sherwood, S. J. Ovenshine, and R. F. King, "A Source of Polarized Deuterons."

G. G. Slaughter, F. W. K. Firk, and R. J. Ginther, "An Improved Li^6 -Loaded Glass Scintillator for Neutron Detection."

G. T. Trammell, "Elastic Scattering by Bound Nuclei."

Neutron Physics Symposium, Troy, New York, May 5-6, 1961

J. A. Harvey (invited paper), "Present Status of Intermediate Energy Cross Section Measurements with Fast Choppers."

International Conference in the Field of Nuclear Spectroscopy, Copenhagen, Denmark, May 23-27, 1961

P. H. Stelson (invited participant), "Discussion Series Aimed at a Survey of Present Knowledge of Low Energy Nuclear Spectra."

Fifth European Congress on Molecular Spectroscopy, Amsterdam, Holland, May 29-June 3, 1961

W. G. Trawick, J. R. Lawson, and H. W. Morgan, "Infrared Spectra of the Nitrate and Carbonate Ions in KBr."

Symposium on Molecular Structure and Molecular Spectra, Ohio State University, June 12-16, 1961

H. W. Morgan and P. A. Staats, "The Calibration of Infrared Spectrometers Using Solid Solution Spectra."

Symposium on Neutron Time-of-Flight Methods for Energies Below 0.1 Mev (sponsored by the European-American Nuclear Data Committee), Saclay, France, July 24-27, 1961

J. H. Gibbons (invited paper), "Radiative Capture Measurements by Time-of-Flight Methods."

W. M. Good (invited paper), "Pulsed Electrostatic Accelerator as a Source of Pulsed Neutrons."

J. A. Harvey (invited paper), "Time-of-Flight Measurements Applied to Nuclear Physics."

R. C. Block, G. G. Slaughter, L. W. Weston, and F. C. VonderLage, "Neutron Radiative Capture Measurements Utilizing a Large Liquid Scintillator Detector at the ORNL Fast Chopper."

F. W. K. Firk and J. H. Gibbons, "A Direct Comparison of Gamma-Ray Spectra Obtained from the Capture of Thermal and (30 ± 10) keV Neutrons."

J. A. Harvey and S. E. Atta, "Shape and Area Analysis of Low Energy Neutron Resonances Using an IBM-7090 Computer."

G. G. Slaughter, F. W. K. Firk, and R. J. Ginther, "A Li^6 -Loaded Glass Scintillator for Neutron Detection."

Conference on Physics of Fast and Intermediate Reactors (sponsored by the International Atomic Energy Agency), Vienna, Austria, August 3-11, 1961

J. H. Neiler, "Neutron Capture Cross Sections for Energies Above a Few Hundred eV."

Fisk University Infrared Spectroscopy Institute, Nashville, Tennessee, August 27-September 1, 1961

H. W. Morgan, "Molecular Environments and Molecular Spectra."

P. A. Staats, "A Practical Approach to Analytical Problems" and "Qualitative and Quantitative Analyses by Infrared."

International Symposium on Chemical Physics of Non-Metallic Crystals, Chicago, Illinois, August 28-31, 1961

H. W. Morgan and P. A. Staats, "Infrared Spectra of Dilute Solid Solutions."

Rutherford Jubilee International Conference on Nuclear Physics, Manchester, England, September 4-8, 1961

A. B. Clegg and G. R. Satchler, "Gamma-Rays from Inelastic Scattering of High Energy Nucleons."

E. C. Halbert, R. M. Drisko, G. R. Satchler, and N. Austern, "Finite-Range Distorted-Waves Calculation of Direct Reactions."

G. R. Satchler, "Direct Nuclear Reactions with Polarized Targets."

B. Zeidman, J. L. Yntema, and G. R. Satchler, "Energy Dependence of the $\text{B}^{10}(d,p)\text{B}^{11}$ Angular Distribution."

Second Congress on Mössbauer Effect, Saclay, France, September 13-15, 1961

S. Bernstein and E. C. Campbell, "Total Reflection of Gamma Rays over the Region of Nuclear Anomalous Dispersion in Fe^{57} ."

F. E. Obenshain, M. E. Rose, and H. H. F. Wegener, "A Mössbauer-Parity-Experiment with Ni^{61} ."

F. E. Obenshain and H. H. F. Wegener, "Mössbauer Effect with Ni^{61} ."

International Conference on Magnetism and Crystallography, Kyoto, Japan, September 25-30, 1961

W. C. Koehler, J. W. Cable, E. O. Wollan, and M. K. Wilkinson (invited paper), "Recent Progress in Magnetic Structure Determinations of Rare Earth Metals."

M. K. Wilkinson, H. R. Child, W. C. Koehler, J. W. Cable, and E. O. Wollan (invited paper), "Recent Magnetic Neutron Scattering Investigations at Oak Ridge National Laboratory."

E. O. Wollan, J. W. Cable, W. C. Koehler, and M. K. Wilkinson, "Magnetic Moment Distribution in Palladium and Iron Group Alloys."

l'Institute International du Froid (International Institute of Refrigeration), London, England, September 20–22, 1961

J. W. T. Dabbs, "Reliability in Helium Liquefaction."

Conference on Electromagnetic Lifetimes and Properties of Nuclear States (sponsored by National Academy of Science – National Research Council and Oak Ridge National Laboratory), Gatlinburg, Tennessee, October 5–7, 1961

Note: P. H. Stelson served as secretary of the organizing committee for this conference, which was attended by 160 individuals representing 13 countries. He is also editing the conference proceedings, which will be published by the NAS-NRC as Nuclear Science Series Report No. 37, Publication No. 974.

D. E. Arnurius, B. Buck, and G. R. Setchler, "Radial Integrals with Realistic Wave Functions."

F. K. McGowan, P. H. Stelson, and R. L. Robinson, "Coulomb Excitation of Osmium and Chromium Nuclei."

C. W. Williams, R. P. Cumby, and J. H. Neiler, "Pulse Characteristics of Some Fast Phototubes."

Annual Meeting of the German Physical Society, Vienna, Austria, October 15–21, 1961

F. E. Obenshain and H. H. F. Wegener, "A Mössbauer-Parity-Experiment with Ni^{61} ."

Conference on Instrumentation and Technology (sponsored by the Oak Ridge Institute of Nuclear Studies and the Oak Ridge National Laboratory), Oak Ridge, Tennessee, November 13–14, 1961

J. L. Duggan, P. D. Miller, and R. F. Gabbard, " (He^3, n) Time-of-Flight Techniques."

J. H. Gibbons, "Automatic Data Reduction at ORNL Physics Division."

R. L. Macklin, "Large Liquid Scintillator Pulse Shape Calculations."

Conference on Magnetism and Magnetic Materials (sponsored by the American Institute of Electrical Engineers and the American Institute of Physics in cooperation with the Office of Naval Research), Phoenix, Arizona, November 13–16, 1961

J. W. Cable, E. O. Wollan, W. C. Koehler, and M. K. Wilkinson, "Neutron Diffraction Investigations of Ferromagnetic Palladium and Iron Group Alloys."

W. C. Koehler, J. W. Cable, E. O. Wollan, and M. K. Wilkinson, "Neutron Diffraction Study of Magnetic Ordering in Thulium."

Tennessee Academy of Science, Martin Branch of the University of Tennessee, November 24–25, 1961

Mary J. Mader and J. L. Fowler, "Phenomenological Nuclear Potentials for Neutrons on Pb^{208} ."

American Physical Society, Chicago, Illinois, November 24–25, 1961

J. K. Bair and H. B. Willard, "The Reaction $\text{O}^{18}(\alpha, n)\text{Ne}^{21}$."

E. C. Campbell and S. Bernstein, "Recoil-Free Nuclear Resonance Gamma Scattering in Total Reflection from Fe^{57} Mirror."

R. F. Gabbard, P. D. Miller, and J. L. Duggan, "The $\text{C}^{13}(\text{He}^3, n)\text{O}^{15}$ Reaction."

F. A. Khan, W. J. Gavin, and J. A. Harvey, "High Resolution Total Cross Section Measurements on W^{184} ."

American Chemical Society SW-SE Regional Meeting, New Orleans, Louisiana, December 7-9, 1961

H. W. Morgan and P. A. Staats, "Infrared Spectra of the BO_2^- Ion in Solid Solutions."

American Physical Society, New York, N.Y., January 24-27, 1962

C. P. Bhalla and M. E. Rose, "Finite Nuclear Size Effects in Beta Decay."

R. C. Block and L. W. Weston, "A 1.25-meter Diameter Liquid Scintillator Capture Gamma Detector Utilizing Only Two Photomultipliers."

J. W. Cable, G. P. Felcher, E. O. Wollan, W. C. Koehler, and M. K. Wilkinson, "Magnetic Form Factor of Metallic Erbium."

T. A. Carlson, "Recoil and Charge Spectra Following the β^- Decay of Ne^{23} ."

J. L. Duggan, M. M. Duncan, P. D. Miller, and R. F. Gabbard, "The Reactions $\text{Li}^7(\text{He}^3, n)\text{B}^9$ and $\text{Be}^9(\text{He}^3, n)\text{C}^{11}$."

T. K. Fowler, "Plasma Potential in DCX."

A. K. Furr, R. H. Rohrer, and H. W. Newson, "Average Resonance Parameters for Nuclei Near $A = 100$."

J. R. Patterson and J. A. Harvey, "Parameters of Neutron Resonances in Pa^{231} ."

V. A. Pethe and J. H. Neiler, "Improvement in Pulse Shape Discrimination Using Multi-Alkali Cathode Photomultipliers."

H. B. Willard and J. K. Bair, "The $\text{Si}^{28}(\alpha, \alpha)\text{Si}^{28}$ Reaction."

ANNOUNCEMENTS

Assignments to the various groups within the Physics Division during the past year have been as follows: J. R. Bird¹ of the Atomic Energy Research Establishment, Harwell, England (Fast Chopper Group); W. H. duPreez¹ of the South Africa Atomic Energy Board, Pretoria, South Africa (High Voltage Group); T. K. Fowler, formerly with the Neutron Physics Division (Sherwood Theory Group); T. Fuketa¹ of the Japanese Atomic Energy Research Institute, Tokai, Japan (Fast Chopper Group); T. Inada¹ of the National Institute of Radiological Sciences, Chiba, Japan (High Voltage Group); W. T. Milner,¹ formerly with the Technical Division of the Oak Ridge Gaseous Diffusion Plant (Charge Particle Compilation Group); M. C. Taylor,¹ a former co-op student from the University of Tennessee (High Voltage Group); and G. S. Vourvopoulos¹ of the Greek Atomic Energy Commission, Athens, Greece (High Voltage Group).

Loanees from other divisions within the Laboratory included: P. M. Griffin and G. K. Werner of the Thermonuclear Division (Optical Physics Group) and G. F. Wells of the Instrumentation and Controls Division (High Voltage Group).

Those completing assignments or terminating employment during this period were as follows: O. Almen¹ of the Chalmers University of Technology, Gothenburg, Sweden (High Voltage Group); H. E. Banta, a loanee from the Instrumentation and Controls Division (High Voltage Group); J. K. Bienlein¹ of the University of Erlangen, Erlangen, Germany (consultant with the Charge Spectrometry Group); J. L. Duggan,¹ ORINS Graduate Fellow from Louisiana State University

¹Temporary assignment.

(High Voltage Group); G. Felsner¹ of the University of Erlangen, Erlangen, Germany (Theoretical Physics Group); F. W. K. Firk¹ of the Atomic Energy Research Establishment, Harwell, England (Fast Chopper Group); H. Muenzer¹ of the Institut für Radiumforschung und Kernphysik, Vienna, Austria (High Voltage Group); K. Nishimura¹ of the Japanese Atomic Energy Research Institute, Tokai, Japan (High Voltage Group); S. J. Ovenshine (High Voltage Group); V. A. Pethe¹ of the Atomic Energy Research Establishment, Bombay, India (Scintillation Spectrometry and Instrument Development Group); R. C. Ritter,¹ ORINS Graduate Fellow from the University of Tennessee (High Voltage Group); M. E. Rose (Theoretical Physics Group); J. E. Sherwood (High Voltage Group); E. van der Spuy¹ of the South Africa Atomic Energy Board, Pretoria, South Africa (Theoretical Physics Group); and H. H. F. Wegener¹ of the University of Erlangen, Erlangen, Germany (High Voltage Group).

S. Bernstein of the Mössbauer Experimental Program is on leave at the University of Miami for the current academic year. He is teaching one course in modern physics and another in general physics at the sophomore level.

R. C. Block of the Fast Chopper Group is presently at the Rensselaer Polytechnic Institute, where for two months he will be conducting a capture gamma experiment.

J. W. T. Dabbs of the Low Temperature Group has completed a six-month Fulbright Lectureship in atomic energy at the Institute of Physics in San Carlos de Bariloche, Argentina.

T. K. Fowler of the Sherwood Theory Group is presently at the Institute of Mathematical Sciences of New York University. His work there for two months, with the Magneto-Fluid Dynamics Division, will deal with theoretical plasma physics.

C. H. Johnson of the Charge Spectrometry Group is assigned this academic year to the University of Minnesota. In addition to teaching an undergraduate physics course, he is conducting a research study of the 60-Mev linear accelerator at Minnesota.

P. D. Miller of the High Voltage Group is on a one-year assignment to the Atomic Energy Research Establishment in Harwell, England. This assignment is a continuation of the profitable liaison in physics between AERE and ORNL, which was initiated in 1959, and is the third such assignment.

Frances Pleasonton of the Charge Spectrometry Group has recently begun a four-month assignment at the University of Erlangen, Erlangen, Germany. She will pursue further at Erlangen studies in progress at ORNL dealing with internal bremsstrahlung accompanying the beta decay of He⁶.

G. T. Trammell of the Theoretical Physics Group is on leave as a Visiting Professor at Rice University. He is conducting research in the field of nuclear physics; teaching duties include theoretical nuclear physics and advanced electricity and magnetism.

M. K. Wilkinson of the Neutron Diffraction Group is on leave as a Visiting Professor at the Georgia Institute of Technology. He is teaching a course in neutron diffraction as well as assisting in the organization of a research program for a reactor under construction there.

N. H. Lazar of the Scintillation Spectrometry and Instrument Development Group (presently on loan to the Thermonuclear Division) has returned to ORNL following an eight-month assignment at the Los Alamos Scientific Laboratory. R. L. Macklin of the High Voltage Group and K. L. Vander Sluis of the Optical Physics Group have also returned to the Laboratory, having completed, respectively, one-year assignments at the Atomic Energy Research Establishment and at the Massachusetts Institute of Technology.

ADVISORY COMMITTEE

Research programs in the Physics Division and the Electronuclear Division are reviewed by a joint Advisory Committee at their Annual Information Meeting. Advisory Committee members at the time of the April 10-13, 1961, meeting were as follows:

Prof. H. Feshbach	Massachusetts Institute of Technology Cambridge, Massachusetts
Prof. W. A. Fowler	California Institute of Technology Pasadena, California
Dr. M. Goldhaber	Brookhaven National Laboratory Upton, Long Island, New York
Prof. M. S. Livingston	Cambridge Electron Accelerator Cambridge, Massachusetts
Prof. J. R. Richardson	University of California Los Angeles, California
Dean J. H. Van Vleck	Harvard University Cambridge, Massachusetts
Prof. J. A. Wheeler	Princeton University Princeton, New Jersey

ACTIVITIES RELATED TO EDUCATIONAL INSTITUTIONS

Research Participants

The following investigators were engaged in research under the cooperative ORINS-ORNL Research Participation Program during the summer months of 1961: C. F. Dam (Associate Professor, Cornell College), Low Temperature Group; R. W. Lide (Assistant Professor, University of Tennessee), Physics of Fission Group; E. Merzbacher (Associate Professor, University of North Carolina), Theoretical Physics Group; G. Oppo¹ (Associate Professor, University of Louisville), Scintillation Spectrometry and Instrument Development Group; J. R. Patterson²

¹Presently with the Polytechnic Institute of Brooklyn.

²Presently with Rockford College.

(Associate Professor, Clemson College), Fast Chopper Time-of-Flight Spectrometry Group; M. F. Steuer (Assistant Professor, University of Georgia), High Voltage Group; and W. G. Trawick³ (Associate Professor, Louisiana Polytechnic Institute), Spectroscopy Research Group.

Summer Visitors

Summer visitors with the Division in 1961 included: J. Kronsbein (University of Florida), Theoretical Physics Group; Jae Park (University of North Carolina), Theoretical Physics Group; M. H. Shelton (University of Tennessee), High Energy Accelerator Research Group; and J. O. Thomson (University of Tennessee), Low Temperature Group.

Student Trainee Program

The cooperative ORINS-ORNL Student Trainee Program (under the sponsorship of the U.S. Atomic Energy Commission) was set up primarily to give students from small southern colleges the opportunity of working in a full-time research laboratory during the summer months between their third and fourth years of college. In 1961, students with the Division under the auspices of this program were: T. B. Kaiser (St. Edwards' University), High Energy Accelerator Research Group; J. W. McWane (Virginia Military Institute), Neutron Diffraction Group; W. G. Mankin (Southwestern at Memphis), Scintillation Spectrometry and Instrument Development Group; L. M. Okun (Wesleyan University), High Voltage Group; B. M. Preedom (Spring Hill College), Charge Spectrometry Group; and J. H. Soper II (Washington and Lee University), Fast Chopper Time-of-Flight Spectrometry Group.

Co-op Students

The Co-op Program of the Oak Ridge National Laboratory is designed for promising students in engineering and science who have completed at least two quarters of undergraduate study. Students selected for the Co-op Program alternate between three months of work as technical assistants at the Laboratory and three months of school attendance. This program has proved to be highly successful, both as a means for promoting the professional development of the students and for providing valuable technical assistants for scientific research in the Laboratory. Nine co-op students were with the Division during the past year and were assigned to the Theoretical Physics Group, the High Energy Research Group, and the High Voltage Laboratory. These students included: J. F. Agnew, J. H. Williams, and L. W. Owen of the Virginia Polytechnic Institute in Blacksburg, Virginia; R. M. Eyer and R. E. Maydole of the Drexel Institute of Technology in Philadelphia, Pennsylvania; and W. A. Hartman,⁴ C. E. Hughey,⁴ D. O. Patterson,⁴ and M. C. Taylor⁴ of the University of Tennessee in Knoxville, Tennessee.

³Presently with Georgia State College.

⁴Assignment completed during this period.

Part-Time University Students

University students currently working with the Division as part-time consultants include:

J. Ginocchio University of Rochester	Theoretical Physics Group
C. E. Hughey ⁵ University of Tennessee	High Energy Research Group
D. O. Patterson ⁵ University of Tennessee	High Energy Research Group
M. R. Patterson University of Tennessee	Charge Particle Cross Section Compilation Group

Thesis Research

Eleven staff members of the Physics Division have served during the past year in an advisory or supervisory capacity for research conducted at the Laboratory by nine Ph.D. candidates, as listed below:

Staff Member(s)	Ph.D. Candidate	Field of Research
T. A. Welton	H. Bertini University of Tennessee	Monte Carlo Calculations on Intranuclear Cascades
P. D. Miller and W. M. Good	J. L. Duggan ⁶ Louisiana State University (now with the University of Georgia)	A Study of the Reactions $\text{Be}^9(\text{He}^3, n)\text{C}^{11}$, $\text{Li}^7(\text{He}^3, n)\text{B}^9$, and $\text{C}^{13}(\text{He}^3, n)\text{O}^{15}$ by Time-of-Flight Techniques
J. A. Harvey and H. W. Schmitt	A. K. Furr ⁷ Duke University (now with the Virginia Polytechnic Institute)	Neutron Capture by Activation Techniques
J. H. Neiler	R. Gwin University of Tennessee	Energy Transport in Alkali Halide Phos- phors
W. M. Good and J. L. Fowler	R. W. Lamphere University of Tennessee	Angular Distribution of Fission from the Fast-Neutron-Induced Fission of U^{234}
T. A. Welton	J. H. Marable University of Tennessee	Nuclear Three-Body Problem
H. W. Schmitt, J. H. Neiler, and L. D. Roberts	W. F. Mruk University of Tennessee	Time-of-Flight and Magnetic Analysis of <i>Fission Fragments</i>

⁵Former co-op student.

⁶ORINS graduate fellowship completed and doctorate received in 1961.

⁷Former ORINS Graduate Fellow.

Staff Member(s)	Ph.D. Candidate	Field of Research
G. R. Satchler	S. K. Penny University of Tennessee	Theory of Nuclear Reactions
P. H. Stelson and F. K. McGowan	R. C. Ritter ⁶ University of Tennessee (now with the University of Virginia)	Coulomb Excitation with Heavy Ions

Consultants Under Subcontract

University personnel currently serving as consultants to the Division are listed below. Numerous other consultants have, throughout the past year, presented seminar talks and are included in the list of speakers in the "ORNL Physics Seminars" section of this report.

L. C. Biedenharn, Jr. Duke University	R. A. Mann University of Alabama
K. A. Brueckner University of California La Jolla, California (on leave to Institute for Defense Analyses, Washington)	J. B. Marion University of Maryland
W. M. Bugg University of Tennessee	A. H. Nielsen University of Tennessee
J. H. Goldstein Emory University	H. W. Newson Duke University
J. M. Jauch University of Geneva Geneva, Switzerland	W. T. Pinkston Vanderbilt University
T. Lauritsen California Institute of Technology	R. H. Rohrer Emory University
R. W. Lide University of Tennessee	J. O. Thomson University of Tennessee
	K. Wildermuth Florida State University
	J. H. Wise Washington and Lee University

Visiting Scientist Lecture Program in Physics

The Visiting Scientist Lecture Program in Physics is sponsored by the American Association of Physics Teachers and the American Institute of Physics. This program, now in its fifth year, is supported by the National Science Foundation. During the past year J. L. Fowler delivered, under the program, the following lectures:

Drew University, Madison, New Jersey, March 8-9, 1961

"Nuclear Science and the Foundation of Future
Technology" (presented as a public lecture)

"The Neutron as a Probe of Nuclear Matter"
(lecture to physics students)

"Electrostatic Accelerators" (lecture to a class
in general physics)

Traveling Lecture Program

The Traveling Lecture Program is conducted in cooperation with the Oak Ridge Institute of Nuclear Studies as a part of the AEC's program of disseminating scientific and technical information to universities, particularly those in the South. Lectures delivered by ORNL personnel present unclassified information to university undergraduate and graduate students and faculty members. The lectures serve to stimulate interest in research in the university departments and also assist the teaching staff in expanding the scope of instruction offered under their regular curricula. Through such personal contacts, ORNL staff members are also able to observe departmental activities at the universities. Listed below are ten members of the Physics Division who participated in the Traveling Lecture Program during the academic year 1960-1961, presenting 31 lectures. To date, five members of the Division have presented 16 lectures under this program for the current academic year; these lectures will appear in the next annual report.

R. L. Becker	Vanderbilt University, January 12-13, 1961 "Studies of Weak Particle-Decay Interactions" and "Theory of the Nuclear Many-Body Problem" Georgia Institute of Technology, April 7, 1961 Louisiana State University, May 11, 1961 University of Texas, May 12, 1961 "Research in Nuclear Many-Body Problem"
H. O. Cohn	Rice University, April 19, 1961 Mississippi State University, April 20, 1961 "Strange Particles in High Energy Physics"
W. C. Koehler	University of Cincinnati, February 10, 1961 "Recent Applications of Neutron Diffraction Methods to Solid State Physics"
F. K. McGowan	Ohio State University, May 11, 1961 "Recent Results from Coulomb Excitation of Nuclei"
P. D. Miller	University of Kentucky, April 21, 1961 "Neutron Time-of-Flight Studies at ORNL"
H. W. Morgan	University of Kentucky, January 11, 1961 University of Cincinnati, January 12, 1961 Mississippi State College, March 9, 1961 Frank Phillips College, March 14, 1961 University of Houston, March 15, 1961 Loyola University, March 17, 1961 Louisiana Polytechnic Institute, March 20, 1961 "The Vibrating Molecule, an Introduction to Molecular Structure and Spectroscopy"
J. H. Neiler	Florida State University, February 21, 1961 "Nuclear Physics and the Recent Theories of Nucleosynthesis" University of Florida, February 22, 1961 Clemson College, April 18, 1961 "Nuclear Spectrometry with Pulsed Electrostatic Accelerators"

M. E. Rose	University of Kentucky, October 11, 1960 "Coherence Effects in Resonance Scattering" University of Miami, December 5, 1960 Florida State University, December 6, 1960 University of Florida, December 8, 1960 University of Maryland, March 15, 1961 "Coherence Effects in Resonance Fluorescence" University of North Carolina, May 15, 1961 "Depolarization of Mu Mesons"
P. H. Stelson	Arizona State University, November 17, 1960 "Coulomb Excitation of Nuclei and the Collective Model"
H. H. F. Wegener	Vanderbilt University, December 16, 1960 Georgia Institute of Technology, May 24, 1961 Florida State University, May 25, 1961 Auburn University, May 26, 1961 "Mössbauer Experiments with Ni ⁶¹ ,"

University Seminars

In addition to the Visiting Scientist Lecture Program in Physics and the Traveling Lecture Program, divisional staff members receive numerous requests from various universities for seminar talks. Fifteen such invitations were accepted during the past report period:

R. C. Block	Rensselaer Polytechnic Institute, April 27, 1961 "Capture Cross Section Measurements with the ORNL Fast Chopper"
J. H. Gibbons	Duke University, June 9, 1961 "Recent Studies of Neutron Capture Gamma Rays" Pennsylvania State University, October 26, 1961 "Capture Experiments with kev Neutrons Using Pulsed Beam Time-of-Flight"
J. A. Harvey	Massachusetts Institute of Technology, March 16, 1961 "Current Status of Low Energy Neutron Spectroscopy"
F. E. Obenshain	University of Tennessee, April 4, 11, and 18, 1961 "Mössbauer Effect"
L. D. Roberts	Princeton University, January 23, 1961 "Mössbauer Studies with Some Gold Alloys"
R. L. Robinson	Indiana University, November 21-22, 1961 "Coulomb Excitation with Alpha Particles"
M. E. Rose	University of Virginia, April 9, 1961 "Coherence Effects in Resonance Fluorescence"
G. R. Satchler	University of Michigan, July 1961 "Distorted Wave Theory of Direct Nuclear Reactions" Florida State University, December 29, 1961 "Recent Nuclear Reactions"
H. W. Schmitt	University of Tennessee, February 6, 1962 "Experimental Studies in Nuclear Fission"

P. H. Stelson	University of Tennessee, February 7 and 14, 1961 "Coulomb Excitation of Collective Motions in Nuclei"
H. H. F. Wegener	California Institute of Technology, April 10, 1961 "Mössbauer Effects on Ni ⁶¹ "
T. A. Welton	Vanderbilt University, November 17, 1961 "Coherent Light"
H. B. Willard	University of Tennessee, February 28 and March 7, 1961 "Parity Non-Conservation Experiments"

University Summer Institutes

Two staff members participated in summer institutes in 1961: R. L. Becker (Theoretical Physics Group) in the Summer Institute for Theoretical Physics at the University of Wisconsin, held June 9–August 4; and G. R. Satchler (Theoretical Physics Group) in the Summer Institute on Nuclear Spectroscopy at the University of Michigan, held July 11–29.

ORINS-ORNL Summer Institute

The Oak Ridge Institute of Nuclear Studies, in cooperation with the Oak Ridge National Laboratory, conducted a Summer Institute for Physics Teachers from Small Colleges, June 26 through August 18, 1961. This institute, sponsored by the U.S. Atomic Energy Commission, was designed primarily to give participants an opportunity to review basic nuclear-energy concepts, acquire an understanding of current nuclear-energy developments, become familiar with new equipment, and gain greater insight into the development of college courses in the field. The institute consisted of both lectures by, and laboratory sessions with, nuclear physicists from ORINS and ORNL. Twenty-two college professors from as many colleges participated in the institute under AEC grants.

Four staff members of the Physics Division were included among the lecturers during the six weeks of the institute. L. D. Roberts and R. L. Becker lectured on "Quantum Mechanics," and J. L. Fowler and P. H. Stelson lectured on "Nuclear Physics." Additionally, M. K. Wilkinson coordinated the laboratory sessions associated with the Physics Division lectures.

ORINS-ORNL Conference on Instrumentation and Technology

A Conference on Instrumentation and Technology Pertaining to Medium Energy Nuclear Physics, sponsored jointly by the Oak Ridge Institute of Nuclear Studies and the Oak Ridge National Laboratory, was held at the Laboratory November 13–14, 1961. This was the first of a contemplated series of meetings and conferences of the Oak Ridge Nuclear Facilities Group, which consists of nuclear physicists from the ORINS region.

The program of the Conference concerned primarily nuclear physics in the 1–70 Mev energy range for protons, with corresponding ranges for heavy ions. J. L. Fowler, Director of the Physics Division and a member of the Steering Committee of the Oak Ridge Nuclear Facilities

Group, was program chairman. W. M. Good, Co-Director of the Division's High Voltage Laboratory, was among the nine invited speakers on the program. Three contributed papers (listed in the section, "Papers Presented at Scientific and Technical Meetings") were presented by members of the Division.

ORNL PHYSICS SEMINARS

Weekly divisional seminars are normally held at the Laboratory each Friday afternoon; for topics of especial timeliness or interest, additional seminars are frequently scheduled. During the period covered by this report, W. C. Koehler served as Seminar Chairman until June 1961, at which time P. H. Stelson became Chairman. Lectures scheduled included the following:

1961	
February 13	Francis Bitter, National Magnetic Laboratory "Generation and Use of High Magnetic Fields"
February 17	T. A. Welton, ORNL "Coherent Light"
February 21	V. P. Kenny, University of Kentucky "Bubble Chambers"
February 24	R. J. Ginther, Naval Research Laboratory "Glass Scintillators"
March 3	G. R. Satchler, ORNL "Distorted Wave Theory of Direct Nuclear Reactions"
March 10	H. H. F. Wegener, University of Erlangen and ORNL "Mössbauer Effect in Nuclear Physics"
March 17	Gerhard Felsner, University of Erlangen and ORNL "Effect of Inelastic Scattering on Polarization Asymmetry"
March 21	S. H. Autler, Lincoln Laboratory "Superconducting Electromagnets"
April 3	Lincoln Wolfenstein, Carnegie Institute of Technology "Weak Interactions"
April 4	"Mu-meson Physics"
April 5	"Possible Experiments Involving Polarized Protons and Neutrons"
April 7	S. Legvold, Iowa State University "Electrical and Magnetic Properties of Rare Earth Single Crystals"
April 14	J. R. Richardson, University of California at Los Angeles "Preliminary Operation of the UCLA 50-Mev Cyclotron"
April 21	S. Bjornholm, University of California at Berkeley "Decay Schemes of the Odd-Odd Protactinium Isotopes"
May 2	W. A. Fowler, California Institute of Technology "Nucleosynthesis During the Early History of the Solar System"

- May 5 H. Postma, Brookhaven National Laboratory
 "Some Experiments on the Beta and Gamma Decay of Oriented ^{166}Ho and ^{160}Tb Nuclei"
- May 11 F. D. Brooks, Atomic Energy Research Establishment, Harwell
 "Partial Neutron Cross Section Measurements with the Harwell Linear Accelerator"
- May 19 J. E. Kunzler, Bell Telephone Laboratories
 "Superconductivity in High Magnetic Fields"
- May 26 C. H. Johnson, ORNL
 "Energy Spectrum of Recoil Ions from the Decay of $\text{He}^{6\alpha}$ "
- June 2 A. Sjölander, Argonne National Laboratory
 "Liquid Dynamics and Neutron Scattering"
- June 8 J. S. Levinger, Louisiana State University
 "The Neutron Gas"
- June 9 J. F. Burns, ORNL
 "Electron Impact Studies of Autoionization of Krypton"
- June 16 Duo-Liang Lin, Ohio State University
 "Charge Dependent Effects on Nuclear Forces"
- June 23 Ernst van der Spuy, South African Atomic Energy Board
 "Baryon-Meson Model"
- June 30 M. A. Melkanoff, University of California at Los Angeles
 "Optical Model Analyses of Proton Scattering Against Carbon at 10-20 Mev"
- July 7 Fred Young, ORNL
 "Dislocation Motion in Copper"
- July 12 M. G. Kelliher, Vickers Research Ltd., Berkshire
 "High Energy Electron Linear Accelerator for Neutron Research"
- July 14 Roger Bender, ORNL
 "Deflection of Ion Beams from the ORIC"
- July 18 Vernon Hughes, Yale University
 "A High Intensity Proton Linear Accelerator"
- July 21 W. A. Arnold, ORNL
 "Wave Mechanics and Muscle Contraction"
- July 28 Norman Lazar, ORNL
 "The DCX-2 Program"
- August 4 R. L. Macklin, ORNL
 "Glass-Loaded Liquid Scintillation Gamma Detector"
- August 11 R. C. Ritter, ORINS and University of Tennessee
 "Coulomb Excitation with Ne^{20} Ions"
- August 16 F. W. K. Firk, Atomic Energy Research Establishment, Harwell
 "Some General Methods of Neutron Resonance Analysis"
 "Photonuclear Measurements at Livermore Using Monoergic Gamma-Rays from Positron Annihilation in Flight"
- August 25 J. L. Duggan, ORINS and Louisiana State University
 "A Study of the Reactions $\text{Li}^7(\text{He}^3, n)\text{B}^9$, $\text{Be}^9(\text{He}^3, n)\text{C}^{11}$, and $\text{C}^{13}(\text{He}^3, n)\text{O}^{15}$."

- September 1 Brebis Bleaney, Oxford University
"Hyperfine Structure in the Rare Earths"
- September 5 G. E. Bacon, Atomic Energy Research Establishment, Harwell
"Some Recent Studies in Neutron Diffraction"
- September 6 Francis Perey and Brian Buck, ORNL
"A Non-Local Potential Model for the Scattering of Neutrons by Nuclei"
- September 15 L. Katz, University of Saskatchewan
"The Generation of Monochromatic Photons by the Annihilation of Positrons in Flight"
- September 22 W. M. Good and G. G. Slaughter, ORNL
"The Saclay Symposium on Time-of-Flight Methods"
- September 29 J. R. Bird, Atomic Energy Research Establishment, Harwell
"Capture Gamma-Ray Spectra for Neutron Resonances in Platinum"
- October 9 Mitsuo Sakai, Institute for Nuclear Study, University of Tokyo
"Nuclear Spectroscopy in Japan"
- October 20 K. Nishimura, Japan Atomic Energy Research Institute
"Gamma Rays from Neutron Inelastic Scattering in Silver and Cadmium"
- October 27 James Ford, California Institute of Technology
"Elastic Scattering of Deuterons from Li^7 "
- November 3 A. Yoshimori, Ohio State University
"The Theory of the Screw Spin Structure"
- November 10 H. Muenzer, Institute für Radiumforschung und Kernphysik, Vienna
"Average Level Spacings"
- November 21 R. L. Becker, ORNL
"The Nuclear Many-Body Problem"
- November 28 E. F. L. Bertaut, Institut Fourier, Grenoble, France
"The Lattice Theory of Spin Configuration"
- December 1 H. O. Cohn, ORNL
"Helium Bubble Chamber Experiment; K^- Interactions"
- December 8 H. C. Schweinler, ORNL
"Statistical Mechanical Calculations for Non-Metals"
- December 15 E. C. Campbell, ORNL
"Recoil Free Nuclear Resonance Gamma Scattering in Total Reflection from Fe^{57} Mirror"
- December 20 J. R. Patterson, Rockford College
"High Resolution Total Neutron Cross Section Measurements on Pa^{231} "
- December 21 E. P. Wigner, Princeton University
"Spacing of Energy Levels"
- 1962
- January 12 F. J. Shore, Queens College
"Transmission of Polarized Neutrons Through Polarized Nuclei"

PHYSICS PROGRESS REPORT

- | | |
|------------|--|
| January 19 | W. C. Koehler, ORNL
"Report on the International Conference on Magnetism and Crystallography" |
| February 2 | William Bugg, University of Tennessee
"Particle Resonances of High Energies" |
| February 9 | G. R. Satchler, ORNL
"Inelastic Scattering of Alpha Particles" |

The following Special Theoretical Physics Seminar Series was arranged during the summer of 1961 by G. T. Trammell:

- | | |
|--------------|---|
| July 19 | H. H. F. Wegener, University of Erlangen and ORNL
"The Physical Meaning of the Vector Potential" |
| July 26 | E. Merzbacher, University of North Carolina
"Single Valuedness of Wave Functions" |
| August 9, 16 | E. van der Spuy, South African Atomic Energy Board
"The Baryon-Meson Model" |
| August 23 | Gareth Guest, North Texas State College
"Time Reversal Invariance in Strong Interactions" |

A weekly lecture course conducted by T. A. Welton on "Relativistic Electron Theory" is in progress, having been arranged by L. D. Roberts and begun November 22, 1961. It is expected that approximately 20 lectures on the subject will be presented.

INTERNAL DISTRIBUTION

1. C. E. Larson
2. Biology Library
3. ORNL – Y-12 Technical Library, Document Reference Section
- 4-6. Central Research Library
7. Reactor Division Library
8. Laboratory Shift Supervisor
- 9-84. Laboratory Records Department
85. Laboratory Records, ORNL R.C.
86. A. M. Weinberg
87. J. P. Murray (K-25)
88. R. G. Jordan (Y-12)
89. J. A. Swartout
90. E. H. Taylor
91. E. D. Shipley
- 92-93. J. L. Fowler
94. M. L. Nelson
95. A. H. Snell
96. A. Hollaender
97. K. Z. Morgan
98. F. L. Culler
99. M. T. Kelley
100. E. O. Wollan
101. H. E. Seagren
102. A. S. Householder
103. L. D. Roberts
104. R. B. Briggs
105. R. N. Lyon
106. W. C. Koehler
107. E. P. Blizard
108. G. E. Boyd
109. R. P. Metcalf
110. R. W. Stoughton
111. W. H. Jordan
112. E. C. Campbell
113. D. S. Billington
114. M. A. Bredig
115. R. S. Livingston
116. F. C. Maienschein
117. F. E. Obenshain, Jr.
118. R. C. Block
119. C. D. Susano
120. C. J. Borkowski
121. M. J. Skinner
122. P. D. Miller
123. J. W. Cable
124. G. deSaussure
125. W. M. Good
126. F. K. McGowan
127. R. W. Johnson
128. J. R. McNally, Jr.
129. J. L. Gabbard
130. G. G. Slaughter
131. Eugene Guth
132. R. W. Peelle
133. P. R. Bell
134. G. G. Kelley
135. C. C. Harris
136. H. G. MacPherson
137. P. H. Stelson
138. J. E. Sherwood
139. W. Zobel
140. R. B. Murray
141. H. B. Willard
142. J. H. Neiler
143. J. A. Harvey
144. C. F. Barnett
145. N. H. Lazar
146. J. W. T. Dabbs
147. J. H. Gibbons
148. J. J. Pinajian
149. F. Pleasonton
150. C. A. Preskitt
151. H. R. Child
152. C. G. Gardner
153. C. J. McHargue
154. J. A. Lane
155. C. S. Harrill
156. A. J. Miller
157. S. C. Lind
158. K. L. Vander Sluis
159. R. L. Robinson
160. G. R. Satchler
161. H. W. Morgan
162. H. W. Schmitt
163. P. M. Griffin
164. A. Zucker
165. R. W. Lamphere
166. C. D. Goodman
167. E. P. Wigner (consultant)
168. L. J. Rainwater

169. M. Goldhaber (consultant)
170. W. A. Fowler (consultant)

171. J. A. Wheeler (consultant)
172. H. Feshbach (consultant)

EXTERNAL DISTRIBUTION

173. R. W. McNamee, Union Carbide Corporation
174-283. Given external distribution
284-915. Given distribution as shown in TID-4500 (17th ed.) under Physics category
(75 copies - OTS)